TRANSMISSION AND SCANNING ELECTRON MICROSCOPIC STUDIES IN DISEASES OF THE LIVER

VOLUME - I

©S.S.M.A.AL-ALOUSI, MB,CHB,

MSc (Medical Sciences) - Research

GLASGOW UNIVERSITY

Supervisor

Professor R.N.M.MacSween, M.D., F.R.C.P., F.R.C.Path.

ProQuest LLC.
789 East Eisenhower Parkway
P.O. Box 1346
Ann Arbor, MI 48106 – 1346

CONTENTS

INTRODUCTION

Ever since Malpighi (1666) introduced the morphological concept of small histological units or lobules within the mammalian liver, many authors have shown close interest in the structural and functional relationships within the organ as applied to the normal as well as the pathological conditions. In the pursuit of this endeavour, liver morphologists applied light microscopy, histochemical techniques and electron microscopy (both transmission and scanning) to hepatic structures. However another era of ultrastructural advances in hepatology is anticipated through the use of freeze-fracture replica and etching techniques.

The four major concepts of the basic structural organisation of the liver have been the hexagonal lobule described by Kiernan in 1833, the portal lobe described by Mall in 1906, the liver acinus defined by Rappaport in 1954 and the hepatic muralium described by Elias (1949a and b). Each of these concepts represented a particular way of looking at an organ of great structural complexity and with a multitude of functions.

The recent SEM studies of Grisham et al (1976a & b) confirmed the initial findings of Elias in which he made a three dimensional reconstruction of the hepatocytes and stated that they are arranged in the form of plates or sheets, one cell in thickness. These plates branch and anastomose with one another to form a complicated system of walls in a maze-like arrangement of partitions between which the sinusoids interweave and interconnect in a continuous labyrinth(MacSween and Scothorn 1979).

In order to understand the details of the ultrastructural changes in alcoholic liver disease and primary biliary cirrhosis, which are

the main objects of this study, it is important to give an account on the light microscopic structures and an elaborate description on the electron microscopic morphology in the normal liver.

Normal light microscopic morphology

In spite of the differences in the various concepts of the hepatic histology, the classic hepatic lobule remained an understandable framework of liver structures. It is hexagonal in outline with a central vein at its centre. Within the lobule the hepatocytes form radially arranged one cell thickness plates (cords) with the sinusoids lying between them.

Each portal tract consists of connective tissue in which are embedded at least one artery, portal vein branch and bile duct in addition to lymphatics and nerves. Bile ducts in the smallest tracts are referred to as interlobular, larger ones as septal or trabecular ducts. Interlobular ducts are lined by cuboidal or low columnar epithelium. Septal ducts are lined by tall columnar cells with basal nuclei (Masuko et al 1964).

Normal bile ducts usually occupy a central position in the portal tracts. The interlobular bile ducts are connected to the bile canaliculi by ductules and canals of Hering. The latter are lined partly by biliary epithelium and partly by liver cells; neither ductules nor canals of Hering are often seen in sections of normal liver. In addition to the abovementioned structures the portal tracts may contain small numbers of lymphoid cells and mast cells (Murata et al 1973).

The hepatocyte has a centrally placed nucleus with a distinct nucleolus, granular cytoplasm with coarse aggregates of rough endoplasmic reticulum usually between the nucleus and the canalicular pole.

The sinusoids are lined by two kinds of cells, endothelial mesenchymal-like cells barely noticeable on light microscopy and larger phagocytic Kupffer cells.

Normal ultrastructural morphology

Since this concerns the main object of this study, an elaborate description of the ultrastructural findings of the normal liver tissue is mentioned below. These will involve description of the hepatic sinusoid, the portal and hepatic vessels, bile canaliculi and the hepatocyte.

Hepatic sinusoid

Mayer (1899) and Minot (1900) believed that the sinusoidal endothelium was comprised of widely separated mesenchymal cells. Fawcett (1955) and Rouiller (1956), utilising electron microscopic techniques, demonstrated that Mayer and Minot were essentially correct.

Cells comprising the sinusoidal lining are usually classified either as undifferentiated endothelial cells or as phagocytic (Kupffer) cells. Microvilli on the surface of parenchymal cells surrounding the sinusoid seem to support the lining endothelium, thus producing the space of Disse. This perisinusoidal space, in normal specimens, contains small amounts of reticulin fibres and variable numbers of fat-storing cells (Ito cells) which are known to synthesize collagen and to store vitamin A in their lipid droplets.

The architecture of the liver sinusoid has been extensively explored by means of TEM. The SEM studies permitted a direct view of the three-dimensional organisation of the sinusoids. Kirn et al (1976) used the perfusion fixation technique to make more distinct and accurate description of the different types of sinusoidal cells. He was able to demonstrate the fenestration of the endothelial cells which measured an average of thirty micron in diameter. These fenestrations allow

direct communication between the blood in the sinusoid and the hepatocytes.

The Kupffer cells bulge into the lumen of the sinusoid, either embedded in the endothelial lining or lying on it and sometimes extending into the space of Disse. The endocytic capacity of these cells is much wider as compared to the endothelial lining cells. They can take up particules of different diameters by phagocytosis or pinocytosis.

The pit cells, a fourth type of sinusoidal cell, described in the rat liver, are located and embedded in the sinusoidal lining and contain granules resembling those in endocrine cells.

The blood flow through the sinusoid is controlled by inlet and outlet sphincters while the flow from the arteriole into the sinusoid being intermittent is controlled by a definitive contractile smooth muscle sphincter. Motta (1975) using SEM supported McCuskey's suggestion (1966) that the spincter activity of the sinusoid is accomplished by thickening of the perinuclear cytoplasm of Kupffer cells. This thickening he attributed to the phagocytic function of those cells. Wisse (1972), however, contested this by describing that the endothelial lining cells can also phagocytose particulate materials, though in small amounts, yet they did not contribute to the sphincteric function of the sinusoid (MacSween and Scothorne 1979).

Portal and hepatic blood vessels

The portal vein subdivides into smaller branches of 400 micron sized interlobular veins which subdivide into venules extending into the hepatic parenchyma. These venules have an endothelial lining with a basement membrane and scanty adventitial fibrous tissue but no muscle in their walls.

The hepatic artery subdivides into terminal branches which open into the peripheral sinusoids. It also gives a peribiliary plexus which surrounds the bile ducts and drain partly into the sinusoids or into portal veins.

The venous blood drains from the central vein into the terminal hepatic veins. These in turn unit to form intercalated veins, interlobular veins and finally to form two or three main hepatic veins which drain into the inferior vena cava.

Bile canaliculi

Biava (1964) made an extensive study of the ultrastructure of the bile canaliculi in the human liver. Bile canaliculi consist of intercellular spaces 0.5-1.5 micron in diameter bound by two liver cells. Their lumina are enclosed by a relatively well defined layer of compact cytoplasm along the inner aspect of the canalicular membrane. The canalicular cell membrane shows the presence of microvilli averaging 0.08 micron in diameter and 0.2 micron in length. In a cross section of a canaliculus, the number of the microvilli ranges from six to thirty. As the canalicular membranes of adjacent liver cells come into contact at the sides of the bile canaliculi, characteristic junctional complexes are formed. These complexes have been described by Farquhar and Palade (1963 and 1965) as tight junctions, desmosomes and intermediate junctions. These junctions extend for a distance of 0.1-0.4 micron from the canalicular lumen.

Desmosomes are located at variable distances from the canalicular tight junctions. They consist of parallel segments of triple-layered membranes averaging 0.2 micron in length, separated by a gap of uniform width, the latter is filled with homogeneous material of moderate electron density. In addition they are characterised by a layer of dense homogeneous material closely apposed to the inner leaflets of

desmosomal membranes. They are not constantly seen between liver cells in any given section. This indicates that in contrast to canalicular tight junctions, they constitute a focal specialisation of cell surface rather than continuous bands running along the entire length of the cell.

Intermediate junctions are less conspicuous in the liver. They are usually located between tight junctions and desmosomes and consist of relatively straight parallel segments of lateral cell membranes separated by a gap of uniform width.

The peribiliary cytoplasm of liver cells contains various organelles among which Golgi complex and the smooth endoplasmic reticulum are particularly prominent. Vesicular elements of these cytoplasmic components are seen reaching the canalicular cell membrane. They were found to extend into the pericanalicular ectoplasm where they appear to undergo progressive dissolution.

Hepatocytes

This is a polygonal-shaped cell approximately 30 micron in diameter and has three distinct interfaces : sinusoidal, canalicular and intercellular which faces neighbouring hepatocytes.

The sinusoidal surface is covered with abundant microvilli each measuring 0.5 micron long. This constitutes a functional surface for absorption and/or secretion. By SEM, the bases of microvilli show indentations representing secretory vacuoles discharging into the perisinusoidal space by exocytosis (Grisham 1976a & b). There is no basement membrane for the hepatocytes.

The canalicular surface is an intercellular space between neighbouring hepatocytes. The intercellular surface extends from the bile canaliculus to the margin of the sinusoidal surface. Occasional plicae and

round mouthed openings representing pinocytic vesicles are found. This surface is separated from the canalicular surface by junctional complexes. The nucleus is large, spherical and has a prominent nucleolus. The mitotic index is very low and the average life span of a hepatocyte is about 150 days in laboratory rodents.

The cytoplasmic organelles include endoplasmic reticulum both rough and smooth (RER, SER), mitochondria, Golgi complex, lysosomes and microbodies. These will be described in the following text.

Endoplasmic reticulum (ER)

The ER of the hepatocyte represents a highly specialised system. It occurs in practically all regions of the cytoplasm and exhibits rich connections with other membranous structures and organelles. The ultrastructural patterns are of basic importance in relation to the functional diversity attributed to this system (Dallner and Ericsson 1976). Earlier EM studies (Dalton et al 1950) described this basophilic structure as lamellar. Bernhard et al (1951 and 1952) described it as filamentous. Porter et al in 1953 and 1954 using improved methods of specimen preparation, found it to consist of intercommunicating membrane-bounded tubules and vesicles which appear as pairs of parallel membranes. The outer surfaces of the membranes are dotted with large numbers of small dense particles. These serve to distinguish the tubular and the vesicular elements of the ER from other membrane-bounded structures in the cytoplasm (Fawcett 1955). Matter et al (1971) used freeze-etched replicas technique to demonstrate the rough ER. He found that the ribosomal particles were difficult to define in the freeze-etched liver. The 8-10 nm particles seen at the outer surface of the double lamellae are only half the diameter of the conventionally treated ribosomes attached to membranes of the RER.

Structural alterations during tissue preparation, including fractures or plastic deformations of the particles, might explain the apparent differences in size observed with the two techniques (conventional and freeze-etched replica). The RER appears as branching tubules, sometimes dilated to form cisternae and sometimes shrunk to form narrow channels (Goldfischer et al 1972).

Jones et al (1977) have produced electron micrographs showing the RER cisternae communicating with the nuclear envelope and the tubules of the SER. The latter communicates with the Golgi complex but not with nuclear envelope. Neither RER nor SER has been found to have any direct connection with the plasma membrane. Morphometric studies have demonstrated that the surface of the ER membranes in one millilitre of liver tissue is of the order of 8-13 square meters. Two thirds of which are made up by the ribosome-carrying RER with an average number of 240-340 ribosomes per squire micron. This means that the hepatocyte contains roughly 9-10 million ribosomes (Dallner and Ericsson 1976). Jones et al (1977) have shown that the periportal hepatocyte contains more RER than the centrilobular cells.

Mitochondria

These granular thread-like organelles were observed by different cytologists over a century ago. They were first stained with fuchsin and named bioblast. Later the term mitochondria was introduced after staining them with alizarin and crystal violet. They were noted to execute continuous slow sinuous movements and to undergo changes in shape. Bensley and Hoerr (1934) and Claude (1945 and 1946) achieved separation of the mitochondria by differential centrifugation of cell homogenates. Later their chemical composition was established and they were found to be the principal site of oxidation reactions.

Golgi complex

The mere fact of the actual existence of this complex remained in doubt for over fifty years. This complex was first discovered by using osmium tetroxide and rubidium bichromate and named "internal reticular apparatus". Dalton et al (1950) observed, in electron micrographs, parallel arrays of membranes and associated vacuoles. Fawcett (1966) described it as aggregations of membrane-bound elements of at least three kinds. The most conspicuous and characteristic of these are clumps of flat cisternae piled one upon the other in close parallel array. Each cisternal unit appears in section as a pair of parallel membranes of considerable length that are continuous with one another at the ends, thus bounding a thin closed cavity of variable length. Four to eight such profiles are commonly spaced to form multilayered arrays of cisternae. Clustered around their ends and along their convex outer surface are small vesicles.

Because of the morphological heterogenecity of this organelle and the persisting uncertainty as to the functional inter-relations of its vesicular, vacuolar and cisternal components, some prefer the term Golgi complex to the older term Golgi apparatus.

While the functions of this organelle have not yet been completely defined, it is clear that the complex plays an important part in the secretory process, the process of segregation and concentration of the product transported to its region through the lumen of a continuous endoplasmic reticulum (Fawcett 1966). The location of this complex near the bile canaliculi confirms its basic secretory function

Lysosomes

This is a membrane-bound particle containing a number of hydrolytic enzymes. These were originally obtained by subfractionation of the classical mitochondrial fraction into heavier and lighter components (Essner et al 1960). It has been shown that the lighter fraction lacked

cytochrome oxidase but had a high concentration of acid phosphatase. This fraction was assumed to consist of cell particles distinct from mitochondria and the name lysosome was given to them to emphasise that they are rich in lytic enzyme. More than ten acid hydrolases have been isolated. Cytochemical staining reactions for localisation of acid phosphatase have led to the identification as lysosomes of a number of cytoplasmic bodies having different appearances (Ashford et al 1962).

The haemosiderin-containing deposits of macrophages have been reported to contain acid phosphatase; this clouded the distinction between these and the lysosomes. Although most of the structures recognised as lysosomes are dense and have a single limiting membrane, it is clear that the various types of particles that have been shown to have hydrolytic activity are so heterogeneous in their fine structure that no particle seen in an electron micrograph can be identified with certainty as a lysosome on the basis of morphological criteria alone (Fawcett 1966).

Microbodies

These are spherical or ovoid organelles that are generally smaller than mitochondria and surrounded by a single membrane. Their matrix is finely granular and often contains a denser body, which at high magnification is found to have a crystalline substructure. These are abundant in hepatocytes. Present indications are that they are independent organelles with a specific function but the exact nature of this function remains obscure (Rouiller et al 1956). Recently they and their enclosed crystals have been isolated and found to be rich in the enzyme uricase (Hruban et al 1964).

They may also contain catalase and D-amino acid oxidase. In the absence of evidence for their release into the blood or the bile it is assumed that their enzymes may exercise their specific function within the liver cell itself.

As the main pathological research materials of this study were from patients with alcoholic liver disease and primary biliary cirrhosis, it is important to give an account of both conditions in general and their ultrastructural changes in particular.

ALCOHOLIC LIVER DISEASE (ALD)

Histological abnormalities are likely to be present in the liver of nearly all alcoholics. Alcoholic liver disease, however, has been divided into three types on the basis of light microscopy: alcoholic fatty liver, alcoholic hepatitis and alcoholic cirrhosis.

In recent decades electron microscopy and new cytochemical procedures have allowed examination of biochemical processes at a subcellular level (MacSween 1979). Bhathal et al (1972) found only eight normal liver biopsies in a group of 98 alcoholics. Fatty liver is almost invariable, develops quickly and is reversible. Hepatitis is less common and can subside but if prolonged causes liver injury progressing to cirrhosis. Cirrhosis, however, occurs in 49% of chronic alcoholics and once established tends to progress.

Alcoholic fatty liver

In biopsies the fat distribution is mainly centrilobular and midzonal and in severe cases involves almost all hepatocytes. Kupffer cells do not contain fat. The overall architecture is not disturbed but focal breakdown of cell membranes may produce fat cysts which if they rupture may form lipogranulomata (Christoffersen et al 1971). Within the hepatocyte the fat makes a single large globule which displaces the nucleus to the periphery. These changes are pronounced if the diet has been poor and are completely reversible in 4-6 weeks. Mild grades of chronic inflammation may be shown in the portal tracts and in severe cases the latter may widen with stellate fibrosis extending into the parenchyma. Massive changes may predispose to cholestasis

and hepatic failure (Popper et al 1957, Ballard et al 1961).

Alcoholic hepatitis

This term was first applied by Beckett, Livingstone and Hill (1961) to describe acute or chronic inflammation of the liver following alcohol-induced parenchymal damage. The essential feature is liver cell necrosis associated with neutrophil polymorph accumulation. The hepatocyte is swollen, its cytoplasm shows an irregular vesicular appearance and Mallory bodies are conspicuous. Fat infiltration is common and lipo-granulomata are of variable features. Lipofuscin pigment is increased in amount. The neutrophils may form extensive microaggregates and there is accompanying Kupffer cell hyperplasia. Occasional giant mitochondria are seen and appear on light microscopy as intensely eosinophilic bodies. The hepatitis characteristically is most marked around the central veins. Variable amounts of fibrosis are most marked also around the central veins.

Pericellular fibrosis extends from the centre into the lobule, within which ductular proliferation develops (Edmonson et al 1963) and may produce portal hypertension (Reynolds 1969). Mallory bodies are a feature of ALD. They stain a homogeneous purplish red with haema-toxylin and eosin, and are PAS-negative. They can be found in other pathological conditions but in ALD they are commonly found in centri-lobular hepatocytes. Birschbach et al (1974) found them in only 32 of a consecutive series of 100 biopsies. They correlate with a more severe hepatitis (Christoffersen 1970 and 1972, Galambos 1972). On alcohol withdrawal they may persist for as long as six months.

Galambos (1975) found 38% of patients with alcoholic hepatitis developed cirrhosis in a mean period of 2.8 years, 52% continued as hepatitis without cirrhosis for a mean of 3.6 years and 10% who abstained recovered a normal liver histology.

Alcoholic cirrhosis

The term cirrhosis first introduced byLaennec (1826), derived from a Greek word meaning brownish-yellow. The liver is micronodular and each nodule is of normal lobule size. The architecture is abnormal and the central veins are indefinable. Gerber and Popper(1972) described the stages in the development of cirrhosis, noting the continued centrilobular damage with central-portal bridging-septa formation. The subsequent collapse of these septa caused cirrhosis with true nodule formation and a variable amount of fat infiltration. This may progress to a macronodular cirrhosis (Popper et al 1972) which is accompanied by a reduction of fat deposit resulting in an end-stage cirrhosis in which the alcoholic aetiology cannot be discerned (MacSween 1978).

Several studies have shown that only about 20% of chronic alcoholics will develop cirrhosis (Viel et al 1966, Christoffersen 1972). The real significance of undernutrition in the development of cirrhosis is unknown. Klatskin (1953) did not find significant differences between the undernourished and the well-nourished cirrhotic alcoholics.Pequignot (1962) and Lelbach (1967b) found a closer relationship between the level and the duration of alcohol consumption and cirrhosis.

The main cell responsible for fibre formation in portal tracts is the fibroblast, and in the lobules it is the lipocyte (Ito cells). The stimulus for their activation is probably hepatocytic degeneration with or without necrosis (Schaffner and Popper 1970). The fibres formed initially have the characteristic of reticulin or type III collagen, as demonstrated by immuno-fluorescence and supported by chemical analysis (Rojkind and Paloma 1976). There are sites of connective tissue formation in ALD. The first is seen in alcoholic hepatitis as pericellular fibrosis in the region of centrilobular veins. The second is parenchymal fibrosis seen around lipogranulomata. The third location

is portal, around the bile ductules.

Ultrastructural changes

Alcohol does not produce specific ultrastructural abnormalities, similar changes being found in a variety of other hepatic conditions. The hallmarks of alcoholic hepatitis, such as Mallory bodies and central hyaline sclerosis, are only seen in a small proportion of cases. Since this study concerned this aspect of liver disease, a detailed account on the ultrastructural changes will be given below.

Smooth endoplasmic reticulum (SER)

Alcohol induces proliferation of SER both in man (Rubin and Lieber 1971) and in the rat (Iseri et al 1966). It becomes vesicular and forms labyrinthine tubular aggregates (Lane and Lieber 1967) with cytoplasmic granulation. These are associated with increased activity of microsomal enzymes. These morphological and functional changes are similar to those produced by many drugs. The difference is that most drugs are metabolised in the microsomes while alcohol is metabolised in the cytosol. However, Lieber and De Carli (1970a,b and c) have described a microsomal ethanol oxidising system (MEOS) which oxidises ethanol to acetaldehyde in the liver. This implies that ethanol is not metabolised in the cytosol.

Rough endoplasmic reticulum (RER)

Alcohol disturbs the parallel arrangement of RER which becomes dilated into vesicles with concomitant detachment of ribosomes(Schaffner and Popper). This results in a reduced synthesis of protein including albumin and prothrombin (Schaffner and Popper 1970).

Golgi complex

Alcohol makes this complex prominent. There is evidence of increased activity of glycosyl transferase, catalase and D-amino acid oxidase (Gang, Lieber and Rubin 1972).

Mitochondria

Alcohol causes alteration and enlargement of the mitochondria (Schaffner et al 1963). The cristae are decreased in number and frequently lie free in the matrix. Giant mitochondria may be found in a minority of the hepatocytes. They often contain enlarged granules.The crucial functional disturbance appears to be reduced activity of the citric-acid cycle (Rubin and Lieber 1967).

Cytoplasmic changes

Focal degenerative changes are evident in the form of clumps of osmiophilic material together with degenerate organelles which may occur within the cytoplasm or be present in autophagocytic membrane-bound vacuoles. The space between the cell membrane and the nucleus contains amorphous material or lipid droplets (Edmondson et al 1967).

Disturbance of microtubules and microfilament systems

Recent evidence has accumulated showing that the cytoplasmic matrix displays a specific pattern of organisation depending on the particular activities of the cell (e.g. changes in shape, cytokinesis,intercellular streaming, endo- and exocytosis processes). This pattern is represented by three major systems (microfilament, microtubules and intermediate filaments) which determine the shape and movement of a cell (Brandle and Gabbiani 1983).

Considerable morphologic, immunologic and biochemical studies have revealed the relationship of Mallory body constituents to proteins in intermediate filaments of cytokeratinous components. Progressive derangement of the hepatocyte cytokeratin meshwork and its incorporation into Mallory bodies suggests that alcoholic hyaline may be regarded as the results of specific alteration of hepatocyte cytoskeleton.

Yokoo et al (1972) subclassified Mallory bodies into three types on electron microscopic appearances:

Type I : is characterised by filaments which run parallel to each other and have a zig-zag appearance. Their thickness averaged 14.1nm in diameter.

Type II : is the most common and consists of randomly orientated fibrils averaging 15.2nm thick.

Type III : is the least common and consists of branches which have a tubular appearance (French et al 1974).

Sinusoidal changes

The collagenisation of the perisinusoidal space of Disse is well recognised in ALD. The lipocytes (Ito cells) form 96% of the cells in the mentioned space. The lipid droplets occupy more than 20% of the Ito cell volume. These cells also contain microfilament bundles with dense bodies and pinocytotic vesicles.In alcohol-fed baboons, only 48% of cells were Ito cells, whereas 52% were transitional cells. These latter cells were surrounded by abundant collagen fibres. These cells appeared to promote the development of fibrosis which in turn may interfere with the nutrient exchange between sinusoids and hepatocytes (Mak and Lieber 1983). Another recognised change is the decrease in the number of fenestrations of the endothelial surface between the space of Disse and the sinusoids. After 5-10 years alcohol-fed baboons showed a decrease in the number of fenestrations by 59%. The diameter of endothelial fenestrations was increased by 19% (Mak and Lieber 1983).
Basement membrane formation and sinusoidal capillarisation play an important role in the formation of fibrous tissue inside the space of Disse (Johannessen 1979). The Ito cells were not observed around capillarised sinusoidal walls (Minato et al 1983).

Ito cell changes

Normally fat-storing cells occupy 1.4% of total liver volume and are distributed diffusely in the hepatic lobule. Matsuda and Lieber

(1979) have observed an increase in the number of Ito cells in the livers of alcoholic patients and baboons.

Minato et al (1983) have shown a close association between the development of RER in the Ito cells and the amount of collagen deposited in the space of Disse and concluded that they play an important role in collagen fibre formation in alcoholic livers. Kent et al (1976) and McGee and Patrick (1972) suggested that the Ito cells are transformed into fibroblasts. Transitional forms between the two have been observed in alcoholic baboon liver (Matsuda and Lieber 1979).

Bile ductular proliferation

The proliferating ductules are often characterised by an elongated or anastomosing configuration with a poorly defined lumen.The ductules are distributed irregularly in the fibrous tissue extending into the parenchyma and are often associated with a neutrophilic reaction (Uchida et al 1982). Schaffner et al (1961 and 1967) concluded that the ductules might be derived from the proliferation of pre-existing ducts. Histochemical, light and electron microscopic studies have shown that the majority of the proliferating ductules appear to have derived from transformation of the hepatocellular cords. The stimulus for this transformation appears to be related to the necrotizing and fibrotic changes involving the dropout of hepatocyte, accumulation of clusters of macrophages, fresh collagen deposition and some inflammatory reaction (Uchida et al 1982).

PRIMARY BILIARY CIRRHOSIS (PBC)

PBC is a fairly uncommon disease which affects middle-aged woman mainly. It was first described by Addison and Gull in 1851 but the term was first used by Dauphinee and Sinclair in 1949. Rubin, Schaffner and Popper (1965) used the term 'Chronic non-suppurative destructive cholangitis' as they indicated that the true cirrhosis was only established in the later stages.

Female to male ratio is 10-15 to 1 with an age range of 30-70 years. Intense itching is the common presenting feature and usually precedes jaundice. Many cases are discovered with incidental hepatomegaly and confirmed by the laboratory findings. Skin pigmentation is common and xanthoma occur in 30% of patients. Over 50% develop portal hypertension (Zeegen et al 1969; Kew et al 1971). 'Sicca syndrome' of dry eyes and mouth may be found also in over 50% of patients (Golding et al 1970). The course and the prognosis of the disease is very variable and unpredictable. The majority survive over ten years. Deep jaundice, though rare, is a bad sign. Disappearance of xanthomata and of itching implies the development of hepatocellular failure which is the most common cause of death. The disease has been reported from all parts of the world. Chinese, Europeans, Japanese, Indians, Jews and Negroes are among those affected. In England it was found that PBC predominantly affects middle-aged women of social grades 1 and 2 living in an urban situation (Sherlock 1976).

Serum alkaline phosphatase activity is very high in the early anicteric stage. Serum IgM levels are increased and is an important aspect of this disease. Serum cholesterol is often increased. There is moderate elevation of serum aminotransferase levels. The most helpful diagnostic test is the demonstration of serum-M-antibody by an immunofluorescent technique. This antibody is found in more than 90% of patients, usually in titres of over 1/128 (Walker et al 1965; Goudie, MacSween and Goldberg 1966).

Pathology

The liver is large, green and smooth in the early stages but as time passes it becomes nodular. The gall bladder and bile ducts are normal. The lymph nodes in the porta hepatis are enlarged and soft and show phagocytes loaded with bile pigment. The spleen shows pulp

hyperplasia and the changes associated with portal hypertension. The disease is essentially one of progressive granulomatous cholangitis with eventual disappearance of septal and interlobular bile ducts within the liver.

In general four stages can be recognized:

Stage I: Florid duct lesion

Septal and large interlobular bile ducts are damaged and surrounded by a dense infiltrate of lymphocytes, large histiocytes, plasma cells and a few eosinophils. Lymphoid aggregates, with or without germinal centres, may be found. There are usually granulomas near damaged ducts in the portal tracts. The ductal damage is seen as swelling, proliferation and crowding of epithelial cells and as rupture. The epithelial cells of the bile ducts are swollen and have finely granular eosinophilic cytoplasm with little or no vacuolisation. The cells are in a single layer. This must be distinguished from those found in chronic active hepatitis, in which the medium-sized ducts are involved and show ballooning, vacuolisation and stratification of the epithelial cells. Granulomas are never seen and duct rupture is absent in the latter condition. Nuclear pleomorphism is more common and periductal fibrosis is unusual.

Stage II: Ductular proliferation

The lesions are more widespread throughout the expanded portal tracts. There is fibrosis, acute and chronic inflammatory cell infiltration and ductular proliferation. The number of ducts are reduced and their place is taken by ill-defined lymphoid aggregates which give a characteristic appearance. Granulomas are less common. There is a slight to moderate degree of hepatocellular necrosis, swelling and cholestasis.

Stage III: Scarring

There is subsidence of inflammation with extension of fibrous septa from the portal tracts into and around the lobules. There are some lymphoid aggregates. Cholestasis may become severe.

Stage IV: Cirrhosis

Regenerative nodules can be seen. The bile ducts are scanty and lymphocyte accumulations can be seen.

There is considerable overlap between these stages and duct lesions (Hadziyannis et al 1970). The initial duct lesion affects medium-sized bile ducts, but in these the lesions are focal. Parenchymal changes are mild initially but with progression become more marked and comprise scattered small foci of liver cell necrosis with a related chronic inflammatory cell infiltrate and some increased sinusoidal cellularity due to accumulation of mononuclear cells with some reactive Kupffer cell hyperplasia.

The destruction of the medium-sized bile ducts progresses and the portal areas further expand and become distorted. The inflammatory and fibrotic reaction spreads into the parenchyma. This spread is characterised by ductular proliferation. The ductules are lined mostly by a flattened elongated structure, separated by loose fibrous tissue and infiltrated by inflammatory cells. Focal lymphocytic aggregates are present, macrophages are often prominent and foamy fatty cells may be present too.

Cholestasis is most marked in the periphery of the lobules in which swelling and vacuolisation of the affected hepatocytes may be noticed. Virtually all portal tracts are affected at this stage.

Transition into the scarring stage is difficult to delineate. In general, ductular proliferation becomes less evident and the inflammatory infiltration also becomes less. The fibrous septa extend out

from portal areas into the parenchyma and trapping single or aggregates of hepatocytes. Peripheral cholestasis is well marked and typical Mallory bodies may be found in over 25% of cases. Regenerative activity by development of twin-cell plates may be found, but without regenerative nodular formation.

The transition into cirrhotic stage is often slow. Continued fibrous linking results in more severe lobular disturbance and nodular regeneration. In general the liver is bile stained, firm and micronodular. Microscopically, PBC may be suspected on the following features:

1) Presence of focal lymphocytic aggregates within the fibrous septa and an irregular margin between the septa and the nodules.
2) Virtual absence of medium and small bile duct radicles.
3) Peripheral cholestasis within some nodules.
4) Mallory bodies.
5) The bile duct lesion and granulomas of the early stage of the disease may be evident (MacSween 1973 and 1979).

Ultrastructural changes

Cholestatic liver disease has been investigated by electron microscopy and although the bile duct epithelium has been established as the basic site of injury in PBC considerable attention has been devoted to changes in hepatocytes and bile canaliculi too.

1) Changes in the bile duct epithelium

The changes observed in the small and medium-sized bile ducts appear to be more characteristic.

At the early stages of PBC, the bile ducts show normal basement membrane. The plasma membranes are normal but their cell cytoplasm is occupied by numerous cytophagosomes indicating the phagocytosed bile components, lysosomes containing myelin-like figures and a few filamentous structures. The mitochondria, rough endoplasmic reticulum

and ribosomes are of normal appearance.

At the intermediate stage, i.e. stage of ductular proliferation and destruction, the cytophagosomes and lysosomes are decreased within the bile duct epithelium. The filaments are more abundant, closely packed and disposed in short thick bundles, grouped around other organelles, mainly mitochondria which show fewer circular and curled cristae. The rough endoplasmic reticulum is vesicular and ribosomes are scanty.

At both of these stages the biliary cells exhibit various necrotic abnormalities. The shape of the nucleus was often irregular but fragmentation of the nuclear chromatin can be seen. There may be dilatation of the endoplasmic reticulum and swollen mitochondria. The most striking feature was the focal cytoplasmic necrosis with abundant cytophagosomes.

2) Changes in hepatocytes

The hepatocytes also contain numerous cytophagosomes, but the most prominent changes are observed in mitochondria when two types of changes are seen:

a) curling of cristae, and b) prominent intramatrical crystalline inclusions.

In addition occasional glycogen bodies composed of large concentrically laminated membranous whorls with intervening glycogen rosettes, are seen. They surround either mitochondria or lysosomes. Large microbodies with homogeneous matrices and single membranes are also present.

At the intermediate stage, the glycogen bodies and large microbodies are no longer observed but intramitochondrial crystals are still present. Cytophagosomes are less prominent.

At the end stage the hepatocytes very frequently contain giant mitochondria with large crystalline, extremely complicated structures in their matrices. The pericanalicular zones of hepatocytes are said to be dense and show numerous vacuoles containing different bile

components and increased numbers of lysosomes as well as hypertrophic Golgi complexes and smooth endoplasmic reticulum. These changes are inconstant, irregular and frequently absent in neighbouring hepatocytes.

3) Changes in bile canaliculi

In the pre-cholestatic stage the lumina of the bile canaliculi are widely patent with microvilli which are either absent or scanty, short and stunted. The basement membrane is normal. At the intermediate stage, the microvilli are entirely absent from the lumina of bile ducts but their basement membranes are still intact.

At the end stage, the basement membrane is split, disrupted and invaded by polymorphonuclear leukocytes but the intercellular membrane is intact; the lumina are narrow and devoid of microvilli.

Most observers have found the bile canaliculi dilated, containing dense non-homogeneous laminated whorls or fibrillar material. Their microvilli were absent, distorted or bleb-like.

The ultrastructural findings permit the suggestion that electron microscopy may be a useful tool to follow the progression of PBC or help in its diagnosis when clinical, biochemical or histological criteria are inconclusive or equivocal.

MATERIALS AND METHODS

For the assessment of the normal morphological features of the liver, different species of animals were used to obtain normal specimens, since normal human liver specimens were inaccessible. Slight species variations were noted, details of which are dealt with in the appropriate paragraphs and illustrations. Different techniques were employed which appeared to illustrate different aspects of hepatic morphology.

The TEM techniques allowed the ultrastructural studies of small areas of the hepatocytes. On the other hand the plasma-oxygen etching techniques offered a three dimensional ultrastructural study of larger areas. The whole section can be examined without the need for trimming the section as is the case in TEM. The SEM technique allowed a study of the hepatic surface structure of the whole specimen. Furthermore, different fracturing techniques appeared to disclose different aspects of hepatic morphology. In the frozen-resin cracking technique the fracture plane passes through the cells showing the outlines of intracellular organelles. In the dry-cracking technique the fracture plane passes between the cells and adequately discloses the external surfaces of hepatic parenchyma, the lining of the sinusoids and the sinusoidal cells. However, breaking the liver by these techniques destroys most of the connective tissue and occasionally strews connective tissue fibres over the broken parenchymal surface. The portal tracts and the hepatic veins are avulsed by the fracture process leaving empty portal and hepatic canals.

Details of the materials used and the methods applied in this study are explained in the following section.

MATERIALS

Animal specimens and human biopsies.

Reagents.

Fixative employed for electron microscopy.

Embedding media.

Tissue mounting and coating.

METHODS

1) Collection of liver tissue.

2) Light microscopy (LM).

3) Specimen preparation for transmission electron microscopy (TEM):

   a) Fixation

   b) Dehydration

   c) Sectioning

   d) Staining

   e) Electron microscopy

4) Specimen preparation for scanning electron microscopy (SEM):

   a) Fixation and dehydration

   b) Fracturing

   c) Drying

   d) Mounting

   e) Electron microscopy

   f) Post-scanning embedding for TEM and LM.

5) Specimen preparation for oxygen plasma etching:

   a) Sectioning and mounting

   b) Etching

   c) Shadowing

   d) Electron microscopy

6) Specimen preparation for scanning electron microscopy from wax blocks:

   a) Dewaxing

   b) Fracturing

   c) Drying

   d) Mounting and coating

   e) Electron microscopy

7) Electron microscopy:

   a) Conventional transmission electron microscopy (TEM)

   b) Scanning electron microscopy (SEM)

8) Photographic techniques:

   a) Micrographs

   b) Montage

   c) Stereopairs

   d) General photography.

1) MATERIALS

a) Animal:

The sources of the hepatic tissue were: 10 mice, type BALB/C, 4 rats type Albino White Rat and one baboon.

All these animals were healthy, of either sex and aged between 4 and 18 weeks.

b) Human:

The sources of the hepatic tissue were: 10 patients with alcoholic liver disease, 8 males and 2 females; age range 37-55 years. 10 patients with primary biliary cirrhosis, 2 males and 8 females; age range 43-71 years (Appendices 1 and 2).

Biopsies were obtained from patients with the abovementioned conditions in the medical wards of Gartnavel General Hospital, Glasgow.

2) REAGENTS

Unless otherwise stated 'ANALAR' Grade reagent supplied by British Drug and Chemicals Ltd., Hants, were used throughout. All aqueous reagents were made up using water produced in or from a 'Fi-stream bi-distillation Unit'. Liquid carbon dioxide research grade (99.95%) supplied by Distillers Company Ltd.

Liquid nitrogen and argon gas supplied by British Oxygen Company Ltd.

Glutaraldehyde fixative supplied by E.M. Chemical Ltd.

Osmium tetroxide supplied by Johnson, Matthey and Co. Ltd.

Araldite embedding medium supplied by E.M. Scope Laboratories Ltd.

a) Fixative employed for electron microscopy

Glutaraldehyde

The fixative was prepared by mixing a pure stock solution of 25% glutaraldehyde with Sorensen's phosphate buffer (SPB) (8mls glutaraldehyde plus 92 mls SPB) to give a final concentration of 2% at pH 7.4. This working solution was made up weekly and kept at 4 degrees Centigrade (Glauert 1974).

Osmium tetroxide

The working osmium fixative combined in a solution of equal parts of 2% osmium tetroxide and SPB. All osmium handling was carried out within a fume-cupboard (Glauert 1974).

Sorensen's Phosphate Buffer (SPB)

The buffer was prepared by mixing 3.786 gm of M/15 sodium phosphate (Di-basic) with 0.967 gm of M/15 potassium hydrogen phosphate with 500mls double distilled water to give a buffer of pH 7.4. This was stored at 4 degrees Centigrade (Glauert 1974).

b) Embedding media

Tissue was embedded in araldite using the following proportions in the final embedding mixture:

Araldite resin (CY 212)	10 mls
Dodecenyl succinic anhydride	10 mls
2,4,6-tri dimethyl amino-ethyl phenol	0.5 ml
Dibutyl phthalate	1 ml

(Glauert 1958 and 1974).

Extreme care (wearing protective clothing and gloves and using a fume cupboard) was exercised in the handling of these compounds which may cause dermatitis and some of which may be carcinogenic.

c) Tissue mounting and coating

Aluminium specimen mounts and quick dry colloidal silver paint were supplied by Polaron Ltd. Electron microscopic grids, apertures, etc. were supplied by Veco Ltd.

METHODS

Collection of liver tissue

Animal specimens

All the mentioned animals were sacrificed without anaethesia except for the baboon for which halothane gas was employed. The liver tissues were immediately excised, immersed in a petri dish full of 2% glutaraldehyde in phosphate buffer and puncture-perfused according to the methods of Itoshima (1978). A G23 needle was employed and the tissue gently perfused with a chilled isotonic solution of saline until it became pale in order to remove as much blood from the liver sinusoids as possible. Puncture perfusion was repeated every 2-3mm and the tissue then re-perfused with several mls of 2% glutaraldehyde in phosphate buffer, pH 7.4. Blocks 1-5mm thick were prepared with a sharp blade. These blocks were further fixed in glutaraldehyde solution overnight.

Human biopsies

The liver tissue was obtained by percutaneous needle using a trucut needle and was immediately cut under the surface of chilled isotonic saline solution. Two thirds of the tissue was fixed in formaldehyde solution for routine light microscopic examination. The remainder was cut into thin blocks (1-3mm) and fixed in a solution of 2% glutaraldehyde in phosphate buffer pH 7.4 overnight (Grisham 1976).

Specimen preparation for light microscopy

Tissue preparation, fixation, embedding, sectioning and staining were carried out by the routine surgical histology laboratory at the Pathology Department, Western Infirmary, Glasgow. A brief account of the procedure is given below.

The freshly obtained liver tissue was transferred to a 10% formal saline fixative and a suitable fixation was accomplished after 3-12 hours at room temperature. The tissue was loaded into the casette and washed in the histokine washer, then transferred into the automatic tissue processing machine (Histokine and Histokinette). In this machine the tissue underwent a 22 hour cycle:

1 hour in 50% spirit

1 hour in 80% spirit

2 hours in 8% phenol in methylated spirit

3 hours in 8% phenol in methylated spirit

3 hours in 8% phenol in methylated spirit

1½ hours in absolute alcohol I

1½ hours in absolute alcohol II

7 hours in absolute alcohol and chloroform

¾ hour in Xylol

¾ hr in Xylol.

The tissue was then blocked in fresh paraffin wax and left to cool on a coded plate. The 3 micromillimeter thick section was then cut from the block using a microtome and the section was then floated on a hot water bath of around 50 degrees centigrade. Twelve sections from each block were made. Each section was 3-5 micromillimeter thick. Alternate sections were used for the following staining procedures and the rest were stored (Drury and Wellington 1973; Scheuer, 1981).

1) Haematoxylin and eosin stain

2) Van Gieson's stain (1889)

3) Masson's trichrome stain (Modified from Masson, 1929)

4) Silver impregnation for reticulin fibres (Gordon and Sweets)

5) Modified Perls' Prussian blue stain for iron

6)Periodic Acid Schiff method

7) Periodic Acid Schiff after diastase

8) Orcein stain for hepatitis B surface antigens, copper associated protein and elastic fibres (Shikata et al 1974).

Specimen preparation for transmission electron microscopy (TEM)

1) Fixation

The freshly obtained liver tissue was fixed overnight in 2% glutaraldehyde in phosphate buffer. The tissue was washed for 1-2 hours in several changes of phosphate buffer and post-fixed in isotonic 1% osmium tetroxide pH 7.4 for 45-60 minutes. The tissue was then washed for 1-2 hours in several changes of Sorensen's phosphate buffer.

2) Dehydration and embedding

Dehydration was achieved by passing the tissue through the following graded series of ethanol and allowing them to remain 5-10 minutes in each of the following in turn: 25% ethanol in water, 50% ethanol in water and 75% ethanol in water. The tissue was infiltrated with propylene oxide by immersion for 5-10 minutes each in propylene oxide/ethanol (1/1, v/v) and propylene oxide (2 changes). This procedure aids in the subsequent penetration of the tissue by araldite, which was carried out as follows:

The tissue was immersed for 1-2 hours each at room temperature in araldite/propylene oxide (1/1, v/v) and araldite/propylene oxide (3/1, v/v) and finally placed in fresh araldite. Embedding was either in trays or capsules. The resin was cured in an oven at 60 degrees Centigrade for 16 hours.

3) Thin sectioning procedure

Thin sections from araldite blocks prepared as above were cut on an LKB-Ultratome, model III. The sections were cut using glass knives

prepared on an LKB knife maker and were floated on to the surface of distilled water contained in a trough attached to the glass knife. Compression within the sections was released by chloroform vapour treatment (a swab in chloroform was held close to the sections until they were seen to elongate). 1-2 micromillimeter thick sections were cut using a glass knife and stained with 1% toluidine blue in water (w/v) for 2-3 minutes (Lewis and Knight, 1974). Sections were examined under a Leitz-Wetzlar type microscope. This was used for area selection and orientation. The ultratome and the glass knife were then adjusted until gold to silver sections were being cut from the blocks. These sections were mounted on 3mm (200 mesh copper) grids (Reid 1975).

4) Staining of thin sections

A double staining procedure was used employing a saturated solution of uranyl acetate in 50% ethanol and Reynold's lead citrate solution (Reynolds 1963). Grids plus attached sections were immersed in uranyl acetate solution in a small bottle for 10 minutes in the dark. The grids were then rinsed in the water and immersed in a similar manner in lead citrate solution, 1-2 minutes being allowed for staining. The grids were finally washed and air-dried (Lewis and Knight 1977).

5) Electron microscopy

The transmission electron microscope employed was a Philips Model EM 301 G. The microscope was used routinely with double condenser illumination system and with a liquid nitrogen anti-contamination device in operation. A 300 micromillimeter aperture was employed in the first condenser lens and a 200 micromillimeter aperture in the second condenser lens. A 50 micromillimeter aperture was employed in the objective lens. Astigmatism was corrected routinely before high resolution microscopy. Microscope alignment was maintained on a weekly basis.Micrographs were taken using Kodak EM Film 4489.

Specimen preparation for scanning electron microscopy (SEM)

1) Fixation and dehydration

The tissue fixation and dehydration was carried out in the same way as for TEM. After the reagent grade ethanol stage the specimen was then passed in turn through the following graded series of ethanol and amyl-acetate, allowing it to remain 10-15 minutes in each:
75 ethanol/25 amyl acetate (v/v), 50 ethanol/50 amyl acetate (v/v),
25 ethanol/75 amyl acetate (v/v) and 100% amyl acetate.

2) Fracturing

The next step in preparing liver for SEM is to expose the undamaged surface of the cells or the tissue for examination. The outer portions of the blocks prepared as above will show various artefacts and should not be used for the ultrastructural examination. Once a surface is prepared as below it must be carefully protected from damage during all subsequent procedures. Internal surfaces of hepatic tissue can be exposed for SEM examination as follows:

a) Freeze-fracturing techniques

The tissue was dried from amyl-acetate on paper, then rapidly immersed in liquid nitrogen and held in a shallow container. After a few minutes the tissue became frozen and hard and could be cracked into two halves along its longitudinal axis using a thick blade and a hammer. The two halves were then immersed in amyl-acetate. In this method the fracture planes go both through and between cells (Brooks, 1973; Grisham, 1976).

b) Frozen-resin cracking

The tissue blocks were embedded in araldite resin without catalyst for 12 hours in gelatin capsules. Hardening was effected by plunging the capsule into liquid nitrogen. When "boiling of liquid nitrogen" ceased after 2-3 minutes the resin was hard. The capsule was placed on a teflon slab and cracked into two halves with a thick blade and a hammer. The

resin was removed at once from the cracked halves by several washes in propylene oxide for 2 hours, the two final washes being in amyl-acetate. In this method the fracture planes go through the intracellular structures (Jensen and Prause 1979).

c) Dry-cracking

This method was performed after the tissue was dried at critical point (see below). The dried tissue cracked along its longitudinal axis into two halves under a stereomicroscope with the aid of two needles (G25 size) bent at an angle of 45 degrees. This method produced a clean fracture plane which passes through the intercellular junctions (Jensen and Prause 1979).

3) Drying (critical point drying)

The tissue was dried in a Polaron Critical Point Dryer (Watford, Herts). The tissue was first placed in an open boat containing amyl-acetate (as intermediate fluid) within a pressure chamber. Research grade liquid carbon dioxide (as transition fluid) was then passed under pressure into the chamber where it displaced the amyl-acetate which was vented as a gas. The fluid exchange within the sealed chamber took an hour. The final drying process took between 15-20 minutes during which the sealed chamber was gradually warmed to the critical value (12,000 Psi). At this point the vapour phase and the liquid phase co-existed providing the condition of zero surface tension. The chamber was then slowly opened allowing the carbon dioxide to vent as a gas, the rate of release being monitored directly on the chamber pressure gauge (Lewis et al, 1973; Humphreys,1974; Boyde, 1978).

4) Mounting and Coating

The dried tissue was finally mounted (with its fractured surface facing upwards) on an aluminium stub. Electrically conducting colloidal

quick dry silver paint was employed to fasten the tissue on the stub. The tissue was then placed in the Polaron Low-Vacuum Sputter Coater E 5000 (Watford, Herts). Argon gas was allowed to pass for two minutes at 1.2 KV in order to give a thin, evenly distributed gold-palladium coat (Echlin, 1974).

5) Scanning electron microscopy

The electron microscope employed was a Jeol 200 T. Two objective lens apertures were employed (120 and 300 micromillimeter). Astigmatism was corrected routinely before high resolution microscopy. Microscope maintenance was carried out on a weekly basis. The microscope was used with a saturated filament at 10-25 KV and with a tilting angle of 0-60 degrees. Micrographs were taken using 120 Ilford FP4 film. The camera employed was Mamiya 67 using an aperture No. P11 (Joy, 1973), the spot size being employed for low resolution and a smaller one for high resolution.

6) Post-scanning embedding for TEM and LM

After examination in the scanning electron microscope, some of the specimens were re-processed for light microscopy, making possible detailed correlation of the different images. Orientation marks on the SEM stub were made with a fluorescent overhead projection pen and these were then used to align the tissue in a suitable orientation for embedding. The tissue was removed from the stub and washed with several changes of 100% amyl-acetate over a period of 2 hours and passed through 3-4 changes of reagent grade absolute ethanol. It was allowed to remain for 20-60 minutes in each. The tissue was infiltrated with propylene oxide by immersion for 5-10 minutes each in propylene oxide/ethanol (1/1, v/v) and propylene oxide (2 changes). Further embedding, cutting and staining of the tissue was carried out in the same way as for the transmission electron microscopy.

Specimen preparation for oxygen plasma etching

1) Sectioning and mounting

Sections 1 micromillimeter thick were floated on to the surface of distilled water contained in a trough attached to the glass knife. The sections were picked up from the surface of the water with a wire loop and placed on a fragment of cover slip 10X10 mm. The cover slip fragments bearing 1 micromillimeter sections were placed on a microscope slide and allowed to dry evenly with the application of gentle heat.

2) Oxygen plasma etching

The microscope slide, prepared as above, was then placed with 0.5 cm teflon tape (polytetra fluoro ethane) in the reaction chamber of a plasma Prep 100 generator. The chamber was evacuated using a mechanical pump and oxygen gas obtained from standard grade commercial oxygen bottles was admitted at a controlled flow rate (13.8 KPa and 2-5 pounds per square inch) to obtain an operating pressure in the range of 6-130 Pa. Radiofrequency power was applied around the chamber at 13-20 RF (Radio-Frequency). A Kv power setting of 60W was chosen and the sections were etched for a period of 1-2 minutes. The highly reactive gaseous plasma caused gentle, low temperature combustion of the organic materials in the sample. The combustion products were carried away in the gas stream leaving behind the thick sections with exposed surfaces etched (Humphreys, 1979).

3) Shadowing and Coating

The etched sections were coated by vacuum evaporation of platinum-palladium wire in an Edwards II 12E6/1447 High Vacuum Coating Unit. The specimens were then lightly sputter-coated with gold-palladium using the Polaron Low-Vacuum Sputter-Coater E 5000. The etched sections were examined in a Jeol 200 scanning microscope at an operating voltage of 15 Kv with the specimen tilted to an angle of about 20-25 degrees.

Specimen preparation for scanning EM from wax blocks (Dewaxing)

The excess wax surrounding the tissue blocks were trimmed off with a sharp knife. The tissue was then washed with several changes of xylene at room temperature for a period of 6-12 hours depending on the size and the thickness of the block. The tissue was then immersed in a mixture of xylene/reagent grade absolute ethanol (1/1, v/v) overnight and then passed through two changes of amyl-acetate for 15-30 minutes each. Further tissue fracturing, critical point drying, mounting and coating were carried out in the same way as for scanning electron microscopy.

Photographic techniques

1) Micrographs

Development of the exposed flat film in the TEM was accomplished by Kodak D19 developer at 20 degrees centigrade for 3.5 minutes. The film was then fixed for five minutes using Kodak rapid fix. The developer used for the film Ilford PF4, after exposure in the SEM, was Icthyol diluted in water (1/10, v/v) at 20 degrees centigrade for 7.5 minutes. The film was then fixed using Kodak rapid fix for five minutes. Prints were made using:

a) an Omega D2 point source enlarger with a 105mm Rodagon Lens, in the case of TEM micrographs.

b) a Leitz Wetzler Focomat 11C with two lenses (60mm and 100mm), in the case of SEM micrographs.

The micrographs were processed in an automatic printing machine (Rapidprint processor) using Agfa-Gevaert Rapitone printing paper. The prints were finally processed using:

Activator Agfa-Gevaert G 182 b

Stabilisator Agfa-Gevaert G 382 b

Rapid Fixer Agfa-Gevaert G 333 c diluted 2L/5L water.

2) Montage

Areas of interest were selected from both SEM and TEM micrographs. High resolution micrographs of these areas were then taken in strip fashion. The micrographs were developed and fixed in the same way mentioned in the previous paragraphs. Finally they were mounted together in strips matching the corresponding areas.

3) Stereopairs

Stereopairs were obtained using the scanning electron microscope in the following way: An area of interest was chosen. Focusing and astigmatism were adjusted. First photographs were taken at a tiling angle of 25 degrees and labelled RH (right hand). A mark was placed on the screen and the tiling angle then changed to 20 degrees. The field was brought back to the mark described above on the screen by rotating the stage. Minimal adjustment of the focusing was used and a second photograph was taken. The latter was labelled LH (left hand). The stereopairs produced were then examined in a viewer supplied by Polaron (Brighton).

4) General photography

Photographs were taken using a Nikomat FT2 Camera fitted with a micronikkor Auto 50mm lens. For copy work incident lighting was employed and Kodak fine grain release positive film used to give a contrasting negative. Development was carried out using Kodak D8 for 2.45 minutes at 20 degrees centigrade, acetic acid for one minute and Kodak rapid fix for five minutes.

RESULTS

I. Normal (Animal) materials

1) The surface liver capsule

2) Portal tract

- A. Portal vein
- B. Hepatic artery
- C. Bile ducts
- D. Canal of Hering

3) The hepatocellular plate

- A. Hepatocellular surfaces
- B. Junctional complexes
- C. Cytoplasmic organelles

4) The sinusoids

- A. Endothelial cell
- B. Kupffer cell
- C. Space of Disse and content

II. Human ALD materials

1) Alcoholic fatty liver

2) Alcoholic hepatitis

3) Alcoholic cirrhosis

III. Human PBC materials

1) Pre-cirrhotic stage

2) Cirrhotic stage

I. Normal (Animal) materials

1) The surface liver capsule

The surface capsule (Glisson's capsule) is composed of relatively thick twisted connective tissue fibres overlaid by continuous layer of mesothelial cells.

SEM examination revealed that the serosal surfaces of the mesothelial cells are studded with a large number of filamentous microvilli. The microvilli are club-ended. Some cells appear to possess only a few scattered stunted microvilli (bare area). (Figs. 1.1, 1.2 and 1.3).

2) The portal tract

The substructures of the portal tracts are readily identifiable on the sliced surface by SEM. The slicing procedure, however,will damage the hepatocytic surface rendering it unsuitable to study. On the other hand the fractured surface is unsuitable to study the substructure of the portal tract due to the shredding of the connective tissue over the broken surface.

A. Portal vein

The portal vein as revealed by SEM shows variation in calibre. The endothelial surfaces, however, are generally smoother than those of the hepatic artery and occasionally contain a few stubby microvilli between which scattered holes of various sizes can be seen. (Figs. 2.1 and 2.2). The TEM shows the thin wall of the vein which is lined by thin endothelial cells. The nuclei bulge into the venous lumen (Figs. 2.3 and 2.4).

B. Hepatic artery

The hepatic artery as revealed by SEM is identified by its relatively smaller size and comparatively thick walls. The endothelial nuclei are bulging sharply into the arterial lumen. (Fig. 2.5).

C. Bile duct

The perilobular bile ducts of various orders do not show notable differences in ultrastructure except in the number of cells of which they are comprised. The wall of the ductule and ducts is formed by tightly arranged cuboidal or columnar biliary epithelial cells lying on a basement membrane and bearing microvilli on the luminal surface. The cells have relatively large nuclei of low density, the small nucleolus is only infrequently seen. Cytoplasmic organelles are scanty; the mitochondria are arranged around the nucleus. There is a little irregularly arranged endoplasmic reticulum and the Golgi complex is usually localised between the nucleus and the apical pole. Differently orientated fasicles of delicate filaments are present in the cytoplasm.

The biliary epithelial cells are attached to one another partly by an intricate system of lateral glove-like interdigitations and partly by numerous desmosomes. The tight jucntion seals the apical zone. Various amounts of orientated collagen fibrils are seen around the basement membrane. (Figs. 3.1 and 3.2).

D. Canal of Hering

This comprises the transitional pathway between the bile canaliculi and the bile ductule. At one end it is lined by flattened or cuboidal cells and at the other by columnar type. (Fig. 3.3)

3) The hepatocellular plate

The hepatic parenchymal cells form distinct plates, as revealed by SEM and TEM. The plates appear to be continuous except when they are penetrated by sinusoids or large vessels. Neighbouring plates are seen to be separated by sinusoids. The plates are orientated in a generally straight direction between terminal portal and hepatic veins. (Figs. 4.1, 4.2 and 4.3).

A. Hepatocellular surfaces

The hepatocytes appear as rather irregular polyhedral cells of variable dimensions and geometrical shape. The numbers of these cells as well as the different cell size is likely to depend on their location in the liver walls of the hepatic labyrinth. However, most hepatocytes present at least three surfaces, each of which is structurally distinct. (Figs. 5.1, 5.2 and 5.3).

i) The canalicular surface

This surface forms the boundaries of the bile canaliculus which is formed by grooves in adjacent hepatocytes. The fractured surface disclosed unroofed canaliculi which appeared to run in the centre of the hepatocellular plates. Typically they run straight and unbranched but sometimes might bifurcate into two or more branches running over the surface of a single cell. (Fig. 6.1). Further, also in many situations, the bile canaliculi possess branches ending blindly very close to the sinusoidal surface, but direct connections between the spaces of Disse and the bile canaliculi were never found. In a number of cases the same facet of a single hepatocyte facing another adjacent hepatocyte could provide a border for more than one bile canaliculus. (Fig. 6.5)

SEM revealed the canalicular lumen densely covered with microvilli projecting perpendicularly or obliquely and occasionally they appear to have an overlapping arrangement. The microvilli seem to concentrate mainly around the margins of the canaliculi. There is a relatively smooth band running along the sides of the bile canaliculi which probably coincides with the limits of intimate contact between adjacent hepatocytes, although the specialisation of adjacent plasma membrane which is evident in TEM cannot be clearly identified by SEM (due to its lower resolving power). It is reasonable to suggest that the smoothest band running along the bile canaliculi corresponds to the junctional complexes. (Fig. 6.3).

On the other hand the TEM examination revealed the microvilli have a well developed fuzzy coat. The canaliculi were sealed at both ends by the tight junctions. The cytoplasm adjacent to the canaliculi appeared to be more dense than the rest of the cytoplasm. Different sizes of membrane-bound vesicles appeared near the canaliculi. A well developed stack of Golgi apparatus is a constant finding (Fig. 6.5 and 6.6).

ii)The intercellular surface

This surface laterally borders bile canaliculi and forms the smoothest surface of the hepatocyte. The flat intercellular surface is not completely structureless but contains a variety of holes and protrusions. These processes and holes are analogous to the studs or collar-button processes and they are presumed to be involved in cellular attachement (Fig. 6.4).

iii) The sinusoidal surface

This surface forms the border of the space of Disse. As revealed by SEM, this surface is densely covered with microvilli (Fig. 7.1). Microvillous surface continuous with sinusoidal surface extends around corners of adjacent hepatocytes towards the centre of hepatic plate forming the peri-sinusoidal recess which approaches bile canaliculi. No apparent connection between the two could be detected (Figs. 5.2 and 5.3). The SEM images show that this recess and the sinusoidal surface appear more complex than is generally evident from TEM observation (Fig. 7.2).

B. Junctional complexes

The intermediate junctions were less conspicuous. They were usually located between tight junctions and desmosomes and consisted of relatively straight parallel segments of lateral cell membranes separated by a gap of uniform width (Fig. 8.1).

The desmosomes consist of parallel segments of triple-layered membranes and separated by a gap of uniform width. Occasionally more than one desmosome could be seen on one side of the hepatocyte (Figs. 8.2 and 8.3).

On the other hand, with the SEM technique, this complex is not very well demonstrated. Sometimes SEM revealed thick ridges between the bile canaliculi and the rest of the smooth intercellular surface which probably correspond to the junctional complexes (Fig. 6.3). The stud projections and the holes which were recognised frequently on the smooth surfaces of the hepatocytes might also correspond to the intermediate junctions (Fig. 6.4).

C. Cytoplasmic organelles

The hepatocytes often have one oval or roundish centrally placed nucleus. Binucleated cells are often also found. The nuclear chromatin is evenly distributed and sometimes slightly condensed along the nuclear membrane. The granular and fibrillar components of the nucleolus are in the form of a loose network making up the nucleolemma. Mitochondria are the most conspicuous cytoplasmic organelles of the hepatocyte. They are roundish and rod-like in shape having a medium electron dense homogeneous matrix and a lamellar cristae. Mitochondria share a close relationship with rough endoplasmic reticulum (RER) and are more concentrated near the nucleus and along the sinusoidal surface (Fig. 5.1).

Abundant amounts of RER are present forming a branching network. The greater part of these form parallel organised cisternae which are usually in the vicinity of the mitochondria. RER is found most commonly near the nucleus, adjacent to the Golgi complex in the pericanalicular zone and under the sinusoidal surface. On the other hand, the smooth endoplasmic reticulum forms small vesicles or branching tubules and

is found in the glycogen-rich areas mostly distant from the nucleus (figs. 9.1 and 9.2).

The Golgi complex itself is well developed and usually multiple in number (up to three complexes being found per cell section) and is located in the pericanalicular position (Fig. 6.5).

Lysosomes are easily found. They are pleomorphic in character and range from primary lysosomes bounded by a single unit membrane to secondary lysosomes bounded by a double or more unit membrane. Lipofuscin granules which are lysosomal in origin, are localised mainly in the pericanalicular region too. (Fig. 9.3).

The microbodies are also found in the neighbourhood of bile canaliculi and are limited by a single membrane. They have a finely granular matrix of varied electron density.

Variable numbers of lipid droplets are found in the cytoplasm usually not membrane-bound and often in close relation with a mitochondrion.

Variable numbers of vesicles, some of them coated and some smooth surfaced, are present in the cytoplasm in the region of the sinusoid. They represent micropinocytic vesicles (Fig. 7.2). On the other hand the cytoplasm adjacent to the bile canaliculi is slightly thickened with variable numbers of microfilaments often penetrating into the microvilli (Fig. 6.6).

4) The sinusoids

The sinusoids appeared as a complex network of channels as revealed by SEM. In cross section the sinusoids appeared as oval to round in shape and lined by two morphologically distinct cell types, the endothelial and Kuppfer cells (Fig. 7.1).

A. Endothelial cells

Endothelial cells appeared as a single layer of elongated narrow cells containing a few cytoplasmic organelles and extending processes to form loose junctions with one another. Bristle-coated micropinocytic vesicles are numerous within the cytoplasm. The luminal surface is smooth, bulging into the lumen only in the perinuclear region. A basement membrane is absent on the deep surface of the sinusoidal endothelium (Fig. 10.3).

The SEM revealed that the greater part of the cell has a net-like appearance and that the fenestrated sinusoidal endothelium extends outward from a plump central body which probably contains the nucleus. The fenestrations differ greatly in size. The smaller ones are arranged in clusters of 10-50 or more forming sieve plates (Figs. 10.1 and 10.2)

B. Kupffer cells

Kupffer cells are extremely variable in form and position. They usually occur at intervals in the sinusoid.

With the SEM techniques they often appear bulging in the sinusoidal lumen and anchored to the adjacent endothelial cell margins by thin cytoplasmic processes corresponding to microplicae which appeared to be interconnected with each other forming a labyrinthine system of surface membranes. Some irregular particles are also evident in some areas which might be related to the phagocytic process (Figs. 11.1 and 11.2). Thick processes of a Kupffer cell appear to

traverse the sinusoidal lumen (Figs. 11.3 and 11.4). On the other hand TEM shows that the Kupffer cell has a long irregular nucleus with chromatin aggregations forming a dense area at the periphery of the nucleus. The most distinctive cytoplasmic organelles are the lysosomes in both primary and secondary forms. A well-developed endoplasmic reticulum and prominent Golgi complex are also present (Figs. 11.5 and 11.6). There are numerous vacuoles in the cell ranging from large vacuoles resembling pinocytic vacuoles to small micropinocytic vacuoles. Some of these are coated vesicles (Fig. 11.7).

C. The space of Disse and its contents

Space of Disee is observed in SEM through fenestrations or when the sinusoidal endothelial lining is ripped away. It appeared as a tissue space between the sinusoidal lining cells and the underlying sinusoidal surface of the hepatocyte (Fig. 10.1). It is also noted that the spaces extend among adjacent hepatocytes in numerous recesses limited by hepatocytic surfaces. It is largely filled with hepatocytic surface microvilli but also occasionally contains a slender bundle of collagen which is, in fractured specimens, occasionally dislodged from the space of Disse and thrown over the parenchyma (Figs. 10.3 and 11.6).

With the SEM technique the spaces with their sacculation and recesses appeared larger and more numerous than were generally evident from TEM observations (Figs. 5.2 and 5.3).

Also found in the space of Disse is the Ito cell or the fat-storing cell. The SEM revealed that these cells appear to have a fixed localisation underneath the endothelial lining within the space of Disse and in the recesses between the parenchymal cells. They have a spindle shape and their surfaces are covered with few slender cytoplasmic processes (Figs. 12.1 and 12.2).

A slender collagen fibre is often found in close relation to these cells. The cytoplasm of these cells contains a large undulating nucleus and very few cytoplasmic organelles. There were small mitochondria, rough endoplasmic reticulum and a well-developed Golgi complex.

The most conspicuous cytoplasmic organelle is the non-membrane bound lipid globule. The number and the size of these vary tremendously (Figs. 12.3 and 12.4).

II. Results of biopsies obtained from patients with ALD

Ten human liver needle biopsies were used, one with alcoholic fatty liver, one fatty liver and alcoholic hepatitis,two with alcoholic hepatitis, two with alcoholic hepatitis and cirrhosis, and four with cirrhosis. Diagnosis of ALD was made on the basis of light microscopic examination, clinical and biochemical findings, the details of which are listed in Appendix (1).

Each core received measured between 10-14 mm long, 8mm of which was used for the routine light microscopic examination and the rest was used for the ultrastructural study divided equally between TEM and SEM techniques.

For the TEM studies, three resin blocks were used from each case, 1-2 micromillimeter thick section stained with toludine blue for area selection.

The results obtained will be discussed according to the pathological stages of ALD (i.e. alcoholic fatty liver, alcoholic hepatitis and alcoholic cirrhosis). However many biopsies showed mixed findings and reference to the general findings for each stage will be made.

1) Alcoholic fatty liver (steatosis)

a) Light microscopic findings

The normal architecture of the liver was preserved. The fat accumulated in the hepatocyte in two morphological forms:

i) Macrovesicular steatosis in which a large single intracellular lipid globule is present occupying most of the cytoplasm and displaces the nucleus to the periphery of the cell and on many occasions greatly distends the hepatocyte (Fig. 13.1).

ii) Microvesicular steatosis in which the fat forms multiple droplets mostly around the nucleus or disposed at one cell pole pushing the nucleus aside (Fig. 13.2).

The fat storing cells (ITO) appeared clearly on one micron thick plastic sections. These cells have a dark irregular nucleus centrally placed or pushed to one side of the cell. The cytoplasm filled with fat droplets give the cell a foamy appearance (Fig.15.1).

b) Transmission electron microscopic findings

While TEM revealed the appearance of macro- and microvesicular steatosis which were consistent with the light microscopic findings. A remnant membrane can be seen between two fat droplets illustrating the process of fat cyst formation (Figs. 14.1 and 14.2).

Among the cytoplasmic organelles, the mitochondria and the endoplasmic reticulum are most affected at the fatty liver stage. The mitochondria showed diversity in the shape, size, matriceal density and most of them contained homogeneous dense inclusion bodies and some occasionally contained paracrystalline inclusions as well. The SER showed mild dilatation with hypertrophy (Figs. 14.3 and 14.4). The Ito cells were more easily found in the section. This might suggest a slight increase in their number. Most of them were in the resting form (Fig. 14.6). Kupffer cells showed a slight increase in the number of cytoplasmic lysosomes (Fig. 14.5).

c) Scanning electron microscopic findings

The most striking changes revealed by SEM are that the surfaces of some hepatocytes became very rough, wrinkled and covered by numerous

short flat microvilli, some look like blebs, giving the smooth surface of the liver a microvillous appearance (Fig. 15.2). Occasionally some swollen hepatocytes demonstrate pouch-like structures on their surfaces (Figs. 15.3 and 15.4).

Some of the fracture surfaces are covered with tissue debris which was assumed to be due to the fragility and thinness of the fat laden cells which make them break down easily during the processing technique (Fig. 15.1).

The collagen fibres in the spaces of Disse stand out more prominently giving the appearance of a slight increase in fibrous tissue at this stage of ALD.

2) Alcoholic hepatitis

a) Light microscopic findings

The prominent features seen were focal hepatocellular degeneration and necrosis with neutrophil polymorph infiltration. In one alcoholic hepatitis was mixed with fatty changes in which the overall changes were very mild and consisted of variable degrees of macro- and microvesicular steatosis with focal hepatocellular degeneration, necrosis with neutrophils and mixed inflammatory cell infiltration around the damaged hepatocytes. Mild Kupffer and Ito cell hyperplasia and minimal pericellular fibrosis were also noted mostly in the mid-zone of the lobule (Fig. 16.1).

The more severe changes were noted in cases of hepatitis and/or hepatitis superimposed on an already established cirrhosis. There was more widespread hepatocellular damage associated with mixed inflammatory reaction, neutrophil infiltration, pericellular fibrosis,central vein sclerosis and Kupffer and Ito cell hyperplasia. Portal tract changes included expansion of the portal tract with oedema, mixed inflammatory cell infiltration, fibrous tissue and bile ductule proliferation dissecting between the hepatocytes breaching the limiting

plates. Ito cells were noted adjacent to the damaged hepatocytes (Fig. 16.2).

The cytoplasmic inclusions which were occasionally found in some hepatocytes and appeared as dense homogeneous globules turned out to be giant mitochondria, giant lysosomes or Mallory bodies in the subsequent TEM examination.

b) Transmission electron microscopic findings

The prominent findings seen were in the hepatocyte whereby the overall architecture was disturbed and the hepatocytes were misshapen.

The cytoplasm of some hepatocytes, especially in the periportal area, showed focal degeneration (Cytolysis) evidence by autophagic vacuoles and myelin figures which ranged from an occasional one involving a small area of the cytoplasm to the more severe one in which a greater area was affected (Figs. 17.3 and 17.4).

The bile canaliculi of these hepatocytes showed signs of membraneous damage which denuded them of microvilli so that they appeared dilated with bile deposition within their lumen. Membraneous debris and various electron dense granules were also seen. The junctional complexes were usually preserved. These changes assumed to be due to the intracellular cholestasis accounted for the focal cytolysis within the cells (Fig. 17.2).

There was a general increase in the number of lysosomes within the hepatocytes. They contained variable amounts of heterogeneous materials of different electron density, some of which contained lipid vacuoles (Figs. 18.1 and 18.2).

The smooth endoplasmic reticulum showed marked hypertrophy with a variable degree of vesicular and/or vacuolar transformation. It occupied most of the cytoplasm (Figs. 17.1, 19.1 and 19.3). On the other

hand the rough endoplasmic reticulum seemed to be reduced in amount. It had lost its parallel arrangement and became dilated and degranulated with only a few ribosomes.

The mitochondrial changes were the most striking among the cytoplasmic organelles. In general there was reduction in their number and increase in their matriceal density. Their cristae became fewer in number and lay free in the matrix. In some instances only a remnant of cristae was left against the mitochondrial wall. The mitochondrial size ranged between 2-10 microns. Giant mitochondria with size equal to the nucleus were frequently found (Figs. 20.1 and 20.2). One to three giant mitochondria could be found per cell usually spheroidal but occasionally displaying bizarre shapes (Fig. 20.3). A frequent finding was where a number of small sized mitochondria could be seen joining together in the process of forming a larger one. This supports the theory that giant mitochondria are formed by fusion of smaller ones rather than a single mitochondrion growing to a hugh size. In many instances of the bizarre form of mitochondria, one could still see the smaller ones joining the large with a narrow rim of cytoplasm lying in the vicinity or with a thin rim of cytoplasm separating them (Fig. 20.3). A frequent observation was where two small mitochondria started to join together and assumed a drum-stick appearance (Figs. 20.6 and 20.7). Among the mitochondrial inclusions were the dense bodies and the paracrystalline inclusions which displayed various geometrical shapes on cross section (Figs. 20.4 and 20.5). On a few occasions lipid-like vacuoles were found inside the mitochondria among other inclusions (Figs. 20.6 and 20.7).

Alcoholic hyaline (Mallory body) was found in one case.It appeared to have a filamentous architecture. The microfilament branches crossed each other and some of them appeared to have tubular structures (Figs. 21.1 and 21.2).

Bile canalicular changes were variable and not uniform. Some of them appeared to have normal structures with a very prominent adjacent Golgi complex (Fig. 22.1). Others showed signs of membrane damage with few microvilli, or were devoid of microvilli, and showed thickened pericanalicular ectoplasm with evident microfilament structures (Fig. 22.2).

The sinusoids were usually filled with tissue debris and various amounts of inflammatory cells. Among them were lymphocytes (Fig. 23.2) and occasionally neutrophils were found in the sinusoids (Fig. 23.1). The endothelial cells were swollen and slightly thickened with variable amounts of electron dense material within their cytoplasm (Figs. 23.3 and 23.4). Kupffer cells were bulky and bulging into the sinusoidal lumen. Their cytoplasm was filled with lysosomes (fig. 23.3).

The spaces of Disse appeared thickened, devoid of microvilli and filled with tissue debris which were evident as variable sized electron dense materials (Fig. 23.4).

The fat-storing cells (ITO) were found in abundance, probably indicating an increase in their number. They displayed various forms. TEM sections of fatty liver with hepatitis showed typical resting Ito cells in the space of Disse where substantial collagenisation had not occurred (Fig. 24.1). These cells were characterised by many fat droplets, small amounts of endoplasmic reticulum and a somewhat convoluted nucleus. On the other hand in areas of hepatocellular degeneration and inflammation, in alcoholic hepatitis, Ito cells occasionally were increased in number together with collagen deposition and neutrophilic infiltration. The cells in these areas had a well-developed dilated RER (Figs. 24.3 and 24.4), few fat droplets and its nucleus had a smoother contour (Fig. 24.2). These cells were designated as activated or transformed Ito cells and could be identified only by EM.

Activated Ito cells were observed in the vicinity of hepatocytes which were undergoing degenerative changes including Mallory body formation. Electron dense amorphous materials were noted around these activated Ito cells (Figs. 24.5, 24.6 and 24.7). Collagen bundles were noted adjacent to these cells. They varied in thickness from very slender few fibrous bundles to very thick ones. Some of them were located between the activated Ito cells and the cytoplasm of a degenerate hepatocyte (Figs. 25.1 and 25.2) while other thick bundles were lying in the space of Disse between the activated Ito cells and the hepatocytes. Probably these cells account for collagenisation of the space of Disse (Figs. 24.8 and 24.9).

Periportal hepatocytes commonly showed signs of cholestasis evident as bile canaliculi dilated and devoid of microvilli in some places or with very few stunted flat ones. The pericanalicular ectoplasm was thickened with increased numbers of microfilaments. The lumina contained bile deposit and variable sized electron dense granules (Figs. 26.1 and 26.2).

The cytoplasm of hepatocytes showed increased numbers of lysosomes, focal cytoplasmic degeneration evident by phagocytosomes and many multivesicular bodies. A striking form of lysosomes found in these cells had central laminated bodies with numerous electron dense granules and a dark irregular periphery presumably containing bile deposits (Figs. 26.3 and 26.4). Bile deposits were also present in the intercellular spaces which showed marked dilatation (Fig. 26.6).

Proliferation of bile ductules is commonly seen in expanded portal tracts and periportal areas. Such ductules are usually tortuous and irregular. They are composed of cuboidal cells and frequently have a poorly defined lumen (Fig. 27.1). The epithelial cells were similar

to those of normal bile ductules and small bile ducts, the nucleus was round or ovoid with uniformly and densely packed chromatin. The cytoplasm had scanty small organelles including mitochondria and endoplasmic reticulum. The Golgi complex and the tonofilaments were well developed. There were many microvilli projecting into the irregularly shaped lumen with occasional bleb formation. The intercellular connections were straight and tight with distinct junctional complexes in the luminal half and widened interdigitations with lacunae formation. In the basilar half there were basal lamina surrounding the ductules which were slightly thickened (Figs. 27.2 and 27.3).

c. Scanning electron microscopic findings

In scanning the specimens of alcoholic hepatitis, in the majority of cases, the fracture line passes through the intracellular plane rather than the intercellular one exposing the interior of the cells. Large areas of fracture surfaces were covered with tissue debris probably due to the fragility of the degenerated hepatocytes. In general there is an increase in the amount of fibrous tissue which looks thick, twisted and strewn over the surfaces of the hepatocytes (Fig. 28.1).

The surfaces of the hepatocytes look rough, irregular and covered by numerous tiny flat microvilli. Occasionally they display a striking microvillous appearance (Figs. 28.2 and 28.3) which is consistent with the TEM findings where the cell wall in some areas was thrown into a complex net of cytoplasmic folds interdigitating with each other (Figs. 28.4, 28.5 and 28.6).

The hepatic sinusoids, more often, were filled with tissue debris, inflammatory cells and RBCs (Fig. 29.1). Occasionally the empty sinusoids revealed a rough, thickened and folded endothelial lining which was usually covered by tissue debris (Fig. 29.2). There were fewer microvilli seen through the fenestrations giving the impression of

a reduction in their number (Figs. 29.3 and 29.4).Kupffer cells were swollen and their surfaces were rough bulging across the sinusoids anchoring their cytoplasmic filopodia to the endothelial lining (Fig. 29.5).

Ito cells were more easily identified suggestive of an increased number which is consistent with TEM findings. They usually appeared lighter than the rest of the cells, triangular or spindle shaped, located in the space of Disse (Figs. 30.1 and 30.2) or when the sinusoid was ripped away by the fracturing technique, they could be seen clinging to the surface of a hepatocyte. A constant findings was a bundle of collagen seen in close apposition to these cells (Fig. 30.3). The surfaces of these cells were rough and irregular with mild folding and a few tiny microvilli (Fig. 30.4).

With the SEM technique the pericellular fibrosis was evident. It looks more prominent wrapping the hepatocyte with a mesh of fibrous tissue of different thicknesses consistent with a chicken-wire appearance of light microscopy (Fig. 31.1). More thickened bundles of collagen fibres were frequently found in the spaces of Disse usually run along both sides and some appear to encircle the hepatocytes (Fig. 31.2). Comparison with TEM findings showed that the earliest appearance of pericellular fibrous accumulation was where the wall broke into a labyrinth of cytoplasmic folds and interdigitations. Between these folds different sized vesicles were evident. The two leaflets of the cell wall appeared to connect to these vesicles with negative stained collagen bundles in between (Figs. 31.3 and 31.4). Occasionally a more thickened intercellular bundle of banded collagen appeared to be herniated towards the cytoplasm (Figs. 31.4 and 31.5). In some

degenerate hepatocytes the whole length of intercellular wall appeared irregular and thrown into folds. More than one thick bundle of banded collagen fibres were evident (Figs. 31.6 and 31.7).

With the SEM technique the fractured surfaces of the portal areas revealed the striking features of the proliferated bile ductules. It appeared as a honeycomb structure among the tissue debris, inflammatory cells and fibrous tissue of the expanded portal tract (Figs. 32.1 and 32.2). This is consistent with the TEM findings.

The inflammatory cells demonstrated various sizes, round or spheroidal structures with slightly irregular surfaces covered by folded ruffles and various pits. Some of these cells were avulsed by fracturing techniques leaving a crater in the tissue (Fig. 32.3).

The honeycomb structure of the proliferated bile ductules consisted of several opened lumina grouped together and surrounded by bands of connective tissue. The lumina are covered by variable numbers of tiny flat microvilli which in some places appeared as a delicate web of interlacing fibres. The walls were thick and irregular and contained several small translucent holes which probably corresponded to the nuclei of the ductular cells (Fig. 32.4). Several bile ductules appeared among the vascular canals in the portal area as discrete from each other. Some had ill-defined lumen, and were surrounded by thick twisted fibrous tissue (Figs. 32.5 and 32.6).

3. Alcoholic cirrhosis

a) Light microscopic findings

Four cases of established alcoholic cirrhosis and two with superimposed alcoholic hepatitis were of micronodular type. No normal architecture was identifiable and in particular central veins were difficult to define. Within the nodule the hepatocytes were arranged in plates two or three cells thick. The amount of fat present was variable.

Within the sinusoids, lymphocytes and Kupffer cells were evident. The perinodular fibrous septa contained inflammatory cells, proliferating bile ducts and some scattered trapped hepatocytes often in an acinar or rosette arrangement (Figs. 33.1 and 33.2).

b) Transmission electron microscopic findings

The ultrastructural changes included in alcoholic cirrhosis were studied both in the cirrhotic nodule and in the perinodular fibrotic septa.

The cirrhotic nodule

Plates of more than one cell thick were present consistent with the LM findings. The hepatocytes were often arranged in a rosette form around the sinusoid. The amounts of macro- and microvesicular steatosis were variable. The hepatocellular changes in a cirrhotic nodule were: marked dilatation of RER, vesicular transformation of SER, increased number of lysosomes and bizarre shaped giant mitochondria with paracrystalline inclusions and dense bodies.

The bile canaliculi within the nodule were little affected while those of the periphery adjacent to the septa showed signs of membranous damage (Figs. 34.1, 34.2 and 34.3).

Inside the hepatic nodule, the sinusoid appeared to contain abundant amounts of tissue debris, increased numbers of lysosomes within the cytoplasm of Kupffer cells and frequent lymphocytes. The lymphocytes were present in close contact with degenerate hepatocytes (Figs. 34.2, 34.3, 35.1 and 35.2).

The spaces of Disse were usually narowed and the hepatocellular vascular poles were smooth and the microvilli were sparse (Fig. 35.1). The presence of electron dense structures were frequent findings. Collagen fibres ran along a considerable length of the sinusoid clinging to the flat attenuated microvilli in the space of Disse underneath

the epithelial lining (Figs. 35.2,36.1 and 36.2) or were present at periodic intervals. It was noted that when basement membranes were present there was no collagen fibres in the space of Disse (Figs. 36.3 and 36.4). Occasionally an Ito cell was found in the space of Disse, usually of the activated form containing a few lipid droplets in the cytoplasm and with a thick bundle of collagen in close contact.

A conspicuous ultrastructural finding in cirrhotic nodules was the considerable dilatation of the intercellular spaces. The lateral cell surfaces facing the intercellular spaces carried a rich array of microvilli especially in those areas in which the liver cell plates were several rows thick. The microvilli projecting into the dilated intercellular spaces created a cavernous appearance (Fig. 37.1). Increased collagen fibrils were found in the dilated intercellular spaces (Figs. 37.2 and 37.3).

The perinodular fibrotic septa

The ultrastructural changes of these septa were associated with marked ductular proliferation (Figs. 38.1 and 38.2), accompanied by an inflammatory reaction and various numbers of trapped hepatocytes in the marginal zone of the septa which was surrounded by thick fasicles of fibrous tissue (Figs. 38.3 and 38.4).

c) Scanning electron microscopic findings

Fracture surfaces of cirrhotic liver confirmed a complete loss of normal lobular architecture, abundant tissue debris and a marked increase in the fibrous tissue which covered the fractured surfaces. Portal tracts and structures within the perinodular fibrous septa were difficult to define due to the increased amount of fibrous tissue which was strewn over the surfaces during fracturing, rendering the examination of the structure in those areas very difficult. In general, with scanning, there were two areas, a more peripheral one which

consisted of fibrous tissue and tissue debris which probably corresponds to the portal tract and/or perinodular fibrous septa adjacent to a round area of hepatocellular tissue which might comprise the cirrhotic nodule (Fig. 39.1).

Within the cirrhotic nodule the hepatocytes were arranged in groups of more than one cell surrounded by thick wavy fibrous bands which appeared to run in the space of Disse and in close contact to the hepatocyte. The sinusoids were difficult to define partly due to abundant tissue debris and increased amount of fibrous tissue and partly due to hepatocytes which were arranged in groups rather than plates (Figs. 39.2 and 39.3). However plates more than one cell thick were occasionally present (Fig. 39.4).

Frequently part of the whole surface of the hepatocyte was crumbled away by the fracturing techniques exposing the inside of the cell which appeared to consist of numerous variable sized spheroidal bodies probably corresponding to the mitochondria. They frequently contaminated the fractured surface (Fig. 40.1). Some of these spheroidal bodies appeared to be of larger size and probably consisted of giant mitochondria as revealed by TEM (Fig. 40.2). A larger spheroidal body was occasionally exposed and might correspond to the nucleus (Figs. 40.3 and 40.4).

The endothelial lining of the sinusoid, frequently, was ripped away exposing the vascular pole of the hepatocytes which appeared smoother. The flat short or plump microvilli were sparse (Figs. 39.4 and 41.1). On the other hand the intercellular surfaces of the hepatocytes appeared as irregular and were thrown into folds and ruffles with scanty numbers of plump microvilli. The bile canaliculi appeared

to be buried between these folds (Figs. 41.1 and 41.2).

The canaliculi surfaces of the hepatocytes were difficult to define in the majority of the cases probably due to the increased amount of tissue debris and fibrous tissue which covered the fractured surfaces or because the surfaces of the hepatocyte crumbled away during the fracturing technique (Figs. 41.1 and 41.2). However the bile canaliculi occasionally appeared more clear. It ran a more tortuous course in the hepatic surfaces. Its microvilli appeared intact within the slightly dilated lumen (Fig. 41.3).

There were increased numbers of inflammatory cells present in the sinusoids and between the hepatocytes. Among these inflammatory cells, round cells were noted with slightly wrinkled surfaces and a few plump blebs or microvilli probably consistent with lymphocytes (Fig. 42.1). These cells were frequently found adjacent to the hepatocytes or wedged between them in close contact with its surfaces. An occasional finding was a lymphocyte clinging to a degenerate hepatocyte with numerous slender cytoplasmic processes (Fig. 42.2). These findings were consistent with the TEM findings (Figs. 42.2 and 42.3). The degenerate hepatocyte usually appeared as a wrinkled cell which lost most of its surface specialisation and was covered by tiny numerous plump microvilli. Usually these cells crumbled during the fracturing technique exposing part or the whole of the cell interior. Occasionally spheroidal bodies appeared to protrude through the surfaces of these cells (Figs. 42.3 and 42.4). In general the sinusoids were covered by tissue debris which either wedged between or filled the sinusoids. However occasionally opened and relatively clear sinusoids were found allowing the study of the ultrastructural changes (Fig. 43.1) The endothelial lining frequently appeared thick and wrinkled with a

decreased number of fenestrations and fewer large pores while the sieve plate was difficult to define.

With scanning microscopy, pericellular fibrosis appeared more prominent. The hepatocytes appeared to be either buried in a thick mass of fibrous tissue or rested in a nest of wavy delicate fibres completely surrounded by fibrous tissue (Figs. 44.1 and 44.2). This was in contrast to the TEM in which the pericellular fibrosis appeared to be more focal than general (Fig. 44.3).

Occasionally Ito cells were found in close contact with a thick fibrous band adjacent to the hepatocyte. A constant finding was a thick band of collagen in close contact with the Ito cell.

III. Results of biopsies from patients with PBC

Ten patients underwent liver needle biopsy, four of them were pre-cirrhotic and six had established cirrhosis. Diagnoses were made on clinical features, biochemical findings and light microscopic examination. (Appendix 2). Specimens were prepared and processed the same as for alcoholic liver disease.

1. Light microscopic findings

For practical purposes the classical staging into, florid duct lesion, ductular proliferation, scarring and cirrhotic stages was not applicable due to marked overlap between these stages at a given time. For descriptive purposes the pathological stages can be divided into pre-cirrhotic and cirrhotic.

a) Pre-cirrhotic stage

The prominent features were irregular expansion of portal tracts with increased numbers of chronic inflammatory cells. The majority of them were lymphocytes and plasma cells which breached the limiting plates and accumulated at their edges. Piecemeal necrosis with proliferating bile ductules was evident (Fig. 45.1). Small ductules, many

of them without obvious lumen, were seen in clusters with various signs of epithelial cell injury. These cells were swollen and pale. Others were crowded or surrounded by a heavy infiltration of lymphocytes and plasma cells. A number of bile ductules were obliterated and their places were taken by an ill-defined hyaline mass surrounded by chronic inflammatory cells (Fig. 45.2). Sinusoids were infiltrated with mononuclear cells. Kupffer cells were enlarged and there was commonly diffuse liver cell hyperplasia as indicated by twin-cell plates (Fig. 45.3).

Occasionally various degrees of steatosis are noted with several Ito cells present, wedged between the sinusoid and the liver cells (Fig. 45.4).

b) Cirrhotic stage

The prominent features of this stage were the extension of fibrous septa from the portal tracts into and around the lobules. Ducts were reduced in number (Fig. 46.1). There was piecemeal necrosis with focal accumulation of proliferated ductules in the septa (Figs. 46.2 and 46.3). Within the lobule there were small aggregates of mononuclear cells, increased numbers of them within the sinusoid. The hepatocytes were often arranged in rosette form. Mild steatosis was noted (Figs. 46.4 and 46.5).

2. TEM findings of pre-cirrhotic stage

a) Bile duct changes

Within the portal tract small bile ductules or a ductule with signs of injury or damage were selected for the ultrastructural study. Most biliary epithelial cells lining the ducts and the proliferating ductules were swollen with few cytoplasmic organelles forming the so-called pale cells, between which were wedged smaller dark cells with less cytoplasmic volume but more abundant in organelles and rich

in mitochondria which displayed circular cristae (Fig. 47.1). The mitochondria were few in number in the epithelial cells, aggregated to one side of the nucleus and showed various signs of cristal injury.

The Golgi zone of the biliary epithelial cell was usually hypertrophic and the scanty rough endoplasmic reticulum showed vesicular or even vacuolar dilatation. The interdigitating junctional structures located near the cell bases sometimes appeared flattened and at other times slack with lacunar dilatation of the adjacent intercellular spaces. However the junctional structures located near the apical pole of the biliary cells were well-preserved.

Cytolysosomes and lysosomes were present in the cytoplasm (Fig. 47.2). Filamentous structures were evident either as small bundles loosely aggregated around the nucleus or around the mitochondria and appeared to be more prevalent towards the apical pole and the lateral wall of the ductular cell, while becoming very scanty around the basal part of the cell (Fig. 48). The ductular lumen showed paucity of microvilli and sometimes appeared narrowed and ill-defined (Figs. 47.1 and 48).

The basement membrane was thickened, stratified, disrupted in places and infiltrated by polymorphonuclear leukocytes. Lymphocytes and macrophages appeared in close contact to the basement membrane (Figs. 49 and 47.1). The intercellular membranes of the ductular epithelial cells remained intact. The bile ductules frequently appeared to be embedded in a thick band of connective tissue with various amounts of pigment present in the extracellular spaces (Figs. 50.1 and 50.2). The canal of Hering was occasionally found composed of several hepatocytes and a few ductular cells. There was an increased amount of lysosomes within the cytoplasm of the hepatocytes. The lumen was dilated, devoid of microvilli and contained amorphous material

of medium electron density. Macrophages wedged between the cells and neutrophils in close contact to both ductular cells and hepatocytes were present (Figs. 51.1 and 51.2).

b) Hepatocellular changes

Some hepatocytes showed alteration due to cholestasis while others were intact. The altered cells frequently showed marked dilatation of the endoplasmic reticulum with vesicular and/or vacuolar transformation. An increased amount of bile pigment deposition within the cytoplasm was found. This pigment was membrane-bound, present either as fine granules of medium electron density or a mass of high electron density and more often a mixture of both (Figs. 52.1 and 52.2). Large lysosomes were also frequently seen which contained various electron dense masses and lipid-like vacuoles probably bile and bile-related substances (Fig. 52.3).

Mitochondrial alteration in the form of condensed mitochondria (Fig. 52.1), curling of the cristae and the appearance of crystalline inclusions in the matrix was most conspicuous (Fig. 54.1). Giant mitochondria with various paracrystalline inclusions adjacent to smaller mitochondria separated by only a thin rim of cytoplasm were also found (Fig. 54.2).

Injury to the bile apparatus was present in the altered hepatocyte. Bile canaliculi were dilated and frequently herniated into the cytoplasm either devoid of microvilli (Fig. 52.2) or with a few stunted ones. The lumen contained membranous materials and electron dense granules. The pericanalicular ectoplasm showed marked thickening with increased number of microfilamentous material. Tight junctions were preserved. The intercellular spaces adjacent to the injured bile canaliculi were dilated with marked thickening of adjacent cytoplasm. Golgi complexes showed significant hypertrophy. There was an increased number

of bile pigment containing lysosomes (Figs. 55.1 and 55.2).

The bile canaliculi in the less affected cells showed increase in their number on one side of the hepatocyte suggestive of increased tortuosity. In these cases the bile canaliculi showed normal features except the marked thickening of the pericanalicular ectoplasm, with increased number of microfilaments, marked dilatation of Golgi complex and widening of intercellular spaces adjacent to the canaliculi (Figs. 56.1 and 56.2).

Sinusoidal changes consistent with the LM findings were widening of the sinusoids and mononuclear infiltration which included lymphocytes and plasma cells. There was increased amount of tissue debris wedged in or filling the sinusoids (Fig. 57). Among them the tissue debris, bile pigment and membranous materials were present (Fig. 60.3). The endothelial cell lining was swollen and bulging into the lumen, their cytoplasm packed with lysosomes (Fig. 58.1). Kupffer cells were enlarged and found in increased numbers. Their cytoplasm contained various amounts of bile pigment lysosomes (Fig. 58.2).

The space of Disse appeared thickened and smooth. The vascular pole of the hepatocyte was devoid of microvilli. Amorphous material with fine granularity appeared to fill the spaces, among them various thick collagen bundles were present (Fig. 58.2). Within the spaces of Disse, Ito cells were found, their cytoplasm filled with striking types of lipid droplets. They consisted of a fine granular medium electron dense outer band encircling a light central smooth area. Many droplets in the process of fusion were present in the cytoplasm of hepatocytes adjacent to the sinusoid. They were also found in the cytoplasm of the Kupffer cells (Figs. 59.1, 59.2. 59.3 and 59.4).

Lymphocytes frequently found within the sinusoid, occasionally present in spaces of Disse, demonstrated a cytoplasmic protrusion in contact with degenerate cellular remnants of degenerated hepatocytes

(Figs. 60.3 and 60.1). The double layer between lymphocyte and hepatocyte appeared to have occasional discontinuity and became difficult to define (Fig. 60.2).

3) TEM findings of cirrhotic stage

The ultrastructural changes occurring in the cirrhotic stage were essentially similar to those occurring in the pre-cirrhotic stage except they were more advanced. The ductules and the proliferated bile-ductule basement membranes were thick, stratified and interrupted in places. The intercellular membrane of the ductular epithelial cell was still intact. The ductular lumen was either devoid of or had short scanty microvilli. Some showed oedematous swelling projecting into the lumen forming pseudopodium-like processes (Fig. 61.1). The most conspicuous change was the marked increase in the filaments which cross the entire cytoplasm either singularly or grouped in long bundles (Figs. 61.2 and 61.3). Most ductular cells and proliferated bile ducts were swollen and showed dark and pale cells. There was abundant deposition of bile pigment within the ductular epithelial cells. Phagolysosomes, myelin-like figures and laminated structures were present (Figs. 62.1 and 62.2).

Giant mitochondria with intra-matrical crystalline inclusion were frequently seen in the hepatocytes (Fig. 63).

The ultrastructural studies of Mallory bodies found in one case showed them to be morphologically similar to that found in alcoholic liver disease (Figs. 64.1 and 64.2).

Fascicles of collagen fibrils were present in the space of Disse with other cellular debris among them numerous high electron dense granules of biliary origin. The same granules were found in the endothelial lining of the sinusoid which was usually enlarged and swollen containing increased numbers of lysosomes (Figs. 65.1 and 65.2). A

thick bundle of collagen fibrils was also found in the intercellular space suggestive of severe pericellular fibrosis (Fig.66).

4) SEM of pre-cirrhotic and cirrhotic stages

No differences were found between the two stages. The fractured surfaces of the majority of the specimens showed two distinct areas:

A. An irregular area of fibrous tissue and cellular debris with abundant various sized spheroidal cells embedded in them. Frequently these cells were avulsed by fracturing technique leaving a depression or crater in their place. These cells had an irregular rough surface with a short plump microvilli or bleb. Some had slightly wrinkled surfaces characteristic of macrophages. Other structures within these areas corresponded to an expanded portal tract with a heavy infiltration of inflammatory cells (Figs. 67.1, 67.2 and 67.3).

B. Hepatocellular area. The majority of the cells in these areas had a crumbled surface due to the fracturing technique but the outlines of these cells were well-defined. Few cells preserved their surface structures. The sinusoid was usually packed with cellular debris with collagen fibres running parallel in the space of Disse wedged between the hepatocyte and the sinusoidal lining. Some of the fibres crossed over the fractured surface (Fig. 68.1). The hepatocytes were arranged in plates more than one cell thick in the majority of the cases (Fig. 68.1) and occasionally arranged around the sinusoid in rosette form (Fig. 68.2).

The surfaces of the hepatocytes located away from the fibrous tissue band and the area of inflammation had very smooth surfaces and appeared to be relatively normal (fig. 70.1 and 70.2).

The bile canaliculi ran in the centre of the hepatocyte crossing from one cell to another, were clear and smooth and had numerous microvilli projecting into the lumen (Figs. 68.1 and 69.1).

The hepatocytic surfaces adjacent to the bile canaliculi appeared very smooth except for some gentle wrinkles in places (Figs. 68.2 and 69.1).

The surfaces of the hepatocytes in the vicinity of the fibrous tissue and inflammatory area showed very rough irregular surfaces covered by numerous microvilli (Figs. 71.1 and 71.2).Fibrosis of the space of Disse, usually with slender bundles of collagen and occasional thicker bundles, was evident.

DISCUSSION

For over three decades, electron microscopy has been frequently used in an effort to reach a better understanding of the hepatobiliary diseases. The results, derived from both experimental and clinical studies to date, have been variable.

Electron microscopy of normal human specimens was sporadic. Thus normal baseline findings are lacking precluding a proper evaluation of the changes present in human liver diseases.

In this study, the SEM contribution was significant in studying the surface morphology of the hepatocyte and the sinusoid in ALD. The SEM was valuable also in demonstrating the Ito cells, perisinusoidal and pericellular fibrosis. In PBC, however, the SEM contribution to the surface morphology was limited.

In ALD the TEM showed more frequent mitochondrial changes than Mallory bodies, although they were less specific than the latter. In PBC no essential differences were found between the pre-cirrhotic and cirrhotic stages at ultrastructural level. The increase in the microfilaments, however, was noted in the pericanalicular ectoplasm which may have a role in the intrahepatic cholestasis seen in PBC.

Electron microscopy is essential to establish the precise nature of the cytoplasmic inclusions encountered in light microscopy.

The significance of the observations reported here would be best confirmed by studying a larger series, perhaps involving comparative examination of different conditions.

The previous ultrastructural findings permit the suggestion that electron microscopy may be a useful tool to follow the progression of PBC and ALD or to help in its diagnosis when the clinical, biochemical or histological criteria are inconclusive or equivocal.

While light microscopy is a well established technique in diagnostic pathology, electron microscopy does not greatly improve the precision or accuracy of diagnosis of liver biopsy, mainly because of the severe constraints on the size of tissue available from needle biopsy for adequate fixation and proper sectioning in the EM technique. In diffuse liver diseases this problem would be minimised whilst in the focal lesions, which is common in the majority of liver diseases, this problem will be a significant limiting factor. However, in order to detect focal lesions and to determine their localisation within the hepatic lobule, each biopsy should contain at least several portal tracts and terminal hepatic veins, making it less difficult to precisely localise sectioned hepatocytes in the lobules or to evaluate all hepatic components. Application of TEM to the diagnosis of liver biopsies is further limited by the fact that a sufficient understanding of the organelle pathology of the liver is not yet available to allow recognition of diagnostically useful patterns at the subcellular level. Assessment of organelle or subcellular pathology is clinically helpful in only a few hepatic diseases. In the majority of instances, diagnostic evaluation of liver biopsies depends on recognition of relatively gross pathologic lesions and it requires techniques that facilitate the rapid examination of relatively large areas of tissue. Currently LM evaluation of stained sections of paraffin embedded tissue best meet these requirements.

The SEM has not yet been applied to the diagnostic evaluation of liver biopsies; this method of topographical morphologic study of cells and tissue has several attributes that suggest its potential utility for this purpose. SEM allows detailed study of the structures of the cell and tissue surfaces in three dimensions. Another valuable feature of SEM is the capability to rapidly scan large areas of tissue.

Examination of the surface features of the normal and abnormal may provide new information that will assist the further understanding of hepatic pathophysiology.

The limitations encountered in the SEM were many. It is difficult to obtain a good fracture surface because the small amount of tissue available from the needle biopsy makes it difficult to handle. In diseased liver, frequently the majority of the hepatocytes have crumbled surfaces due to the thinness and fragility of the cells. The cellular debris, therefore, will cover the fractured surfaces adding another difficulty for detailed study.

In the area of marked increase in connective tissue, fibres were especially encountered in the portal tracts in PBC. Inflammatory cells obscured the portal tract substructures making them difficult to define and usually covered by abundant fibrous tissue strewn over broken surfaces.

The sinusoids in the diseased liver are usually filled with inflammatory cells, cellular debris and RBCs, making it difficult to study the detailed changes of the endothelial lining of the sinusoids.

In the earliest fatty stage of ALD, minor organelle changes and variable amounts of steatosis, both minor and major lipid droplets are found. Slight hypertrophy of SER and increased matrical density of mitochondria are present. Ito cells were found more frequently, suggestive of an increase in their number consistent with the findings in the thin LM sections. The majority of them were of a resting form (Fig. 15.1). SEM revealed increased brightness of some cells due to an increase in their electrical charges. Nopanitaya et al in 1977 suggested that a potentially diagnostic feature of necrotic cells is that as seen by SEM they appear to emit a much higher intensity

of secondary electrons than the non-necrotic hepatocytes. This caused the necrotic cells to standout in SEM micrographs because of their relative brightness (Fig. 15.2).

The whole surfaces of these cells are covered by microvilli; among them bile canaliculi are difficult to define; these bright cells, covered by microvilli, might represent an early alcoholic change on the surface morphology of degenerated or necrotic hepatocytes.

In alcoholic hepatitis, while LM shows normal hepatic architecture, focal hepatocytic degeneration and related polymorph infiltration, early pericellular fibrosis was centrally placed and extended outwards in the lobule. TEM showed major cytoplasmic changes with marked hypertrophy of SER either with vesicular or vacuolar transformation. RER was reduced in size, dilated with a decrease in the number of ribosomes, and an increase in the number of lysosomes, but the most constant and frequent changes were mitochondrial with giant transformation being the commonest change. Giant mitochondria probably developed from initially normal organelles. Theoretically this may occur by swelling of individual units or by a process of fusion with consequent diminution in number. Evidence for the latter theory has been found in rat liver (Kimbery and Loeb 1972). In this study suggestive signs of fusion were present (Figures 20.3, 20.6 and 20.7). Giant mitochondria are just visible in light microscopy, but EM was essential for their accurate identification. This also applied to Mallory bodies which were occasionally found (Figs. 21.1 and 21.2).Johannessen (1980) suggested that Mallory bodies in ALD occurred in centrilobular areas while in PBC they occurred in the periphery. They are virtually diagnostic of alcoholic changes when found in the centrilobular hepatocytes. These bodies are also found in longstanding cholestasis and Indian childhood cirrhosis (Gerber 1973). The most conspicuous finding

is ITO cells, confirmed by TEM especially in relation to the area of hepatocellular degeneration and necrosis (Minato et al 1983). Few were in the resting form and the majority in an activated form with well developed RER, well developed Golgi complex, few lipid droplets and a smooth nucleus as compared to the deeply convoluted nuclear shape of the resting form (Figs. 24.2, 24.3 and 24.4).

In SEM, ITO cells were seen more frequently in a constant relationship to a collagen bundle of variable thickness. Matsuda and Lieber in 1979 observed in the livers of alcoholic patients and baboons a significant increase in the number of fat-storing cells (ITO) as well as fibroblasts with enhancement of collagen deposition in the space of Disse. McGee et al in 1972 suggested that fat-storing cells transformed into fibroblasts. Indeed a transitional form between ITO cells and fibroblasts and their proliferation in association with collagen deposition have been observed in alcoholic baboon liver (Matsuda and Lieber 1979). The exact mechanism of biochemical activation of the fat-storing cells and their morphological transformation are unknown (Minato 1983).

In the TEM, proliferated bile ductules were observed in the portal area, most of which had narrowed or no lumen (Fig. 27.1). This is contradictory to the SEM findings in which a cluster of closely packed ductules with patent lumen and a few microvilli could be seen with a fine mesh of fibrous tissue covering the lumen (Fig. 32.4).

Using rats Brookes et al in 1975 demonstrated proliferating bile ducts by SEM after ligation of the common bile duct. These proliferating ducts contained microvilli with a patent lumen and cable-like structures within the lumen. There is great controversy about the origin of the proliferating bile ducts (Schaffner et al 1961). They concluded that they might be derived from proliferation of pre-

existing ducts while Uchida et al in 1983 suggested that they arise from transformation of the hepatic cellular cords. Indeed they demonstrated a transitional cell between hepatocytes and ductular cells.

In this study a transitional cell has not been demonstrated and the cells appeared to be like ductular epithelial cells. Pericellular fibrosis was evident by TEM and confirmed by SEM where collagen fibres were frequently demonstrated encircling the hepatocytes in a chicken-wire mesh (Fig. 31.1). In the very early stage of pericellular fibrosis noted in TEM, focal or occasional diffuse changes in the intercellular space were noted whereby a cellular membrane of adjacent hepatocytes was thrown into a labyrinth of interdigitations, folds and herniations between single or small groups of collagen fibrils (Figs. 31.3 and 31.5). There is no evidence to suggest the involvement of hepatocytes in this process nor any ITO cells or other cells adjacent to these areas. The nature of development of pericellular fibrosis appears to be undecided.

In the alcoholic cirrhosis, the ultrastructural changes were more profound with marked alteration in the cytoplasmic organelles. The mitochondrial injury is the most striking change. Paracrystalline mitochondrial inclusions and giant mitochondria formation were frequently seen.

The hepatocytes constituting the cirrhotic nodule were more than one cell thick with many hepatocytes located distant from the sinusoids and bearing microvilli over their entire surfaces. The intercellular spaces were dilated and the lateral cell surface facing the intracellular spaces carried arrays of microvilli. The microvilli projecting into the dilated intercellular spaces created a cavernous appearance (Figs. 37.1, 37.2 and 37.3).

Johannessen in 1980 advanced various theories on the development of the microvilli on the lateral intercellular borders. He suggested that it may be a primary abnormality of the cells in the cirrhotic nodules and that most cells in the nodules arose by regeneration. The development of microvillous borders is a property of regenerating cells. He has further speculated that the altered space of Disse might act as a barrier to the diffusion of substrate from the sinusoids and this would lead secondarily to the development of microvillous borders as an adaptive response on the part of the hepatocytes.

The space of Disse appeared narrowed and the vascular pole of the hepatocyte appeared smoother with a few flat microvilli. A basement membrane of amorphous electron density was found in the space of Disse under the endothelial lining either at periodic intervals or running across a considerable length of the sinusoid (Figs. 36.1, 36.2, 36.3 and 36.4).

Schaffner and Popper in 1972 described the development of a continuous basement membrane and conversion of the sinusoids into capillaries in advanced longstanding cirrhosis. However, Johannessen in 1980 found the basement membrane developed only a short portion of the sinusoid and was limited to the peripheral areas near the septa.

In this study the development of basement membrane was not uniform. In some sinusoids it appeared at intervals only while in other sinusoids it appeared to run along a considerable length of sinusoid. Moreover occasionally it appeared on one side of the sinusoid and not on the other (Figs. 36.3 and 36.4).

The pericellular fibrosis and the fibrosis of the space of Disse were both marked in alcoholic cirrhosis as revealed by TEM and SEM. Little is known about the site and formation of the collagen and

collagen precursors responsible for the intranodular increase of collagen fibrils.

There is no evidence to suggest the involvement of hepatocytes in this process; probably the perisinusoidal fat-storing cells (ITO) found along the sinusoidal margins play a certain role in collagen genesis to judge from observations on their ability to transform with the development of RER and the close apposition to collagen fibrils. Indeed the scanning microscope shows on several occasions a slender fibril of collagen attached to ITO cells (Figs. 44.4 and 44.5). However, collagen synthesis also occurs in nodular regions distant from sinusoids or limiting septa where no elements capable of fibroblastic transformation are present. This has been attributed partly to the condensation of the original reticular fibre network in consequence of necrosis and collapse of the parenchyma.

In primary biliary cirrhosis the EM study focussed mainly on the abnormalities of the intrahepatic ducts. During the advanced stage of PBC no essential differences were found, a finding that contradicted to some extent the light microscopic observations. Most biliary epithelial cells lining the ducts and proliferating ductules were swollen, so called pale cells, with a luscent cytoplasm; wedged between them were the so-called dark cells with less cytoplasmic volume but more abundant organelles. The interdigitating junctional structures located near the cell bases sometimes appeared flattened or slackened with lacunar dilatation of the adjacent intercellular spaces. However, tight junctions located near the apical pole of the biliary epithelium were well preserved (Fig. 47.1).

The basement membrane showed characteristic changes; thickened, stratified, split or disrupted in places and infiltrated by polymorphonuclear leukocytes (Fig. 47.1). The intercellular membrane of the

ductular epithelium was intact. Another striking feature in PBC was the presence of numerous lymphocytes in close contact with biliary cells, especially the necrotic ones (Fig. 49).

The ultrastructural alteration described by Chedid et al (1974) as characteristic of the end stage (thickening, stratified and occasional disruption of basement membrane) with leukocytic infiltration of the bile duct was not often seen. Johannessen (1980) suggested that there were frequent polymorphs in contact with damaged basement membrane and infrequent contact with lymphocytes in the latter stages. Lymphocyte contact was also observed by Bernnau et al in 1981.

The ductular lumen was narrowed and the luminal surface of the lining epithelial cell was devoid of microvilli (Fig. 47.1 and 48) or had only a few flat short microvilli, while in the advanced stage of the cirrhosis some microvilli showed marked swelling and presented as a pseudopodium-like process into the lumen (Fig. 61.1). Another characteristic change which occurred in the advanced stage was a marked increase in microfilaments within the ductular epithelium which crossed the entire cytoplasm either singly or in a bundle (Fig. 48). Necrosis of biliary cells was conspicuous and characterised by the presence of numerous cytoplasmic cytolysosomes whose contents were often suggestive of bile components (Figs. 50.2 and 60.1). This abnormality was also observed by Chedid et al 1974 in the early stage of PBC and was very rarely observed in the advanced stage. In this study, cytophagolysosomes were found both with biliary epithelial cells and hepatocytes. Other cytoplasmic organelle changes in biliary epithelial cells were hypertrophy of Golgi complexes, paucity of the RER and reduced numbers of ribosomes. Mitochondria showed various cristaecal

injuries consistent with Chedid's observations but prominent intramitochondrial granules were rarely seen (Figs. 47.2 and 50.1). On the other hand, the ultrastructural hepatocellular changes were minor organelle alterations in the majority of cells especially those within the nodule. It has been observed that most of these cells have a virtually normal appearance but minor organelle changes may be present despite the preserved cellular architecture. Numbers of megamitochondria were not infrequently seen (Figs. 54.1, 57 and 63). Mitochondrial paracrystalline inclusions were usually seen in the peripheral hepatocytes adjacent to portal tracts and to the fibrous septa. These are not specific and occur in other liver diseases. The same applied to Mallory bodies which were occasionally observed and have the same morphological characteristics as that of alcoholic hyaline (Figs. 64.1 and 64.2).

The most peripheral hepatocytes frequently showed injury to the biliary secretory apparatus characterised by paucity of bile canaliculi. The latter often herniated into the cytoplasm, were devoid of microvilli and showed marked thickening of the pericanalicular ectoplasm. Numerous microfilaments were present with marked hypertrophy of Golgi complexes and increased amounts of lysosomes which contained material of bile origin (Figs. 52.1, 52.2, 55.1 and 55.2). Bile deposition was present within the lumen of bile canaliculi as electron dense granules and within the hepatic cytoplasm in three forms. A fine membrane bound electron dense granule or a highly electron dense mass being the most frequent, accompanied by focal cytoplasmic degeneration evident as phagolysosomes, and thirdly a laminated body. Chedid et al (1977) described them as occurring in ductular epithelium and only in the early stages of PBC. Johannessen in 1980

also described the frequent encounter of laminated bodies in advanced stages. In this study, laminated bodies were frequently present in both hepatocytes and ductular epithelium (Figs. 62.1 and 62.2). The tight junctions were well preserved (Fig. 52.1). The majority of the bile canaliculi had a rounded appearance and their lumina were filled with microvilli. Moreover there was an increase in the number of bile canaliculi present on the lateral wall of the hepatocytes, a phenomenon suggestive of increased tortuosity of the bile canaliculi (Fig. 56.1). A striking thickening of pericanalicular ectoplasm with increased numbers of microfilaments was present in both injured bile canaliculi and those with normal appearances. The thickening frequently extended to the lateral wall of the hepatocytes with slight widening of the intercellular spaces (Fig. 56.2).

Several theories and suggestions were advanced to study the possible early site and causes of intrahepatic cholestasis. However, the subject remains controversial.

Philips et al in 1975 suggested microfilament dysfunction as a posible cause of intrahepatic cholestasis. Later in 1978 they confirmed microfilament involvement in norethandrolane-induced intrahepatic cholestasis, while Adler et al in 1980 suggested a primary alteration of canalicular plasma membrane with its microvilli to be responsible for cholestasis. This finding suggests that an increase in the number of microfilaments is an early feature of cholestasis, possibly preceding canalicular dilatation. Similar changes occurred in those portions of the bile ductular cells that face the lumen. Philips et al in 1978 suggested microfilaments contain active substances which might facilitate bile flow in the canalicular system of the liver, while Erlinger 1978 suggested the possibility of pump failure or a microvilli defect

or perhaps both as a possible cause of intrahepatic cholestasis.

In this study increased microfilaments in the pericanalicular zone were found around normal looking bile canaliculi and a marked increase in the microfilaments which extended to the lateral wall of the hepatocytes around the injured bile canaliculi. These findings do not rule out the early involvement of microfilaments in the intrahepatic cholestasis occurring in the advanced stage of PBC.

Ultrastructural sinusoidal changes were consistent with that of the LM findings - widening of the sinusoids, enlarged Kupffer cells, increased amount of lysosomes and bile pigment (Fig. 57). Endothelial cells were swollen and contained increased amounts of lysosomes and electron dense granules of biliary origin (Fig. 58.1). Increased numbers of mononuclear cells were present within the sinusoids and the space of Disse where they came in direct contact with degenerate hepatocytes (Figs. 60.1 and 60.2).

The space of Disse appeared filled with tissue debris and amorphous electron dense material with fine granules of biliary origin. Bundles of collagen were present in variable thicknesses suggestive of fibrogenesis in the space of Disse in the advanced stages of PBC (Fig. 58.2).

ITO cells were found occasionally and they were usually of activated form. Their lipid droplets were of a different morphological appearance to that seen in ALD. They had a medium dense granular outer band with lighter smooth centres. These lipid droplets found in the cytoplasm of the hepatocytes and in the space of Disse appeared to be picked up by both Kupffer and ITO cells. It is possible that differences in the chemical composition of the lipid occurring in PBC was responsible for this striking morphological appearance (Figs. 59.1, 59.2, 59.3 and 59.4).

Fibrosis in the space of Disse (figs. 65.1 and 65.2) and pericellular fibrosis (Fig. 66) are present in advanced stages of cirrhosis with slight widening of the intercellular spaces and few microvilli appear at the lateral border of the hepatocyte, a finding confirmed by Johannessen in 1980. While the TEM findings emphasised to some extent the findings present in LM, SEM did not show any outstanding features.

The majority of hepatocytes were arranged in a rosette shape around a sinusoid or in plates two cells thick (Figs. 68.1 and 68.2). The sinusoids were packed with debris and inflammatory cells. The space of Disse appeared narrowed and fibrous tissue was wedged between it and the hepatocytes. The bile canaliculi run along the surfaces of the hepatocytes with microvilli projecting into their lumen (Fig. 69.2). Very little pericellular fibrosis was present. Yoshino in 1979 described dilatation and sacculation of bile canaliculi occurring in PBC. These findings were not found in this study. The majority of bile canaliculi appeared of normal morphology on TEM and this was confirmed by SEM.

While scanning of the portal area showed a marked inflammatory infiltrate, it did not show the substructure of the portal tract. This was due partly to the increased amount of fibrous tissue found in the advanced stage of PBC and which was strewn over the fracture surface, making it difficult to interpret and partly due to the amount of tissue debris found covering the area (Figs. 67.1 and 67.2).

SUMMARY

Light, transmission and scanning electron microscopy has been carried out on a number of normal mouse liver specimens, on needle biopsies from 10 patients with alcoholic liver disease and from 10 patients with primary biliary cirrhosis. The ultrastructural findings in the normal mouse liver are described. In the diseased human livers there was disturbance of normal architecture and of hepatocellular surfaces, the presence of fibrosis, injury to cytoplasmic organelles, sinusoids, the space of Disse, bile canaliculi, canals of Hering and bile ducts. The findings are discussed from the basic research point of view. The application of electron microscopic techniques in diagnostic histopathology requires particular knowledge and interest in this field. Further experience on a routine basis and the use of larger sized biopsies might help to further our understanding of some of the pathogenetic mechanisms involved in these forms of liver disease.

ACKNOWLEDGEMENTS

I wish to thank Professor J.R. Anderson and Professor R.N.M. MacSween for allowing and helping me to carry out this study. I also wish to reiterate my thanks to Professor MacSween for all the support he offered me during all the problems which faced me during this project. I also thank Professor W.R. Lee for allowing me to be trained on the scanning electron microscope in the University Department of Ophthalmology.

I am grateful to Dr. G. Watkinson, Consultant Physician, and Dr. B. Goudie, Medical Registrar, at Gartnavel General Hospital, for allowing and performing the needle biopsies on their patients.

I am very grateful to Dr. I.A.R. More, Department of Pathology, and Dr. K. Carr, Department of Anatomy, for all the help and advice they offered to me during the study as well as in the layout of this thesis.

I am indebted to the staff of the Transmission Electron Microscope Unit at the Department of Pathology as well as the Scanning Electron Microscope Unit at the Department of Pathology, Western Infirmary, in particular, Margaret, Dorothy and Tom for all their valuable help, patience and support.

APPENDIX - 1

DETAILS OF PATIENTS WITH A.L.D. FROM WHOM BIOPSIES WERE STUDIED

Name, Age, Sex	Hosp. No.	Lab. No.	EM No.	Biochemical Data					Pathological Stage (L.M.)
				S.B.	A.P.	O.T.	P.T.	G.G.T.	
1) Enoch McWade, 37, (M)	709338	P83/2464	230/83	11	110	49	50	564	Fatty liver.
2) James Murdoch, 54, (M)	705529	P83/2098	182/83	8	166	31	36	110	Fatty/Hepatitis liver.
3) Hamish McMurphy, 50, (M)	551475	P83/5470	525/83	112	631	387	112	3114	Hepatitis liver.
4) Anne McFadden, 55, (F)	647069	P84/0833	72/84	11	61	25	21	N	Hepatitis liver.
5) Isobel Nielson, 51, (F)	480809	P83/2400	212/83	66	166	129	41	150	Hepatitis/Cirrhotic live
6) John Newton, 38, (M)	235839	P83/5695	532/83	15	94	64	40	305	Hepatitis/Cirrhotic live
7) Francis Hughes, 42, (M)	023802	P83/2741	263/83	78	321	110	48	582	Cirrhosis
8) Ronald Craig, 54, (M)	725918	P81/0196	372/83	12	133	54	45	366	Cirrhosis
9) Narinder Nath, 52, (M)	679675	P83/3778	373/83	23	156	59	35	280	Cirrhosis
10) Charles Mizzi, 46, (M)	7819761	P84/0978	82/84	44	N	45	N	N	Cirrhosis

Normal biochemical values

Serum Bilirubin (S.B.) : 3-18 umol/L

Alkaline Phosphatase(A.P.): 35-130 u/L

SGOT (O.T.): 10-35 u/L

SGPT (P.T.): 10-50 u/L

Serum Gamma Glutamyl Transferase (G.G.T.): 5-50 u/L

L.M. : Light microscopy.

EM : Electron microscopy.

N : Normal value.

M : Male

F : Female

APPENDIX - 2

DETAILS OF PATIENTS WITH P.B.C. FROM WHOM BIOPSIES WERE STUDIED

Name, Age, Sex	Hosp. No.	Lab. No.	EM No.	Biochemical Data					Pathological Stage (L.M.)
				S.B.	A.P.	O.T.	P.T.	G.G.T.	
1) Helga Richards, 58, (F)	745461	P83/3796	376/83	8	504	62	89	N	Pre-cirrhotic
2) Sarah Matheson, 65, (F)	653690	P83/5369	516/83	76	13	503	64	576	Pre-cirrhotic
3) Dorothy Hosie, 67, (F)	616483	P83/7586	642/83	11	590	81	76	N	Pre-cirrhotic
4) Shiela Blyth, 43, (F)	696745	P84/0977	83/84	8	116	38	65	170	Pre-cirrhotic
5) Anne Moffat, 69, (F)	621495	P83/3797	377/83	12	750	56	38	275	Cirrhosis
6) Mary Mackie, , (F)			562/83						Cirrhosis
7) Mary Morrison, 71, (F)	320107	P83/6390	580/83						Cirrhosis
8) Mathew Murray, 69, (M)	540498	P83/7308	624/83	156	465	64	88	162	Cirrhosis
9) Wilma Steele, 64, (F)	480281	P83/7972	670/83	59	554	115	76	151	Cirrhosis
10) Thomas Moffat, , (M)	700431	P83/2742	264/83						Cirrhosis

REFERENCES

1) Addison, T., Gull, W., (1851), On a certain affection of the skin- Vitiligoidea & plana, B tuberosa. Guys Hosp.Rep. 7:265-276.

2) Adler, M., Chung K.W. and Schaffner, F., (1980). Pericanalicular hepatocytic and bile ductular microfilament in cholestasis in man. Amer. Jour.Pathol. Vol.98, No.3, 1980.

3) Ashford, T.P., Porter, K.R., Cytoplasmic components in hepatic cell lysosomes. J.Cell Biol. 42:198, 1962.

4) Ballard, H., Bernstein, M., & Farrar, J.T., (1961), Fatty liver presenting as obstructive jaundice. American Journal of Medicine, 30:196-201.

5) Beckett, A.G., Livingstone, A.V. and Hill, K.R. (1961) : Acute alcoholic hepatitis. Brit.Med.J., 2:1113-1119.

6) Bensley, R.R., Hoerr, N., Studies on Cell structure by freezing-drying method: the preparation and properties of mitochondria. Anat.Rec., 60:449, (1934).

7) Berhard, W., Gautier, A., and Oberling, C. : Elements fibrillaires de nature probablement ergastoplasmic dans le cytoplasme de la cellule hepatique reveles au microscope electronique. Compt. rend. soc.biol. 145:566-569, (1951).

8) Bernhard, W., Haguenau, F., Gautier, A., and Oberling, C. : La structure submicroscopique des elements basophiles cytoplasmique dans le foie, le pancreas, et les glandes salivaires. Ztschr.Zellforsch.mikr.Anat. 37:281-300, (1952).

9) Bernuau, D., Feldman, G., Degott, C., (1981). Ultrastructural lesions of bile duct in P.B.C. Human pathology, Vol.12, No.9, pp 782-793 (1981).

10) Bhathal, P.S., Christie, G.S., A fluorescence microscopic study of

bile duct proliferation induced in guinea pigs by alpha-naphthyl isothiocyanate. Lab.Invest. 20:280-487 , (1969).

11) Bhathal, P.S., Presence of Modified fibroblast in cirrhotic livers in man. Pathology, 4:139-144 (1972).

12) Biava, C., Studies on Cholestasis, A re-evaluation of the fine structure of normal bile canaliculi. Lab.Invest. 13:840-864 (1964).

13) Birschbach, H.R., Harinasuta, U., & Zimmerman, H.J. (1974). Alcoholic steatonecrosis II. Prospective study of prevalence of Mallory bodies in biopsy specimens and comparison of severity of hepatic disease in patients with or without this histological feature. Gastroenterology 66:1195-1202.

14) Brandle, E.R., Gabbiani, G. The role of cytoskeletal and cytocontractile element in pathologic process. American Journal Pathology. Vol.110, 3:361-370 (1983).

15) Brooks, S.E.H. and Haggis, G.H. (1973) Scanning electron microscopy of rats liver. Lab.Invest. Vol.29, 1:60-64.

16) Brooks, S.E.H., Reynold, S.P., Andretsch, J.T. and Geoffrey, H., Scanning electron microscopy of proliferating bile ductules in alcoholic liver disease. A.J.C.P. March 1983, pp 326-333.

17) Boyde, A., Pros and Cons of critical point drying and freeze drying for SEM. In: Scanning electron microscopy pp 303-314, Vol.II (1978).

18) Chedid, A., Spellberg, M.A., and Debeer, R.A. Ultrastructural aspect of primary biliary cirrhosis and other type of cholestatic liver disease. Gastroenterology 67:858-869. (1974).

19) Christoffersen, P., Iversen, K., Nielsen, K., et al : Alcoholic hepatitis. A comparative study of two groups of patients with Mallory bodies with and without liver cell necrosis and neutrophilic infiltration in liver biopsies. Scand.J.Gastroent. 5:633-638, (1970).

20) Christoffersen, P., Braedstrup, O., Juhl. E., Poulsen, H., Lipogranulomas in human liver biopsies with fatty change. A morphological, biochemical and clinical investigation. Acta Pathol. microbiol. Scand. 79:150-158, (1971).

21) Christoffersen, P., Nielsen, K. : Histological changes in human liver biopsies from chronic alcoholics. Acta Pathol.Microbiol. Scand. 80:557-565, (1972).

22) Christoffersen, P., Light microscopical features in liver biopsies with Mallory bodies. Acta Pathol.Microbiol.Scand. 80:705-712.

23) Claude, A., Fullam, F.F., An electron microscope study of isolated mitochondria. J.Exper.Med., 81:51 , (1945).

24) Claude, A., Fullam, F.F., The preparation of sections of guinea pig liver for electron microscopy. J.Exper.Med., 83:499, (1946).

25) Dalton, A.J., Kahler, H., Striebich, M.J. and Lloyd, B., Finer structure of hepatic, intestinal and renal cells of the mouse as revealed by electron microscope. J.Nat.Cancer Inst., 11:439 (1950).

26) Dallner, G., Ericsson, J.L.E., Mollecular structure and Biological implication of the liver endoplasmic reticulum. In: Progress in Liver Diseases, pp 35-68 (1976).

27) Dauphinee, J.A., Sinclair, J.C. (1949) Primary Biliary Cirrhosis. Canadian Medical Association Journal, 61:1-6.

28) Drury, R.A.B. and Wallington, E.A., (1973) Carleton's histological technique (New York, Toronto). Oxford University Press

29) Echlin, P., Coating Techniques for scanning electron microscopy. In: Scanning electron microscopy pp 1019-1028 , (1974).

30) Edmonson, H.A., Peters, R.L., Reynolds, T.B. and Kuzma, O.T., Sclerosing hyaline necrosis of the liver in the chronic alcoholic: a recognizable syndrome, Ann.Int.Med., 59:646-673 (1963).

31) Edmondson, H.A., Peters, R.L., Frankel, H.H. and Borowsky, S., The early stage of liver injury in the alcoholic. Medicine, 46:119-129 , (1967).

32) Elias, H., A re-examination of the structure of mammalian liver. I. Parenchymal architecture. American Journal of Anatomy, 84:311-334 (1949a).

33) Elias, H., A re-examination of the structure of mammalian liver. II. The hepatic lobule and its relation to the vascular and biliary system. American Journal of Anatomy, 85:379-456 (1949b).

34) Erlinger, S. (1978). Cholestasis: Pump failure, microvilli defect, or both. In: The Lancet, March 11, 1978, pp 533-534.

35) Essner, E., Novikoff, A., Human hepatocellular pigments and lysosomes. J.ultrastructure Res. 3:374-391, (1960).

36) Fawcett, D.W., Observations on the cytology and electron microscopy of hepatic cells. J.Nat.Cancer Inst. 15:1475-1502 (1955).

37) Fawcett, D.W., The cell, its organelles and inclusions. An Atlas of fine structures.

38) French, S.W., Davies, P.L., Carr, B.N., The nature of Mallory body filaments. Lab.Invest. 30:374a , (1974).

39) Farquhar, M.G. and Palade, G., Junctional complexes in various epithelia. J.Cell Biol. 17:375-412 (1963).

40) Farquhar, M.G., and Palade, G., Cell junctions in amphibian skin. J.cell Biol. 26:263-291 (1965).

41) Galambos, J.T., Alcoholic hepatitis: its therapy and prognosis. In: Progress in Liver Diseases, Vol.4, ed. Popper, F.Schaffner (1972).

42) Galambos, J.T., Shapira, R., : Natural history of alcoholic hepatitis: IV.Glycosaminoglycuronans and collagen in hepatic connective tissue. J.Clin.Invest. 1973. 52:2952-2962.

43) Galambos, J.T., The course of alcoholic hepatitis. In: Alcoholic Liver Pathology. eds.Khanna, J.M., Israel,Y., Kalant H., Toronto: Addiction Research Foundation of Ontario, 1975:97-111.

44) Gang, H., Lieber, C.S., Rubin, E., Aniline hydroxylase microassay suitable for needle biopsy specimens : effects of phosphate and pyrophosphate on aniline hydroxylation. J.pharmacol.Exp.Therap. pp 183-218 , (1972).

45) Gerber, M.A., Popper, H. Relation between central canals and portal tracts in alcoholic hepatitis: A contribution to the pathogenesis of cirrhosis in alcoholics. Human Pathol.1972, 3:199-207.

46) Gerber, M.A., Orr, W., Denk, H., Schaffner, F. and Popper, H., (1973). Hepatocellular Hyaline in cholestasis and cirrhosis; Its diagnostic significance. In: Gastroenterology Vol.64, No.1, pp 89-97, 1973.

47) Glauert, A.M., (1974), The Fixation, dehydration and embedding of biological specimens. In: Practical methods in electron microscopy. ed.A.M.Glauert (North-Holland, Amsterdam).

48) Glauert, A.M. and Glauert,R.H., Araldite as an embedding medium for electron microscopy. J.biophys.biochem.cytol.4, 191 (1958).

49) Goldfischer, S., Ma,M.H., Biempica,L., Morphology of the Normal Liver Cell. In: Progress in Liver Diseases. ed.Popper,H., Schaffner,F., Vol.IV, pp 1-17 (1972).

50) Golding, P.L., Brown, R., Mason, A.M.S., Taylor,E. "sicca complex" in liver disease. Br.Med. 79:31-36 (1974).

51) Goudie, R.B., Macsween, R.N.M., Goldberg , D.M. : Serolological and histological diagnosis of primary biliary cirrhosis. J.Clin.Pathol. 19:527-538 (1966).

52) Grisham, J.W., Nopanitaya,W. and Compagno, J., Scanning electron microscopy of the liver diseases. eds.H.Popper, F.Schaffner, Vol.V pp 1-21. New York : Grune and Stratton (1976a).

53) Grisham, J.W., Nopanitaya, W., Compagno, J. & Nagel, A.E.H., Scanning electron microscopy of normal rat liver: the surface structure of its cells and tissue components. American Journal of Anatomy, 144, 295-322 (1976b).

54) Hadziyannis, S., Scheuer, P.J., Feizi, T., Naccarato, R., Doniach, D., Sherlock, S., : Immunological and histological studies in primary biliary cirrhosis. J.Clin.Pathol. 23:95-98 (1970).

55) Hering, E., Ueber den Bau der wirbelthierleber. Arch f mikr Anat.3, 88-114,(1867).

56) Hruban, Z., Swift, H., Uricase: Localisation in hepatic microbodies. Science 146:1316-1317 (1964).

57) Humphreys, W.J., Henk, W.G., Ultrastructure of cell organelles by scanning electron microscopy of thick sections surface-etched by an oxygen plasma. In: Journal of microscopy, Vol.116, pp 225-264 (1979).

58) Humphreys, W.J., Spurlock, B.O., Johnson, J.S. , Critical point drying of ethanol- infiltrated, cryofractured biological specimens for scanning electron microscopy. In: Scanning electron microscopy Part 1, pp 275-282 (1974).

59) Ito, T., Shibasaki, S. : Electron microscopic study of the hepatic sinusoidal wall and fat-storing cells in the normal human liver. Arch.Histol.Jap. 29:137-192 (1968).

60) Iseri, O.A., Lieber, C.S., Gottlieb, L.S., The ultrastructure of fatty liver induced by prolonged ethanol ingestion. American Journal of Pathology, 48:535-555 (1966).

61) Johannessen, J.V., The Liver. Electron Microscopy in Human Medicine. Vol.8, pp 89-95 (1979).

62) Jensen, O.A. and Prause, J.U. Frozen resin cracking, dry-cracking and enzyme digestion. Methods in SEM as applied to occular tissues. In: eye Path.Inst.Univer.of Copenhagen.

63) Jones, A.L., Schmucker, D.L., Current concepts of liver structure as related to function. In: Progress in hepatology. Gastroenterology 73:833-851 (1977).

64) Joy, D., The Scanning electron microscope principles and application. In: Scanning electron microscopy, Vol.II, pp 743-750 (1973).

65) Kent, G., Steffen, G., Inonye,T., Bahu,R., Minick,O.T., Popper,H., Vitamin A-containing lipocytes and formation of type III collagen in liver injury. In: Proc.Natl.Acad.Sci.Vol.73, 10:3719-3722 (1976).

66) Kew, M.C., Varma, R.R., Dos Santos, H.A., Scheuer, P.J., Sherlock,S.: Portal hypertension in primary biliary cirrhosis. Gut 12:830-834, (1971).

67) Kimbery, D.V. and Loeb, J.N. (1972) The effects of cortizone administration on rat liver mitochondria. Journal of Cell biology, Vol.55, p 635.

68) Kiernan, F. , The anatomy and physiology of the liver. Philosphical Transactions of the Royal Society of London, Series B, 123:711-770 , (1833).

69) Kirn, A., Gut, J-P., Gendrault, J-L., Interaction of viruses with sinusoidal cells. In: Progress in Liver diseases. Vol.V, pp 377-388 (1976).

70) Klatskin, G., The role of alcohol in the pathogenesis of cirrhosis. Yale Journal of Biology and Medicine, 26:23-37 (1967).

71) Laennec, R.T.H., Traite de l auscultation mediate et des maladies des poumons et du coeur, 2nd.edn., ed.Chaude, T.T. pp 196-197, Paris (1826).

72) Lane, B.P., Lieber, C.S. Effects of butylated hydroxytoluene on ultrastructure of rat hepatocytes. Lab.Invest. 16:341-348 (1967).

73) Lelbach, W.K. Liver damage from different alcoholic drinks. German Medical Monthly. 92:233-238 (1967).

74) Lelbach, W.K., Dose-effect relationship in alcohol-induced liver damage. German Medical Monthly 2:116-118 (1972).

75) Lieber, C.S., De Carli, L.M., Hepatic microsomal ethanol oxidising system. In vitro characterstics and adaptive properties in vivo. Journal of Biological Chemistry, 245:2505-2512 (1970a).

76) Lieber, C.S., De Carlie, L.M., Reduced nicotinamide adenine dinucleotide phosphate oxidase: Activity enhanced by ethanol consumption. Science, 170:78-79 (1970b).

77) Lieber, C.S., De Carlie, L.M. Effect of drug administration on the activity of the hepatic microsomal ethanol oxidising system. Life Sciences, Part II, 9:267-276 (1970c).

78) Lewis, E.R., Nemanic, M.K., Critical point drying techniques. Scanning electron microscopy pp. 767-774 (1973).

79) Lewis, E.R., Knight, D.P. Staining methods for section materials. Practical methods in electron microscopy .
pp 25-27 ed. Glauert, A.M. (North Holland, Amsterdam), (1974).

80) Macsween, R.N.M., Mallory's hyaline in primary biliary cirrhosis. J.Clin.Pathol. 26:340-342 (1973).

81) Macsween, R.N.M., Galbraith, I., Thomas, M.A., Watkinson, G., Ludlam, G.B., Evidence of impaired cell-mediated immunity. Clin.Exp.Immunol. 15:35-42 (1973).

82) Macsween, R.N.M., Alcoholic liver disease, Recent Advances in Histopathology. No.10, eds. P.P.Anthony, N.Woolf. Edinburgh, Churchill Livingstone, pp 193-221, 1978.

83) Macsween, R.N.M., Scothorne, R.J., Developmental anatomy and normal structure. Pathology of the liver. eds.R.N.M.Macsween,P.P.Anthony, P.J.Scheuer, pp 1-30 . Churchill Livingstone (1979).

84) Macsween, R.N.M. primary biliary cirrhosis. Pathology of the liver. Churchill Livingstone, Edinburgh

eds. R.N.M.Macsween, P.P.Anthony, P.J.Scheuer, 1:206-314 (1979).

85) McGee, T.O., Patrick, R.S. The role of perisinusoidal cells in hepatic fibrogenesis. An electron microscopic study of acute carbon tetrachloride liver injury.
In: Lab.Invest. Vol. 26, No.4, pp 429-440 (1972).

86) McCuskey, R.S., A dynamic and static study of hepatic arterioles and hepatic sphincters. Amer.J.Anat. 119:455-478 (1966).

87) Mak, K.M., Lieber, C.S., Ultrastructural changes of lipocytes and endothelial fenestrations in livers of baboons fed alcohol. Hepatology, Vol.3, 5:801 (1983).

88) Masuko, K., Rubin, E. & Popper, H. , Proliferation of bile ducts in cirrhosis. Archives of Pathology 78:421-431 (1964).

89) Matsuda, Y., Lieber, C.S., ultrastructure of perivenular sclerosis in alcoholic liver injury in the baboon.
Gastroentero.Vol.76, 5:1292 (1979).

90) Mayer, S., Anat.Anz. 16, 180 (1899).

91) Mall, F.P., A study of the structural unit of the liver. American Journal of Anatomy, 5:227-308 (1906).

92) Malpighi, M., (1666) quoted by Rappaport (1976).

93) Matter, A., Orci, L., Rouiller, C., A comparative study of freeze-etch replicas and Thin sections of Rat liver.
Ultrastructure Research, 35, (1971).

94) Minato, Y., Hasumura, Y., Takeuchi, J., The role of fat-storing cells in Disse Space fibrogenesis in alcoholic liver disease.
Hepatology, Vol.3, 4:559-566 (1983).

95) Minot, C.S., Proc.Boston Soc. Nat.Hist. 29,185 (1900).

96) Miyai, K., and Hardison, W.G., (1979). Bile duct ligation (Vs) Retention of bile: Pericanalicular microfilaments form bundle only with bile ligation. In: Gastroenterology Vol.76, No.5, p 1292.

97) Motta, P. Fumagalli, G., Structure of rat bile canaliculi as revealed by scanning electron microscopy. Anat.Rec.182, 499-514 (1975).

98) Murata, K., Okudarra, M., & Akashio, K., Mast cells in human liver tissue. Increased mast cell number in relation to the components of connective tissue in the cirrhotic process. Acta Dermato-Venereologica, Suppl. 73:157-165 (1973).

99) Nopanitaya, W., Grisham, J., and Lesensne, H., (1977). A preliminary assessment of the use of scanning electron microscopy for diagnostic evaluation of liver biopsy. In: Scanning electron microscopy. Vol.II, pp 159-170, (1977).

100) Okahoue, T., Burbige, E., French, S., (1983). The role of the ITO cell in perivenular and intralobular fibrosis in alcoholic hepatitis. Arch.Pathol.Lab.Med.Vol. 107, Sept. 1983.

101) Pequignot, G., The role of alcohol in the aetiology of liver cirrhosis. 103:1464-1468 (1961).

102) Phillips, M.J., ODA,M., Mak,E., Fisher, M.M. and Jeebloy, K.N., Microfilament dysfunction as a possible cause of Intra-hepatic cholestasis. In: Gastroenterology Vol.69, pp 48-58, (1975).

103) Phillips, M.J., ODA,M., and Funatsu, K., Evidence for microfilament involvement in Norethandrolone induced intrahepatic cholestasis. In: Ann. J. Pathol. Vol. 93, No.3 , (1978).

104) Popper, H., Szanto, P.B., Fatty liver with hepatic failure in alcoholics. Journal of the Mount Sinai Hospital, 24:1121-1131, (1957).

105) Porter, K.R.: Electron microscopy of basophilic components of cytoplasm. J.Histochem. & Cytochem. 2:346-375, (1954).

106) Porter, K.R., Blum, J., A study in microtomy of electron microscopy. Anat.Rec. 117:685-712 (1953).

107) Pequignot, G., Die Rolle des alkohols bei der Aetiologie von Leberzirrhosen in Frankreich. Munchener Medizinische Wochenschrift, 103: 1464-1468 (1961).

108) Rappaport, A.M., Borowy, Z.L., Lougheed, W.M., Lotto, W.N., Subdivision of hexagonal liver lobules into a structural and functional unit; role in hepatic physiology and pathology. Anat.Rec. 119:11-34 (1954).

109) Reynolds, T.B., Hidemura, R., Michel, H. and Peters, R. : Portal hypertension without cirrhosis in alcoholic liver disease. Ann.Int.Med.: 70:497-506 (1969).

110) Rojkind, M., Martinez-Palomo. Increase in Type I and Type III collagens in human alcoholic liver cirrhosis. Proc. Natl.Acad.Sci.USA 73:539-543 (1976).

111) Rouiller, C., Les canalicules biliares. Acta Anat. (Basel), 26:94-109 (1956).

112) Rouiller, C., Bernhard, W., Microbodies and the problem of mitochondrial regeneration. J.Biophys.Biochem.Cytol. (suppl.)2:355-360.

113) Reid, N., Choice of section thickness. Practical methods in electron microscopy and ultramicrotomy. pp. 296-299 (1975).

114) Rubin, E., Schaffner, F., Popper, H., Primary biliary cirrhosis (chronic non-suppurative destructive cholangitis). Am.J.Pathol. 46:387-407 (1965).

115) Rubin, E., Lieber, C.S., Early fine structural changes in human liver induced by alcohol. Gastroenterology Vol.52, 1:1-13 (1967).

116) Rubin, E., Lieber, C.S., Alvares, A.P., Levin, W., Kuntzman, R., Ethanol binding to hepatic microsomes: Its increase by ethanol consumption. Biochemical Pharmacology 20:229-231 (1971).

117) Schaffner, F., Popper, H., Electron microscopic studies of normal and proliferated bile ductules. Am.J.Pathol.1961 , 38:393-410.

118) Schaffner, F., Popper, H., Capillarisation of hepatic sinusoids in man. Gastroenterology 44:239-242 (1963).

119) Schaffner, F., Popper, H., Electron microscopy of human liver disease. Modern Trends in Pathology. ed.Crawford, T., Vol.2 , pp 252-300 London: Butterworth.

120) Schaffner, F.M.D., Popper, H., Alcoholic hepatitis in the spectrum of ethanol-induced liver injury. Scand.J.of Gastroenterology (suppl.) 7:69-78 (1970).

121) Schaffner, F., Popper, H., Electron microscopy of the liver. pp 50-83. Diseases of the liver. L.Schiff ed.Lippincott Publ., Philadelphia (1972).

122) Scheuer, P.J., Techniques. Liver biopsy interpretation. 2:8-14. ed. P.J.Scheuer, 3rd edition, Baillier Tindal, London (1981).

123) Shikata, T., Uzawa, T., Yoshiwara, N., Akatsuka, T. & Yamazaki, S., Staining methods of Australia antigen in paraffin section-detection of cytoplasmic inclusion bodies. Jap.J.of Experimental Medicine. 44:25-36 (1974).

124) Sherlock, S., The presentation and diagnosis of 100 patients with primary biliary cirrhosis. The liver and its diseases. ed. Schaffner, F., Sherlock, S., & Leevy, C.M., New York: Intercontinental Medical Book Corporation (1976).

125) Uchida, T., Peter, R.L., The nature and origin of proliferated bile ductules in alcoholic liver disease. American Journal of Clin. Pathol., Vol.79, 3:326-333 (1982).

126) Viel, B., Donoso, S., Salcedo, D., Rojas, P., Varela, A., & Alessandri, R., Alcoholism and socioeconomic status, hepatic damage and arteriosclerosis. Archives of Internal Medicine, 117:84-91.

127) Wisse, E., An ultrastructural characterisation of the endothelial cell in the rat liver sinusoid under normal and various experimental

conditions, as a contribution to the distinction between endothelial and Kupffer cells. J.Ultrastructurct.Res. 38:528-562 (1972).

128) Yoshino, K. (1979), Scanning electron microscopy of the primary biliary cirrhosis.
In: Scanning electron microscopy (1979)M Vol.III, pp 697-704.

129) Zeegan, R., Stansfeld, A.G., Dawson, A.M., Hunt, A.H. : Bleeding oesophageal varices as the presenting feature in primary biliary cirrhosis. Lancet, 2:9-13 (1969).

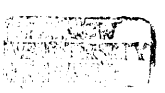

FIGURE 20.2

TEM of alcoholic hepatitis. Hepatocyte showing three spheroidal giant mitochondria with high electron density matrix. Note the presence of dense bodies or paracrystalline inclusions within the mitochondria. (X 6450)

FIGURE 20.3

TEM of alcoholic hepatitis. Shows part of a hepatocyte in which a bizarre shaped mitochondria is seen. Note the close apposition of smaller mitochondria to the giant one. (X 22050)

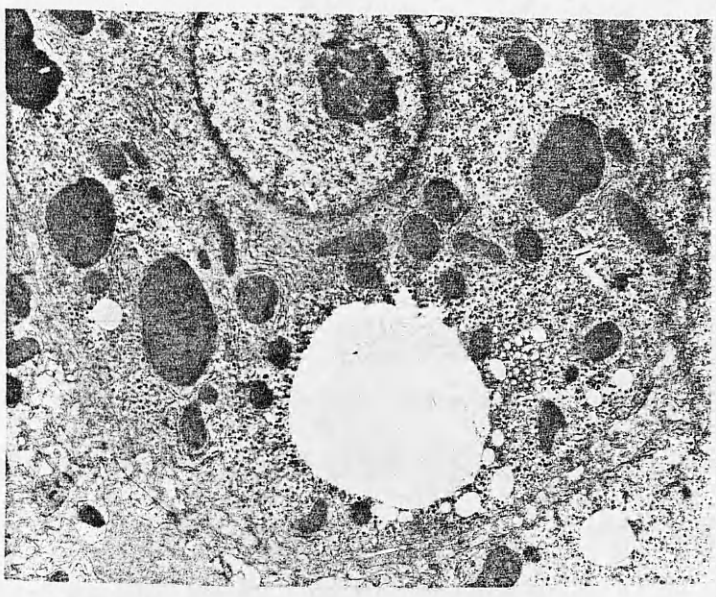

Above : Figure 20.2

Below : Figure 20.3

FIGURE 20.4

TEM of alcoholic hepatitis. Shows a giant mitochondria (gm) fused to the adjacent thinner segment of another smaller mitochondrion. Note the giant mitochondrion displayed a striking paracrystalline inclusions and several dense bodies. (X 16870)

FIGURE 20.5

TEM of alcoholic hepatitis. Shows high magnification micrograph of the paracrystalline inclusions (pi) illustrating its geonatrical arrangement. (X 220500).

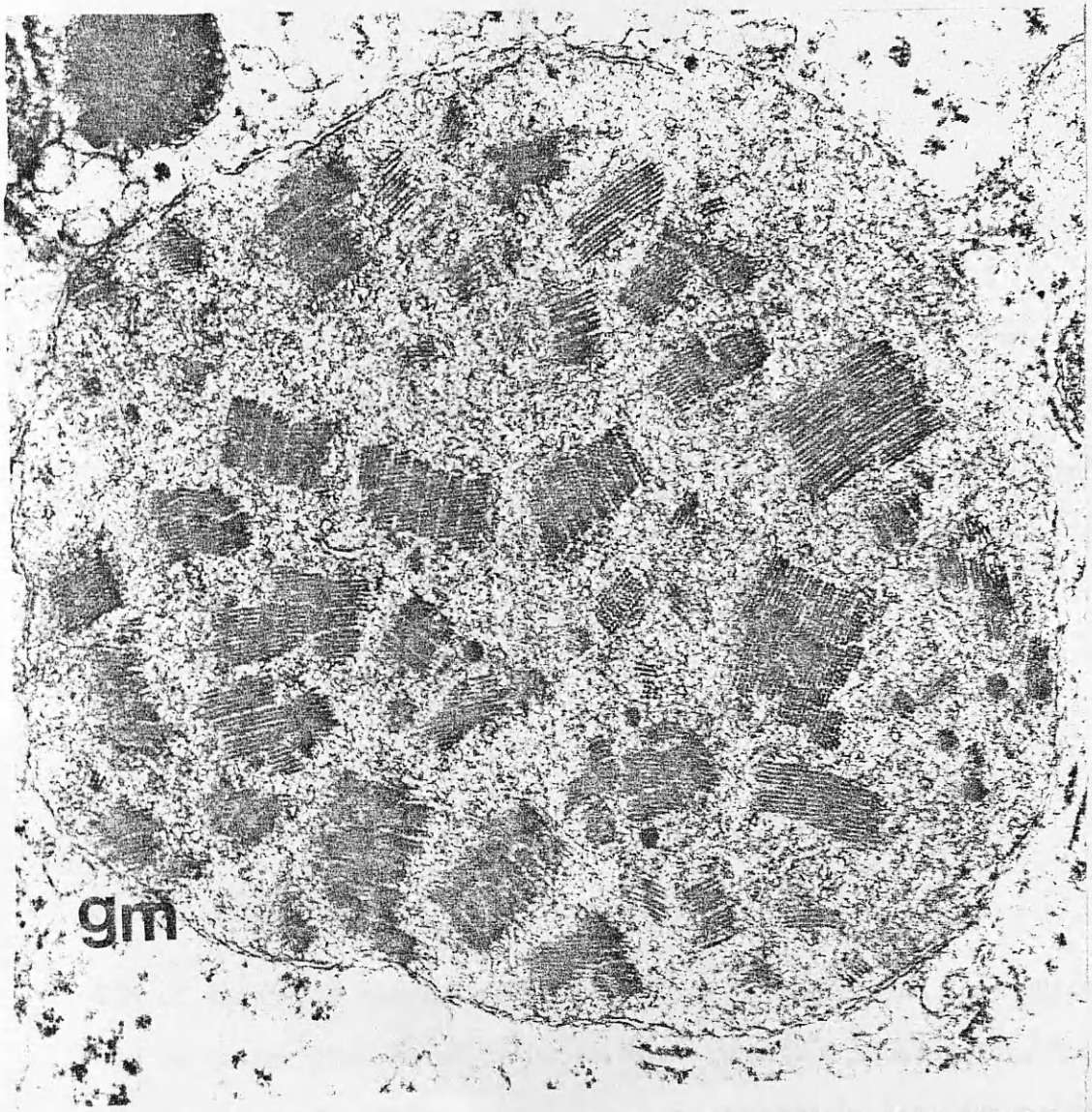

Above : Figure 20.4

Below : Figure 20.5

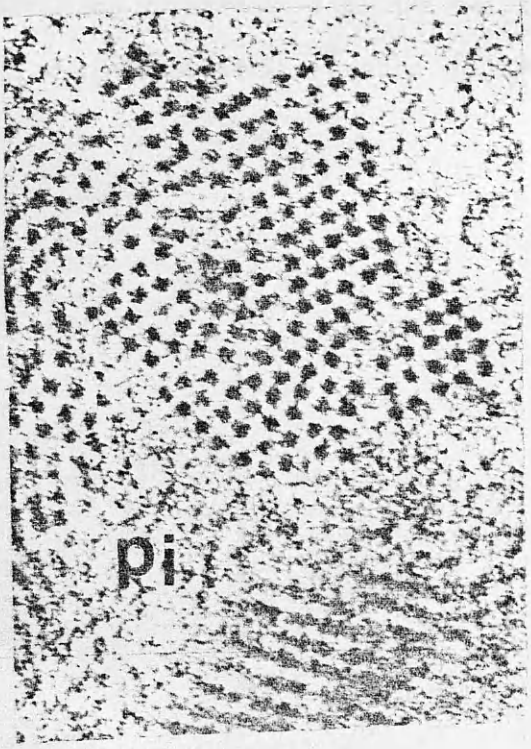

FIGURE 20.6

TEM of alcoholic hepatitis. Shows a giant mitochondrion (gm) displaying paracrystalline inclusion dense bodies and may-be lipid vacuoles. Note many smaller mitochondria in close apposition to each other (arrows). Others assume a drum-stick appearance. (X 9675)

FIGURE 20.7

TEM of alcoholic hepatitis. Shows a giant mitochondrion (gm) which may be in the process of fusion to the adjacent mitochondrion. Note the presence of numerous lipid vacuoles, paracrystalline inclusions, dense bodies and dilated rough endoplasmic reticulum (rer). (X 22050)

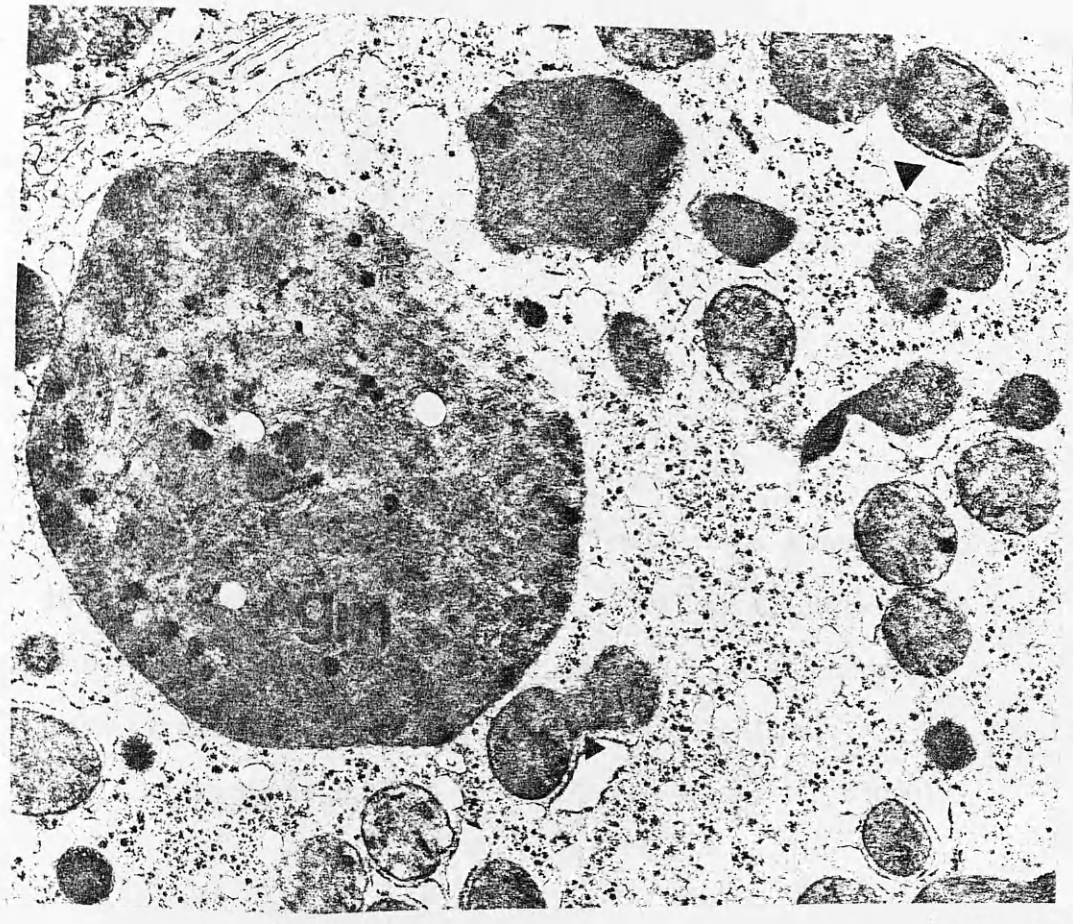

Above : Figure 20.6

Below : Figure 20.7

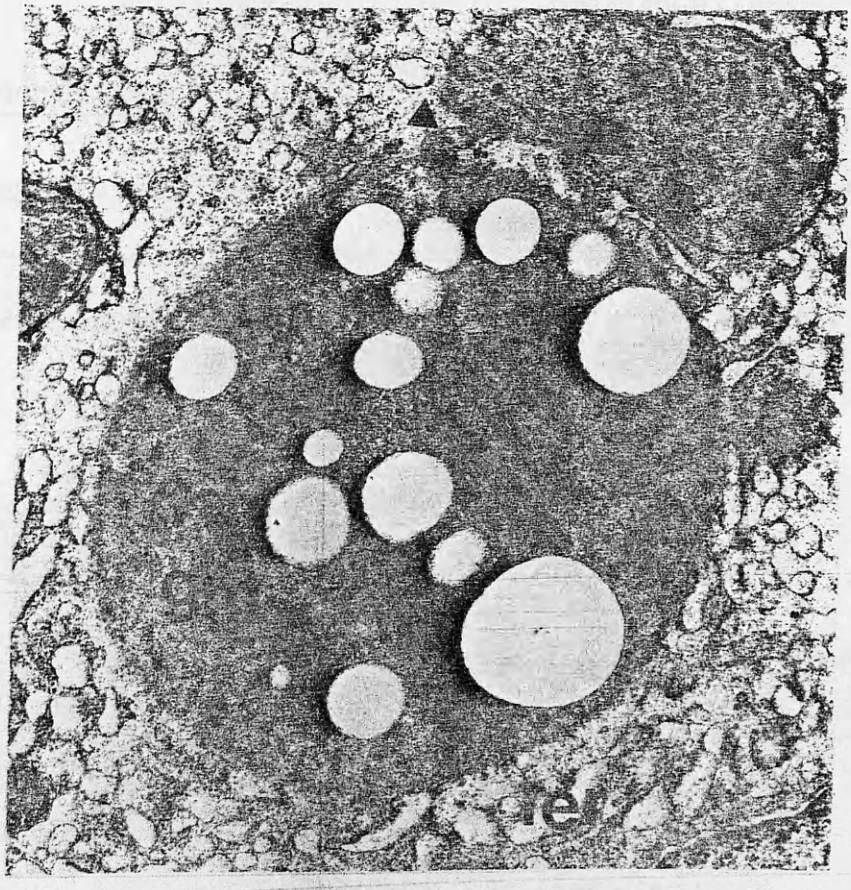

FIGURE 21.1

TEM of alcoholic hepatitis. Part of hepatocyte shows alcoholic hyaline (Mallory body , mb) with fibrillar structure. The insert shows details of the branching fibrils which cross each other. Some of them present in cross-section.
(Main micrograph: X 13275 . The Upper insert : X 63000)

FIGURE 21.2

TEM of alcoholic hepatitis. Alcoholic hyaline shows some microfilament which appeared as tubular striation. Note the condensed mitochondria adjacent to mitochondrion (m) with transverse cristae. (X 40500)

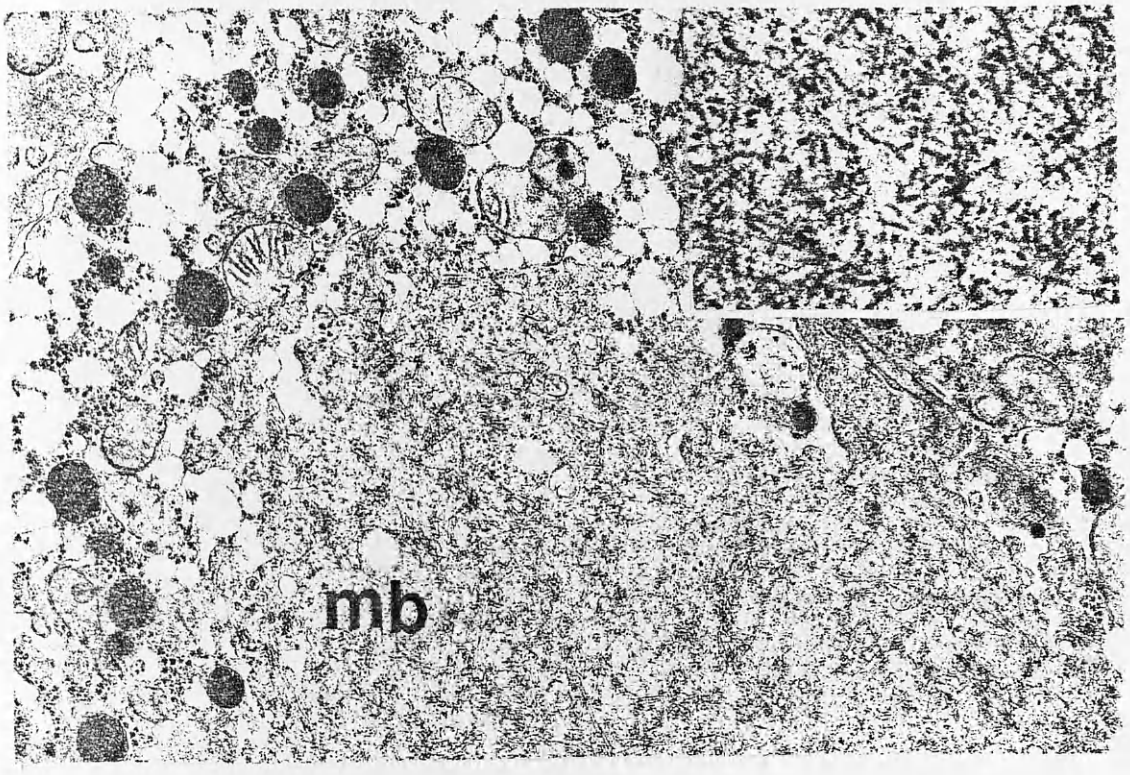

Above : Figure 21.1

Below : Figure 21.2

FIGURE 22.1

TEM of alcoholic hepatitis. Shows a prominent stack of Golgi complexes (gi) adjacent to normal bile canaliculi. Note the penta-laminar structure and the presence of many tonofilaments running parallel to and fusing with the desmosomes (d). (X 40500)

FIGURE 22.2

TEM of alcoholic hepatitis. Shows adjacent part of hepatocytes, dilated bile canaliculi (bc) with outpouches toward the cytoplasm. Only few stunted microvilli are present. Note the thickness of the pericanalicular ectoplasm with evident filament materials. (X 22050)

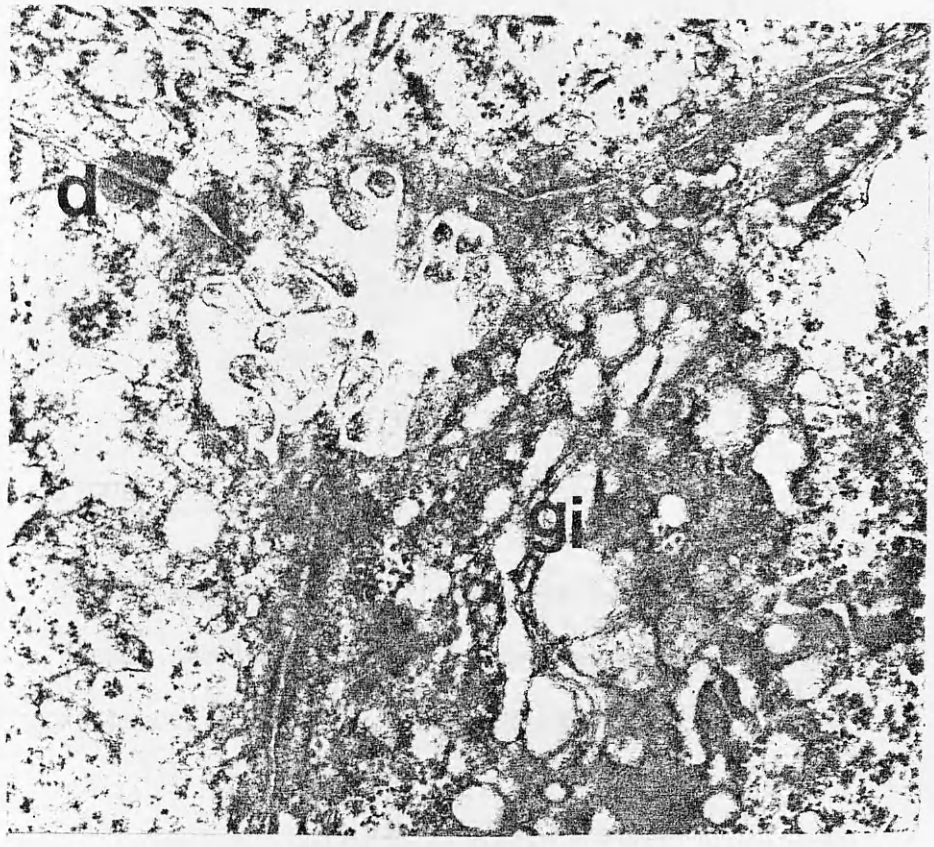

Above : Figure 22.1

Below : Figure 22.2

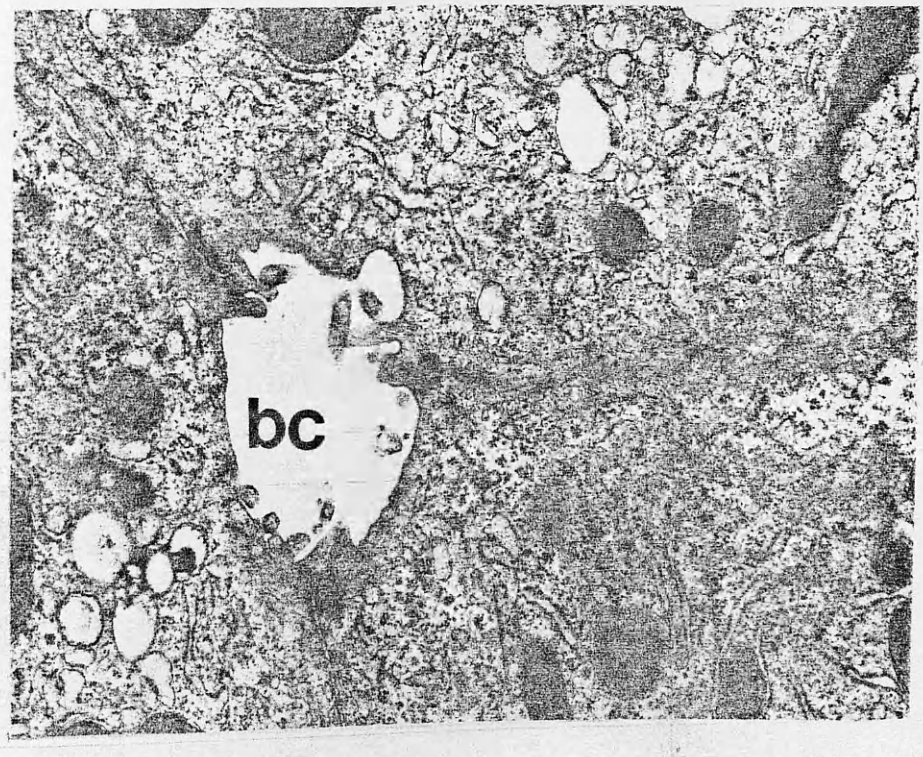

FIGURE 23.1

TEM of alcoholic hepatitis. Shows hepatic sinusoids (s) filled with tissue debris. Neutrophils (ne) are evident within the lumen. Note a slender bundle of collagen in the space of Disse. (X 6300)

FIGURE 23.2

TEM of alcoholic hepatitis. Two lymphocytes (lm) seen within hepatic sinusoid. One lymphocyte appeared in close apposition to the cytoplasm of the hepatocyte and separated only by thin wall. (X 6300)

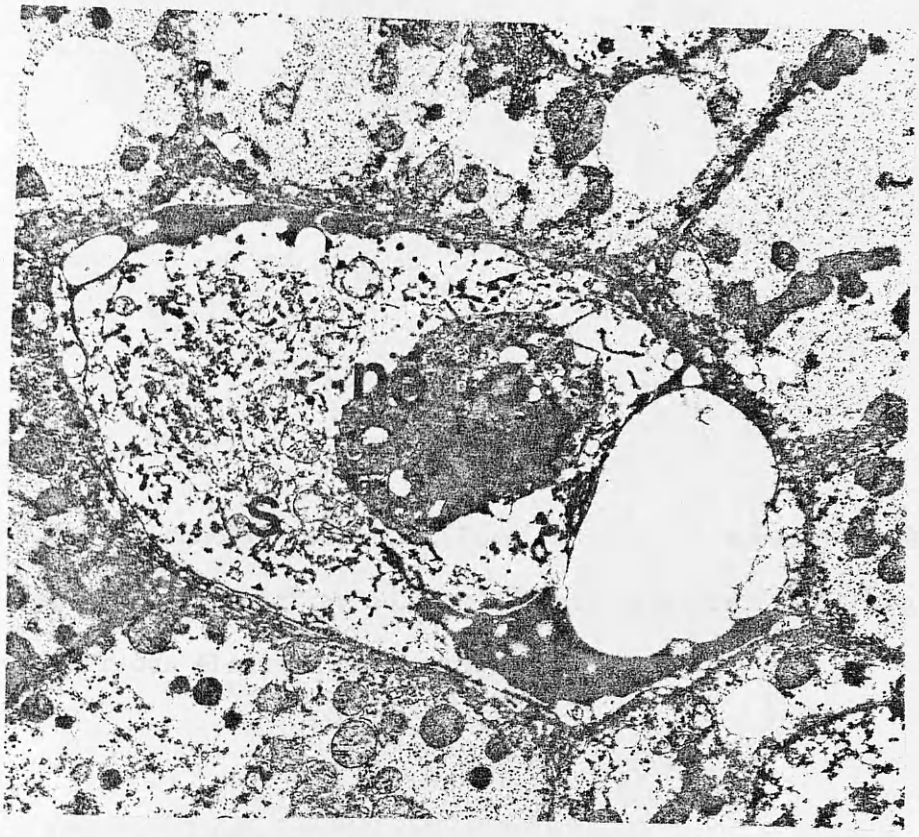

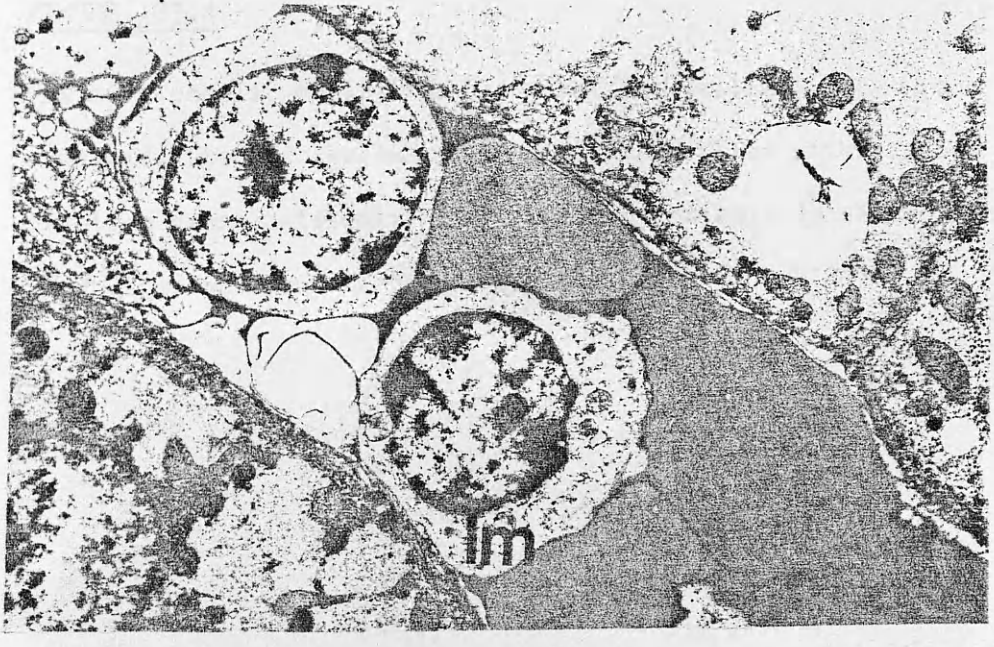

Above : Figure 23.1

Below : Figure 23.2

FIGURE 23.3

TEM of alcoholic hepatitis. Hepatic sinusoid shows a lymphocyte (lm) and probably Kupffer cell (k). Their cytoplasm is filling with lysosomes of various electron dense material. (X 4950)

FIGURE 23.4

TEM of alcoholic hepatitis. Shows Kupffer cell (k) filling the hepatic sinusoid. The endothelial cells (ed) are swollen with various size electron dense materials within their cytoplasm. Spaces of Disse are shown thickened and devoid of microvilli. (X 8100)

Above and Middle : Figure 23.3

Below : Figure 23.4

FIGURE 24.1

TEM of alcoholic hepatitis. Shows resting Ito cell (rit). The cytoplasm is filled with lipid droplets with few deformed mitochondria. Sinusoid contains RBCs and Kupffer cell (k). Note the thin bundle of collagen lying between the Ito cell and the cytoplasm of the hepatocyte (h). (X 5400)

FIGURE 24.2

TEM of alcoholic hepatitis. Shows hepatic sinusoid with Kupffer cell (k). Activated Ito cell (ait) seen in the space of Disse with few lipid droplets and a small smooth contour of the nucleus. Note the electron-dense amorphous material around the cell. (X 9950)

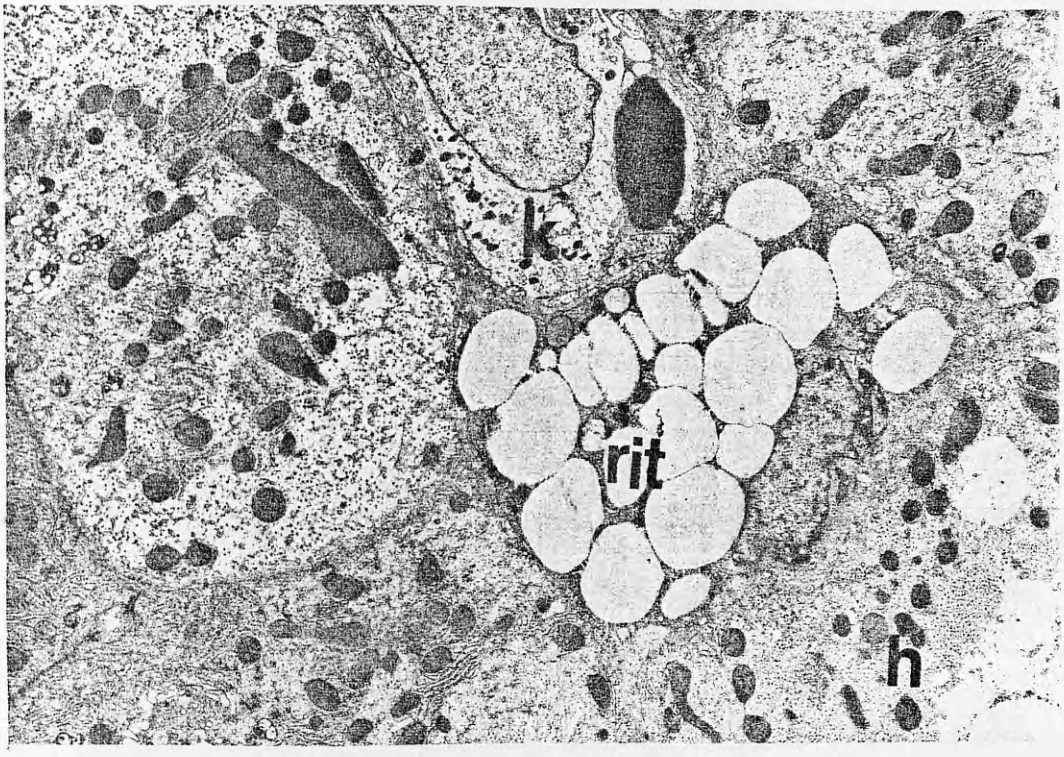

Above : Figure 24.1

Below : Figure 24.2

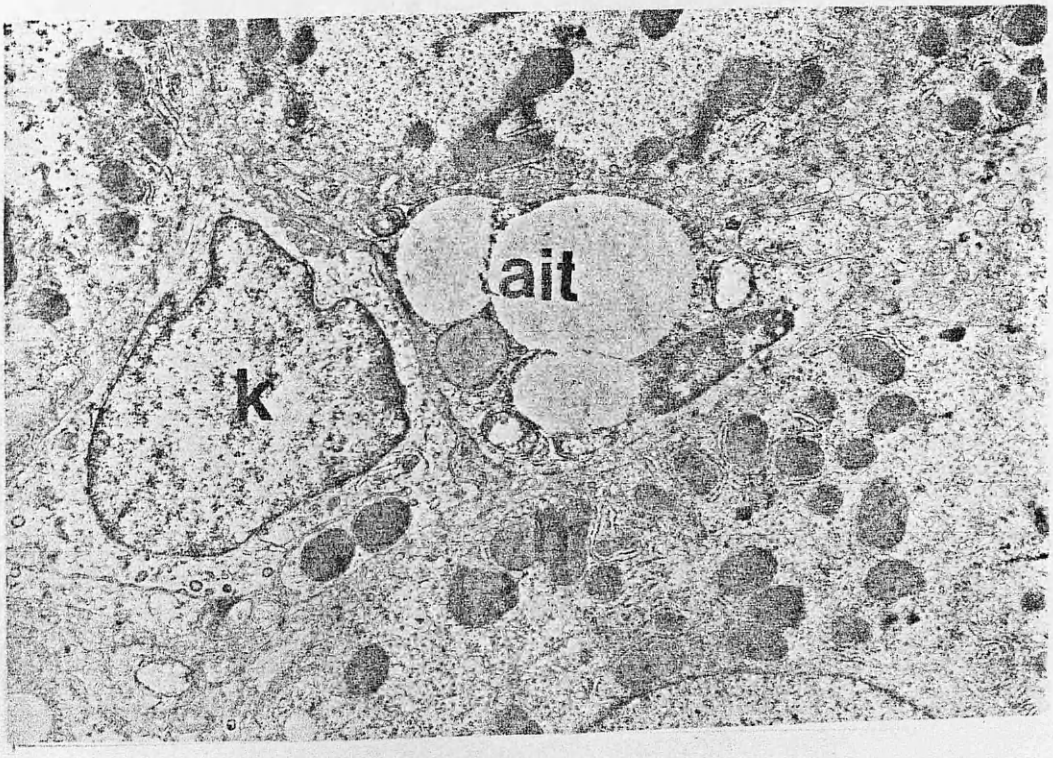

FIGURE 24.3

TEM of alcoholic hepatitis. Shows Ito cell (it) in the perisinusoidal space of Disse with marked dilatation of endoplasmic reticulum. (X 9950)

FIGURE 24.4

TEM of alcoholic hepatitis. Shows high magnification micrograph illustrating details of dilated rough endoplasmic reticulum (rer) with few ribosomes attached to them.(ds : Disse space).(h : hepatocyte) (X 14700)

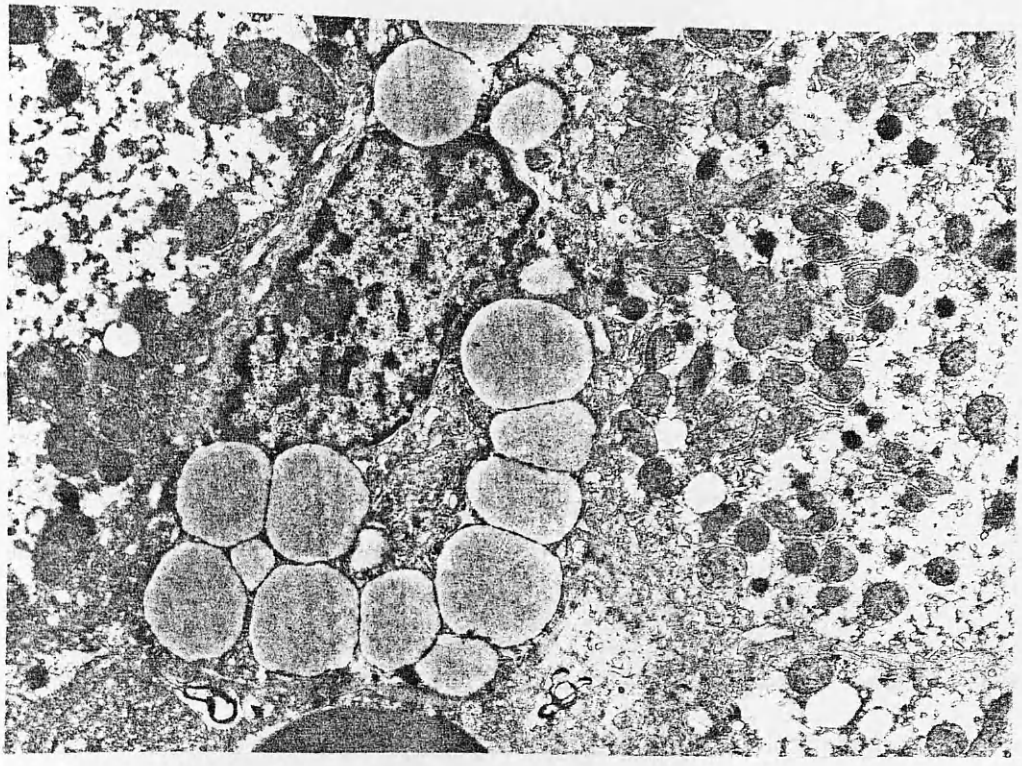

Above : Figure 24.3

Below : Figure 24.4

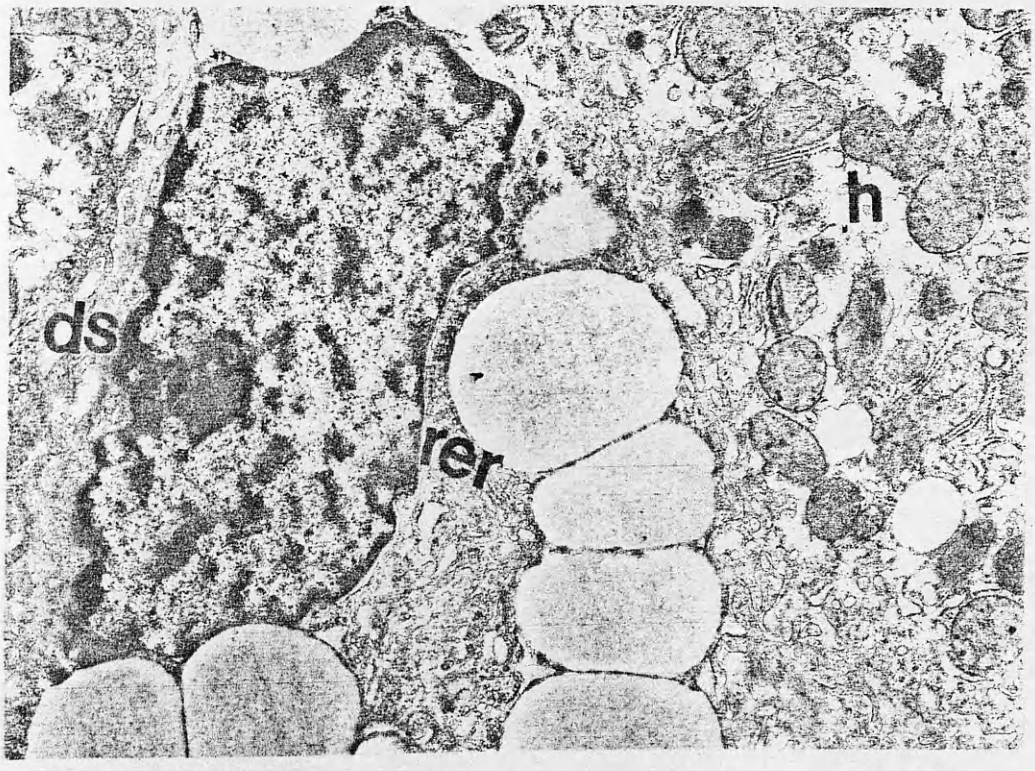

FIGURES 24.5 & 24.6

TEM of alcoholic hepatitis. Shows part of adjacent hepatocytes and activated Ito cell (ait). The cell lie in close apposition to the cytoplasm of hepatocyte (h) which show various amount of lysosomes and dense inclusion probably old coiled Mallory body. Note the collagen bundle (co) adjacent to Ito cell.

(Fig. 24.5 X 9300) . (Fig. 24.6 X 22050).

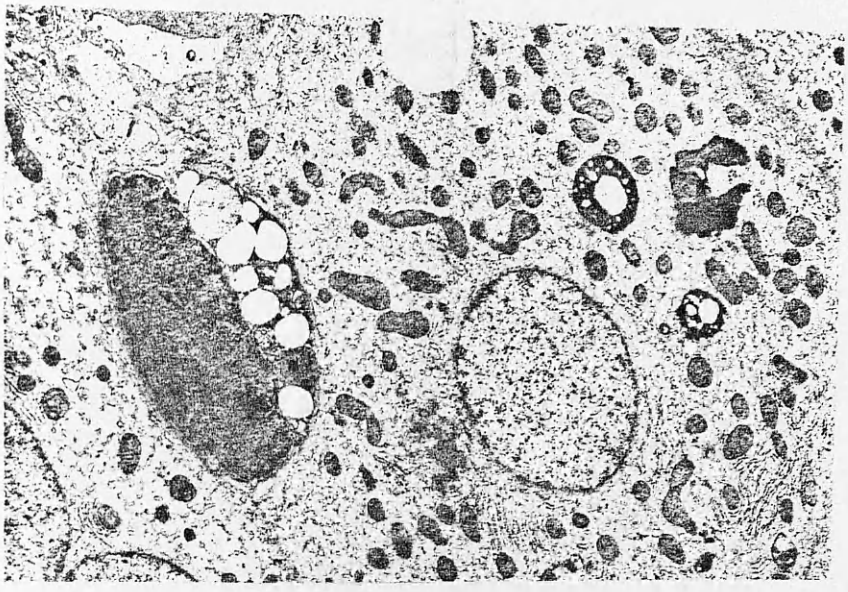

Above : Figure 24.5

Below : Figure 24.6

FIGURE 24.7

TEM of alcoholic hepatitis. Shows high magnification micrograph of activated Ito cell (ait). The nucleus has a smooth margin and few lipid droplets seen. Note the microvesicular bodies (mvb) around the cell and many slender bundles of collagen fibres (co) in close apposition to these cells. (X 22050)

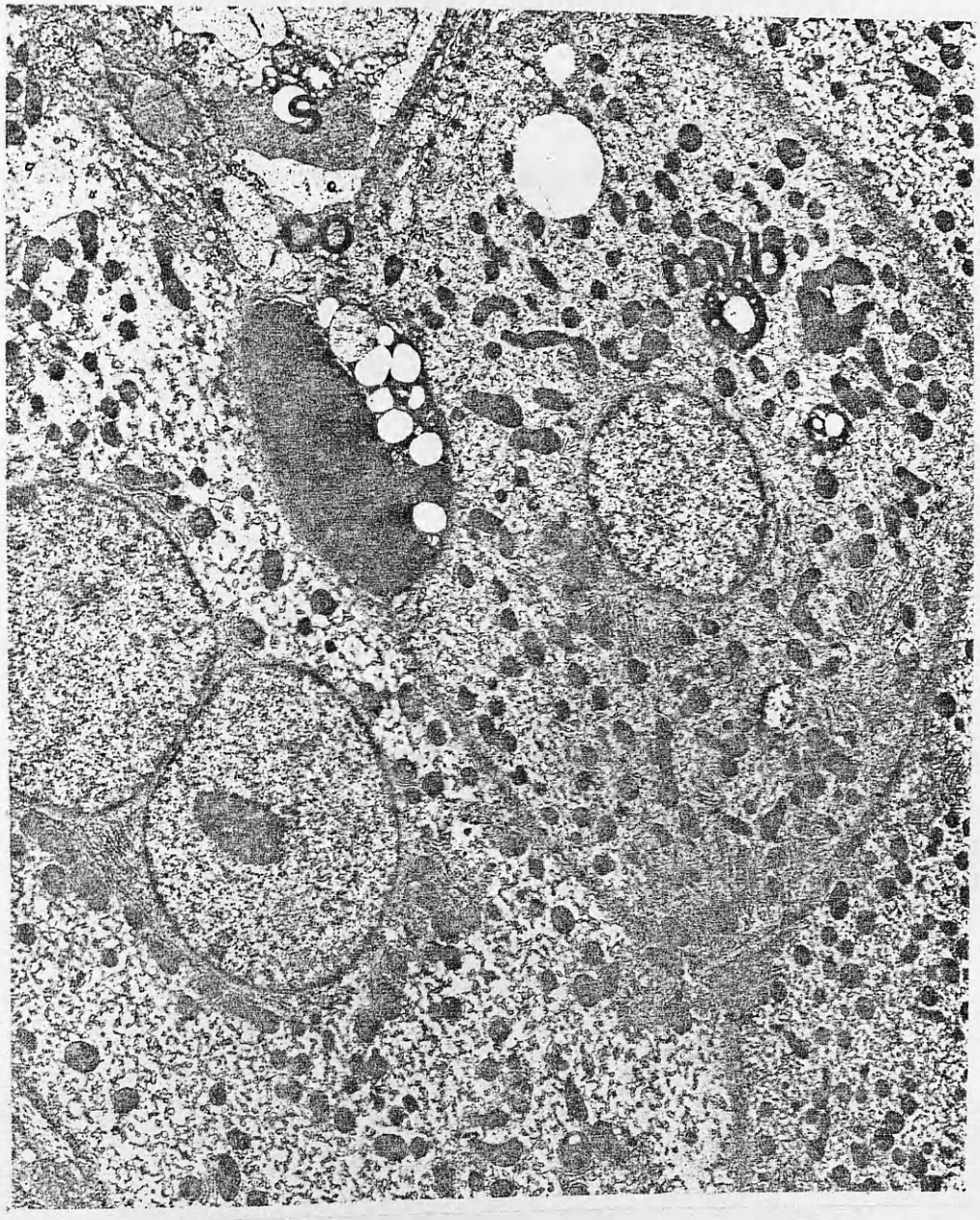

Figure 24.7

FIGURE 24.8

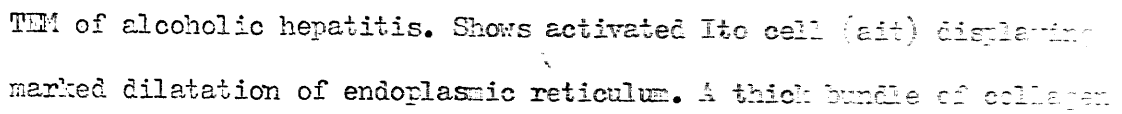

TEM of alcoholic hepatitis. Shows activated Ito cell (ait) displaying marked dilatation of endoplasmic reticulum. A thick bundle of collagen (co) fibre lying adjacent to the cell in the space of Disse.
(X 6450)

FIGURE 24.9

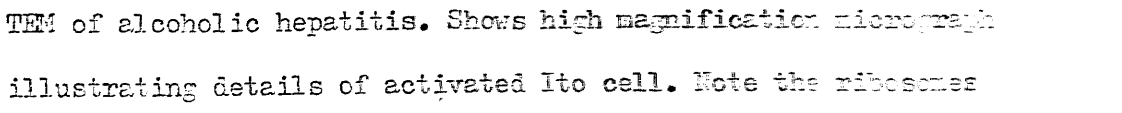

TEM of alcoholic hepatitis. Shows high magnification micrograph illustrating details of activated Ito cell. Note the ribosomes attached to the rough endoplasmic reticulum (rer) and thick collagen bundle (co) in the space of Disse. (X 14700)

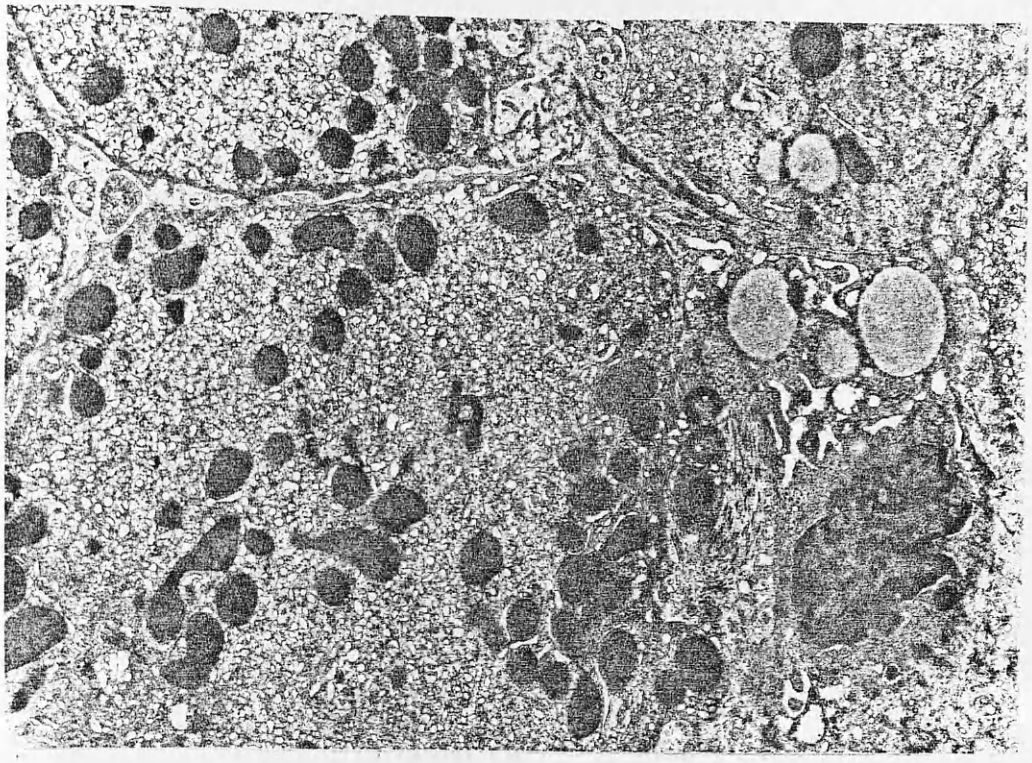

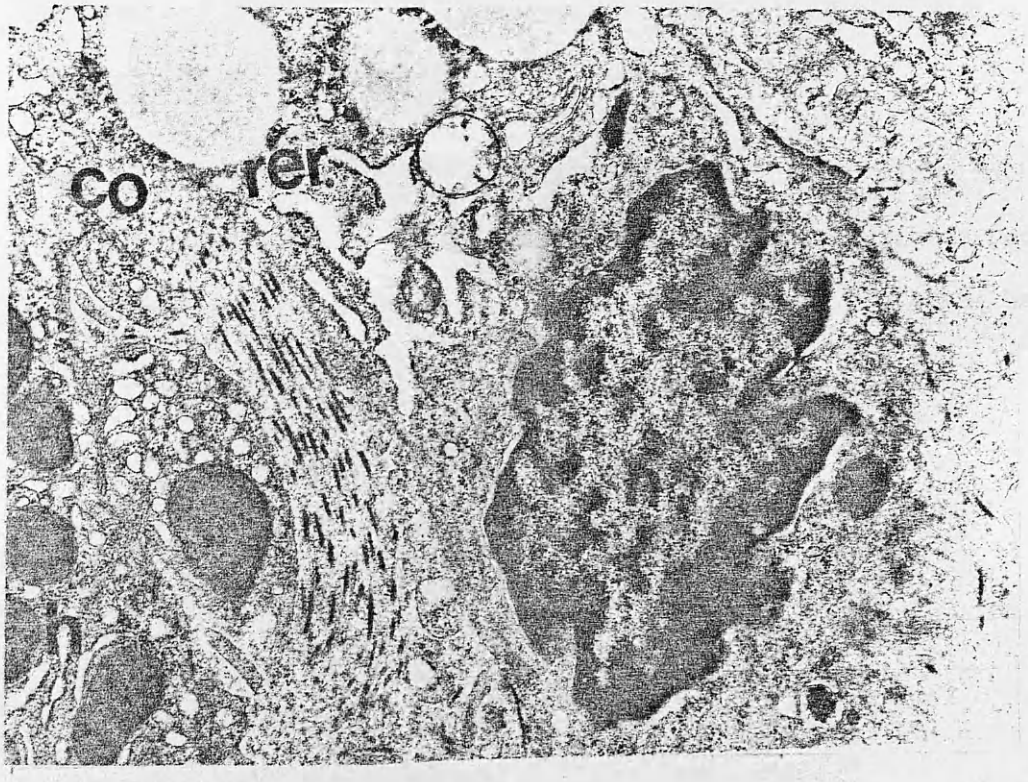

Above : Figure 24.8

Below : Figure 24.9

FIGURE 25.1

TEM of alcoholic hepatitis. Shows activated Ito cell with bundle of collagen in close apposition to degenerate hepatocyte (h). (l : lipid droplet). (n : nucleus). (X 4950)

FIGURE 25.2

TEM of alcoholic hepatitis. Shows high magnification micrograph of activated Ito cell (ait) with details of collagen fibres (co) in close apposition to the degenerate hepatocyte (h). Note the banded form of the collagen. (ds : Disse space). (X 16870)

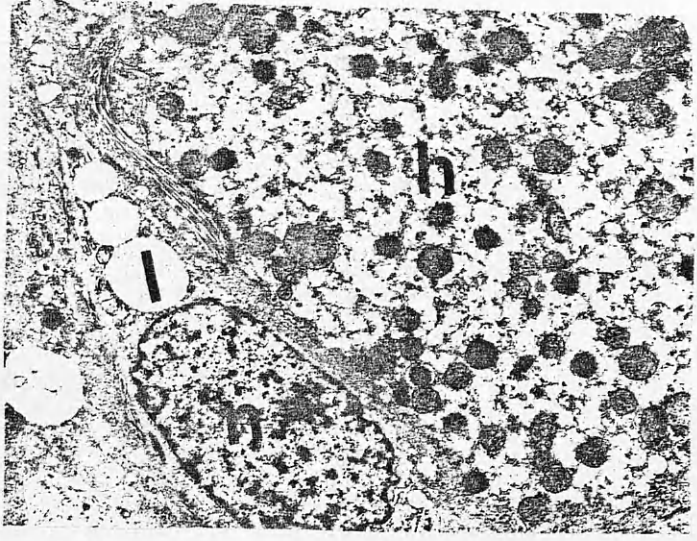

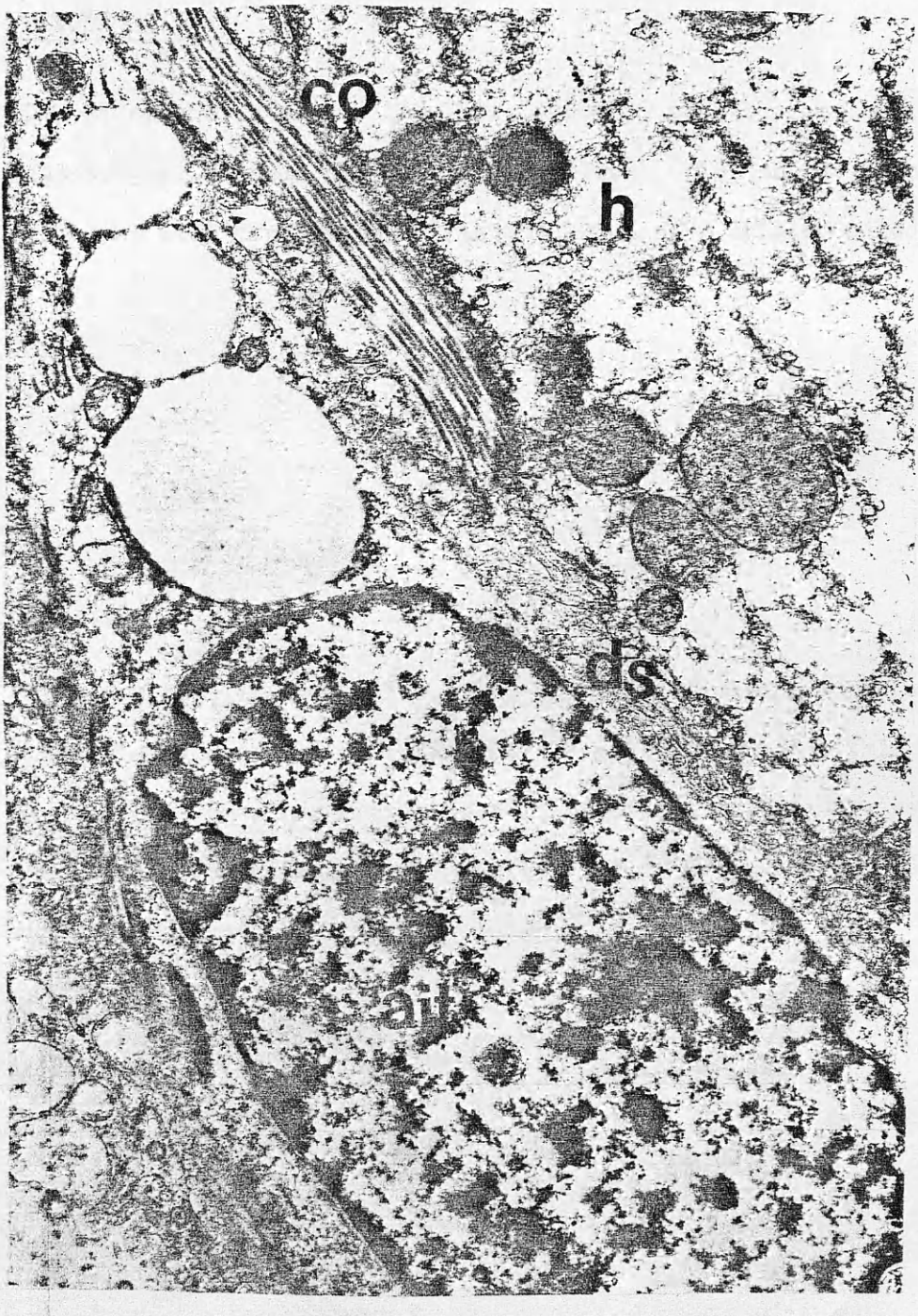

Above : Figure 25.1 Below : Figure 25.2

FIGURE 26.1

TEM of alcoholic hepatitis. Shows parts of adjacent periportal hepatocyte. Several phagolysosomes present (ply) in the cytoplasm. Note the bile deposition within the lumen of a dilated bile canaliculus (bc). (X 8100)

FIGURE 26.2

TEM of alcoholic hepatitis. Shows high magnification micrograph of the bile canaliculus. Bile pigment deposit (bp) shown within the lumen. Note the increased number of microfilaments in the peri-canalicular ectoplasm. (mv : microvilli). (h : hepatocyte). (X 29250)

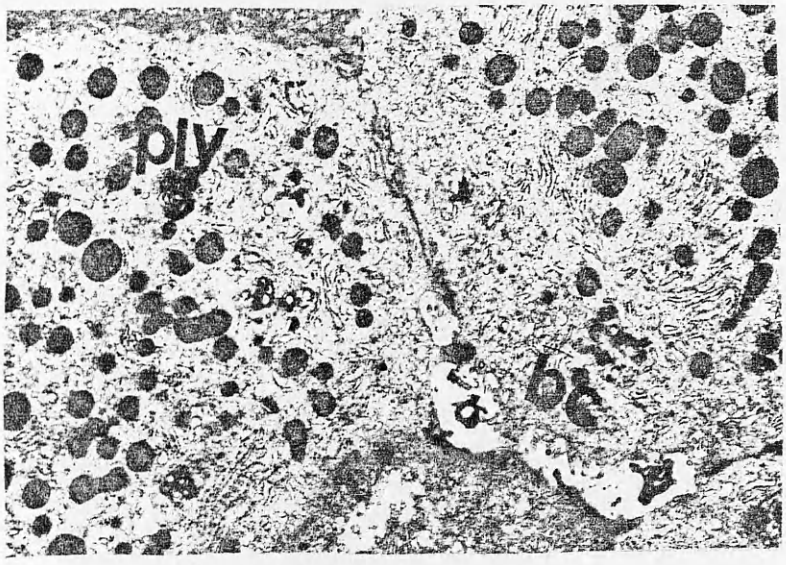

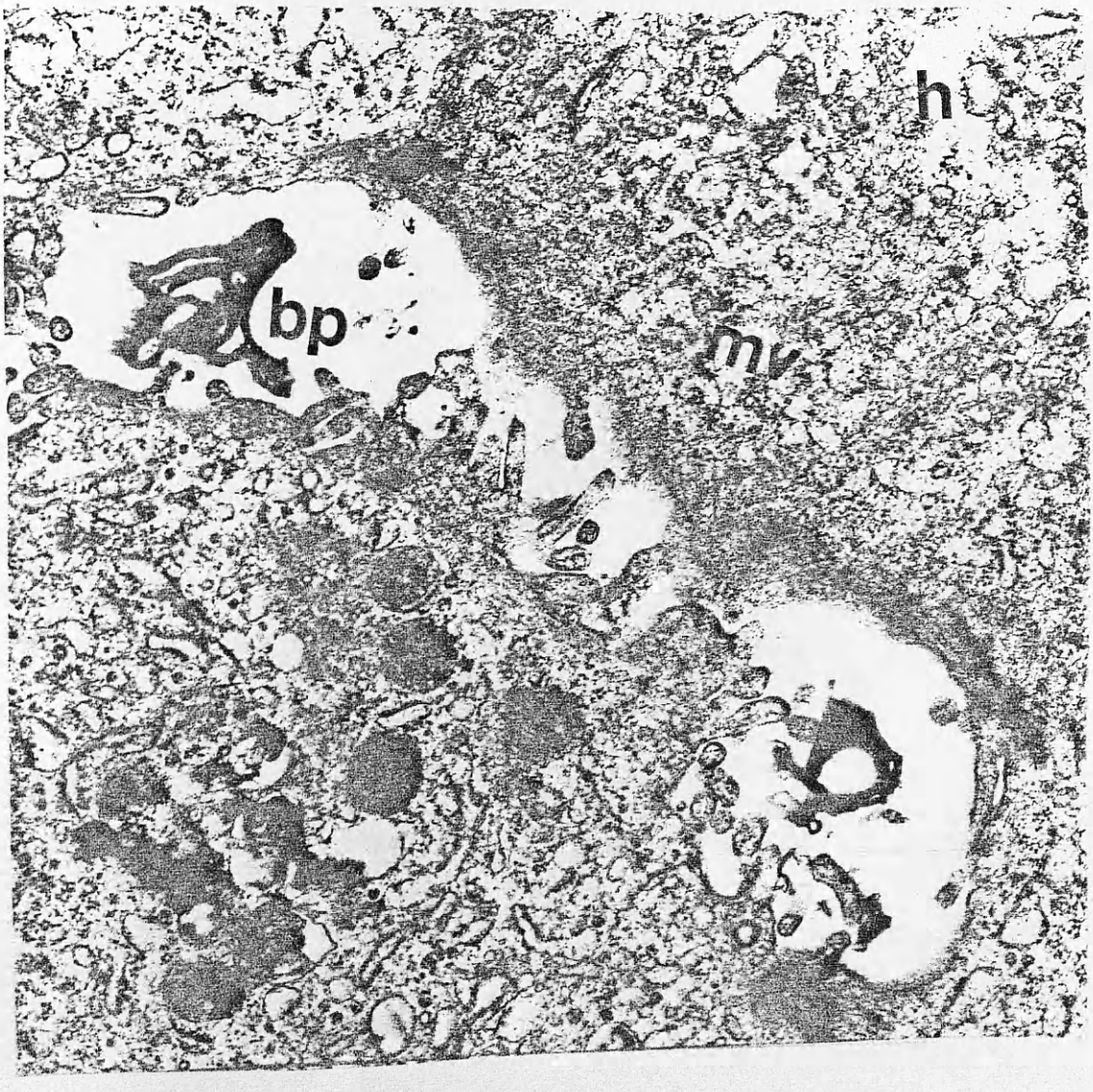

Above : Figure 26.1

Below : Figure 26.2

FIGURE 26.3

TEM of alcoholic hepatitis. Shows periportal hepatocyte with increased number of lysosomes (ly). (bc : bile canaliculus). (X 4950)

FIGURE 26.4

TEM of alcoholic hepatitis. Shows high magnification micrograph with details of the laminated lysosomes (ly). Note the electron dense granules within the laminated structure and the multivesicular bodies (mvb). (X 9675)

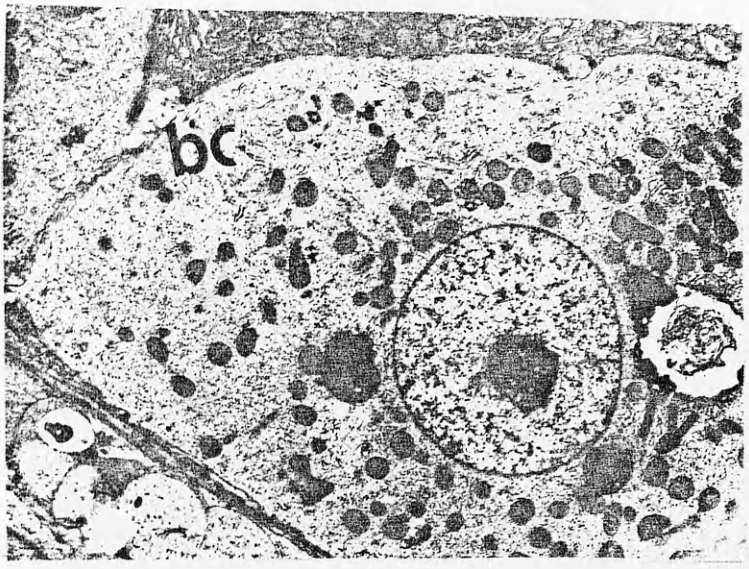

Left: Figure 26.3

Below: Figure 26.4

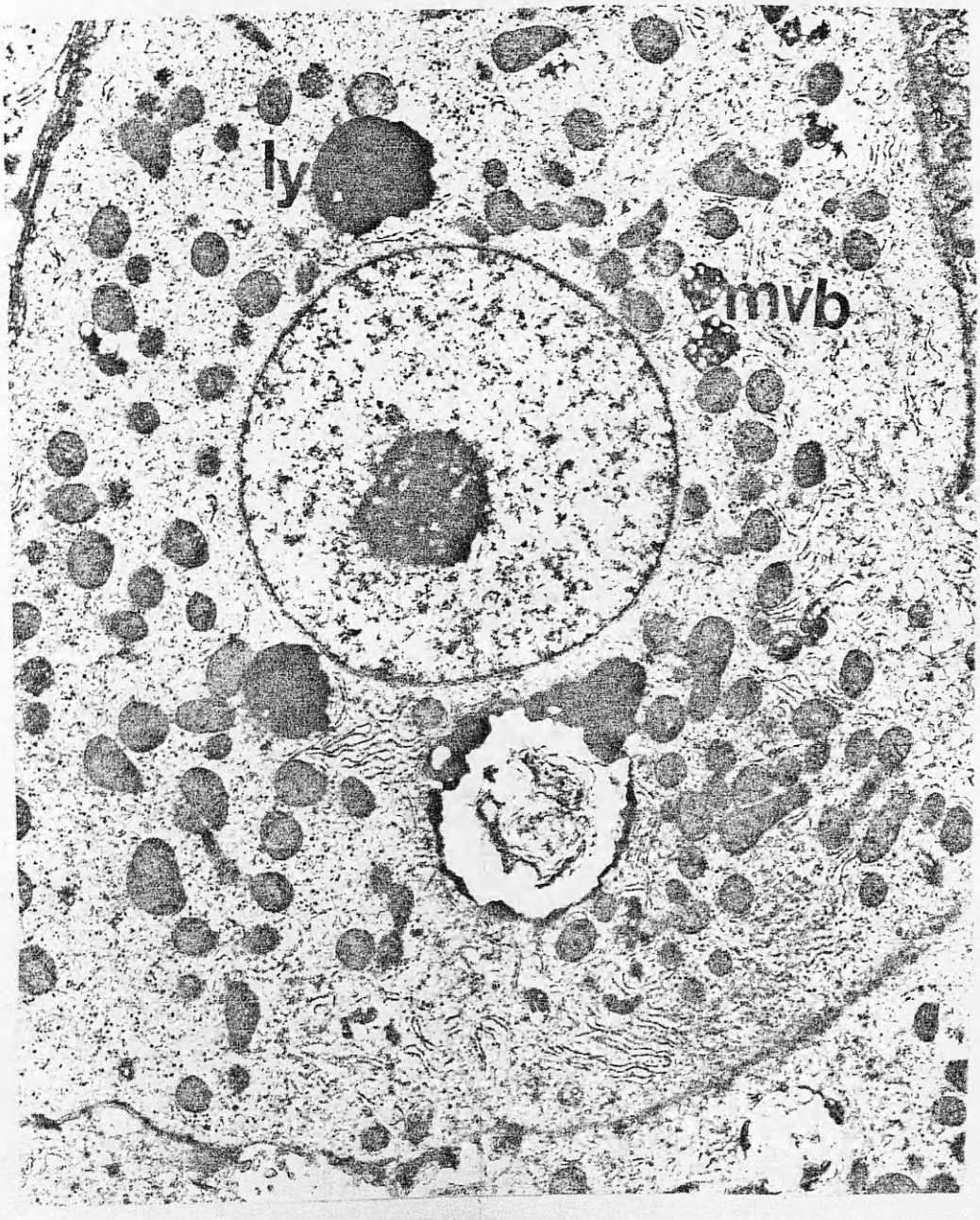

FIGURE 26.5

TEM of alcoholic hepatitis. Shows several periportal hepatocytes (h) with wide spread bile pigment (bp) deposition within the intercellular spaces. Marked dilatation shown evident by wide cytoplasmic inter-digitation. (X 5400)

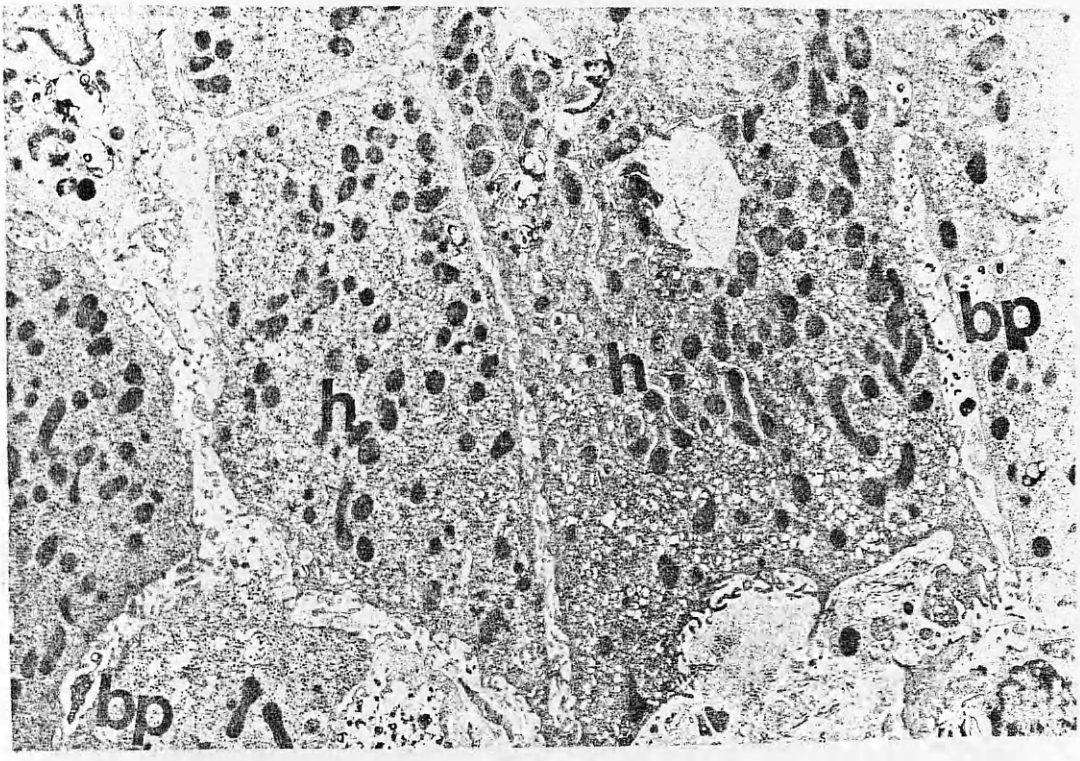

Figure 26.5

FIGURE 27.1

TEM of alcoholic hepatitis. Shows proliferated bile ductule (dc) with ill-defined lumen. The epithelial cells resemble those of normal ducts with relatively scanty cytoplasm. The intercellular connection is straight in the luminal half and interdigital in the basal half. The basal lamina (bl), surrounds the ductule, is thickened in places with stratified appearance. (X 4050)

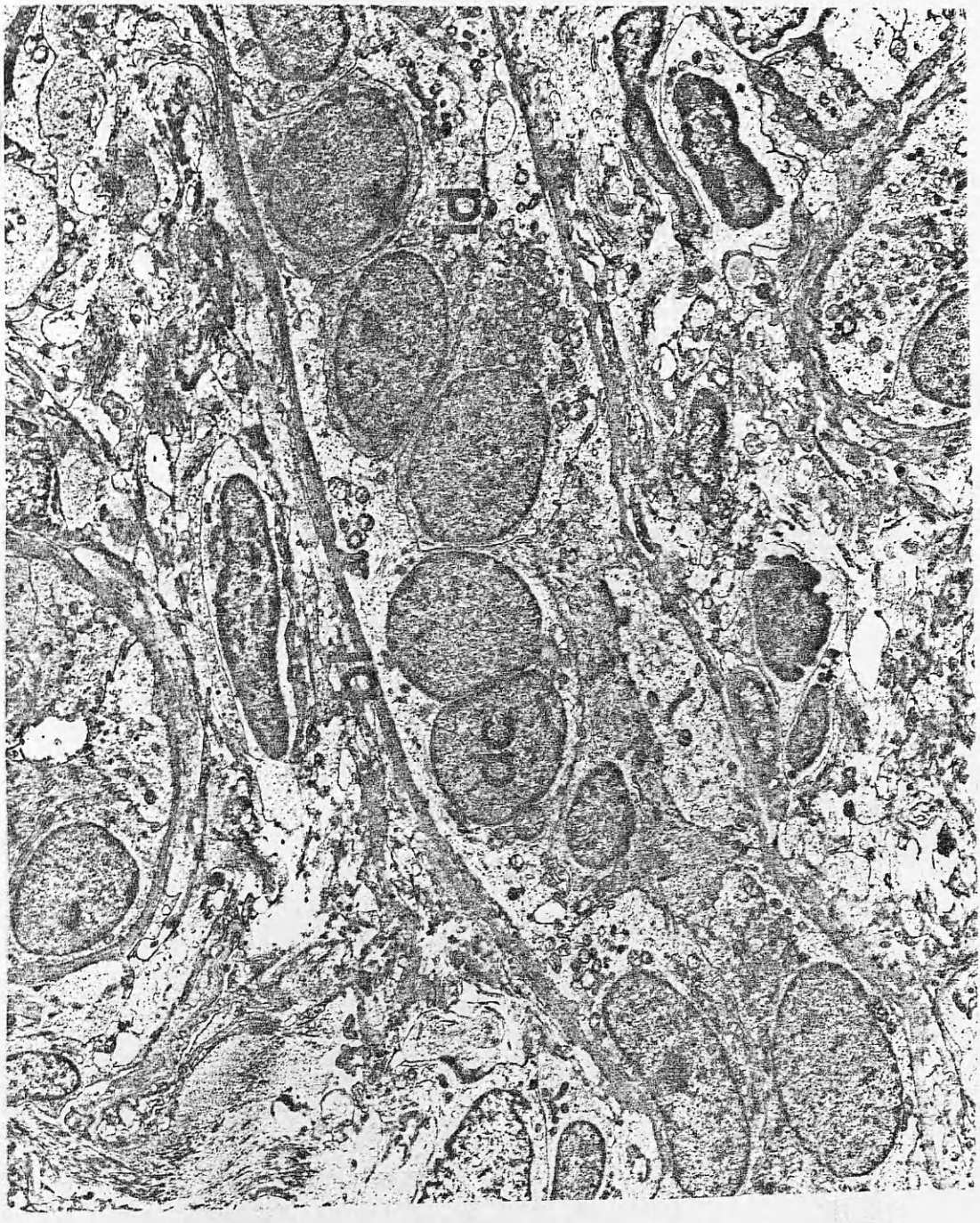

Figure 27.1

FIGURE 27.2

TEM of alcoholic hepatitis. Shows parts of proliferated bile ductules with few microvilli projecting into the lumen (lu). The epithelial cell contained increased number of lysosomes (ly), some with lipid-like vacuoles. (ne : neutrophil). (X 5400)

FIGURE 27.3

TEM of alcoholic hepatitis. Shows high magnification micrograph with details of the lysosomes and the cytoplasmic organelles. The basal lamina (bl) is thickened in places. (X 11250)

Above : Figure 27.2

Below : Figure 27.3

FIGURE 28.1

SEM of alcoholic hepatitis. Shows several plates of hepatocytes (h) separated by sinusoids (s). There is increased amount of collagen fibres (co), A thick band of fibrous tissue seen in the space of Disse. Some sinusoids seen filled with tissue debris and inflammatory cells. (X 2250)

Figure 28.1

FIGURE 28.2

SEM of alcoholic hepatitis. Shows several hepatocytes with striking microvillous appearance. The microvilli (mv) covered almost all the hepatic surfaces. Bile canaliculi run in the centre of one hepatocyte giving a blind loop. There are two small spindle-shaped cells in close apposition to the hepatocyte with delicate mesh of fibrous tissue (co). Probably Ito cells were exposed when the sinusoidal lining is ripped away during fracturing technique. (X 7675)

FIGURE 28.3

SEM of alccholic hepatitis. Shows high magnification micrograph with details of the microvillous appearance of the hepatocyte surface (h). (bc : bile canaliculus). (X 10125)

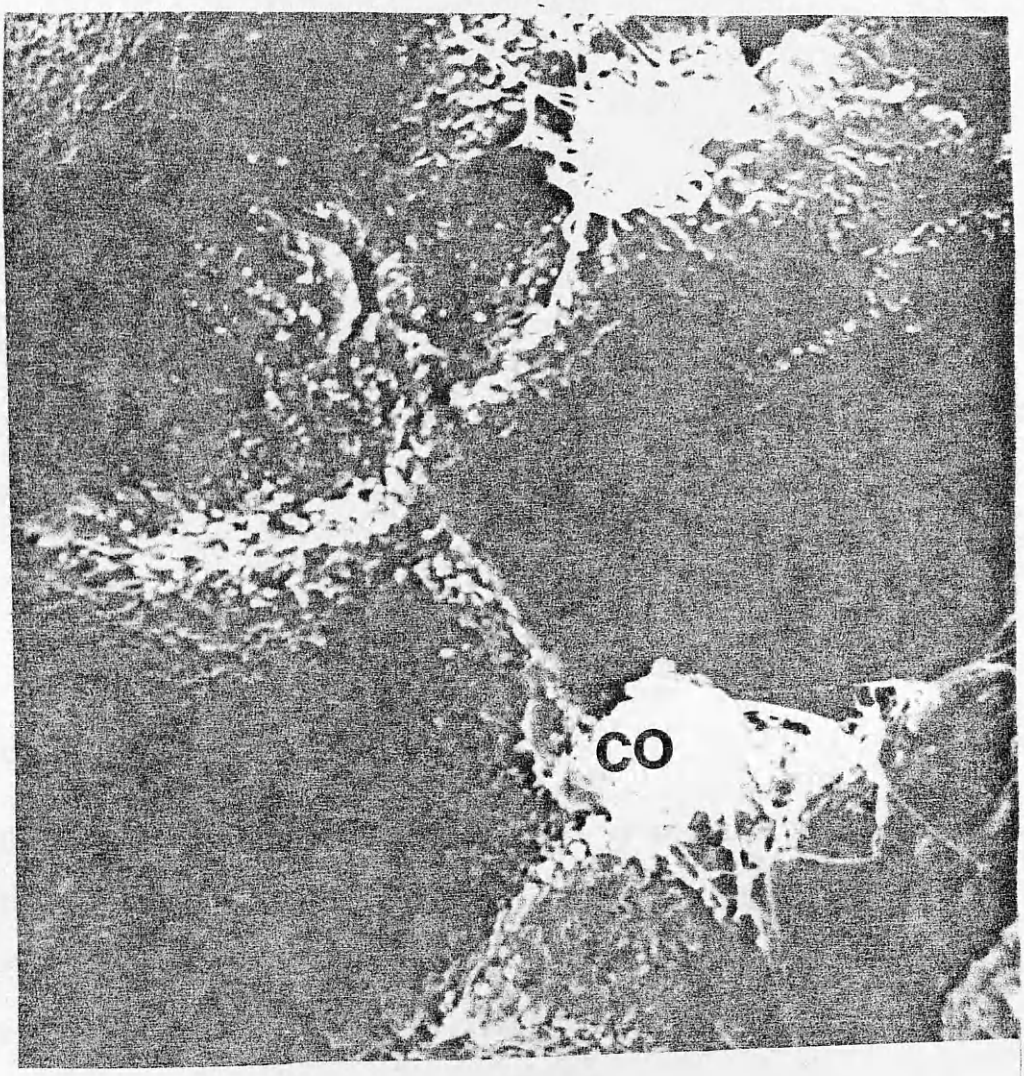

Above : Figure 28.2

Below : Figure 28.3

FIGURE 28.4

TEM of alcoholic hepatitis. Shows the intercellular wall (iw) between two hepatocytes. Note the folds and the herniations of the wall into the cytoplasm. (X 49500)

FIGURE 28.5

TEM of alcoholic hepatitis. Shows parts of adjacent hepatocyte (h) with the cell wall (iw) displaying a striking labyrinth appearance of the cytoplasmic folds and interdigitations. Electron-dense, granular materials are shown between the digitations. (X 49500)

FIGURE 28.6

TEM of alcoholic hepatitis. Shows high magnification micrograph of the cell wall (iw) with much granular material and many folds. (X 81000)

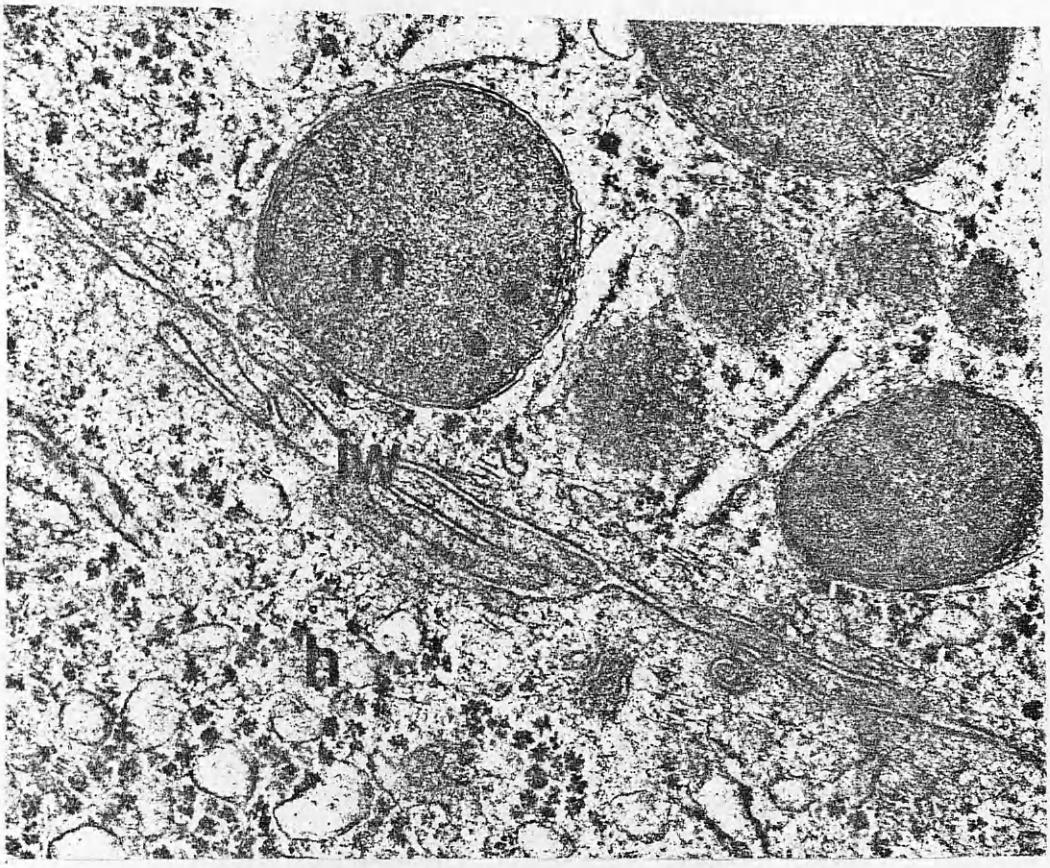

Above: Figure 28.4 Middle: Figure 28.5 Below: Figure 28.6

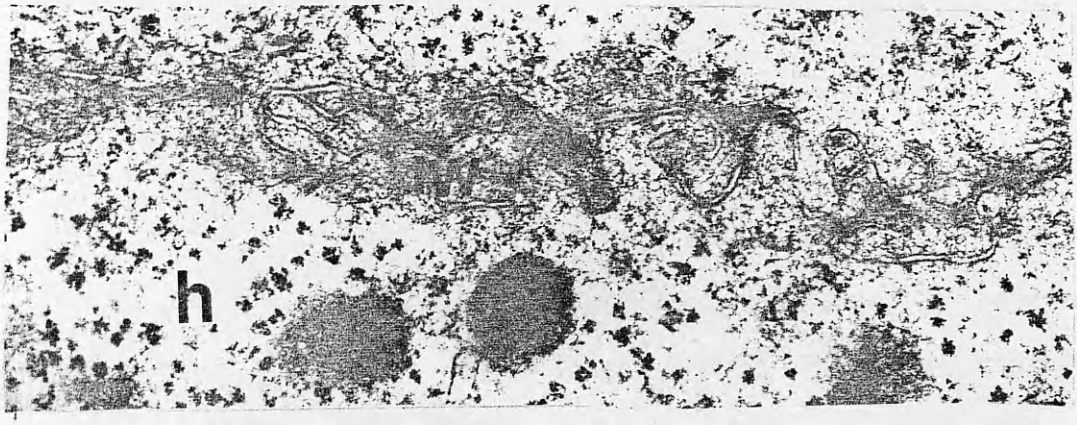

FIGURE 29.1

SEM of alcoholic hepatitis. Shows two plates of hepatocytes (h) and an opened hepatic sinusoid filled with tissue debris (td) and RBCs (rb). The bile canaliculi run in the centre of one plate. Note the rough and irregular surfaces of the hepatocyte and the thin compressed space of Disse. (X 7875)

FIGURE 29.2

SEM of alcoholic hepatitis. Shows empty hepatic sinusoids between two plates of liver cells with the endothelial lining (ed) rough, thick and thrown into folds with very few tiny microvilli. Note the thick collagen fibres (co) in the space of Disse (ds) on both sides wedged between the endothelial lining and the hepatocytes. (X 4500)

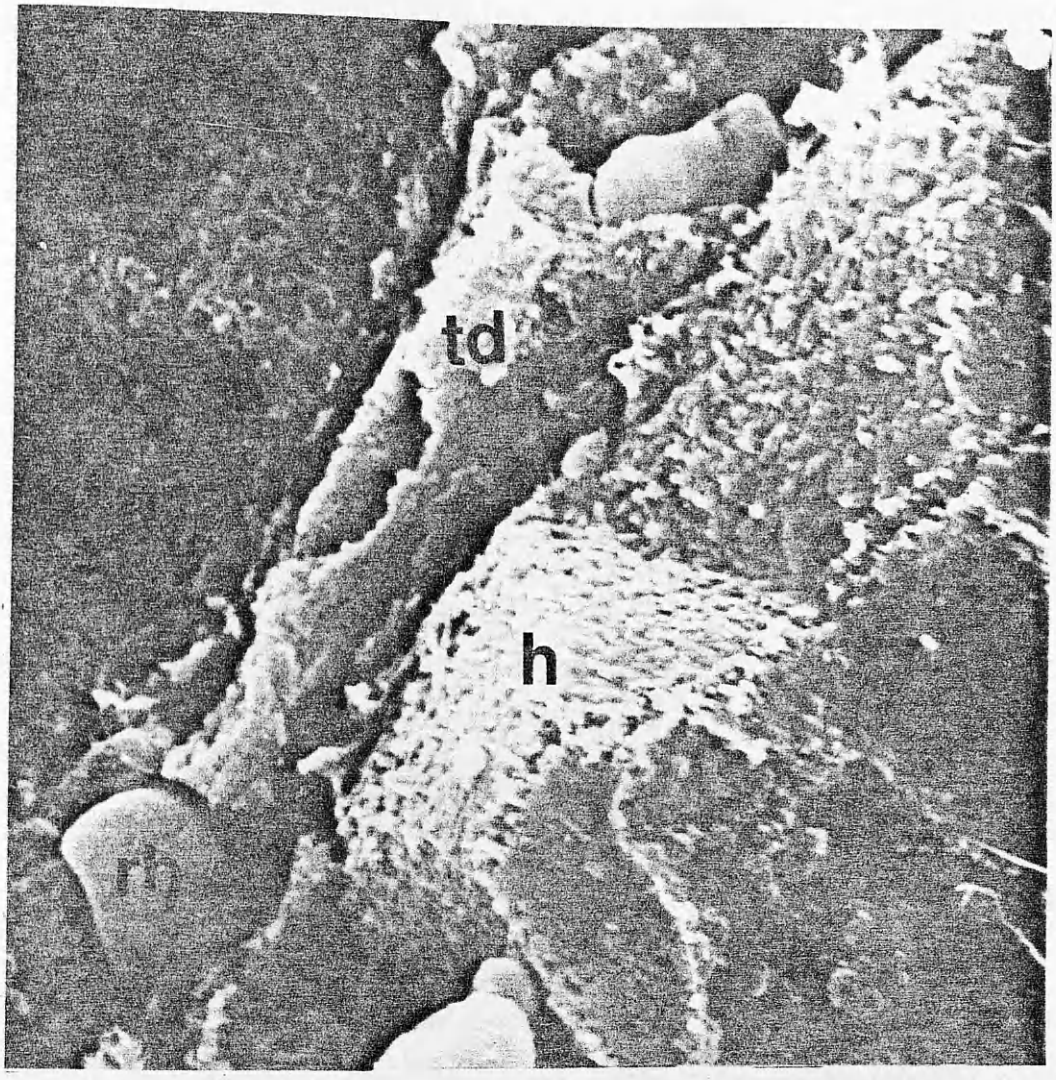

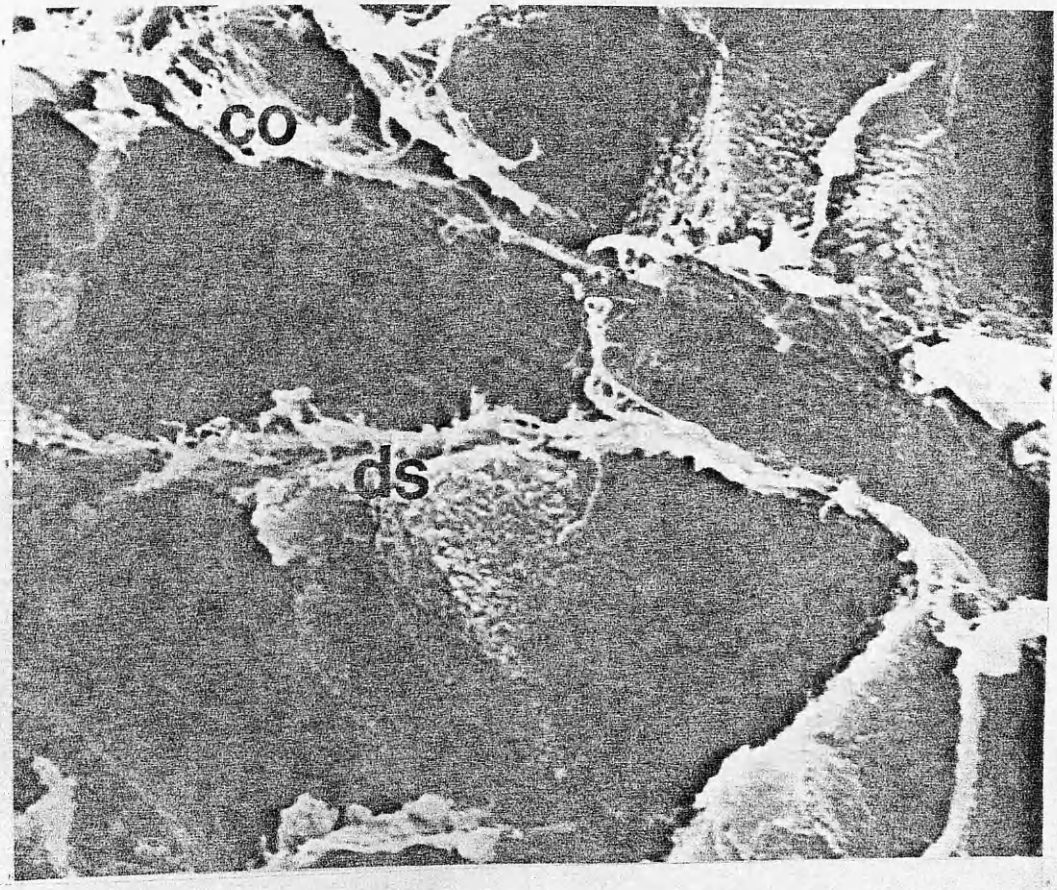

Above : Figure 29.1

Below : Figure 29.2

FIGURE 29.3

SEM of alcoholic hepatitis. Shows opened sinusoids (s) and several hepatic plates (h). The surfaces of the hepatocytes are covered by numerous tiny microvilli. The endothelial lining (ei) is thick, folded and covered by tissue debris. Note the Kupffer cell (k) anchoring its long cytoplasmic extension into the sinusoidal wall. (X 4500)

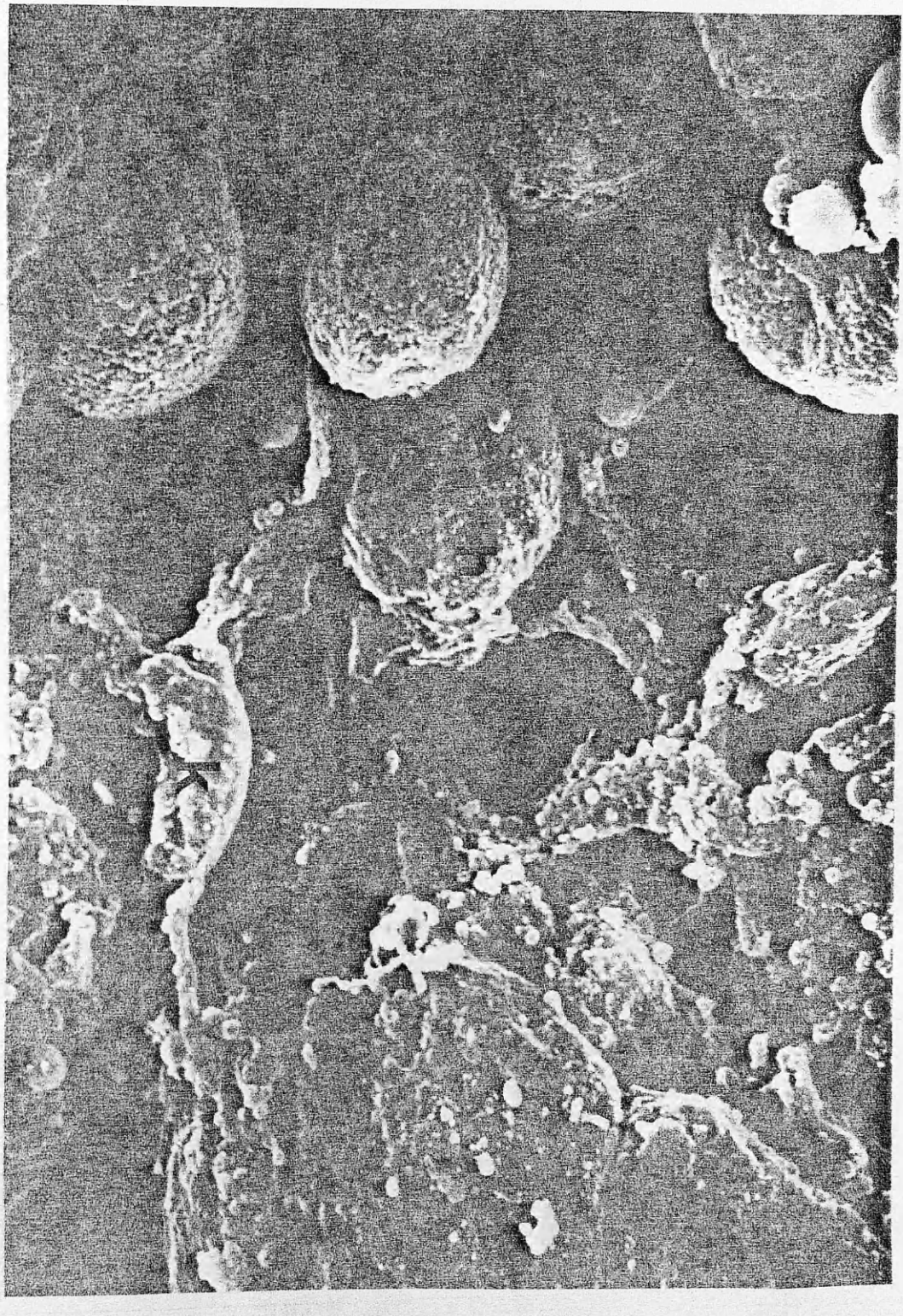

Figure 29.3

FIGURE 29.4

SEM of alcoholic hepatitis. High magnification micrograph of the hepatic sinusoids showing details of the endothelial lining. Large and small fenestrations (f) are evident. Few microvilli protruding through the fenestrations are seen. Part of the sinusoid is covered by tissue debris.(sv : sieve plate). (X 22500)

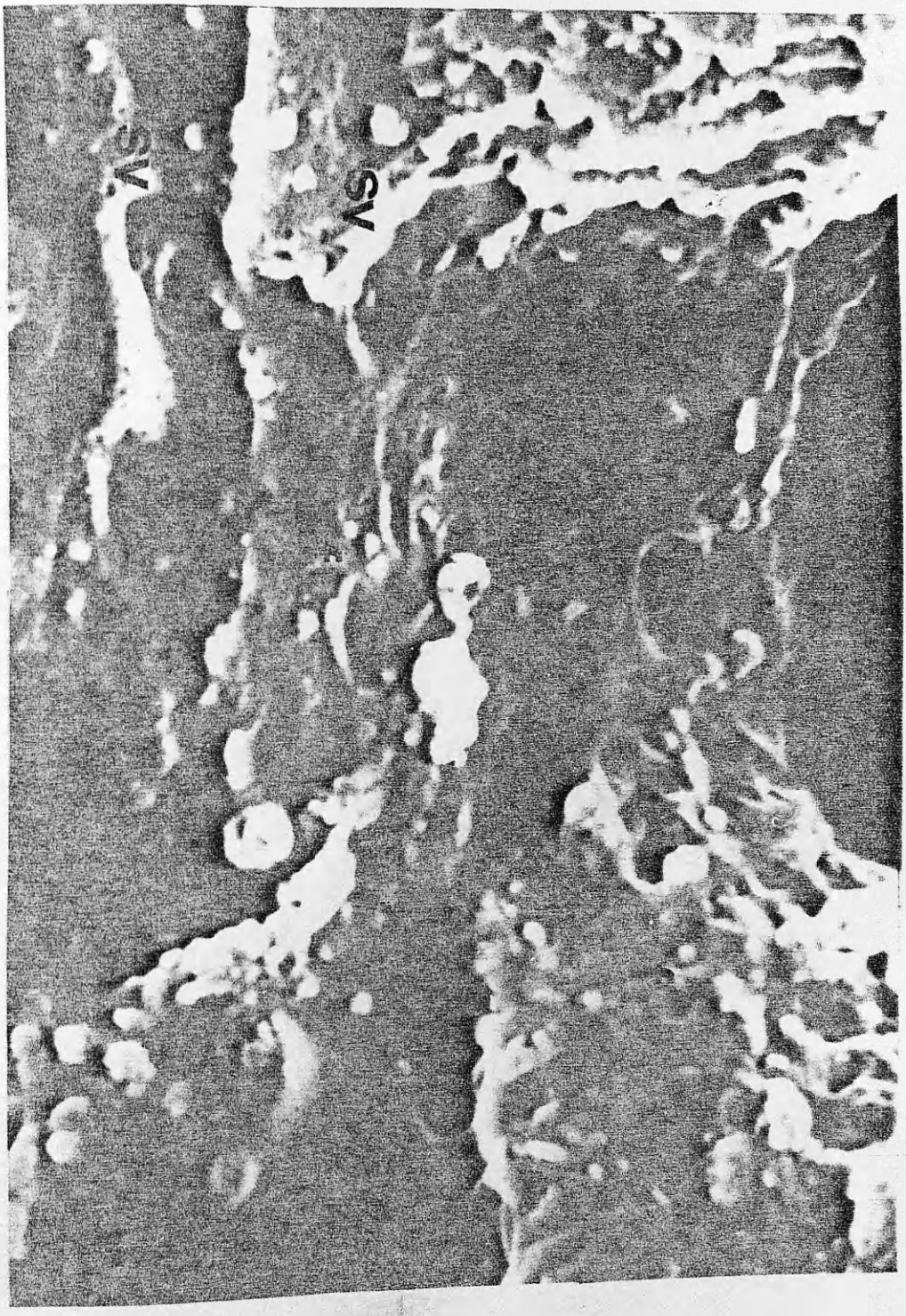

Figure 29.4

FIGURE 29.5

SEM of alcoholic hepatitis. High magnification micrograph of Kupffer cell (k) showing details of surface morphology. (ed : endothelium) (lp :Limbopodium). (X 11125)

Figure 29.5

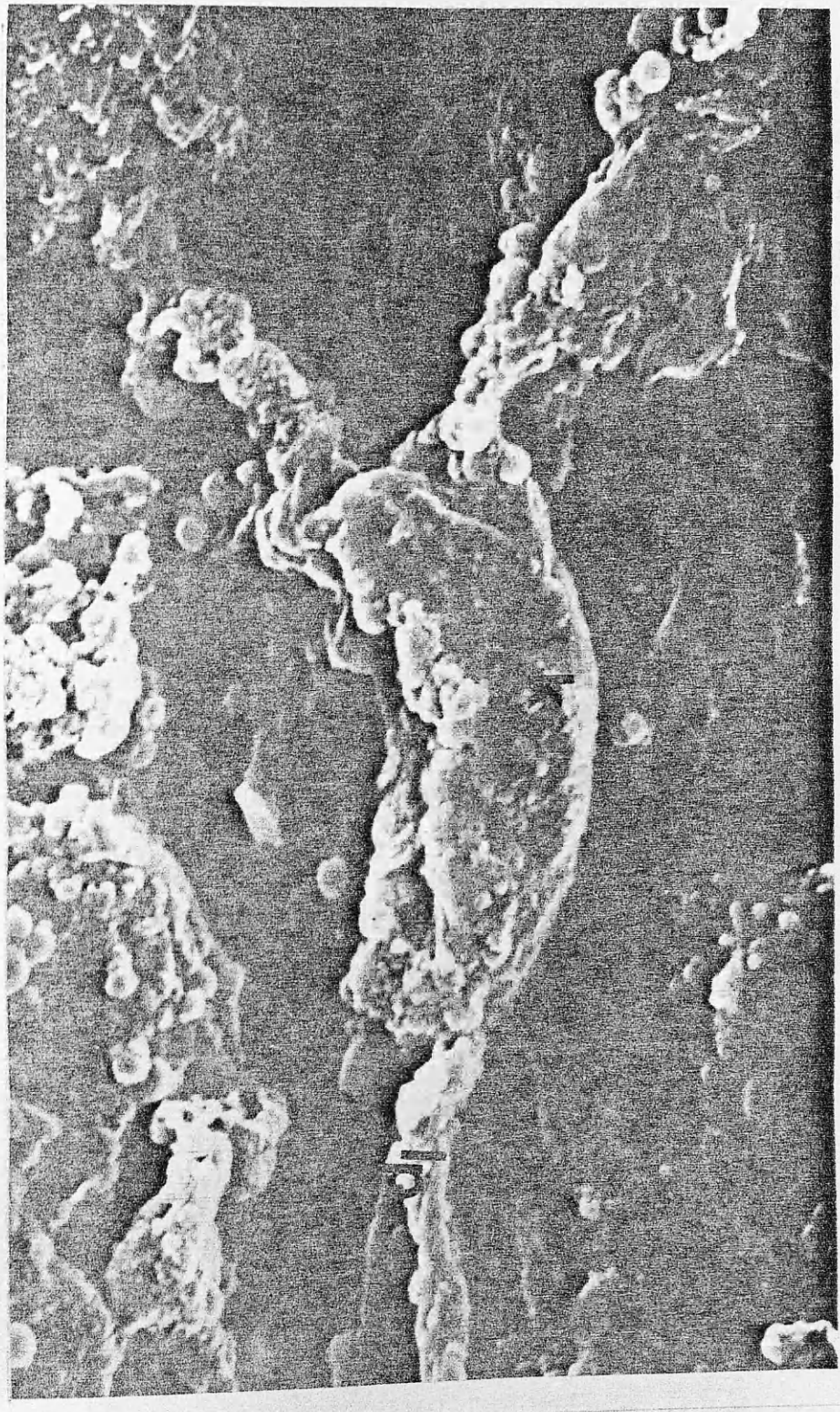

FIGURE 30.1

SEM of alcoholic hepatitis. Shows several plates of hepatocytes and sinusoids which are filled with tissue debris, inflammatory cells and RBCs.(rb). Note the Ito cell wedged between the hepatocyte and the sinusoid. Two thick bundles of collagen seen in close apposition to the cell. (ds : Disse space) (X 3375)

FIGURE 30.2

SEM of alcoholic hepatitis. High magnification micrograph shows details of Ito cell (it). Note the few tiny microvilli on its rough surface and the close apposition of collagen bundles (co) to both ends of the cell.(S : Sinusoid).(rb : RBC).(bc : bile canaliculi). (X 7875)

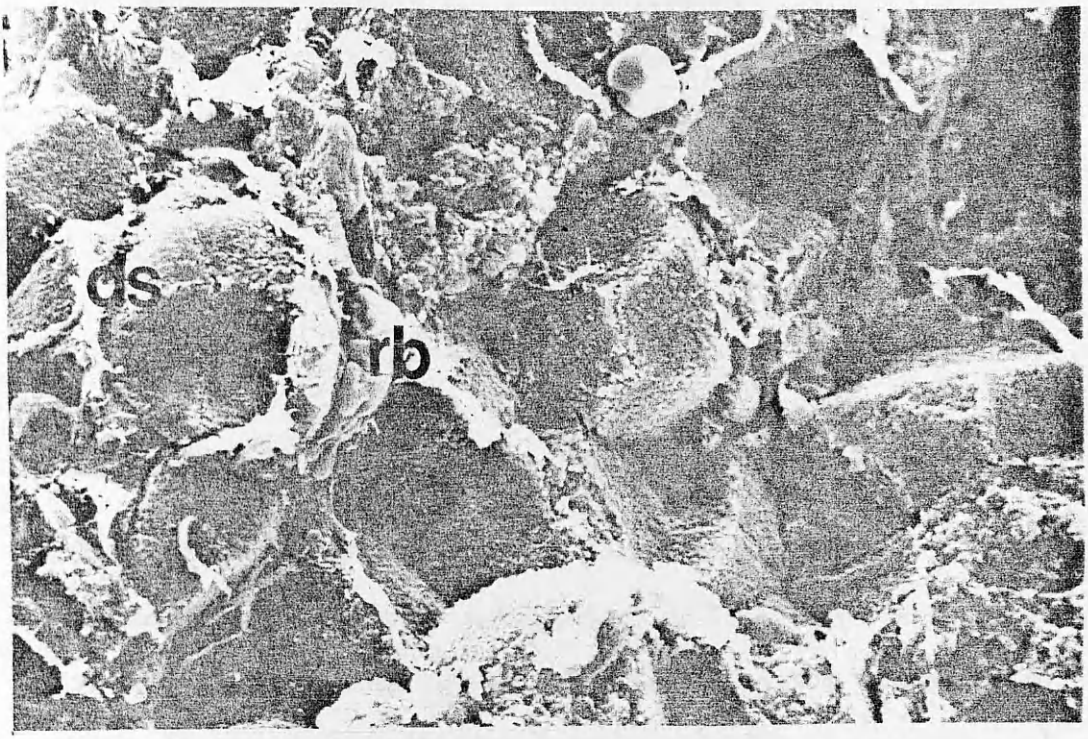

Above : Figure 30.1

Below : Figure 30.2

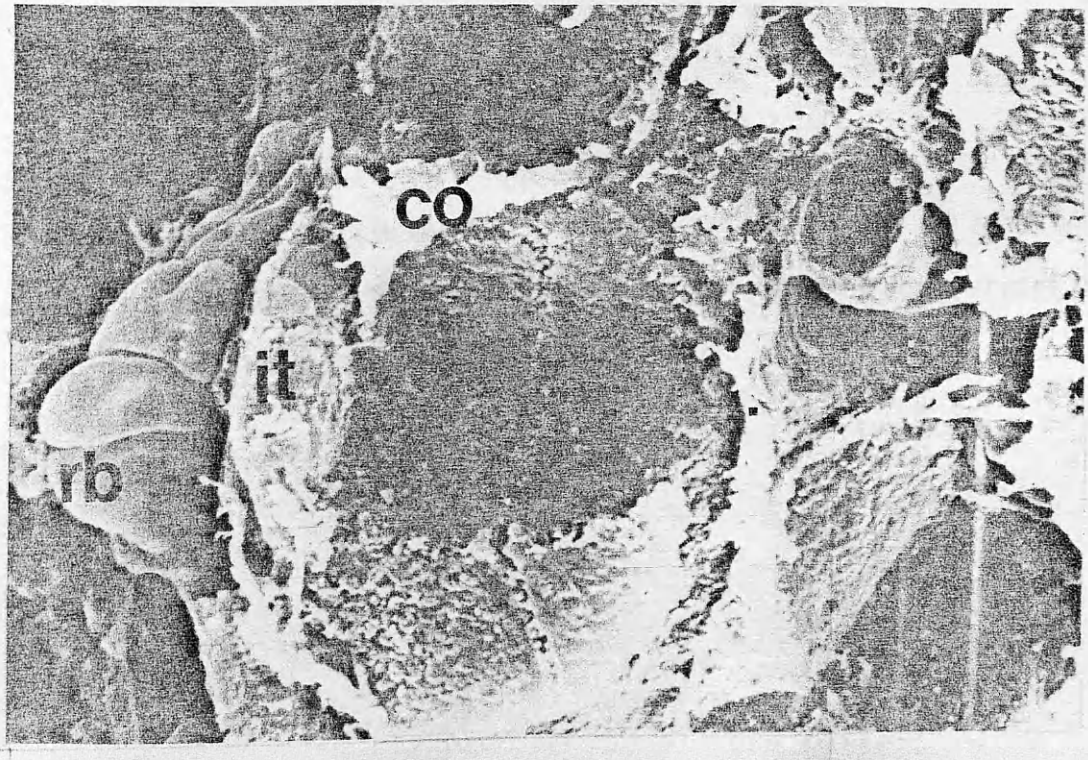

FIGURE 30.3

SEM of alcoholic hepatitis. Shows plates of hepatocytes (h) and sinusoids (s) filled with inflammatory cells and tissue debris. Ito cell (it) appears as a bright spindle cell clinging to the surface of the hepatocyte and adjacent to a thin bundle of collagen (co). Note the bile canaliculi run in the middle of the hepatic plates. (X 4500)

FIGURE 30.4

SEM of alcoholic hepatitis. High magnification micrograph of Ito cell (it) showing the surface displaying mild folding. There is tiny microvilli and a slender bundle of collagen fibre (co) is seen clinging to the surface of the hepatocyte. (X 7875)

Above : Figure 30.3 Below Figure 30.4

FIGURE 31.1

SEM of alcoholic hepatitis. Shows striking appearance of hepatocyte surrounded by mesh of fibrous tissue(pf : pericellular fibrosis). Some delicate bundles appeared to be anchored to the surface of the hepatocyte. Note the bile canaliculi (bc) run along the surface of hepatocyte and show slight dilatation. (X 11250)

FIGURE 31.2

SEM of alcoholic hepatitis. Shows an open hepatic sinusoid (s) with adjacent hepatocyte (h). Note a thick bundle of collagen fibre (co) in the space of Disse which appears to encircle the cell. Few RBCs are evident in the sinusoid. (bc : bile canaliculus) (X 7860)

Above : Figure 31.1 Below : Figure 31.2

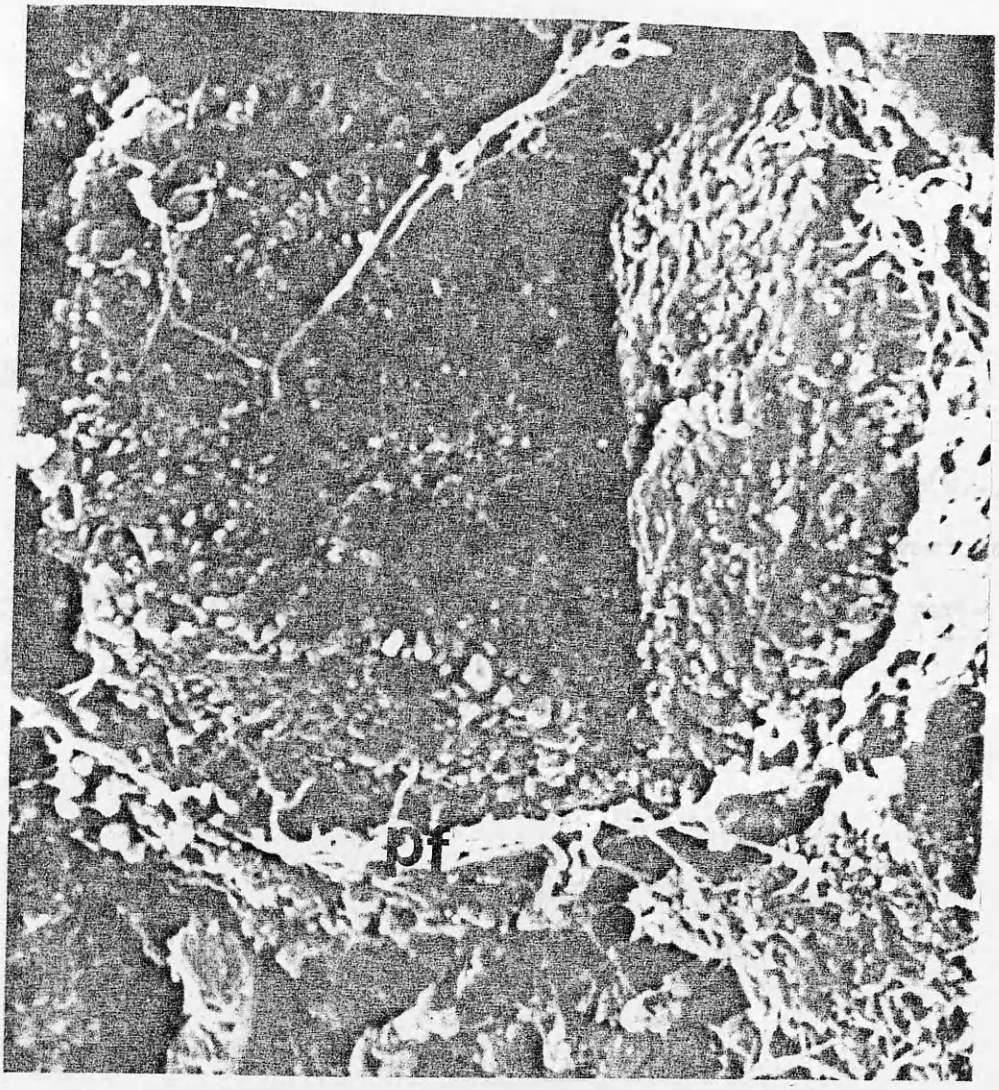

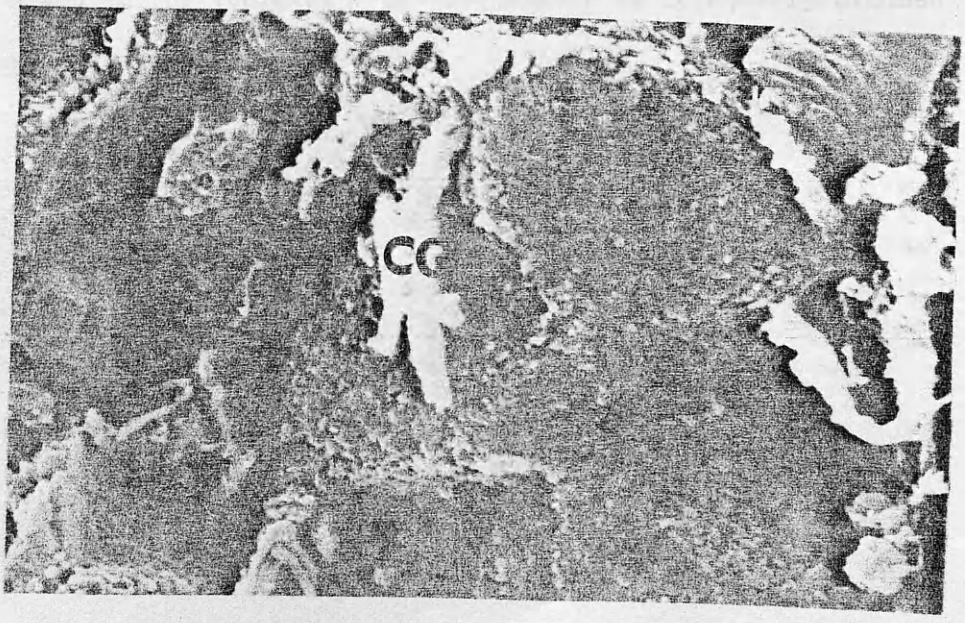

FIGURE 31.3

TEM of alcoholic hepatitis. Shows part of adjacent hepatocytes(h). Their cell wall break into labyrinth of folds between which various sized vesicles are evident. Note the early appearance of the peri-cellular fibrosis. (X 22050)

FIGURE 31.4

TEM of alcoholic hepatitis. High magnification micrograph of the cell wall. Note the two leaflets of the cell wall appear to be connected to the vesicle. A slender bundle of negatively stained collagen (co) is evident. (X 63000)

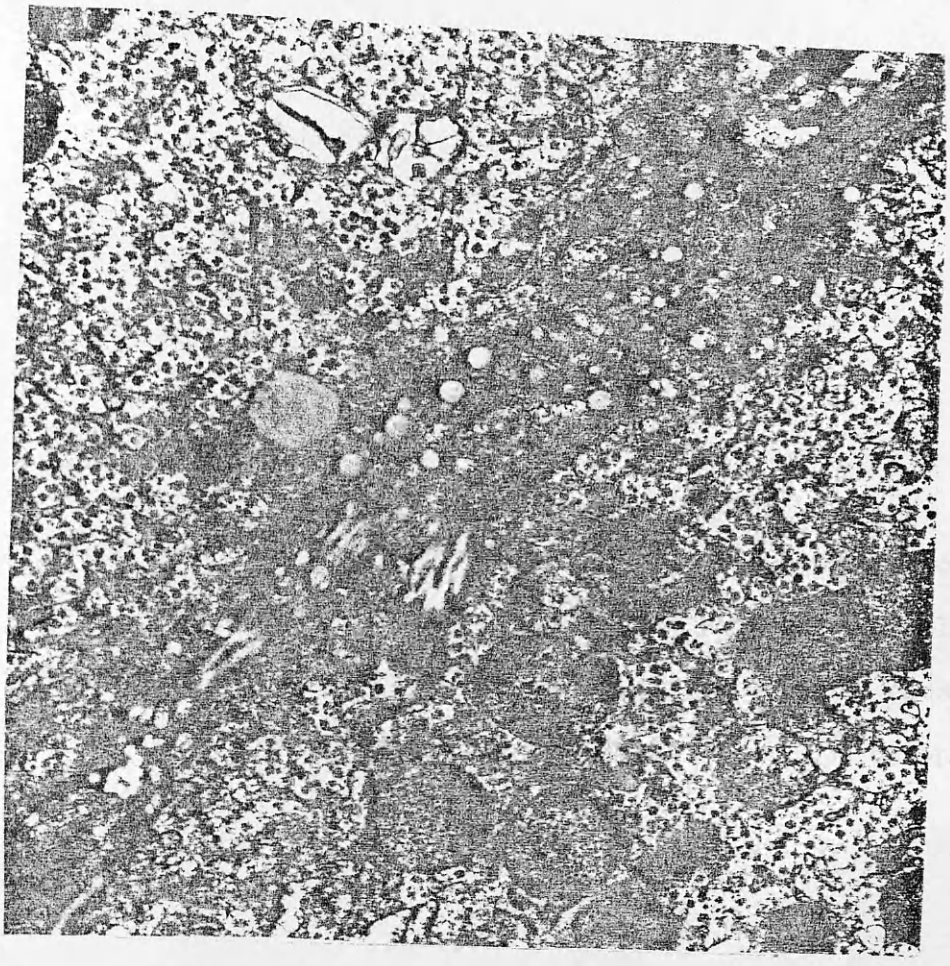

Above : Figure 31.3

Below : Figure 31.4

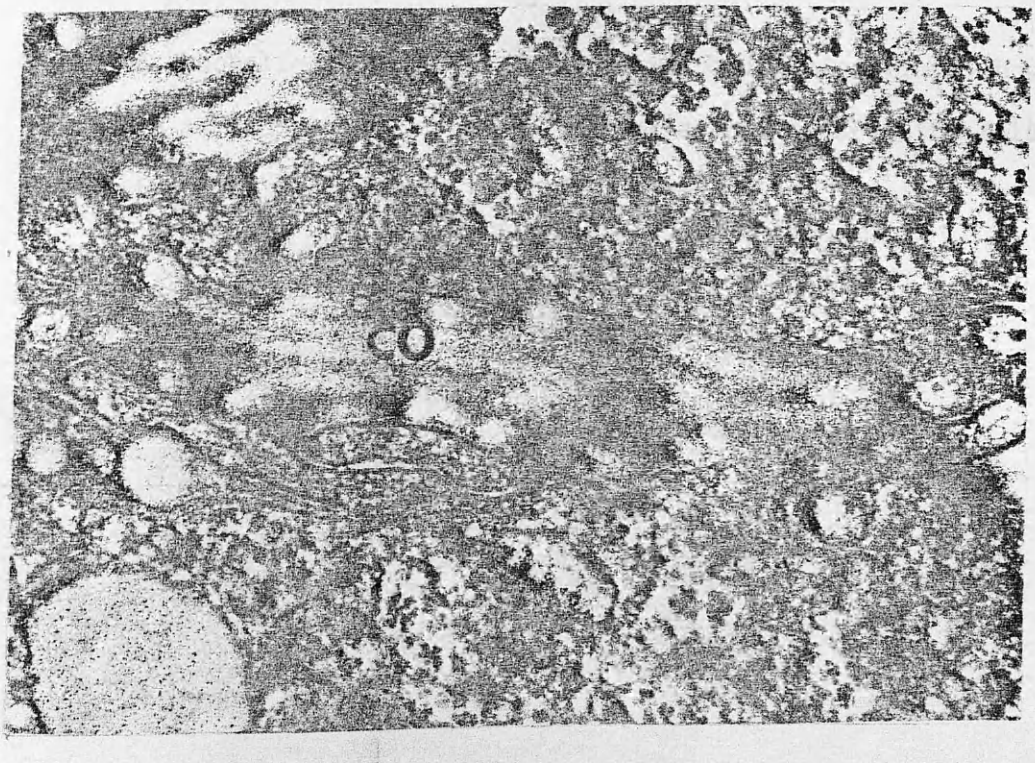

FIGURE 31.5

TEM of alcoholic hepatitis. Shows part of adjacent hepatocytes (h) with thick band of a cross-section of the pericellular collagen (co) appearing to be herniated into the cytoplasm. Note the close apposition of the mitochondria to the lipid droplets (l) in the cytoplasm. (X 13275)

FIGURE 31.6

TEM of alcoholic hepatitis. High magnification micrograph shows details of the banded intercellular collagen(co). Note the folds into the cell membrane. (X 16870)

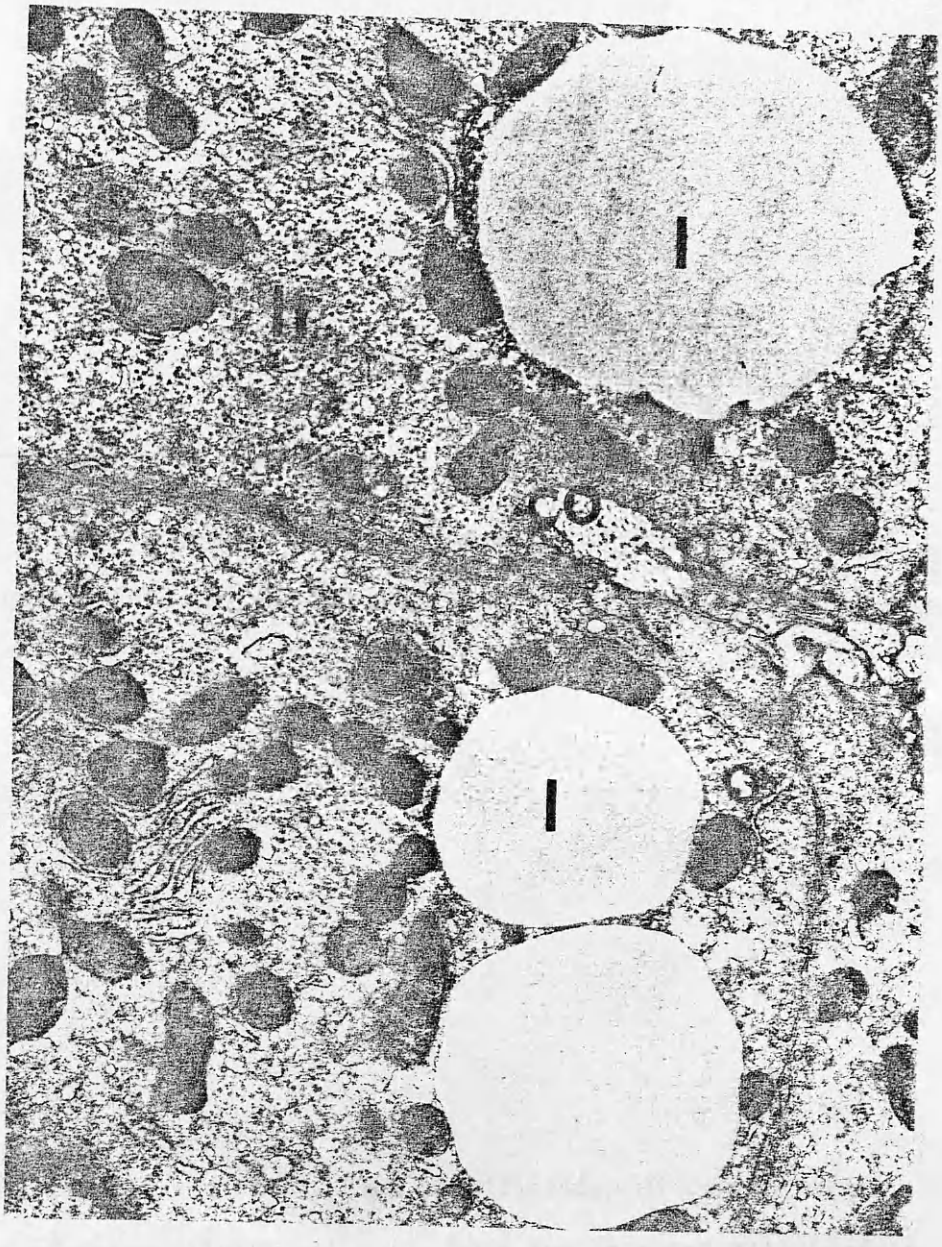

Above : Figure 31.5
Below : Figure 31.6

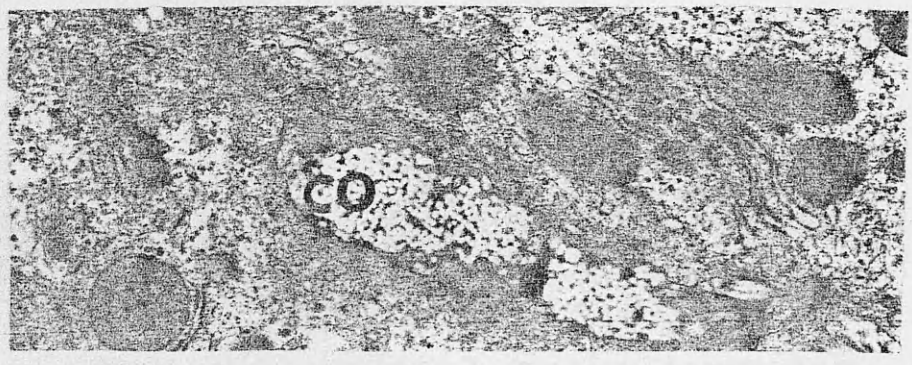

FIGURE 31.7

TEM of alcoholic hepatitis. Shows parts of adjacent degenerated hepatocytes. Note the thick bundle of intercellular banded collagen. (X 8100)

FIGURE 31.8

TEM of alcoholic hepatitis. High magnification micrograph shows details of intercellular collagen. Note the adjacent mitochondria with various matrical inclusions in close apposition to the collagen. (X 16870)

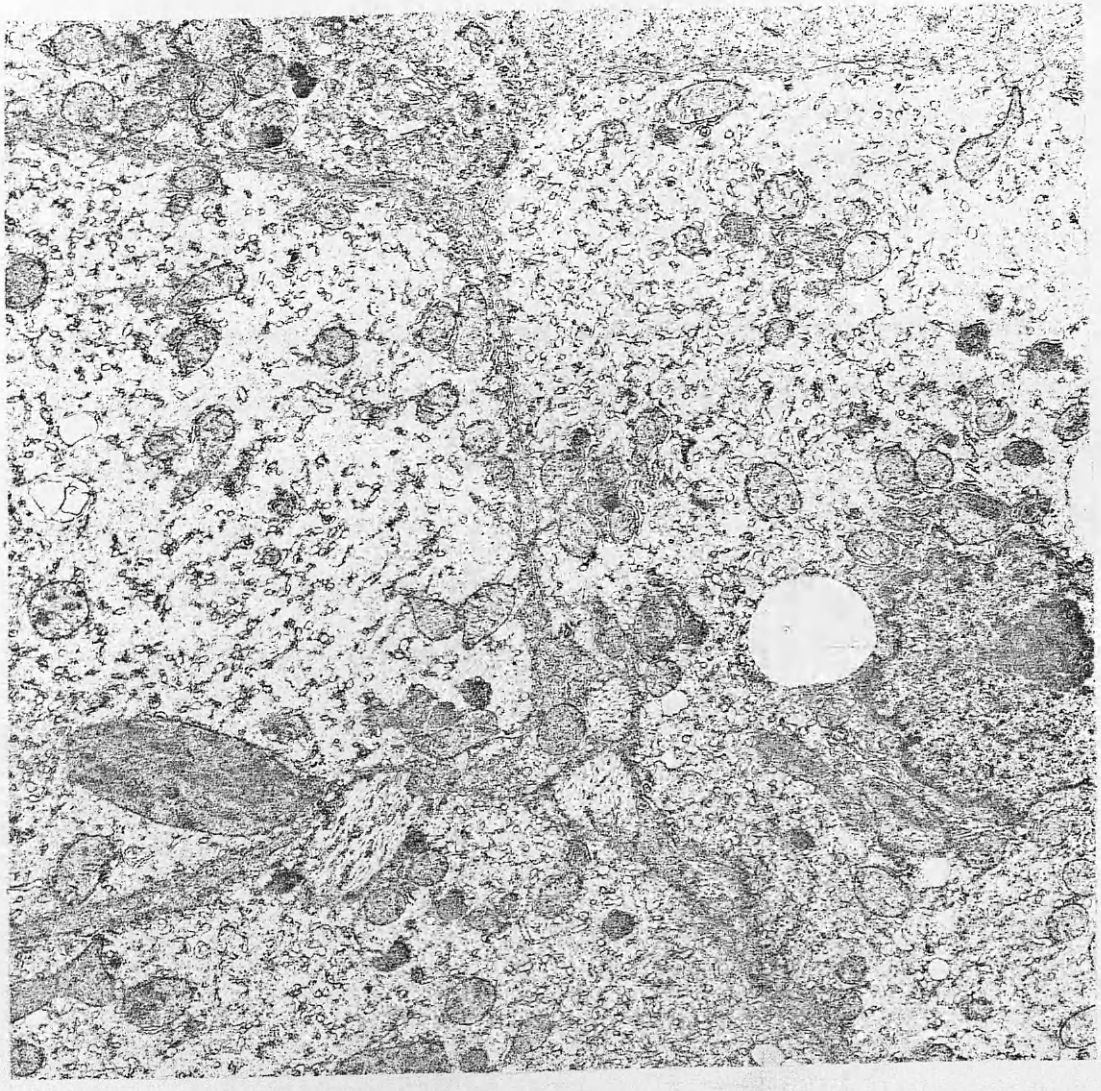

Above : Figure 31.7 Below : Figure 31.8

FIGURE 32.1

SEM of alcoholic hepatitis. Fractured hepatic surface showing portal area with numerous inflammatory cells and tissue debris. Fibrous tissue bands seen thrown over the broken surfaces. Honeycomb structure of proliferated bile ductules are evident. (X 225)

FIGURE 32.2

SEM of alcoholic hepatitis. High magnification micrograph shows details of various inflammatory cells, fibrous tissue and different thickness and several lumina of bile ductules among the tissue debris. Note the small translucent round holes which probably correspond to the nuclei of the ductular cells. (X 1125)
(pd : proliferated ductule) (co : collagen) (n : nucleus)

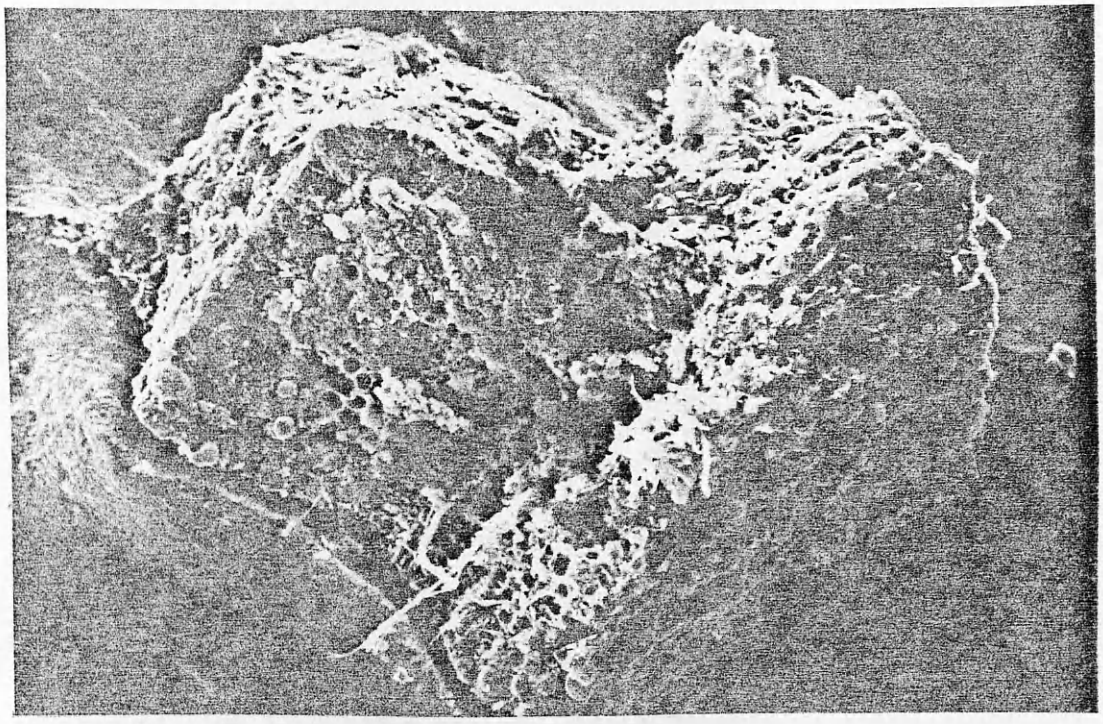

Above : Figure 32.1

Below : Figure 32.2

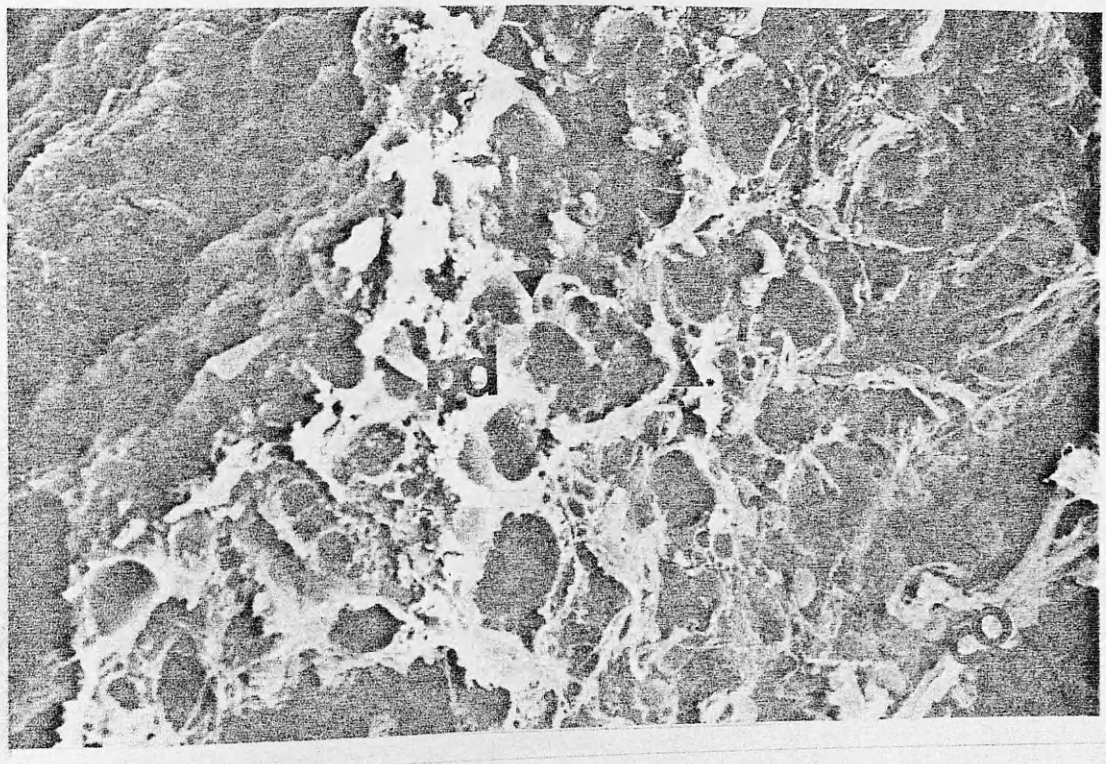

FIGURE 32.3

SEM of alcoholic hepatitis. Shows inflammatory cells of various sizes with folds, ruffles and pits. A honeycomb structure of proliferated bile ductules(pd) consisting of six lumina are present. (ma : macrophage). (X 1125)

FIGURE 32.4

SEM of alcoholic hepatitis. High magnification micrograph of proliferated ductules showing details of their lumina (lu), covered by numerous tiny flat microvilli and thin web of delicate fibres. Note the several small holes of the nuclei(n)present in the wall. Part of fibrous tissue band surrounding the ductules are present. (X 4500)

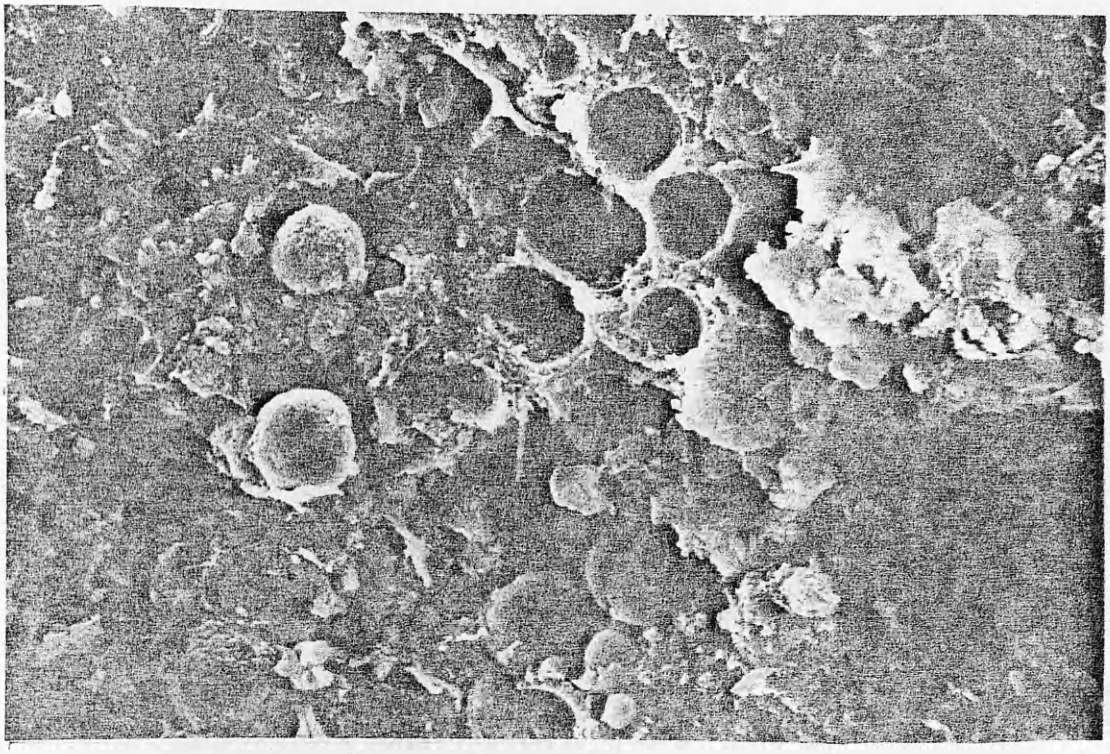

Above : Figure 32.3

Below : Figure 32.4

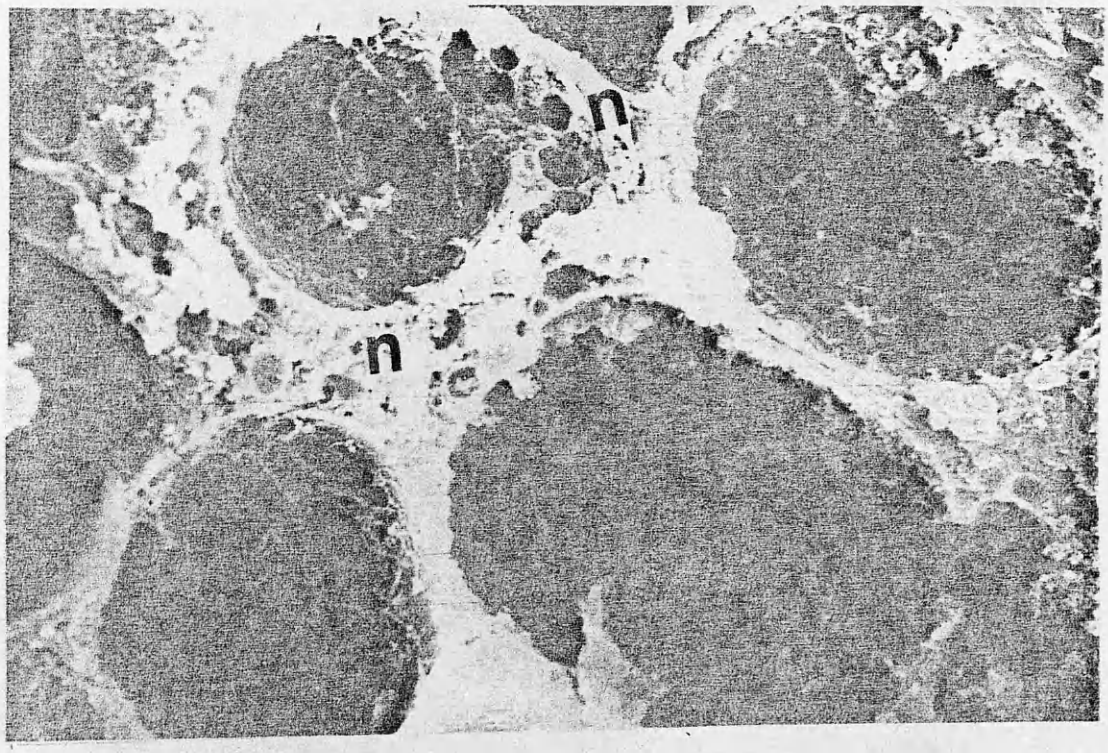

FIGURE 32.5

SEM of alcoholic hepatitis. Shows bile ductules with ill-defined lumen. The walls have several nuclei surrounded by twisted fibrous band adjacent to a relatively normal size bile ductule. (X 2250) (co : collagen).(n : nucleus).(arrow : bile ductule).

FIGURE 32.6

SEM of alcoholic hepatitis. Shows high magnification micrograph of the bile ductule. (X 4500)

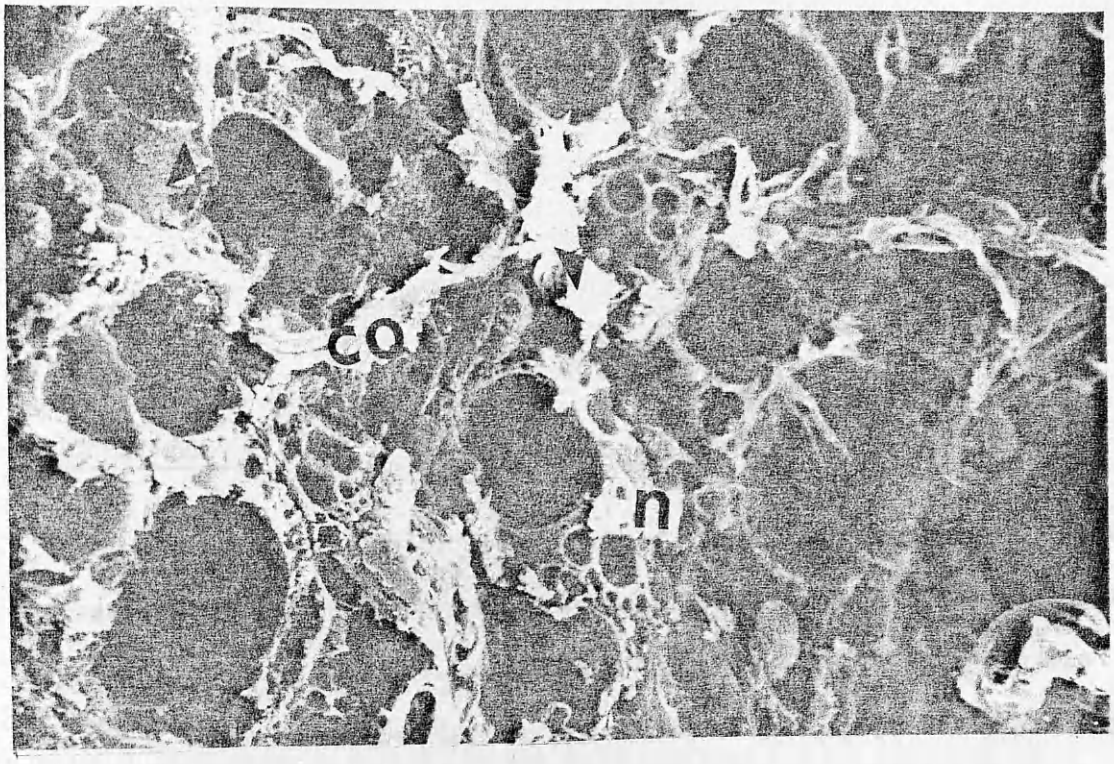

Above : Figure 32.5

Below : Figure 32.6

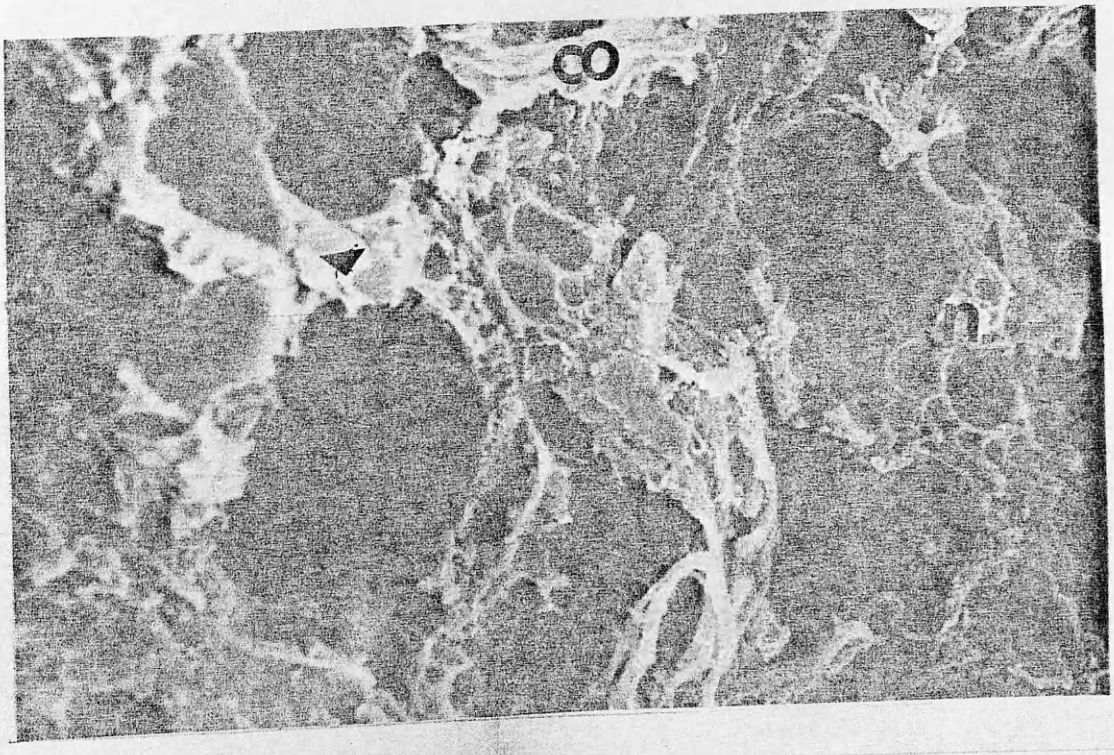

FIGURE 33.1

LM of alcoholic cirrhosis. Shows part of cirrhotic nodule, the cells arranged in more than one cell thick plate. Macro- and Microvesicular fat droplets are abundant. Sinusoidal and pericellular fibrosis are evident. Note the coiled dark cytoplasmic inclusions probably Mallory bodies.

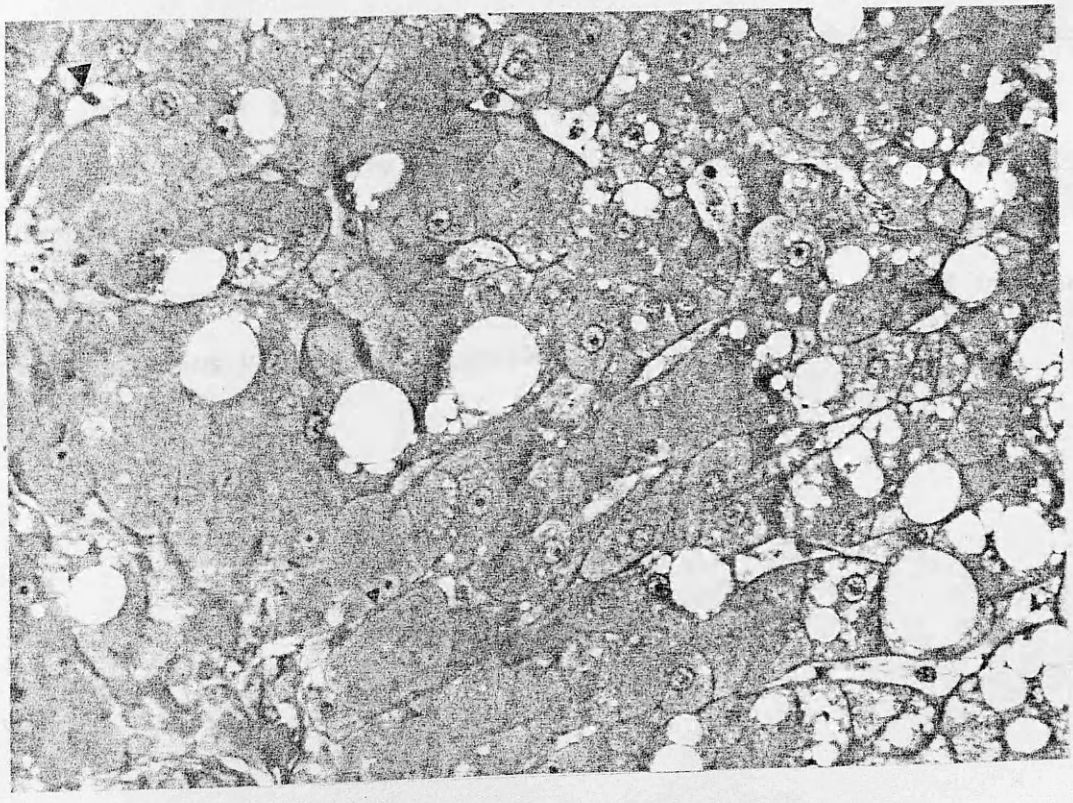

Figure 33.1

FIGURE 33.2

LM of alcoholic cirrhosis. One micron thick resin section shows part of perinodular fibrous septa where proliferated bile ductules are evident among the heavy chronic inflammatory cell infiltrate. Trapped hepatocytes are evident. The hepatocytes within the nodule have a rosette arrangement. There is Kupffer cell hyperplasia and lymphocytic infiltration within the sinusoids.

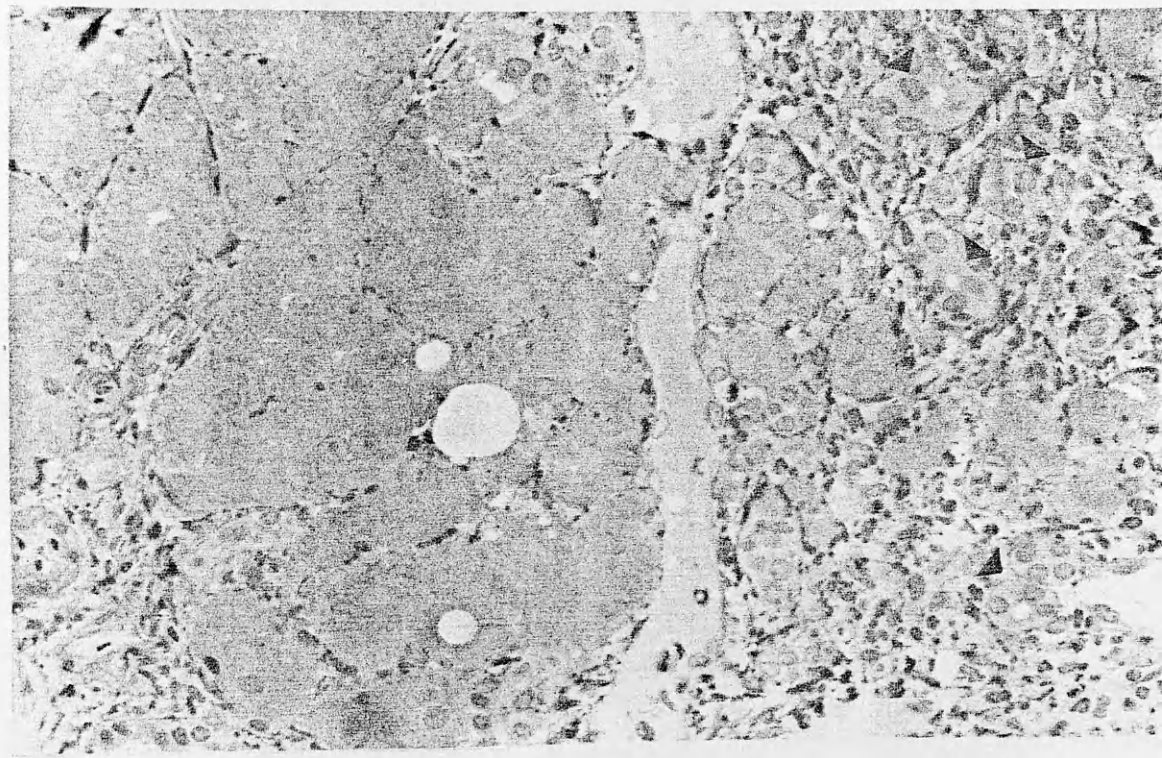

Figure 33.2

FIGURE 34.1

TEM of alcoholic cirrhosis. Shows several hepatocytes arranged in rosette form around hepatic sinusoid (s). There is marked dilatation of RER, hypertrophy of SER, increased number of lysosomes (ly) and giant mitochondria (gm) are evident. (X 4050)

Figure 34.1

FIGURE 34.2

TEM of alcoholic cirrhosis. Shows several hepatocytes (h). The hepatic sinusoid (s) seen containing abundant cellular debris. The space of Disse appeared narrowed and devoid of microvilli. (ly : lysosome).(k : Kupffer cell). (X 4050)

FIGURE 34.3

TEM of alcoholic cirrhosis. High magnification micrograph showing details of hepatic sinusoid (s). Lymphocyte, Kupffer cell and lysosome-filled cytoplasm are evident. Note the space of Disse devoid of microvilli. (X 4050)
(bc : bile canaliculi).(h : hepatocyte).(n : nucleus).

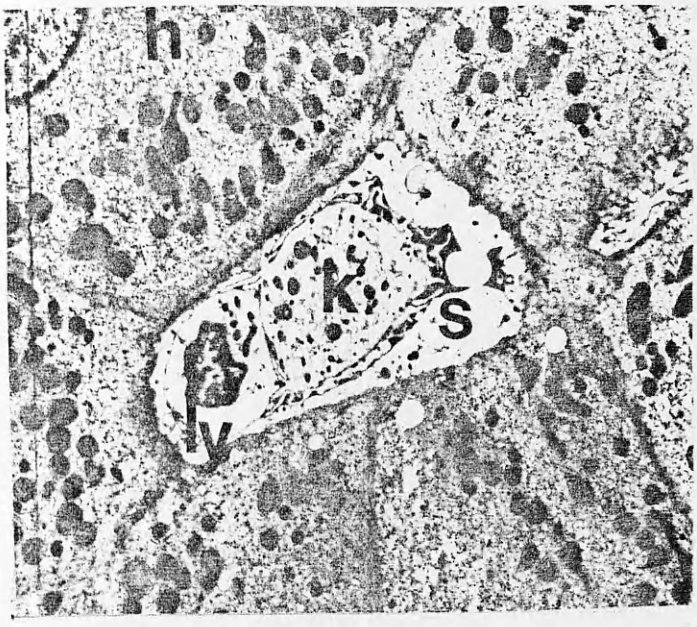

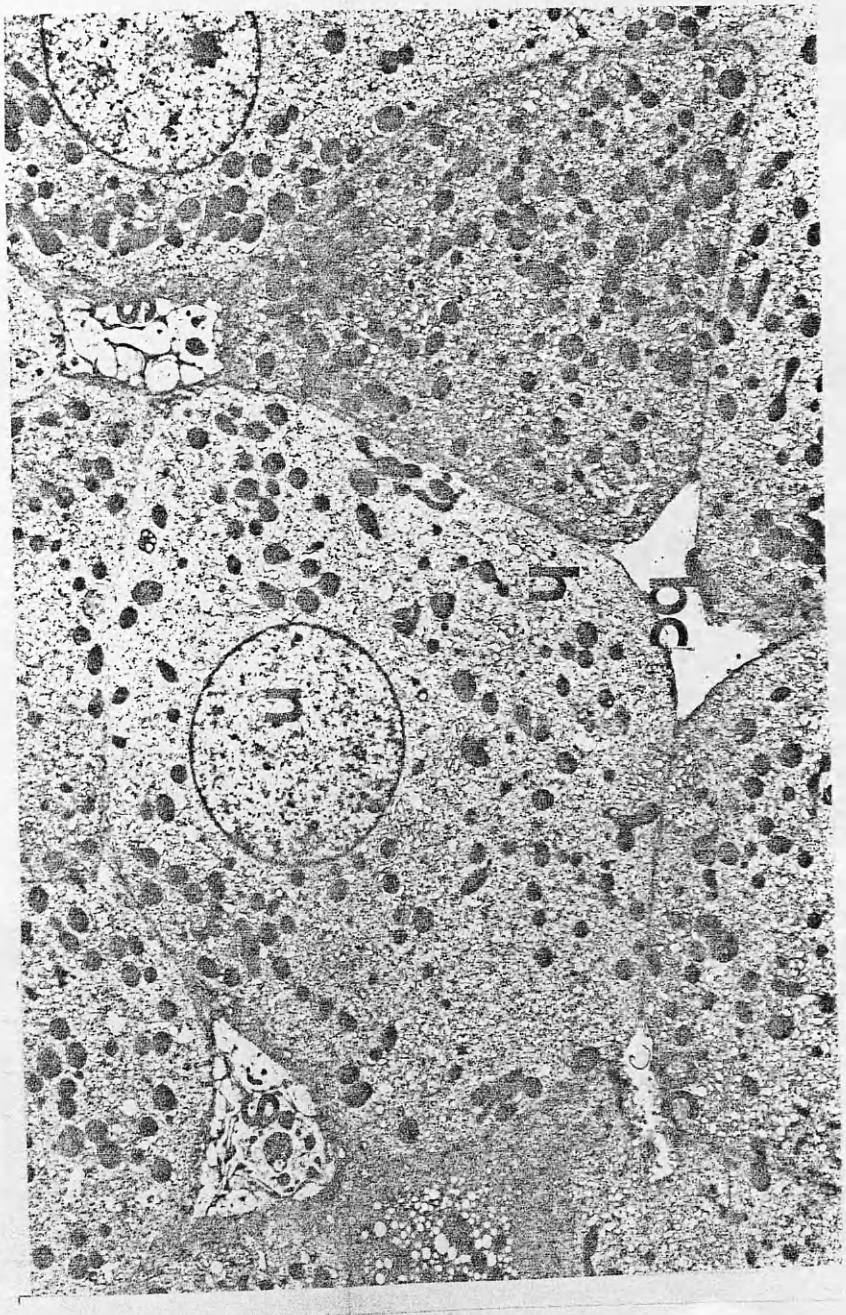

Above : Figure 34.2 Below : Figure 34.3

FIGURE 35.1

TEM of alcoholic cirrhosis. Shows part of cirrhotic nodule. Hepatocytes located close to a sinusoid. The space of Disse is narrowed. The vascular pole of most hepatocytes is smooth and microvilli are sparse. Within the sinusoid a lymphocyte (ly) is present in close apposition to degenerated hepatocyte (dh). Note the presence of basement membrane (bm). (X 8100)

FIGURE 35.2

TEM of alcoholic cirrhosis. Shows part of cirrhotic nodule. High magnification of hepatic sinusoid showing details of the space of Disse. The basement membrane runs a considerable length underneath the endothelial lining. Note the close contact of the lymphocyte (ly) with degenerated hepatocyte (dh). A slender collagen fibre is present in the space of Disse on the other side of the sinusoid. (X 9675)

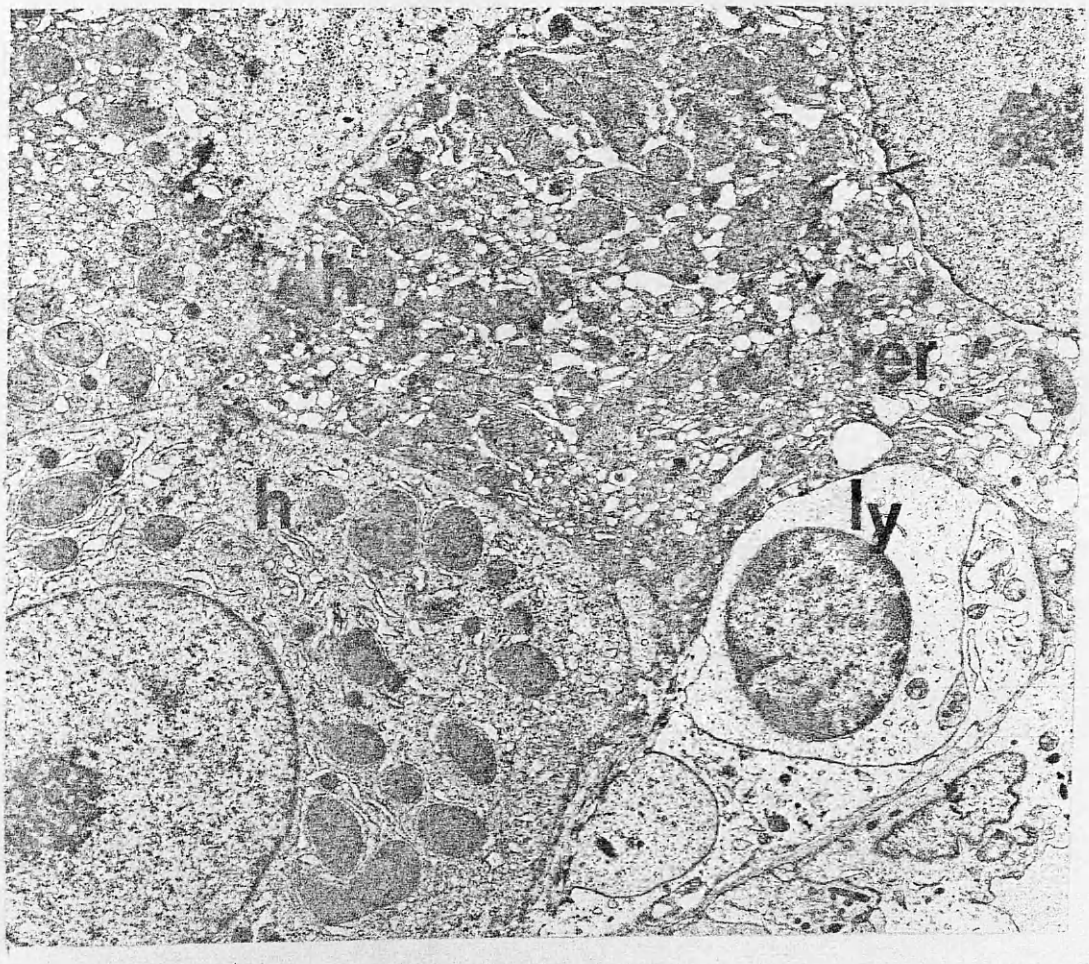

Above : Figure 35.1 Below : Figure 35.2

FIGURE 36.1

TEM of alcoholic cirrhosis. Shows part of cirrhotic nodule. Hepatocyte seen close to a sinusoid. The space of Disse (ds) is narrowed with few flat microvilli (mv). Electron dense membrane is evident clinging to the microvilli. Nucleus of Kupffer cell (k) is evident. (X 22050)

FIGURE 36.2

TEM of alcoholic cirrhosis. Shows part of cirrhotic nodule. The hepatic sinusoid showing basement membrane resting on the microvilli (mv) in the space of Disse (ds). Note the presence of high electron dense area on periodic intervals. (X 22050)

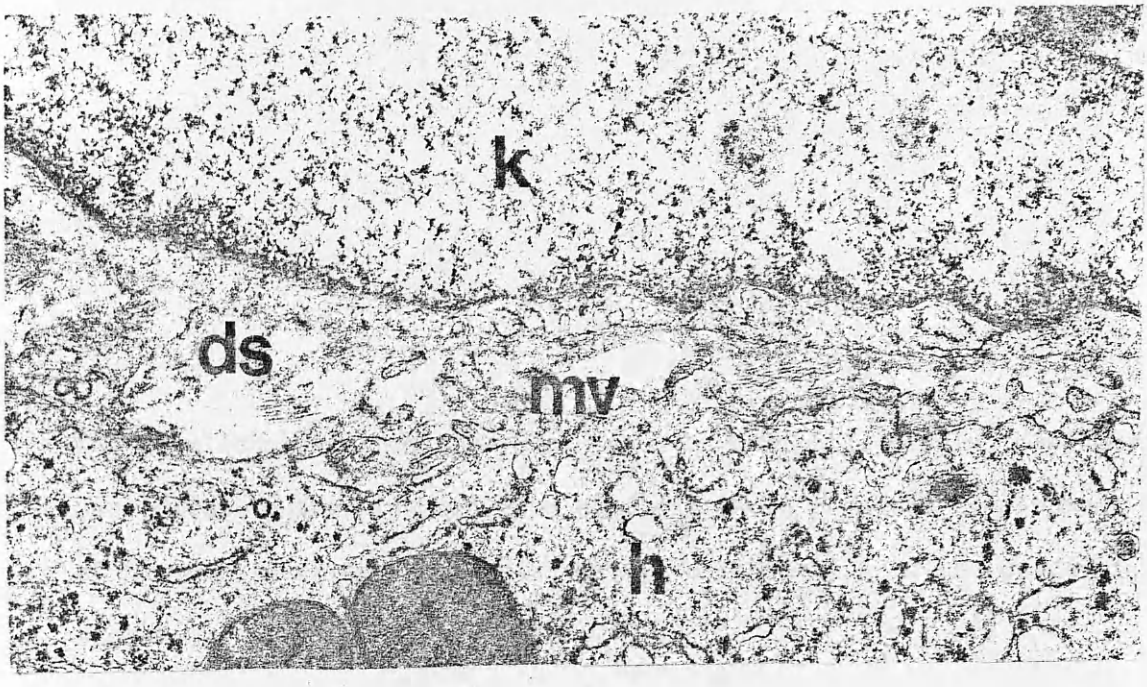

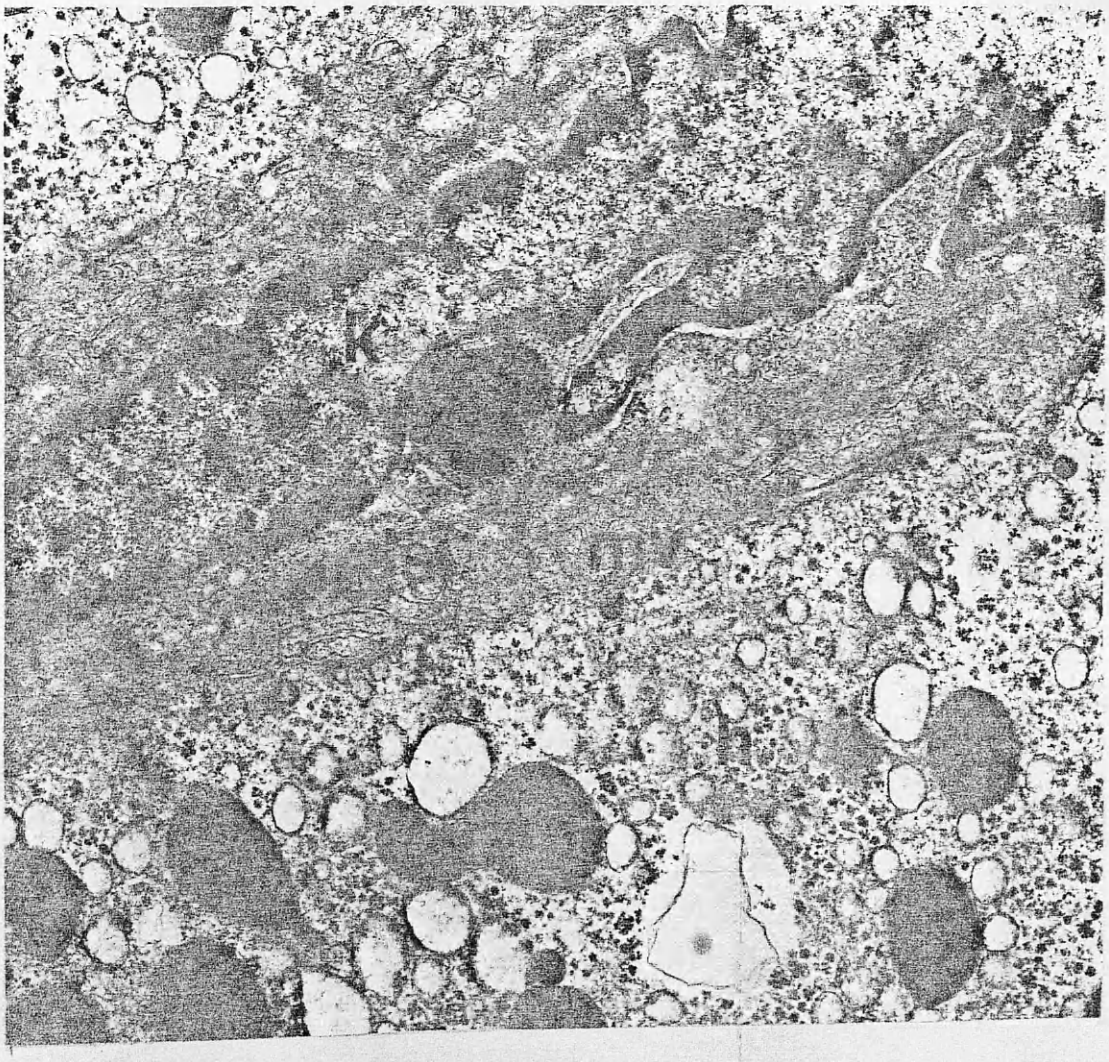

Above : Figure 36.1 Below : Figure 36.2

FIGURE 36.3

TEM of alcoholic cirrhosis. Shows part of cirrhotic nodule. Hepatocyte seen close to the sinusoid. The sinusoid shows periodic development of basement membrane (bm) which clings to microvilli in the space of Disse. (X 9675)

FIGURE 36.4

TEM of alcoholic cirrhosis. High magnification micrograph showing details of the basement membrane which have slight granular appearance. (mv : microvilli).(h : hepatocyte).(k : Kupffer cell). (X 29250)

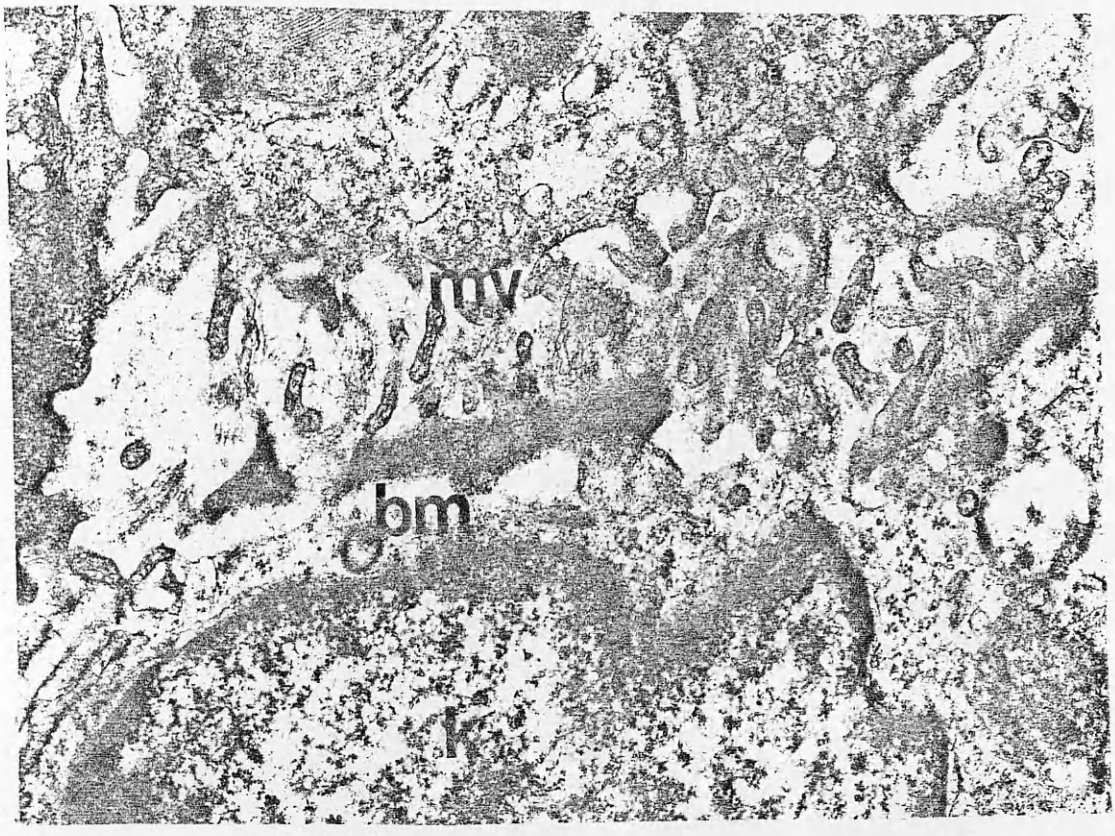
mv
bm
f


m
h

FIGURE 37.1

TEM of alcoholic cirrhosis. Shows the lateral surfaces of neighbouring hepatocyte in a cirrhotic nodule. The intercellular spaces (iw) are dilated and the hepatocellular surfaces (h) are covered by microvilli creating a cavernous appearance. Giant mitochondria (gm) with para-crystalline inclusions are present.(ply: phagolysosome). (X 22050)

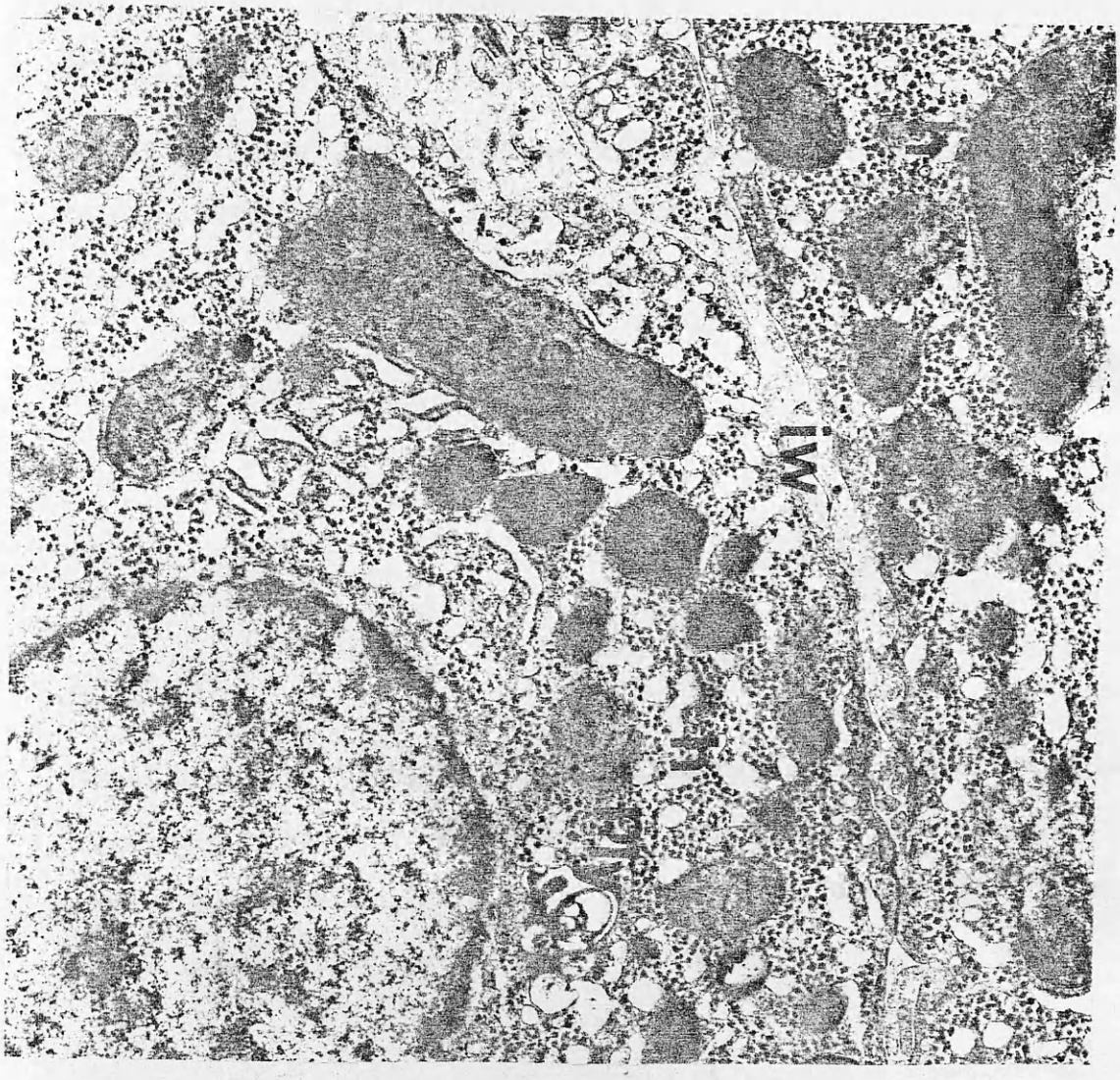

Figure 37.1

FIGURE 37.2

TEM of alcoholic cirrhosis. Shows part of adjacent hepatocytes. Collagen fibrils present in dilated intercellular space (iw). Note the vacuolar dilatation of the endoplasmic reticulum. (X 16870)

FIGURE 37.3

TEM of alcoholic cirrhosis. High magnification micrograph of the dilated intercellular spaces (iw), the lateral surfaces of both hepatocytes covered by microvilli (mv), banded collagen (co) fibrils are evident in the intercellular spaces. (X 40500)

Above : Figure 37.2 Below : Figure 37.3

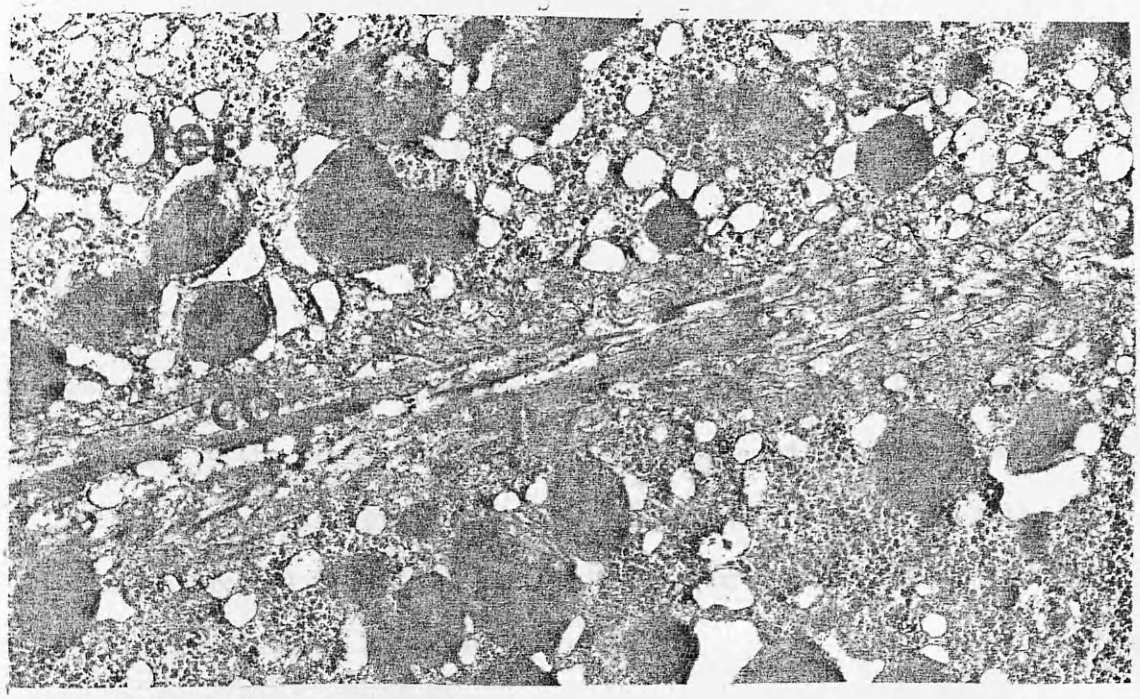

FIGURE 38.1

TEM of alcoholic cirrhosis. Proliferated bile ductule (dc) shown embedded in the connective tissue and surrounded by thick basal lamina. Note a bleb projecting from the apical pole of the cell and a neutrophil (ne) in close apposition to the ductules. (X 2205) (lu : lumen).(co : collagen fibre).

Figure 38.1

FIGURE 38.2

TEM of alcoholic cirrhosis. A proliferated bile ductule (dc) with thick wavy basal membrane (bm) surrounded by thick fascicle of fibrous tissue. Some of the lumens are ill-defined while the others have few microvilli. Several stromal cells are evident. (co : collagen) (ma: macrophage). (X 4050)

Figure 38.2

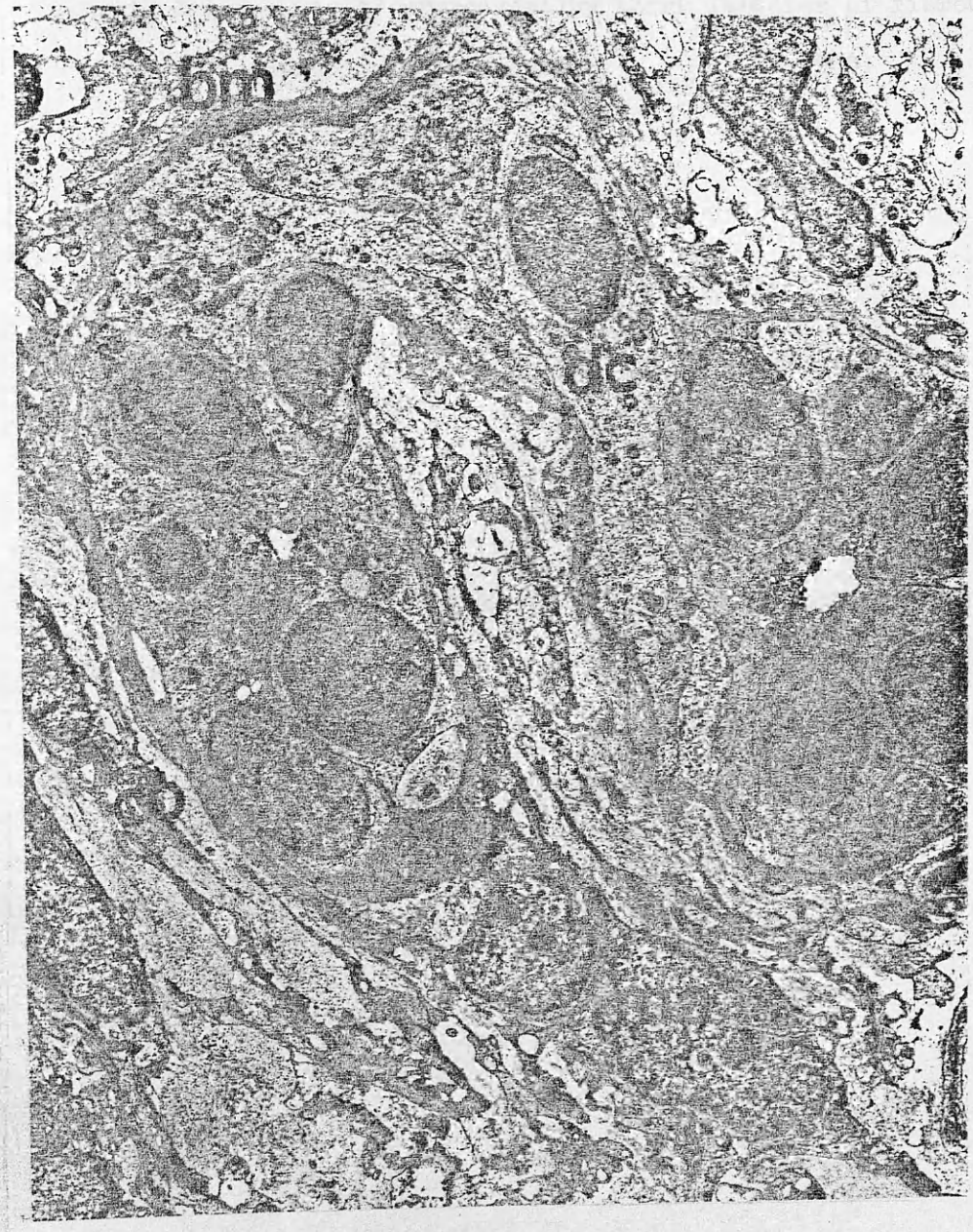

FIGURE 38.3

TEM of alcoholic cirrhosis. Marginal zone of cirrhotic septa showing trapped hepatocyte (h) surrounded by thick fasicles of fibrous tissue. Fibroblast is shown in close contact. (X 4950)

FIGURE 38.4

TEM of alcoholic cirrhosis. Marginal zone of cirrhotic septa showing thick fasicles of connective tissue dissecting between hepatocyte (h). Several stromal cells are present. (ma : macrophage). (X 4950)

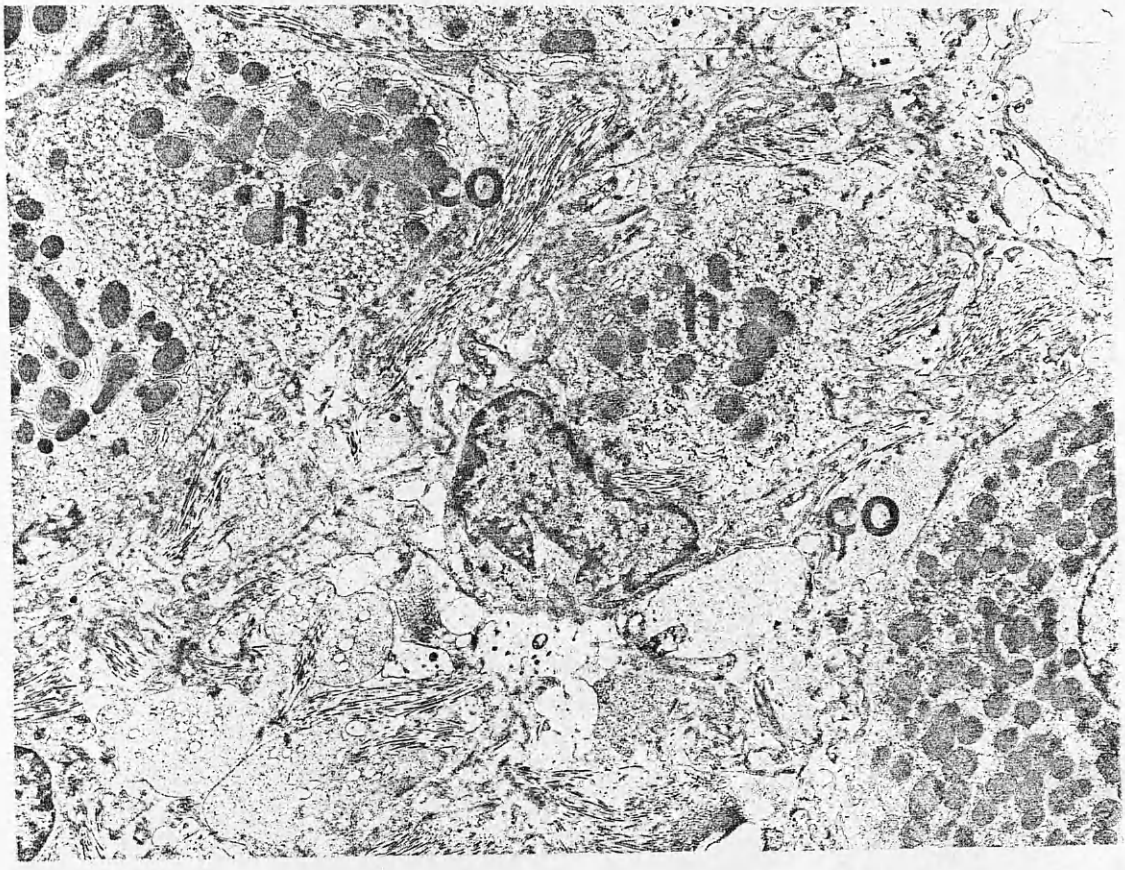

Above : Figure 38.3

Below : Figure 38.4

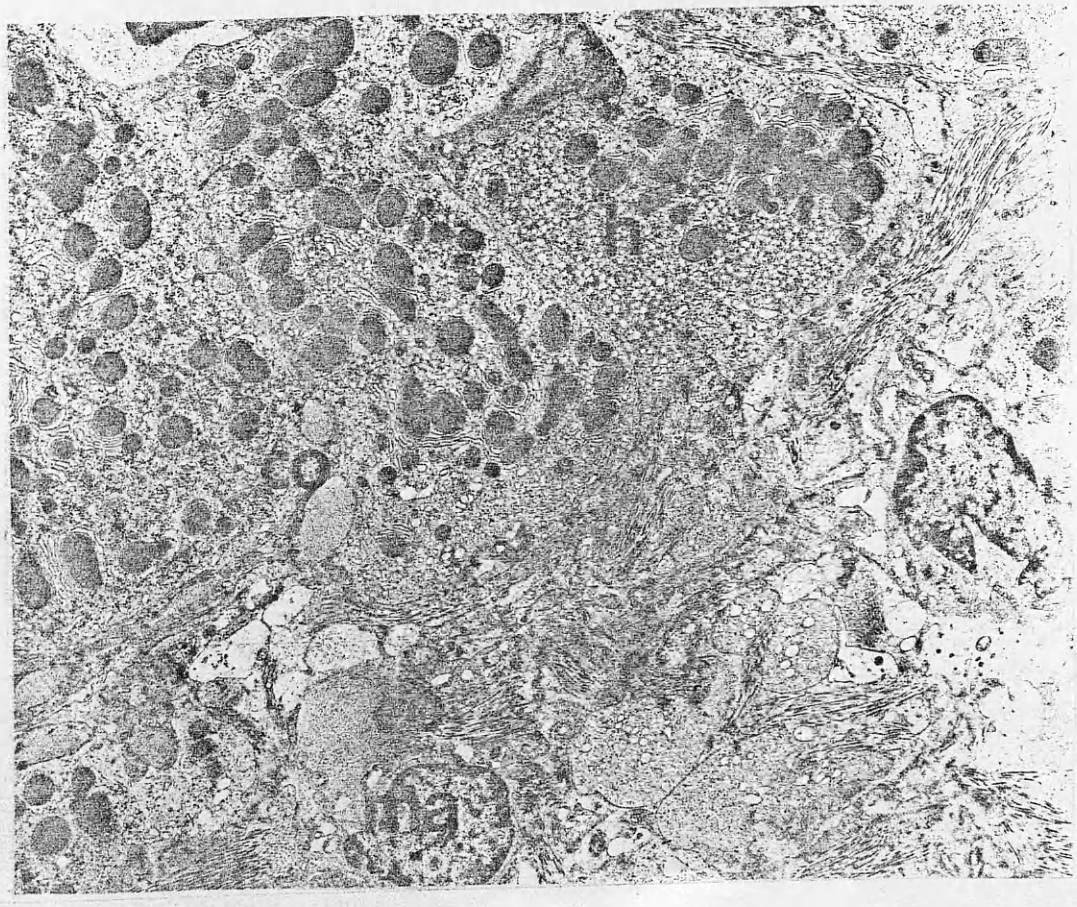

FIGURE 39.1

SEM of alcoholic cirrhosis. Fractured surface showing a cirrhotic nodule surrounded by thick bands of connective tissue. Within the nodule the cells are arranged in groups. Note the increased amount of fibrous tissue between the cells and the fine tissue debris covering the fractured surface. (co : collagen).(h : hepatocyte). (X 450)

Figure 39.1

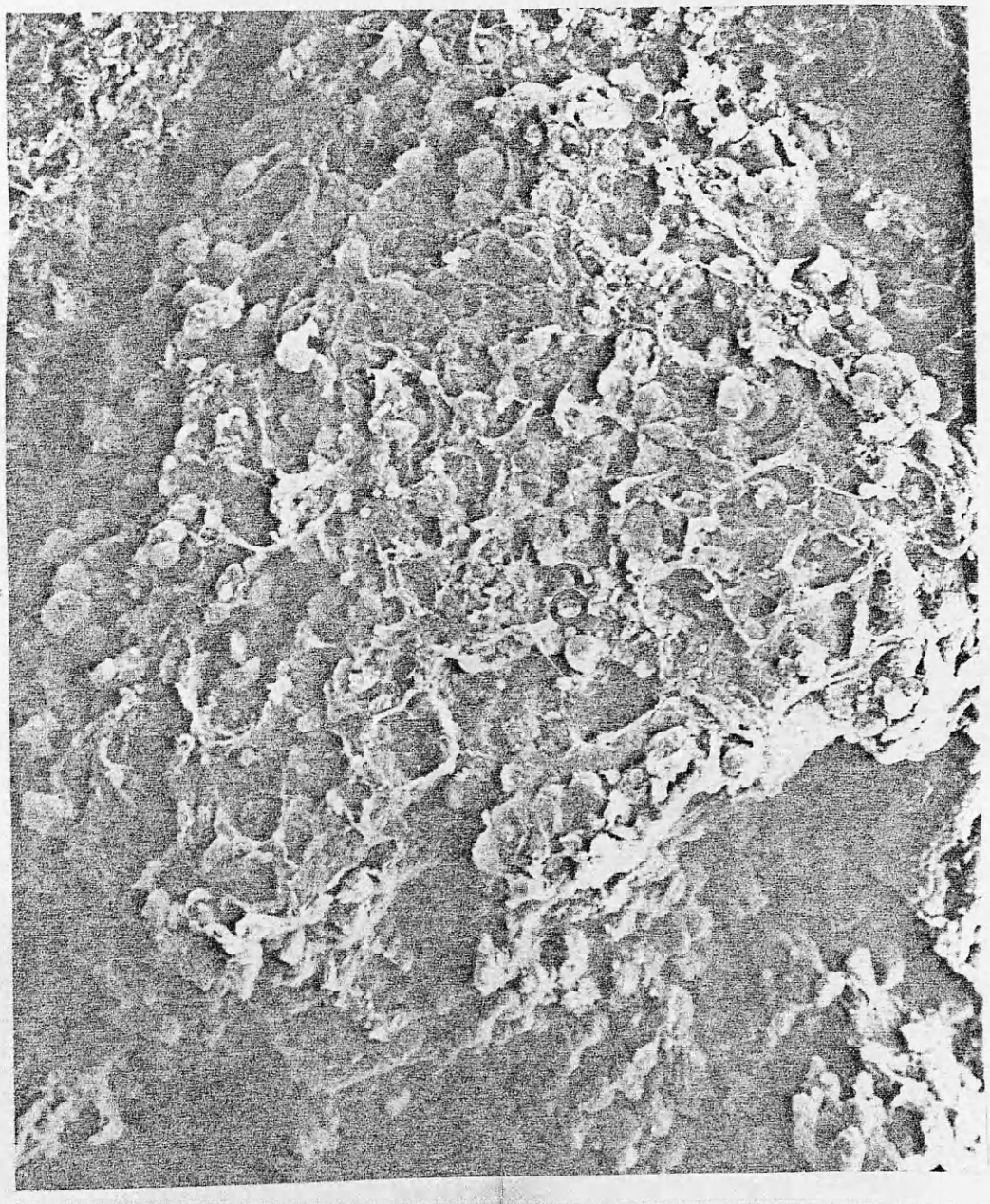

FIGURE 39.2

SEM of alcoholic cirrhosis. Shows group of hepatocytes (h) surrounded by fibrous tissue and covered by thin layer of debris. The fibrous tissue stands more prominently and some is strewn over broken surfaces. Increased amount of inflammatory cells is evident. (X 1125)

Figure 39.2

FIGURE 39.3

SEM of alcoholic cirrhosis. High magnification micrograph showing group of hepatocytes (h) surrounded by thick fibrous bands which appear to be composed of variable thickness fibres and localised in the space of Disse. The surface of the cell is irregular, wrinkled and covered by flat tiny microvilli. The bile canaliculi are difficult to define. (X 3375)

Figure 39.3

FIGURE 39.4

SEM of alcoholic cirrhosis. Fractured surfaces displaying two thick plates of hepatocytes (h). Some of the cells, during fracture process, break in some places exposing the interior of the cells in which are numerous tiny spheroidal bodies probably corresponding to the mitochondria (m). Some of these bodies are spilled all over the cell surfaces. There is increased number of inflammatory cells and RBCs (rb). Note the marked increase in the fibrous tissue. (X 4500)

Figure 39.4

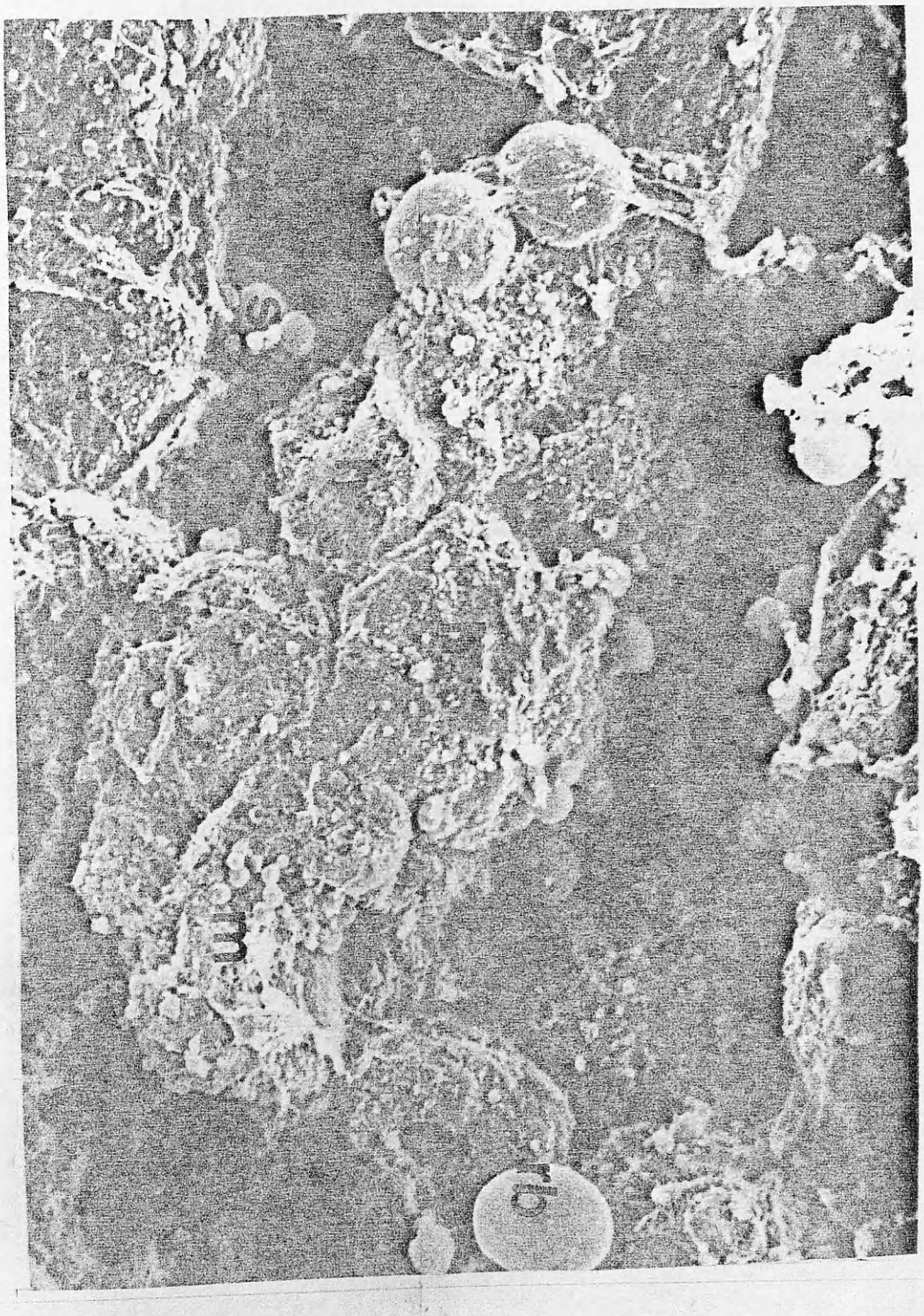

FIGURE 40.1

SEM of alcoholic cirrhosis. Fractured surfaces show the hepatocytes arranged in more than one cell thick plate, the endothelial lining is ripped away from the sinusoid in which few RBCs are still present. Hepatocyte with part or whole surface is crumbled exposing its entire structure. The cells are covered by fine tissue debris. Note the prominent collagen fibres (co), some in close apposition to the cells; others appear as a fine mesh covering the surfaces. (X 1687)

Figure 40.1

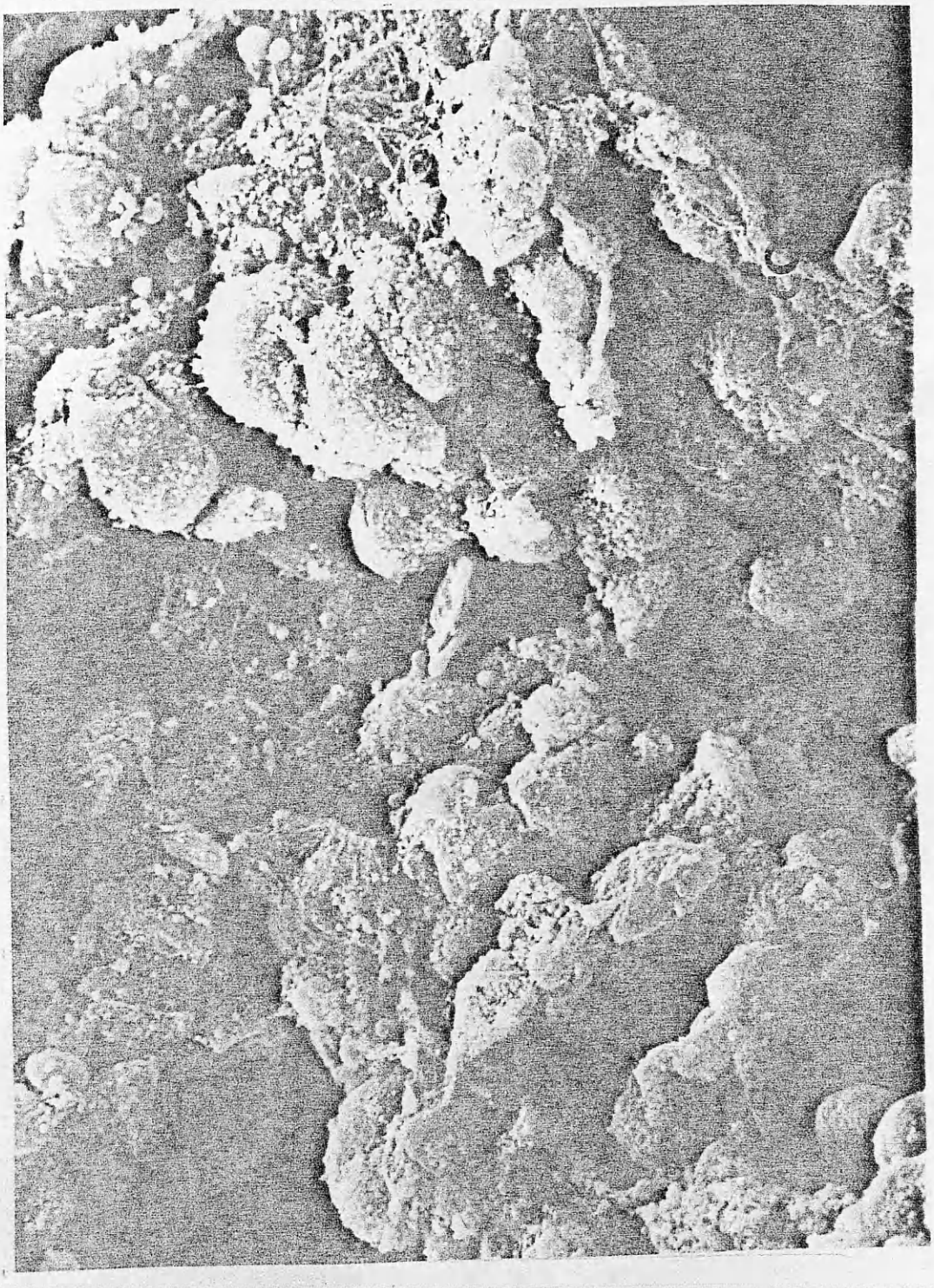

FIGURE 40.2

SEM of alcoholic cirrhosis. Fractured surfaces showing details of several hepatocytes, partially exposing the interior of some of the cells, demonstrating numerous various sized spheroidal bodies among which a large one might correspond to a giant mitochondria (m). Note a thick bundle of fibrous tissue running alongside the cells and some covered the fractured surface. The bile canaliculi are ill-defined. (X 4500)

Figure 40.2

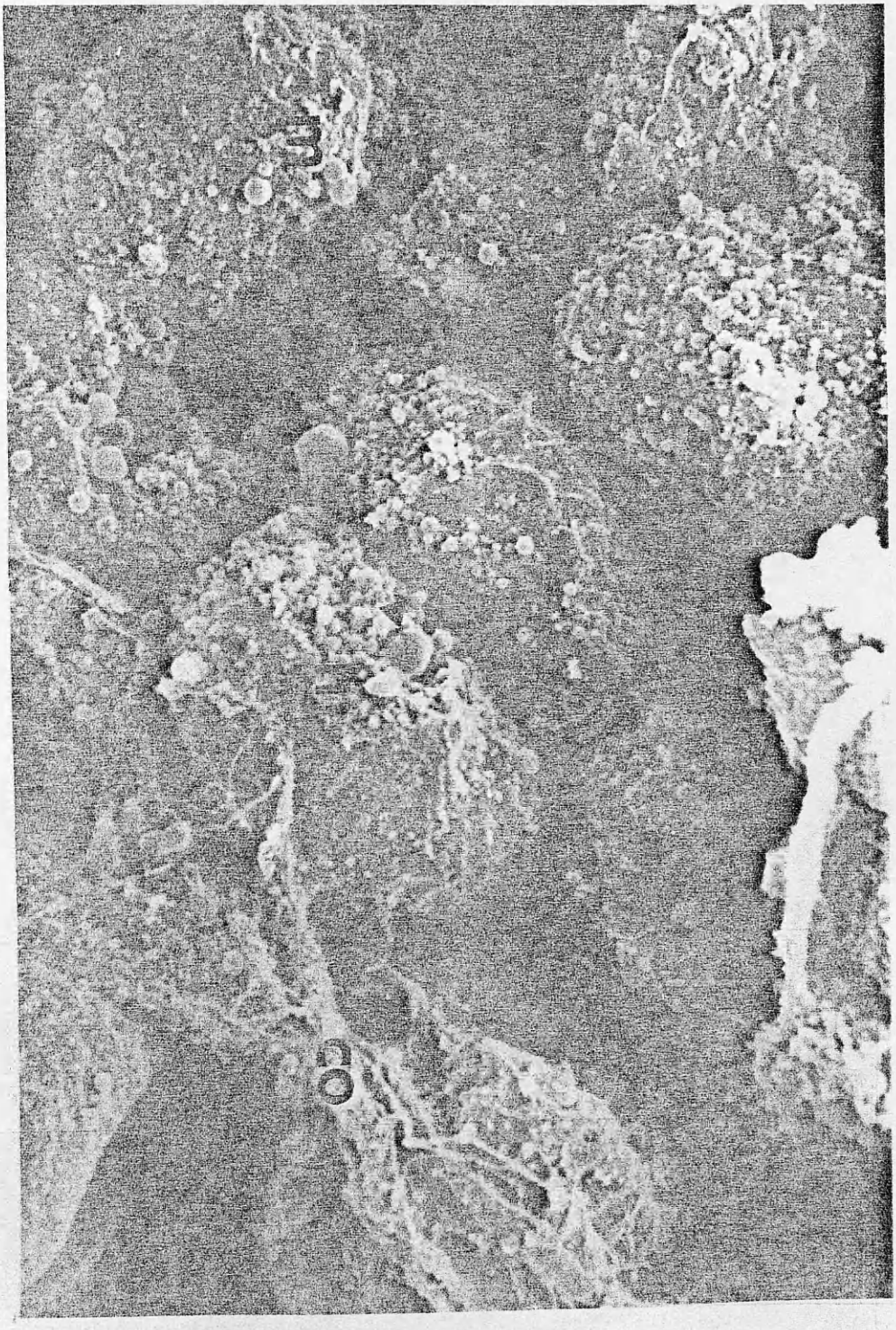

FIGURE 40.3

SEM of alcoholic cirrhosis. A group of hepatocytes are present. Several spheroidal bodies are evident through a partially crumbled cell surface. Some are contained within the cells while others are spilled over the fractured surface. Note some hepatocytes displayed a bizarre shape. (X 2250)

FIGURE 40.4

SEM of alcoholic cirrhosis. High magnification micrograph showing a large spheroidal body evident through broken cell surface and probably corresponding to the nucleus. Several spheroidal bodies within the cells and over the fractured surfaces are evident. Note the bile canaliculi are ill-defined. (X 4500)

Above : Figure 40.3 Below : Figure 40.4

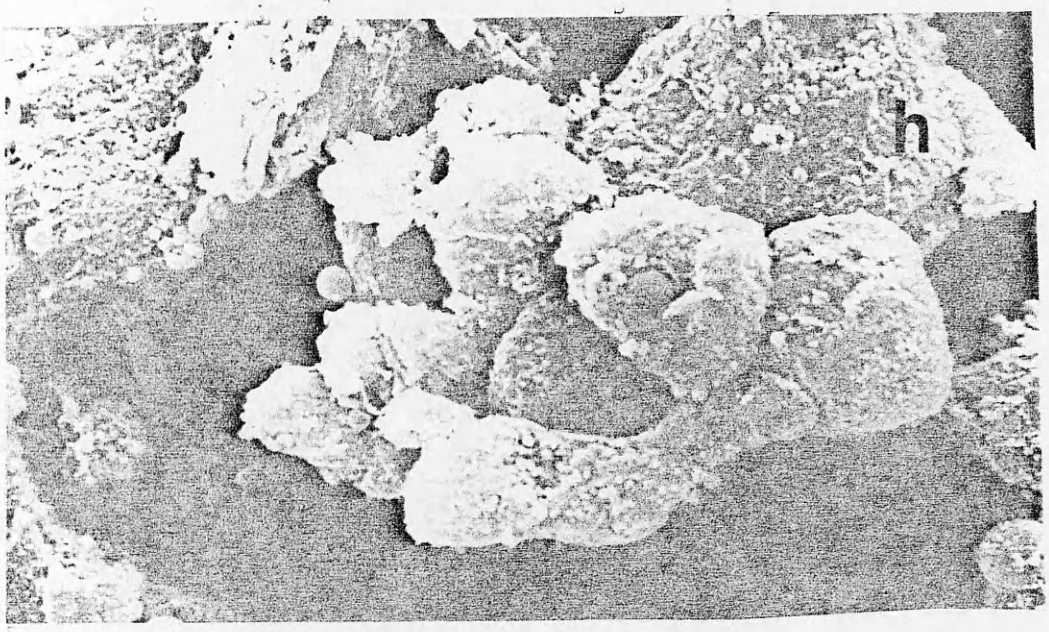

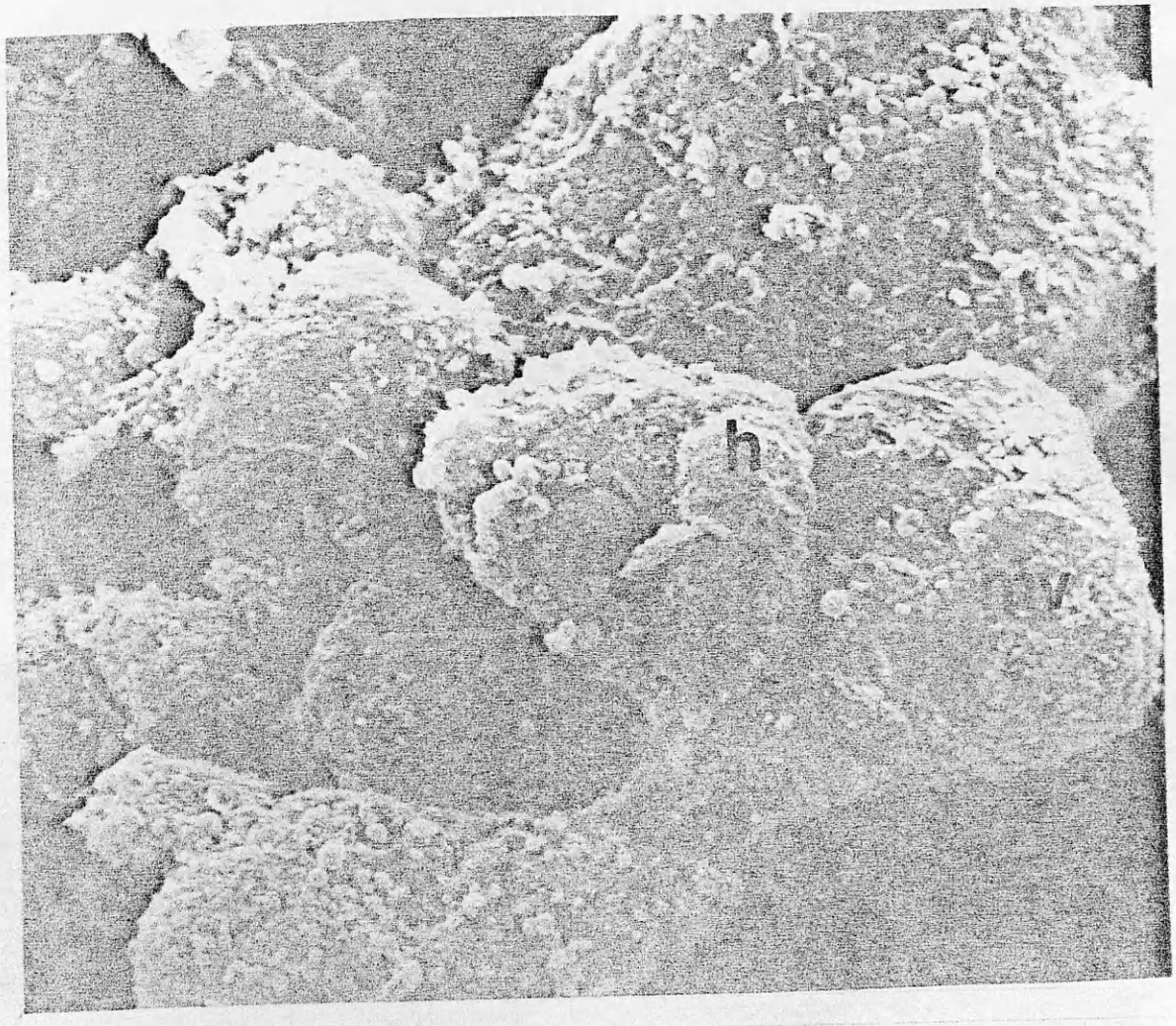

FIGURE 41.1

SEM of alcoholic cirrhosis. Several cells thick plates are present. The endothelial lining is ripped away from the sinusoid. Several RBCs still present. The vascular pole of the hepatocyte is exposed in places demonstrating a relatively smooth surface with few flat microvilli. The intercellular surfaces are folded and rough. (X 4500)

Figure 41.1

FIGURE 41.2

SEM of alcoholic cirrhosis. Fractured surfaces show several hepatocytes The bile canaliculi are difficult to define in any cell. The vascular poles are exposed demonstrating a ruffle appearance of the surface. Few flat microvilli are present. (X 4500)

Figure 41.2

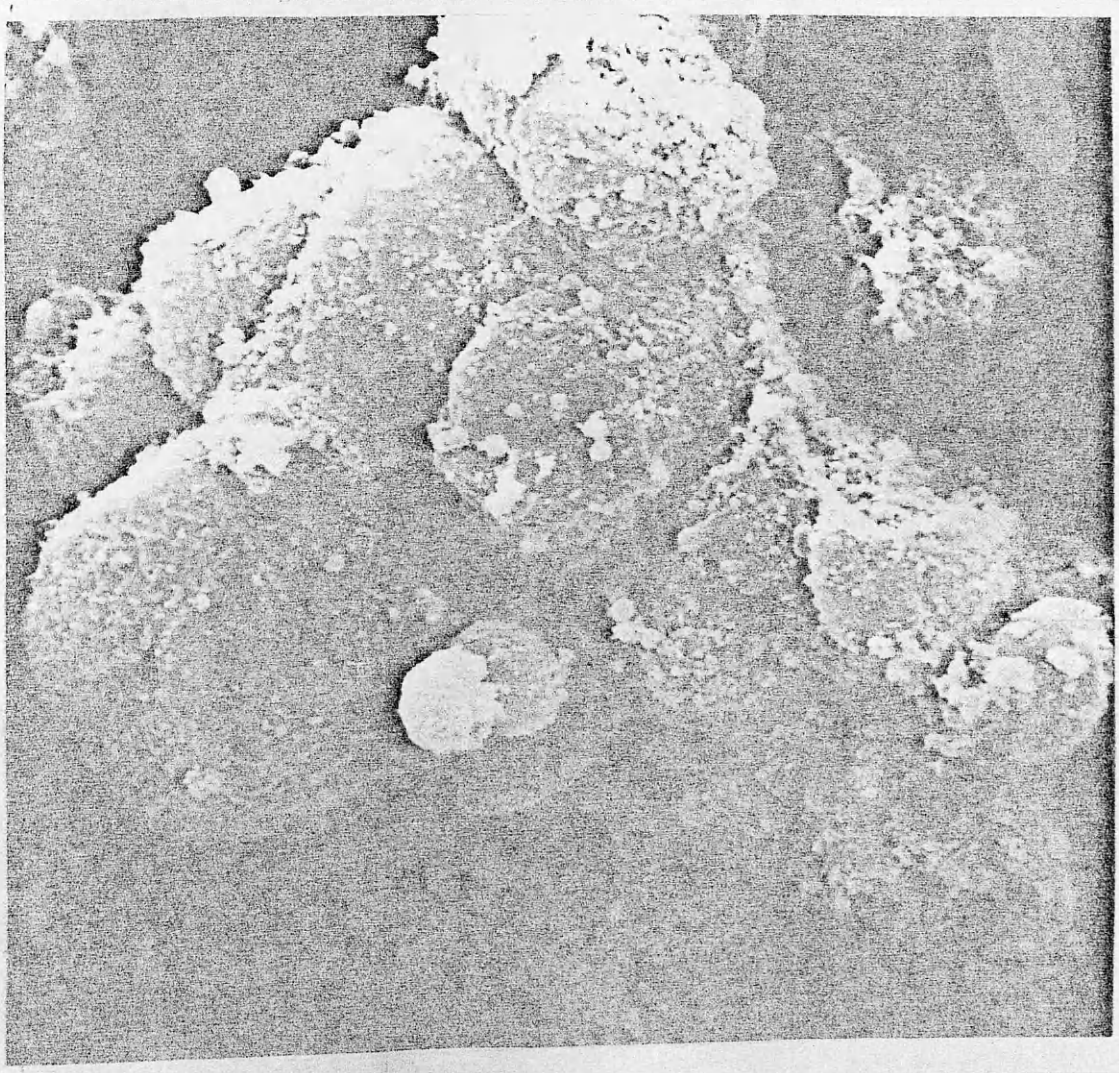

FIGURE 41.3

SEM of alcoholic cirrhosis. Shows several hepatocytes. The bile canaliculi (bc) appear to run a tortuous course. Across the surfaces of the hepatocytes and in the lumen, numerous microvilli are projecting (X 7875)

FIGURE 41.4

SEM of alcoholic cirrhosis. High magnification micrograph showing the bile canaliculi buried between the folds and ruffles of the hepatocytic surfaces. (X 7875)

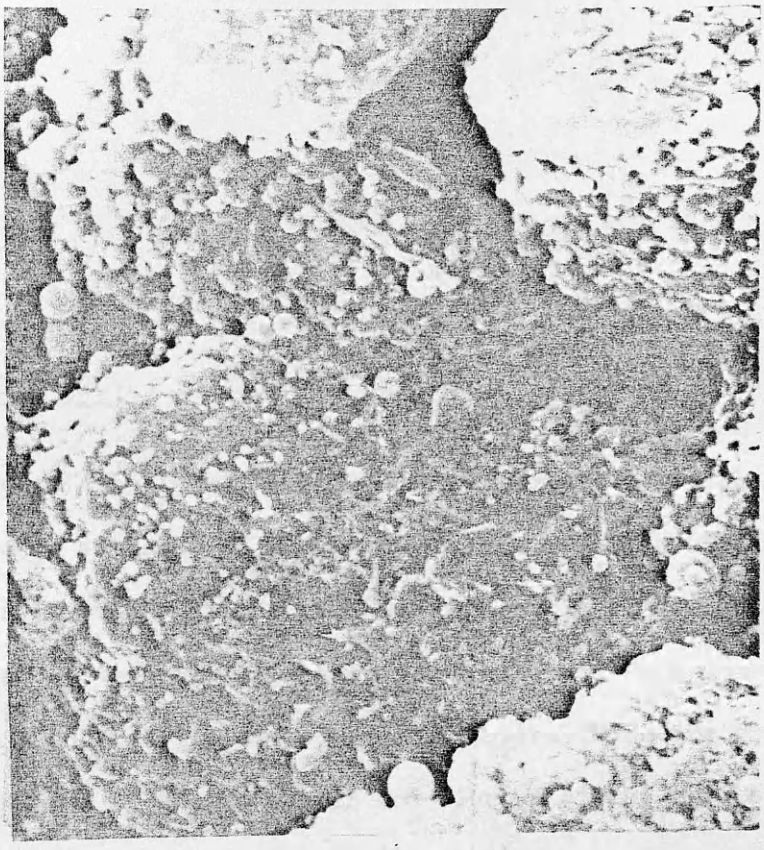

Above : Figure 41.3

Below : Figure 41.4

FIGURE 42.1

SEM of alcoholic cirrhosis. Fractured surface revealed thick fibrous septa on either side of a group of hepatocytes. Several spheroidal cells (probably lymphocyte) are present in close contact, one is wedged between two hepatocytes and attached to a degenerated one with slender cytoplasmic process. Several RBCs are present. Note the amount of tissue debris and fibrous tissue spilled over the fractured surface. (X 4500)

Figure 42.1

FIGURE 42.2

SEM of alcoholic cirrhosis. High magnification micrograph showing details of lymphocytes. Their surfaces slightly wrinkled with few plump microvilli. It appeared to be connected to the degenerated hepatocyte with numerous slender cytoplasmic processes. Note the thick wavy fibrous septa. (X 7875)

Figure 42.2

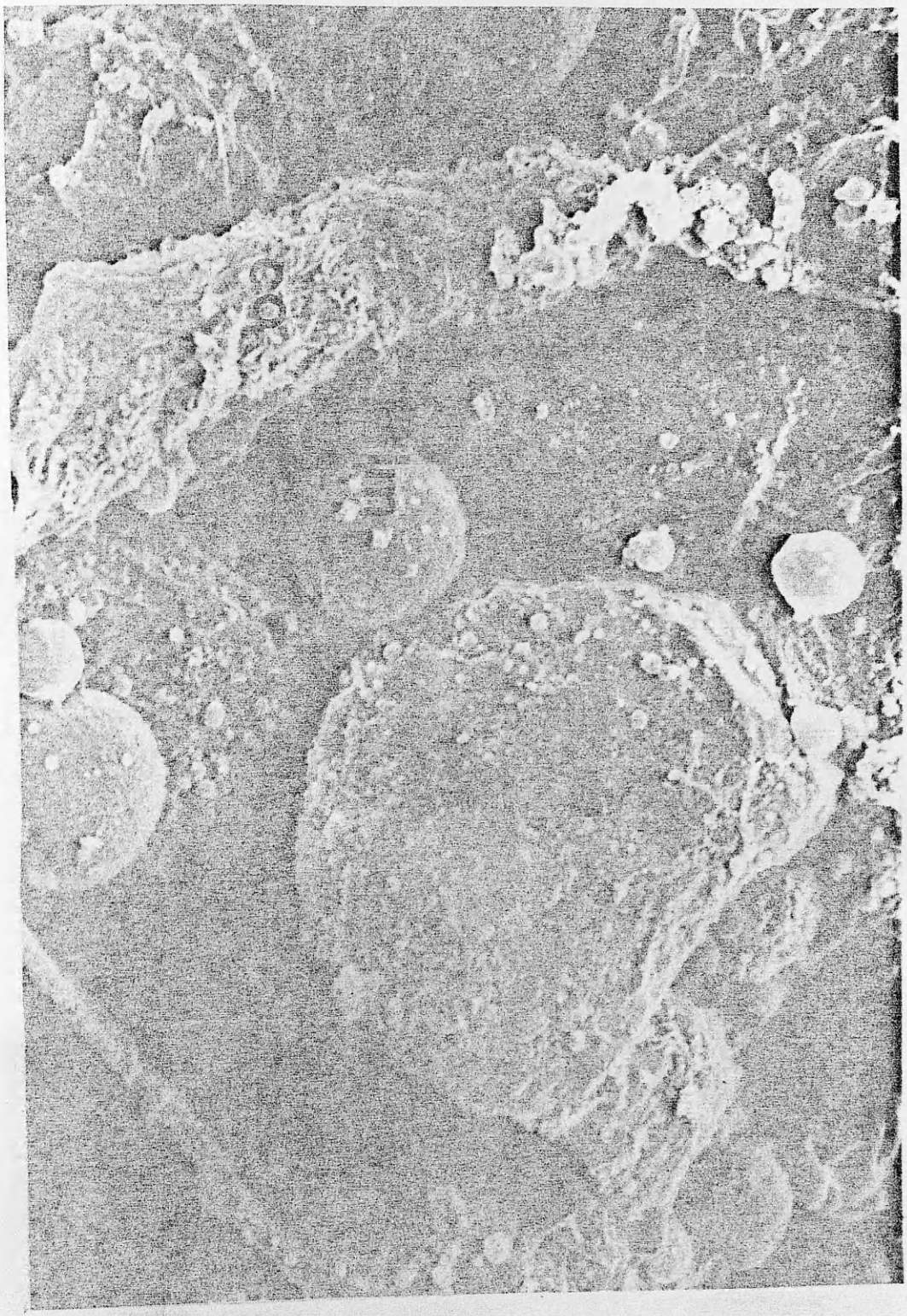

FIGURE 42.3

SEM of alcoholic cirrhosis. Shows thick fibrous band which consists of twisted fibres. Increased amount of tissue debris surrounded the degenerated hepatocyte. Spheroidal body protruded through the surface of one of them. Note the close apposition of a lymphocyte to this cell. (X 4500)

Figure 42.3

FIGURE 42.4

SEM of alcoholic liver cirrhosis. High magnification micrograph of a degenerated hepatocyte. The cell has a wrinkled appearance. The details of its specialised surface are ill-defined. It is covered by plump blebs or microvilli. A shadow of bile canaliculi probably runs across the surface. A lymphocyte in close contact with the cells. Note the spheroidal body which protruded through the surface. (X 7875)

Figure 42.4

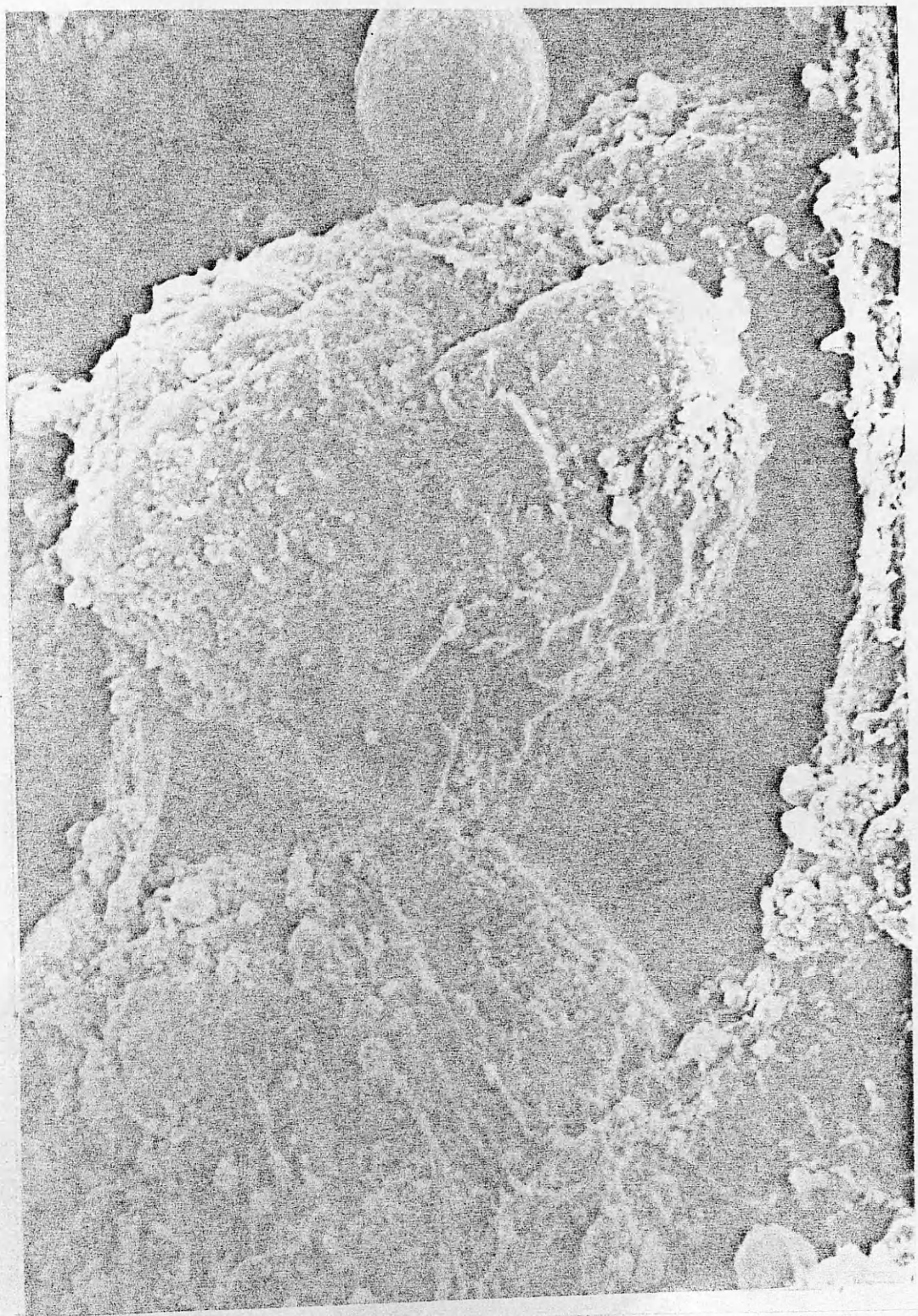

FIGURE 43.1

SEM of alcoholic cirrhosis. Shows an open hepatic sinusoid (s) between groups of hepatocytes (h). A thick band of fibres wedged between the endothelial lining (ed) and the hepatocytes. Various sizes of tissue debris are present within the sinusoid. (X 3375)

Figure 43.1

FIGURE 43.2

SEM of alcoholic cirrhosis. High magnification micrograph of the sinusoid showing details of the endothelial lining which appeared thickened and wrinkled. Few large fenestration (f) are evident. Note the Kupffer cell (k) with its long cytoplasmic processes anchoring to the endothelial lining. (X 16875)

Figure 43.2

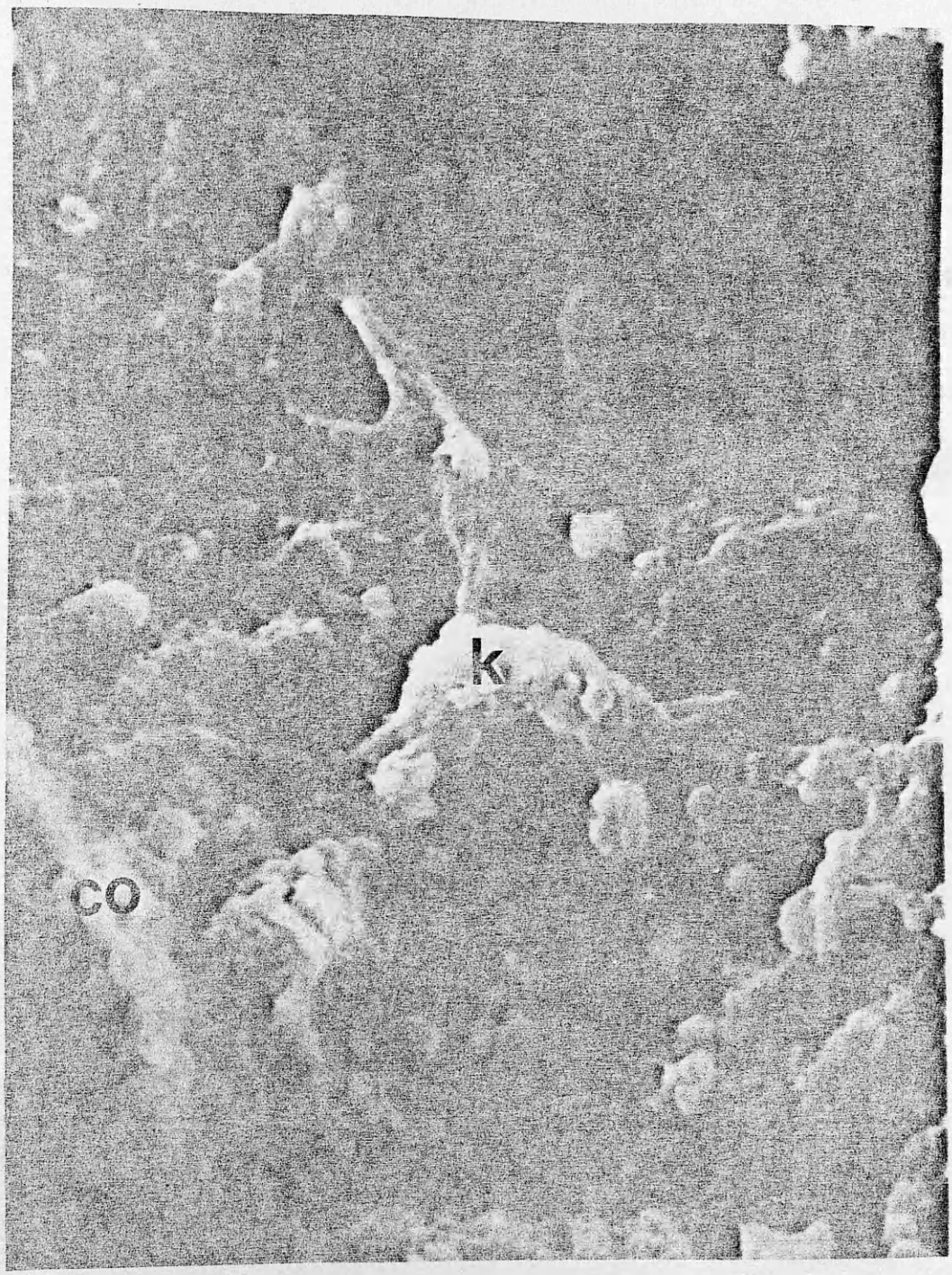

FIGURE 44.1

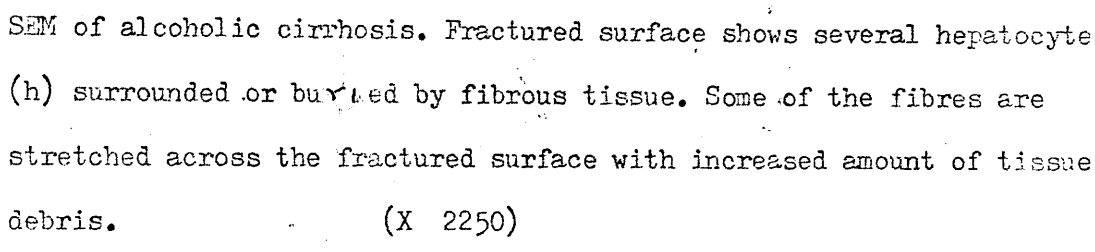

SEM of alcoholic cirrhosis. Fractured surface shows several hepatocytes (h) surrounded or buried by fibrous tissue. Some of the fibres are stretched across the fractured surface with increased amount of tissue debris. (X 2250)

FIGURE 44.2

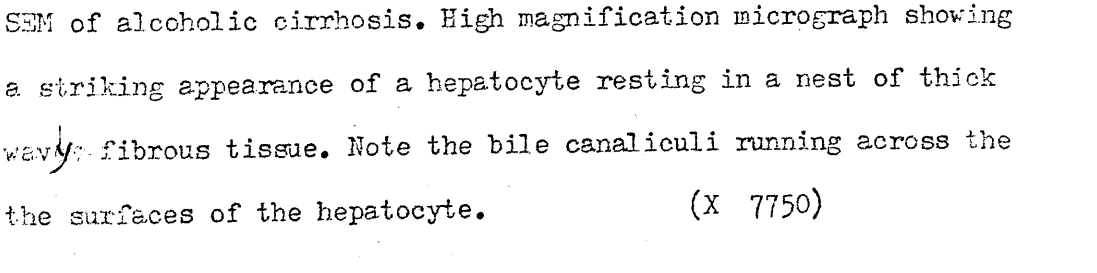

SEM of alcoholic cirrhosis. High magnification micrograph showing a striking appearance of a hepatocyte resting in a nest of thick wavy fibrous tissue. Note the bile canaliculi running across the the surfaces of the hepatocyte. (X 7750)

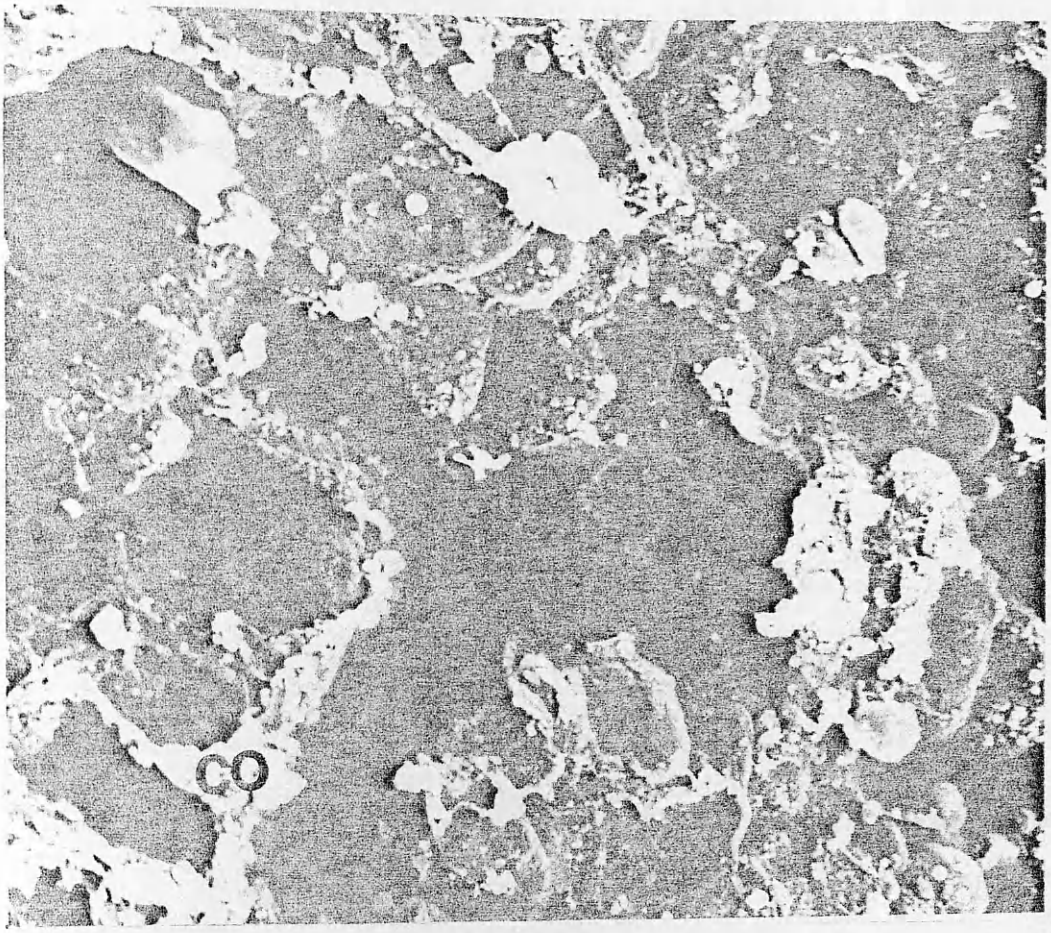

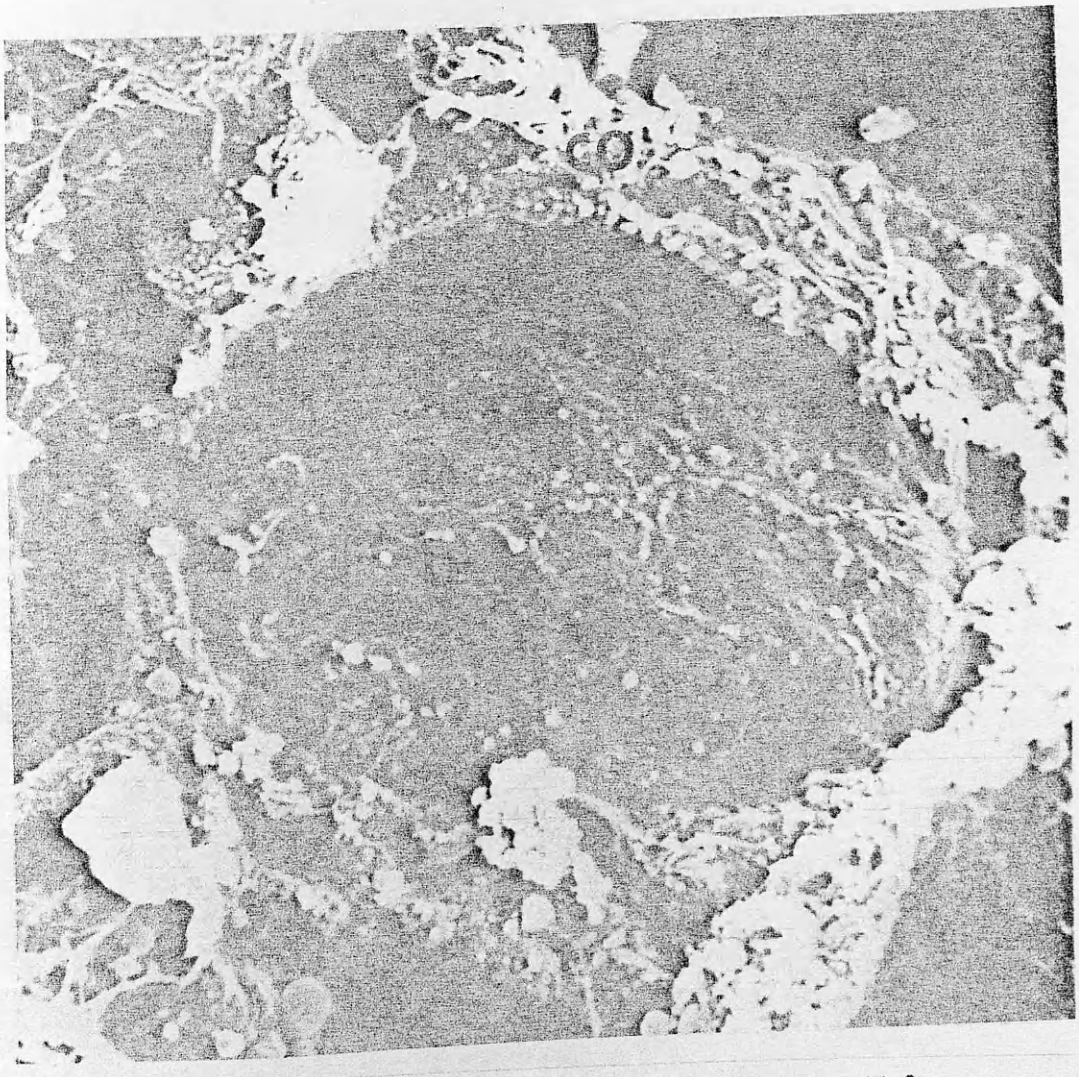

Above : Figure 44.1 Below : Figure 44.2

FIGURE 44.3

TEM of alcoholic cirrhosis. Shows part of adjacent hepatocytes (h). Pericellular fibrosis is evident. Note the phagolysosomes in the cytoplasm. (X 6300)

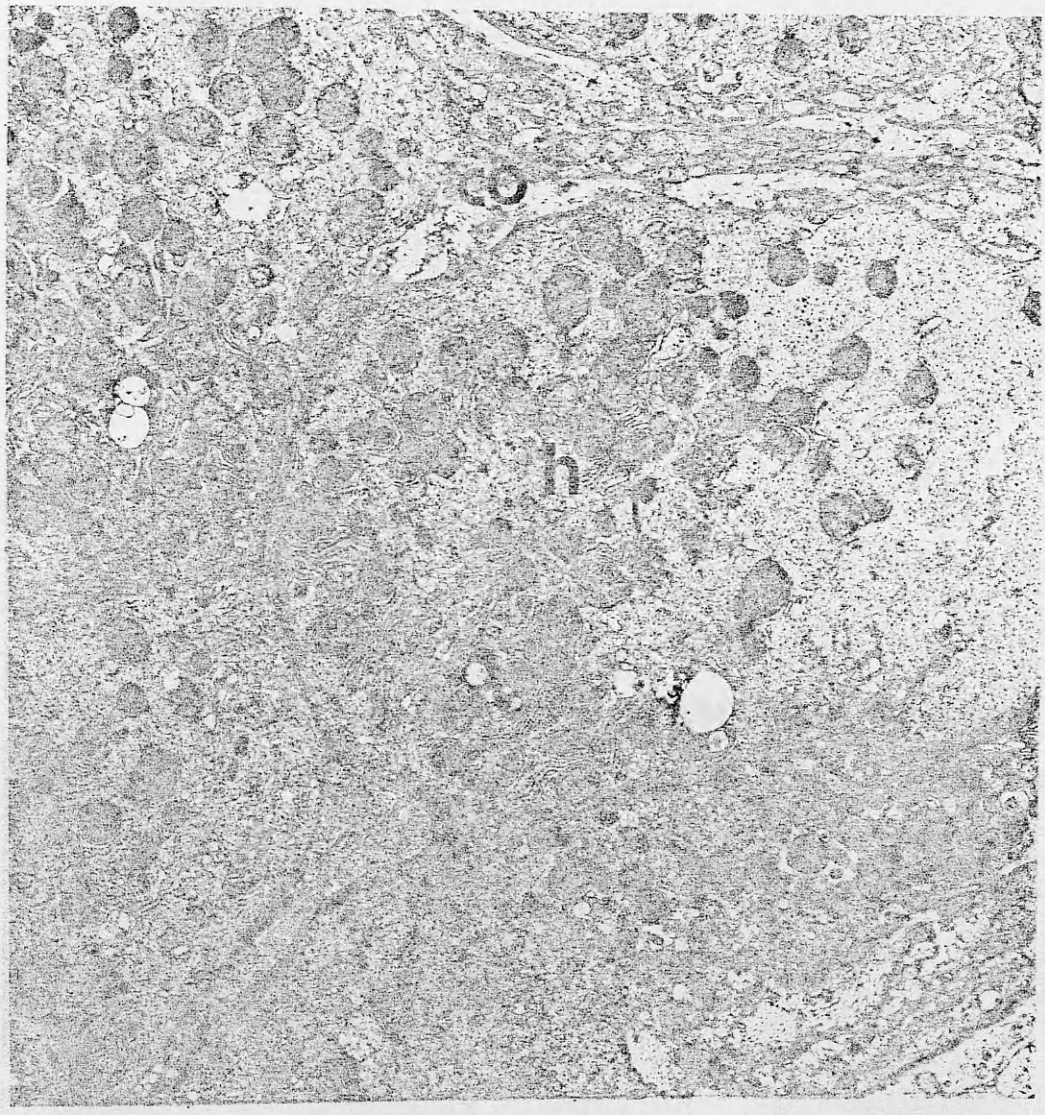

Figure 44.3

FIGURE 44.4

SEM of alcoholic cirrhosis. Shows part of fractured surface. Among the cells a hepatocyte surrounded by a thick band of fibrous tissue. Ito cell is present in close contact. (X 3375)

FIGURE 44.5

SEM of alcoholic cirrhosis. High magnification micrograph showing details of pericellular fibrosis (co) which appear as thick band surrounding the hepatocyte. Ito cell (it) is evident. Note the delicate cytoplasmic process with which the cell clings to the fibrous band. (X 7875)

Above : Figure 44.4

Below : Figure 44.5

FIGURE 45.1

LM of Pre-cirrhotic PBC. Portal tract and periportal area shown irregularly expanded. Heavy infiltration with chronic inflammatory cells seen breaching the limiting plates. There is increased number of the mononuclear cells invading and dissecting between the hepatocytes. The small bile ductules (bd) show some signs of injury with swollen pale epithelial cells surrounded by lymphocytes. Bile ductular proliferation is evident.

FIGURE 45.2

LM of Pre-cirrhotic PBC. Part of expanded portal tracts showing deranged small ductules, many of them without obvious lumen, appeared in clusters (arrows). Some present as ill-defined hyaline mass surrounded by increased number of chronic inflammatory cells. Note the normal medium sized bile ductules.

Above : Figure 45.1 Below : Figure 45.2

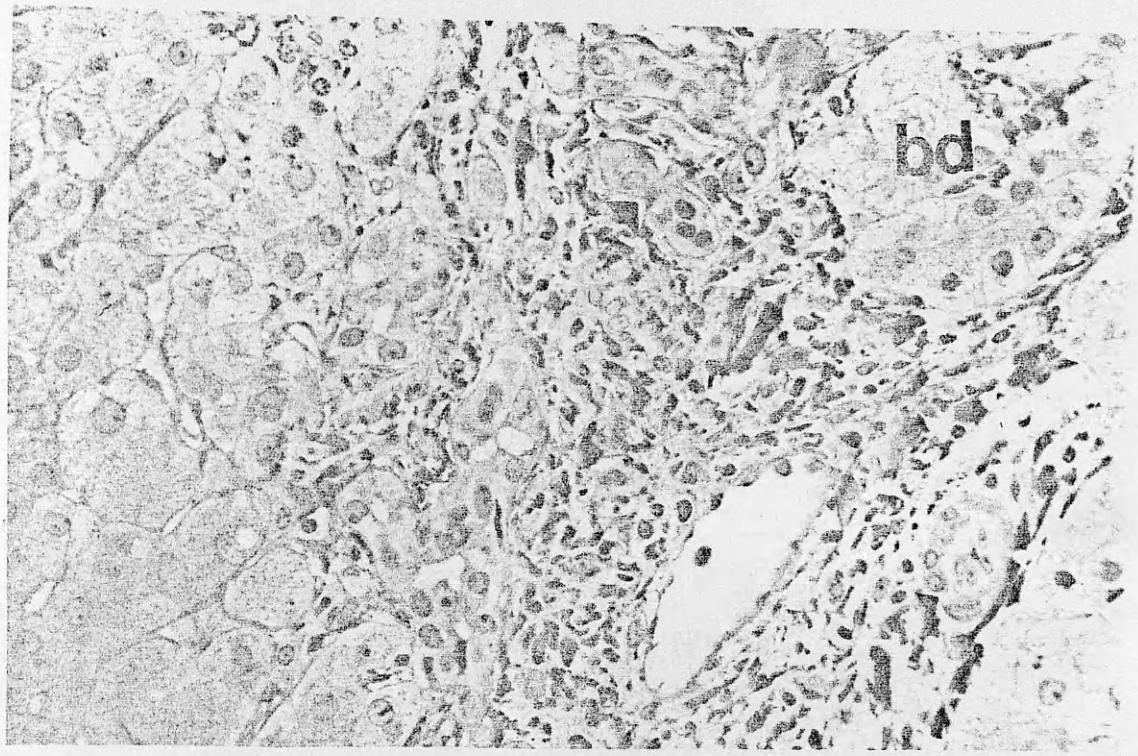

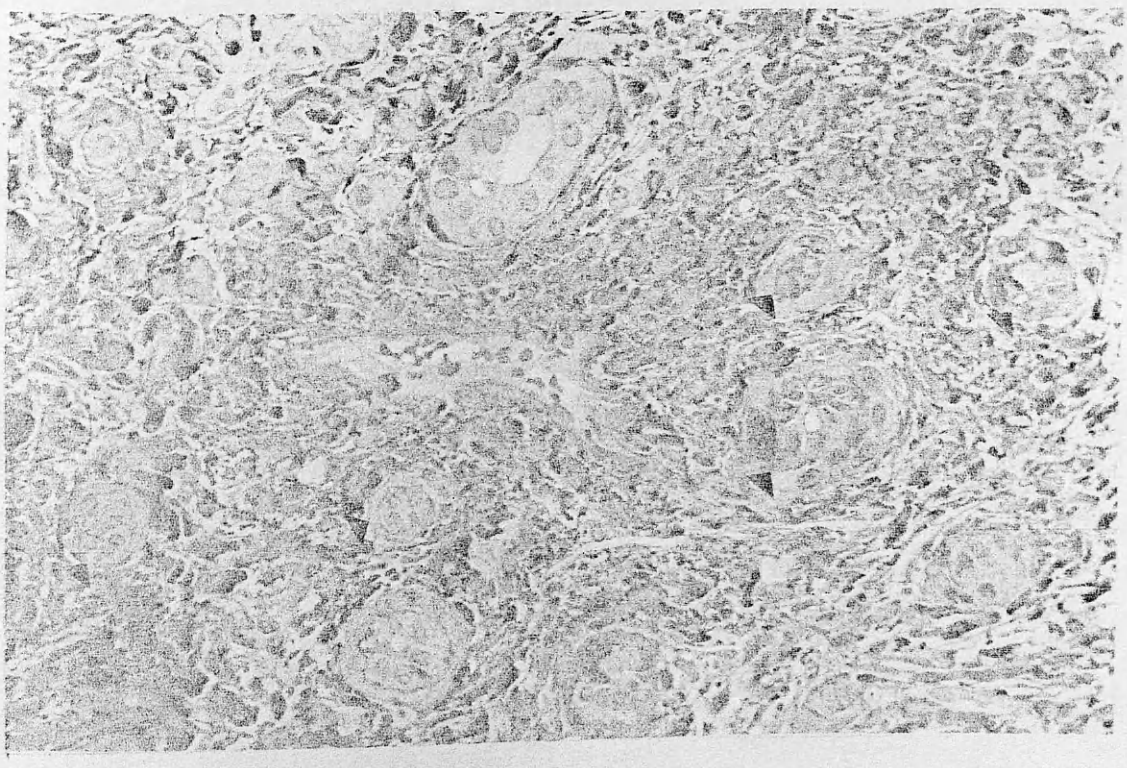

FIGURE 45.3

LM of Pre-cirrhotic PBC. Shows hepatic sinusoids invaded by mononuclear cells, Kupffer cells enlarged, and diffuse twin cell plate arrangement.

FIGURE 45.4

LM of Pre-cirrhotic PBC. Shows liver cells arranged in twin cell plates and containing various size lipid droplets. Increased number of mononuclear cells within the sinusoid and Kupffer cell hyperplasia are seen. Several Ito cells wedged between the sinusoids and the liver cells are evident.

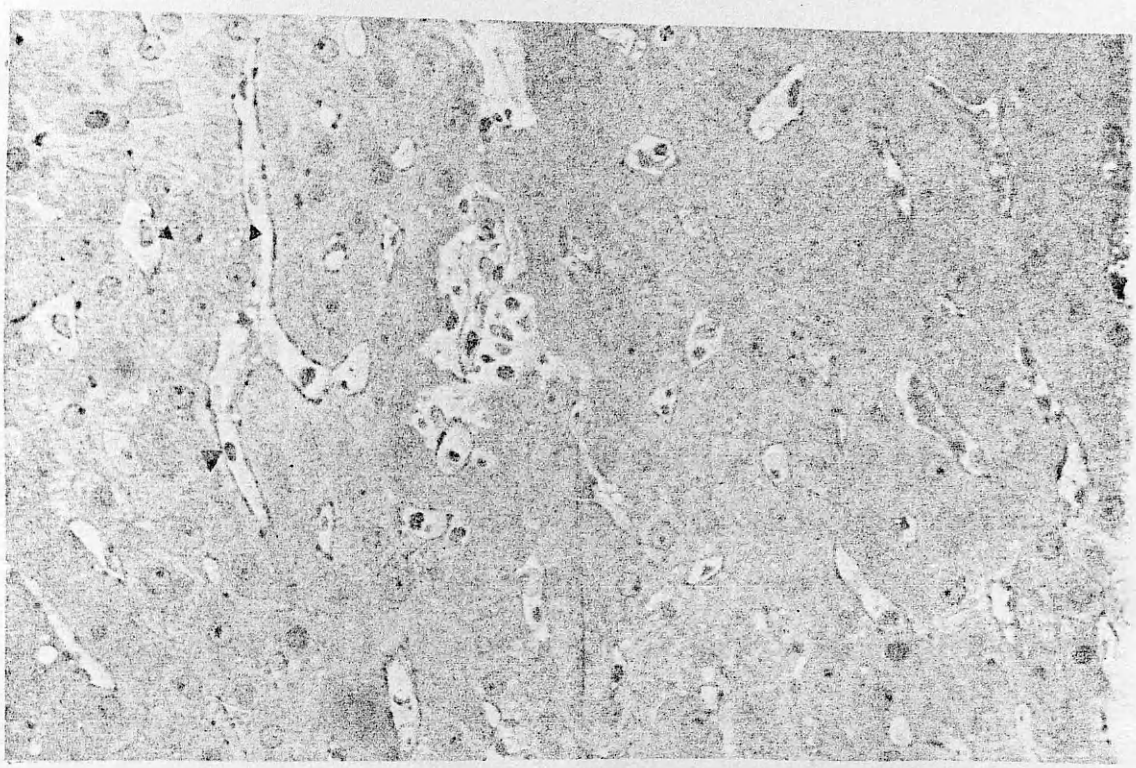

Above : Figure 45.3

Below : Figure 45.4

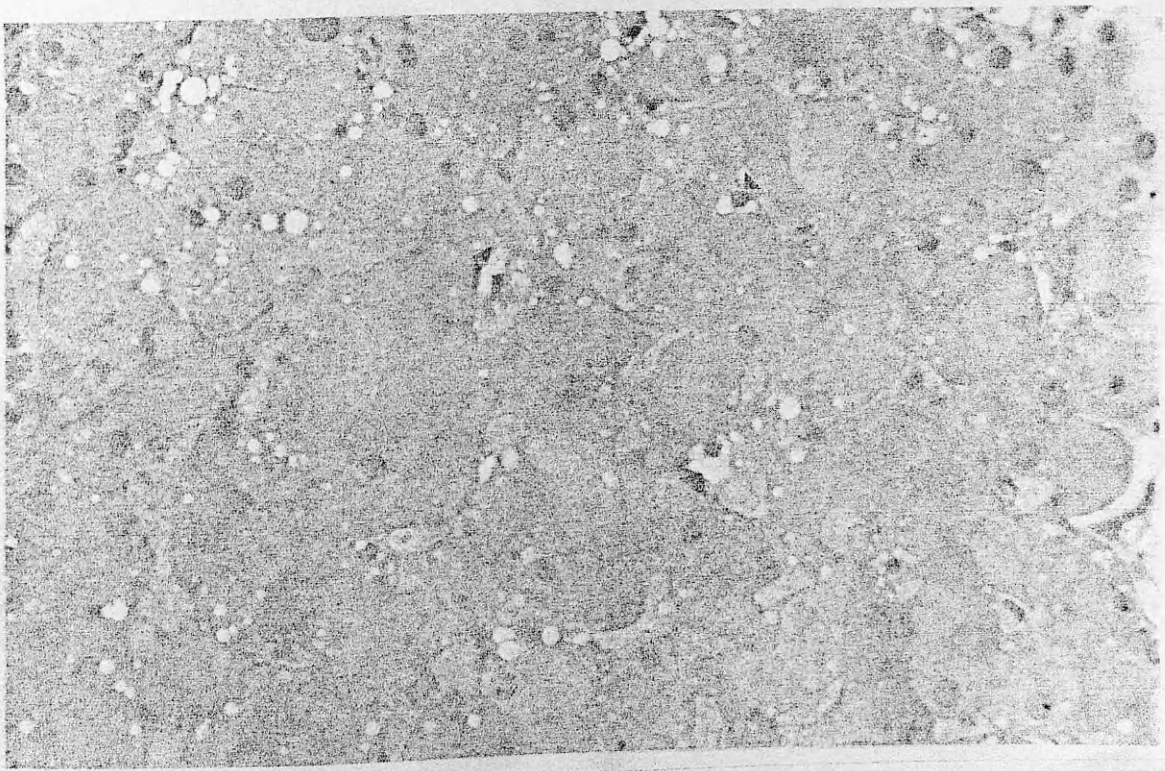

FIGURE 46.1

LM of cirrhotic PBC. One micron thick resin section showing part of portal tract with heavy chronic inflammatory cells infiltration. Marked reduction in the number of small duct, remnant of which usually surrounded by fibrous tissue and inflammatory cells. A large bile duct adjacent to a blood vessel is present.

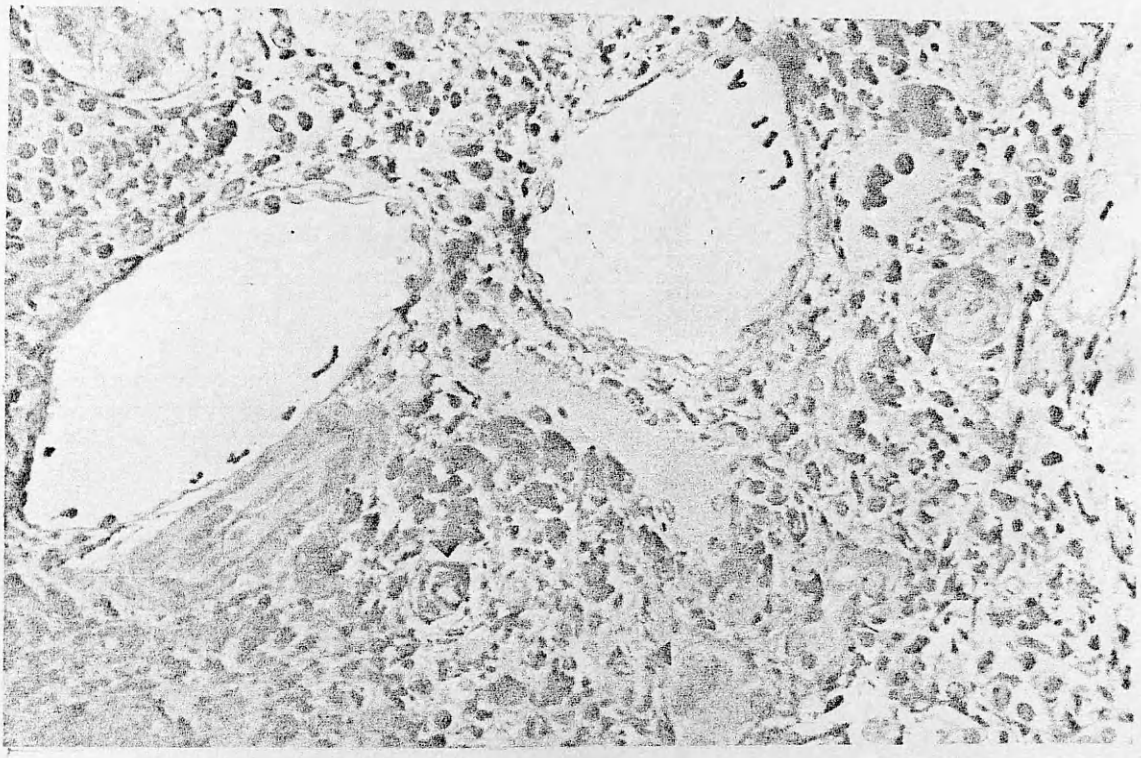

Figure 46.1

FIGURE 46.2

LM of cirrhotic PBC. One micron thick section shows biliary piecemeal necrosis. Heavy infiltration of chronic inflammatory cells invading between the hepatocytes and breaching the limiting plates.

FIGURE 46.3

LM of cirrhotic PBC. One micron thick resin section shows focal accumulation of proliferated bile ducts among the heavy infiltration of chronic inflammatory cells and piecemeal necrosis.

Above : Figure 46.2 Below : Figure 46.3

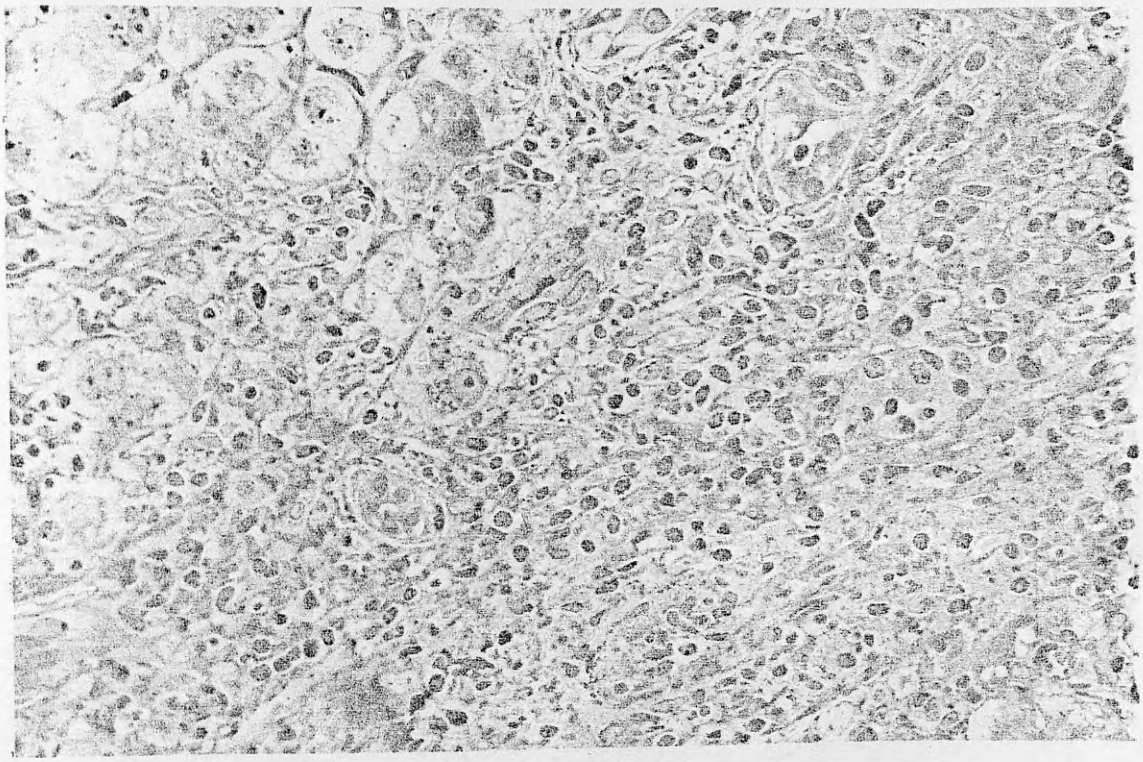

FIGURE 46.4

LM of cirrhotic PBC. One micron thick resin section shows focal mononuclear aggregates among plates of hepatocytes which contain various size lipid droplets.

FIGURE 46.5

LM of cirrhotic PBC. Shows dilatation of the sinusoids with increased number of chronic inflammatory cells and Kupffer cells hyperplasia. Rosette formations of hepatocytes are present.

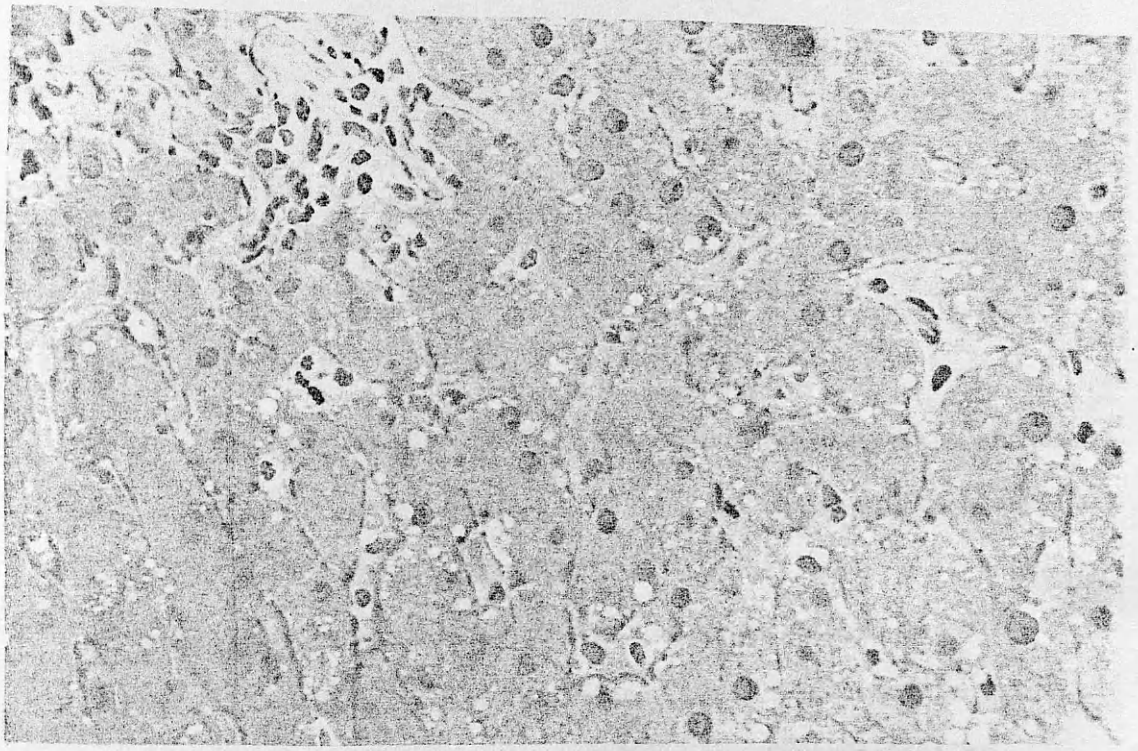

Above : Figure 46.4

Below : Figure 46.5

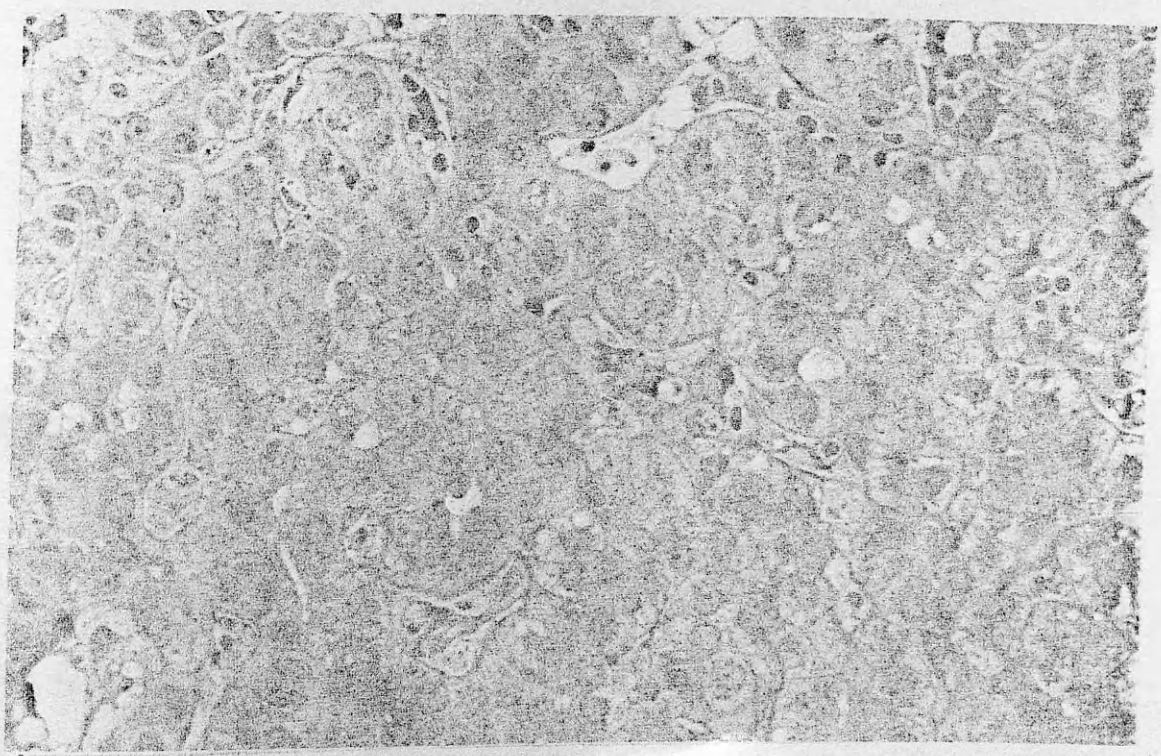

FIGURE 47.1

TEM of PBC. Cross-section of the bile ductule showing pale and dark cells. The lumen is devoid of microvilli. The basement membrane (bm) is thick and stratified. Note the close apposition of plasma cell and macrophage (ma). A neutrophil leukocyte (ne) is seen invading between the swollen biliary epithelial cells. The tight junction near the apical pole was preserved while the interdigitating structures near the cellular bases were flattened. (de : dark cell). (pe : pale cell). (X 4950)

Figure 47.1

FIGURE 47.2

TEM of PBC. High magnification micrograph showing details of the dark cell (de). Its cytoplasm is packed with circular cristae (arrow). Microfilaments present in single and small aggregates around the nucleus and near the apical part of the cell. Cytophagosome (ply) and lysosomes are evident. (X 8100)

Figure 47.2

FIGURE 48

TEM of Pre-cirrhotic PBC. Shows apical part of proliferated bile ductules. Thick bundles of microfilament (mf) are present, oriented in various direction, some wrapped around the mitochondrion (m), others encircling the dilated Golgi complex. The dilated lumen(lu) contained granular material of high electron density. Tight junctions (tj) are well preserved. (X 29250)

Figure 48

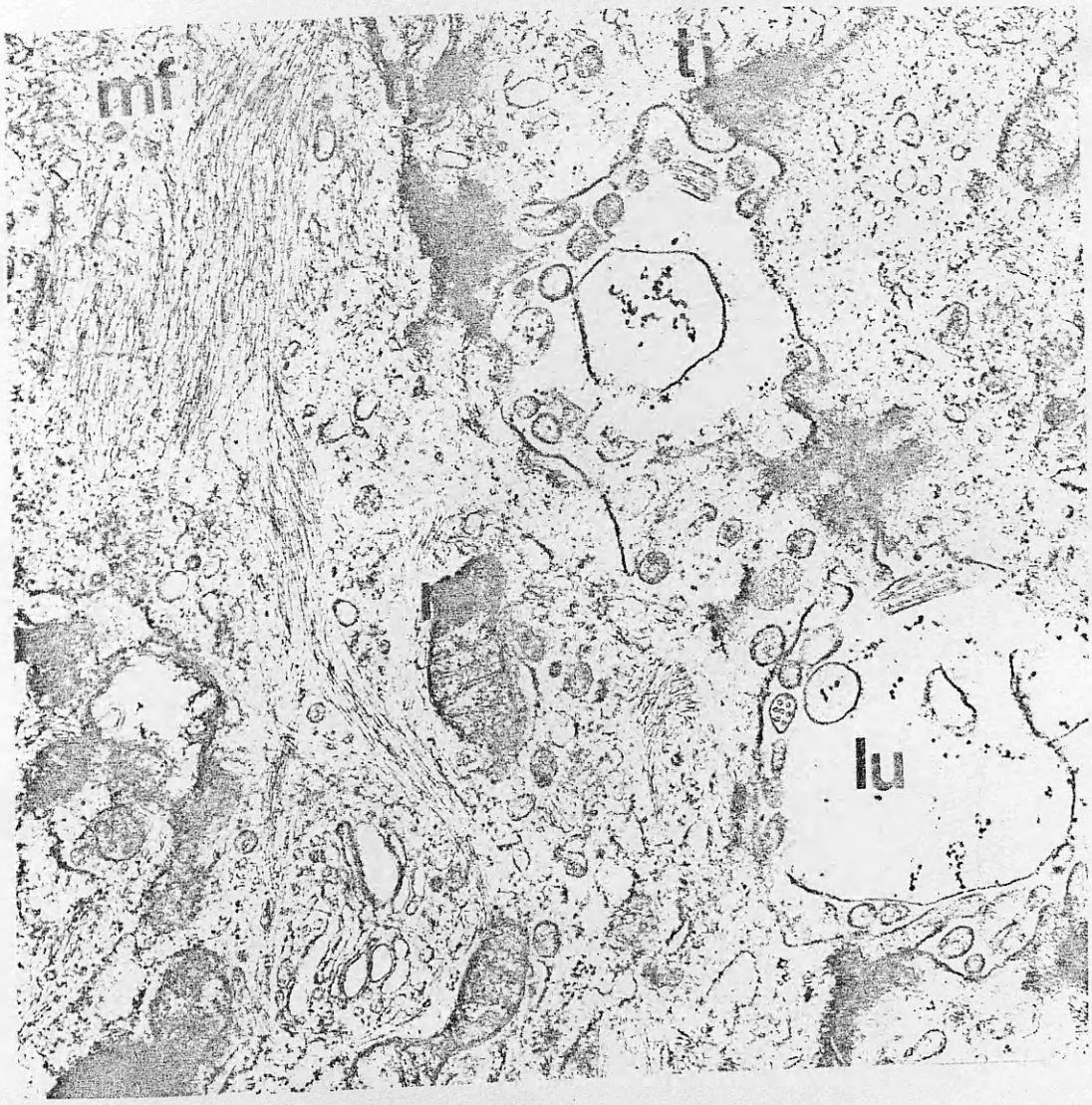

FIGURE 49

TEM of Pre-cirrhotic PBC. Shows a cross-section of bile ductule. The lumen is narrowed and devoid of microvilli. There is lacunar dilatation of the interdigitating structure at the base of the cell. The basement membrane (bm) is thickened and surrounded by thick fascicles of collagen fibres. The ductule is surrounded by macrophages, neutrophils (ne) and lymphocyte (lm) with its cytoplasm protruding and breaching the basement membrane. (ply : Phagolysosome). (id : interdigitation). (X 8100)

Figure 49

FIGURE 50.1

TEM of Pre-cirrhotic PBC. Cross-section of bile ductule showing the basement membrane (bm) thick and stratified in places and wavy in others. The lumen (lu) is dilated, devoid of microvilli and filled with granular materials of medium electron density. (m: mitochondrion) (gi : Golgi complex).(co : collagen). (X 13275)

Figure 50.1

FIGURE 50.2

TEM of Pre-cirrhotic PBC. Cross-section of bile ductule showing narrowed and ill-defined lumen (lu). The cells are swollen with scanty cytoplasmic organelles. Lysosomes (ly) are present. The basement membrane (bm) is thickened and stratified. Bile pigment (bp) deposition within the extracellular spaces is evident. (X 9675)

Figure 50.2

FIGURE 51.1

TEM of pre-cirrhotic PBC. High magnification micrograph showing details of the canal of Hering's lumen. Tight junctions are (tj) preserved. Medium electron dense amorphous materials with fine granularity are present in the centre of the lumen. In the edges the shadow of the microvilli are still present. (X 22050)

FIGURE 51.2

TEM of pre-cirrhotic PBC. Cross-section of Canal of Hering, composed of three hepatocytes and two ductular cells (dc). The lumen (lu) is dilated, devoid of microvilli and filled with medium density amorphous materials. The macrophages (ma) are wedged between the cells while the neutrophils (ne) are in close apposition to parts of hepatocyte (h) and ductular cells. (X 4050)

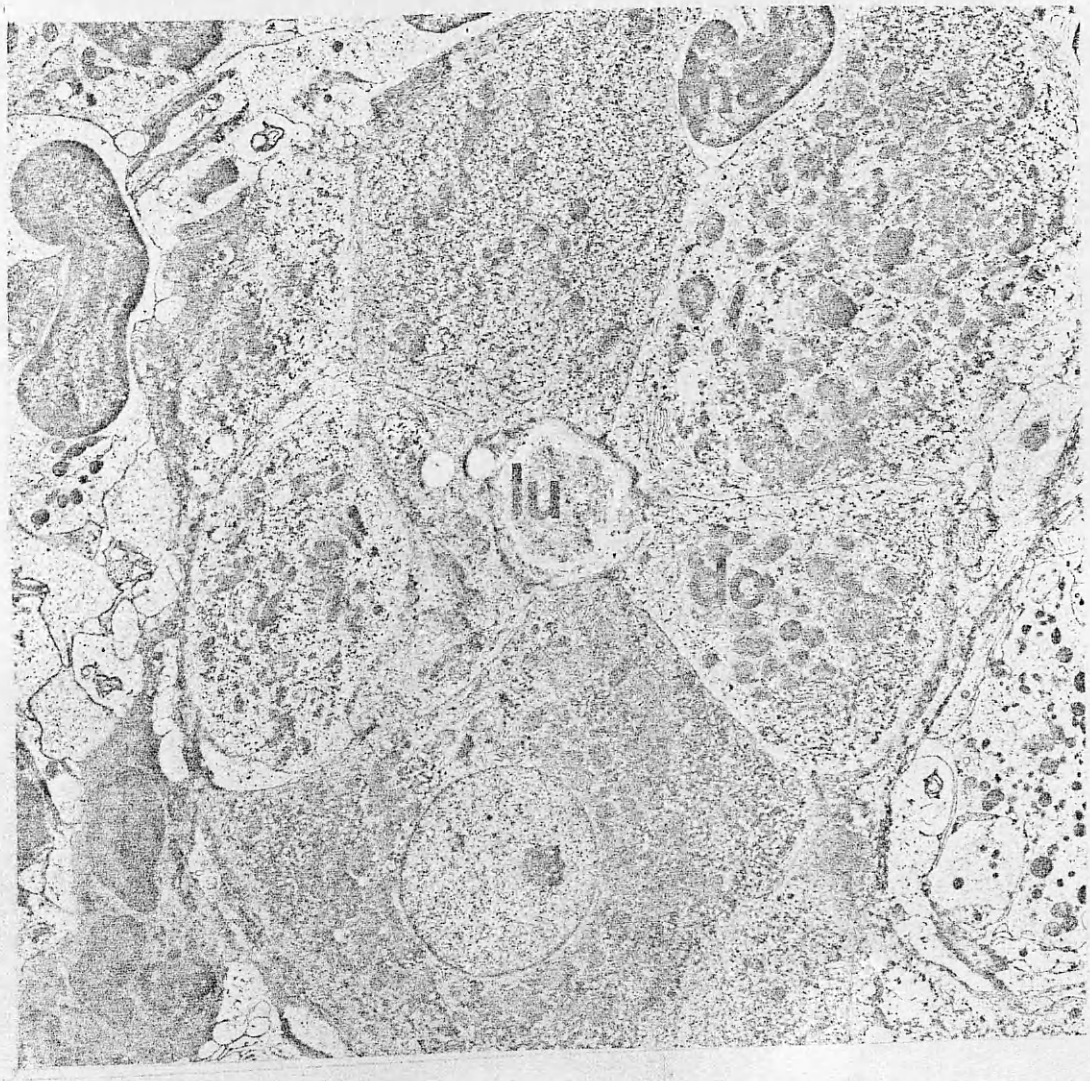

Above : Figure 51.1 Below : Figure 51.2

FIGURE 52.1

TEM of Pre-cirrhotic PBC. Shows parts of several hepatocytes with marked vacuolar dilatation of the endoplasmic reticulum. Mitochondria are small and condensed. There is marked membrane-bound bile pigment (bp) deposition. Tight junctions sealing the bile canaliculi (bc) are preserved. (X 8100)

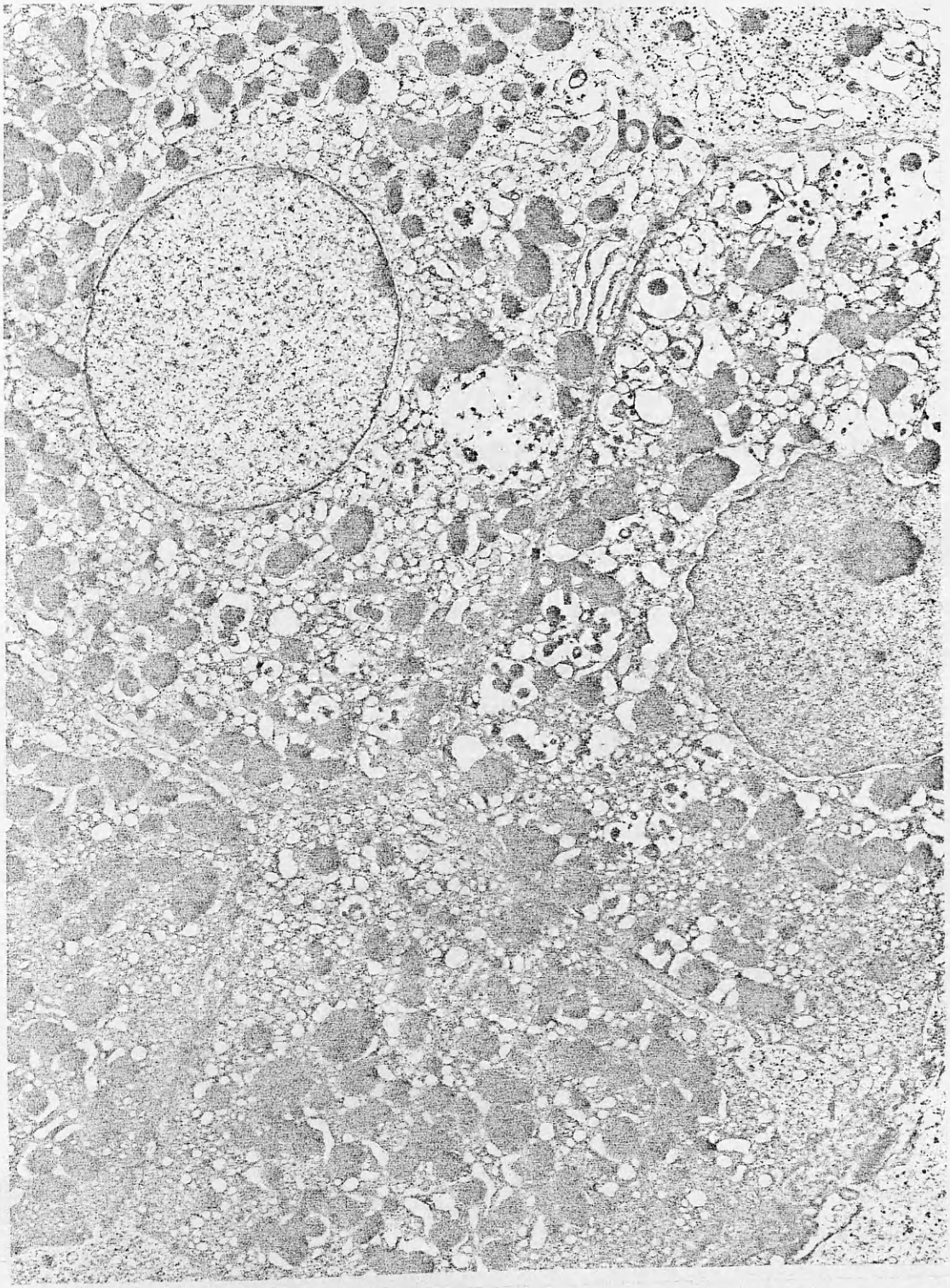

Figure 52.1

FIGURE 52.2

TEM of pre-cirrhotic PBC. Part of adjacent hepatocytes showing marked dilatation of the bile canaliculi (bc) herniated into the cytoplasm. The lumen is devoid of microvilli and contains medium electron density granules. Bile pigment deposition in the cytoplasm is evident. (rer: rough endoplasmic reticulum).(tj : tight junction). (X 8100)

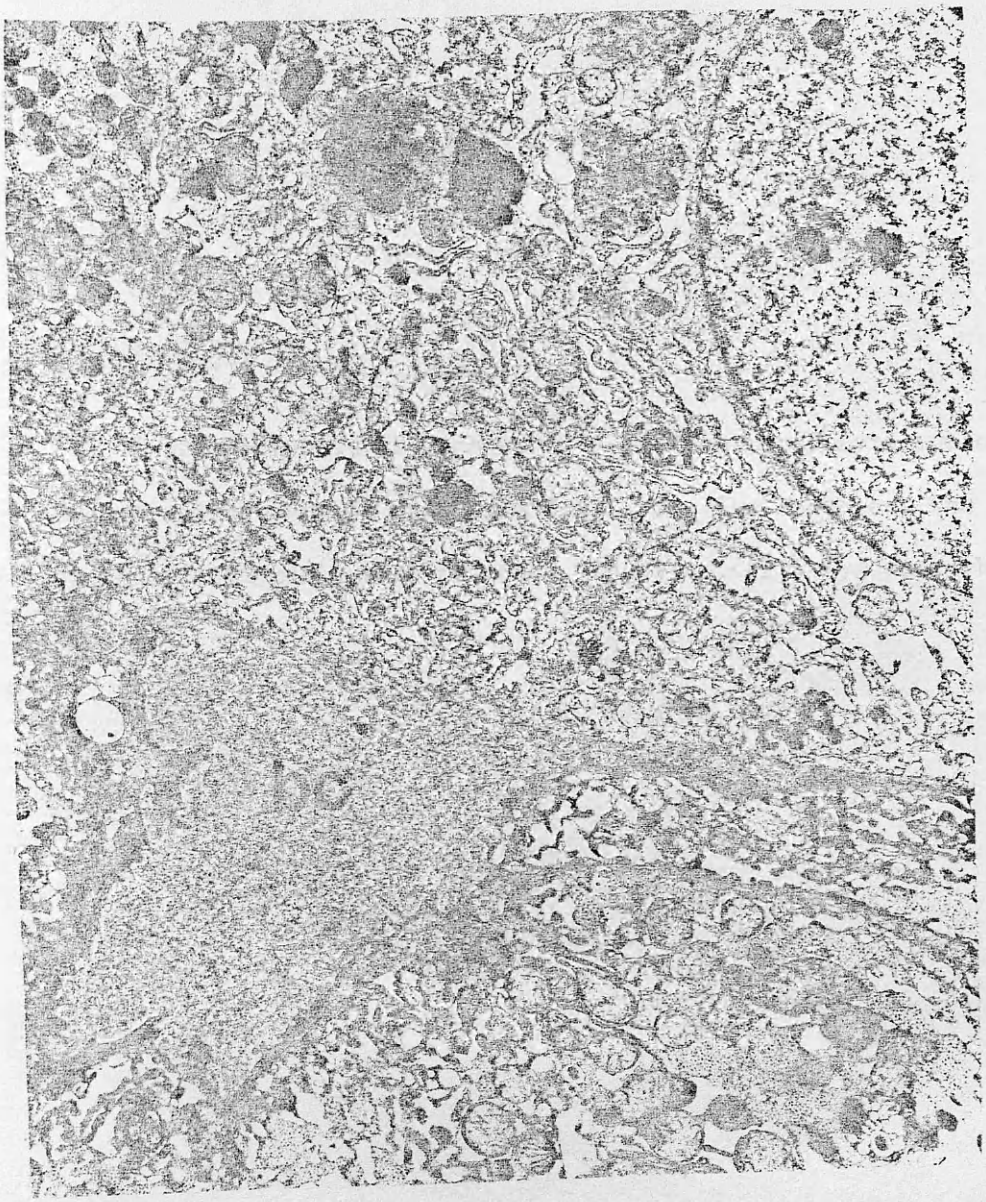

Figure 52.2

FIGURE 52.3

TEM of pre-cirrhotic PBC. Shows twin-nucleus hepatocyte containing high electron density mass with few lipid-like vacuoles. The majority of the mitochondria show cristal injuries. (ly: lysosome)(bc : bile canaliculus). (X 9675)

Figure 52.3

FIGURE 54.1

TEM of pre-cirrhotic PBC. Shows parts of hepatocytic cytoplasm in which several mitochondria manifest curling of the cristae and some paracrystalline inclusions. Note the vacuolar transformation of the endoplasmic reticulum. (X 29250)

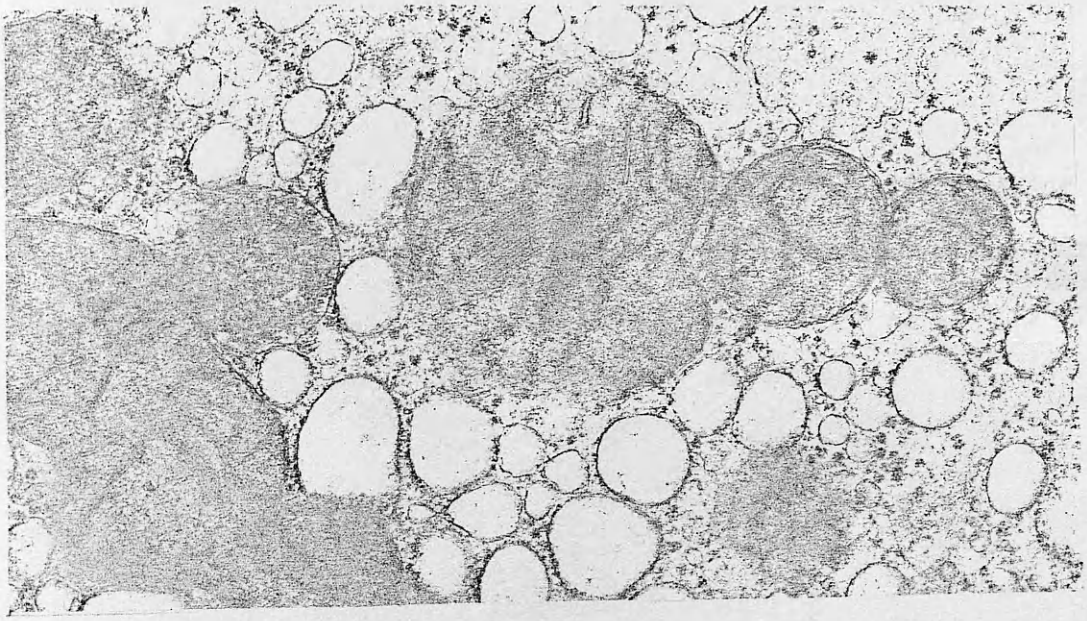

Figure 54.1

FIGURE 54.2

TEM of pre-cirrhotic PBC. A giant mitochondria (gm) with striking paracrystalline inclusions is present. Several smaller mitochondria (arrows) seen in close apposition and only separated by thin cytoplasmic rim. Dilatation of the RER is evident. (X 29250)

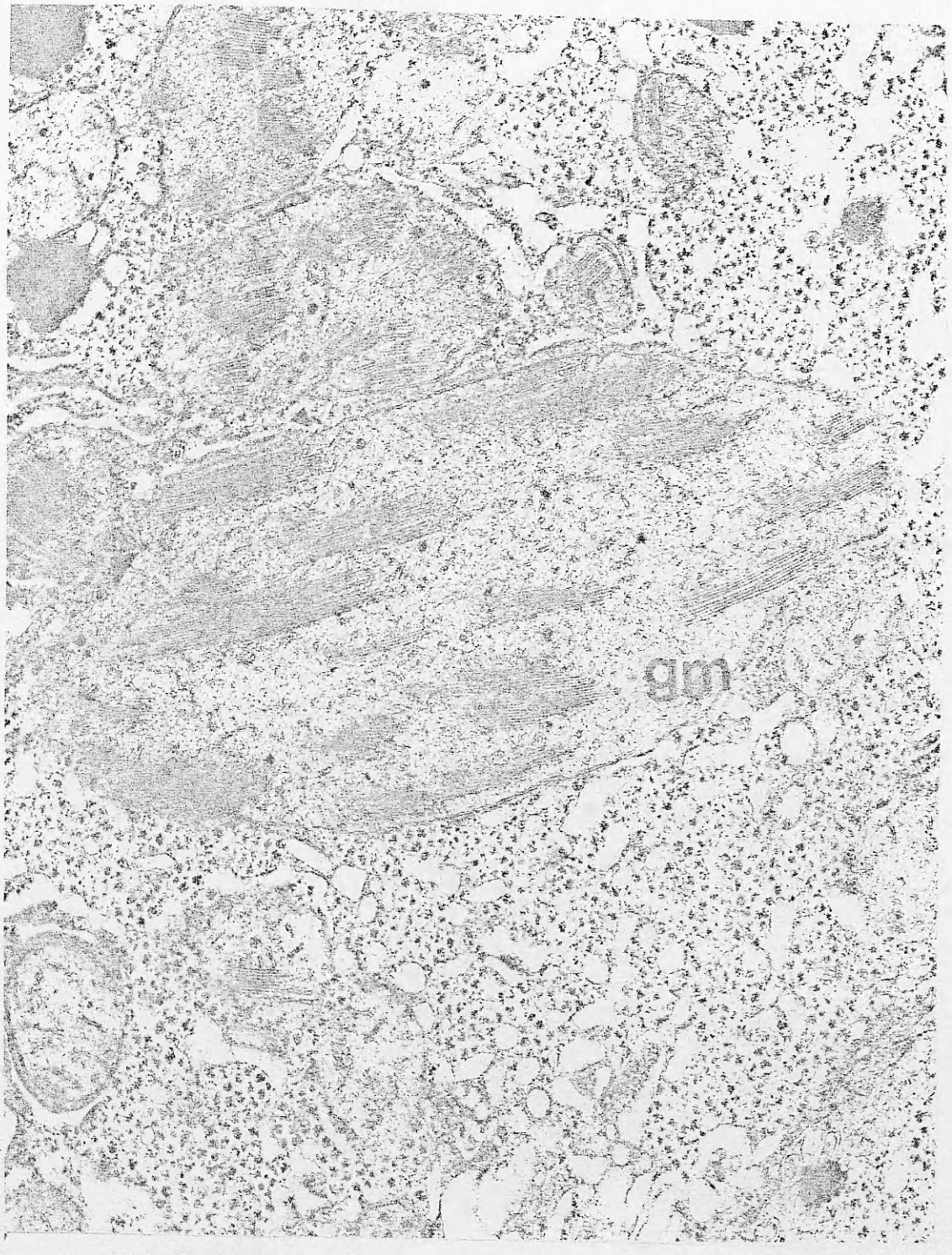

Figure 54.2

FIGURE 55.1

TEM of pre-cirrhotic PBC. Adjacent hepatocytes showing dilated bile canaliculi. The lumen contains membraneous materials and few stunted microvilli. There is marked thickening of the pericanalicular ectoplasm. Bile pigment lysosomes (ly) are abundant. Hypertrophied Golgi complexes (gi) are present. The majority of the mitochondria show cristal -injury and contain dense bodies. Adjacent bile canaliculi appeared to be less affected. (X 4950)

Figure 55.1

FIGURE 55.2

TEM of pre-cirrhotic PBC. A dilated bile canaliculi showing herniation into the cytoplasm. The lumen contains membranous materials with numerous high electron-dense granules. There is marked increase in the filamentous material in the pericanalicular region. Note the dilatation of the adjacent intercellular spaces (iw) and the increased thickening of the adjacent cytoplasm. (d : desmosome) (X 16870)

Figure 55.2

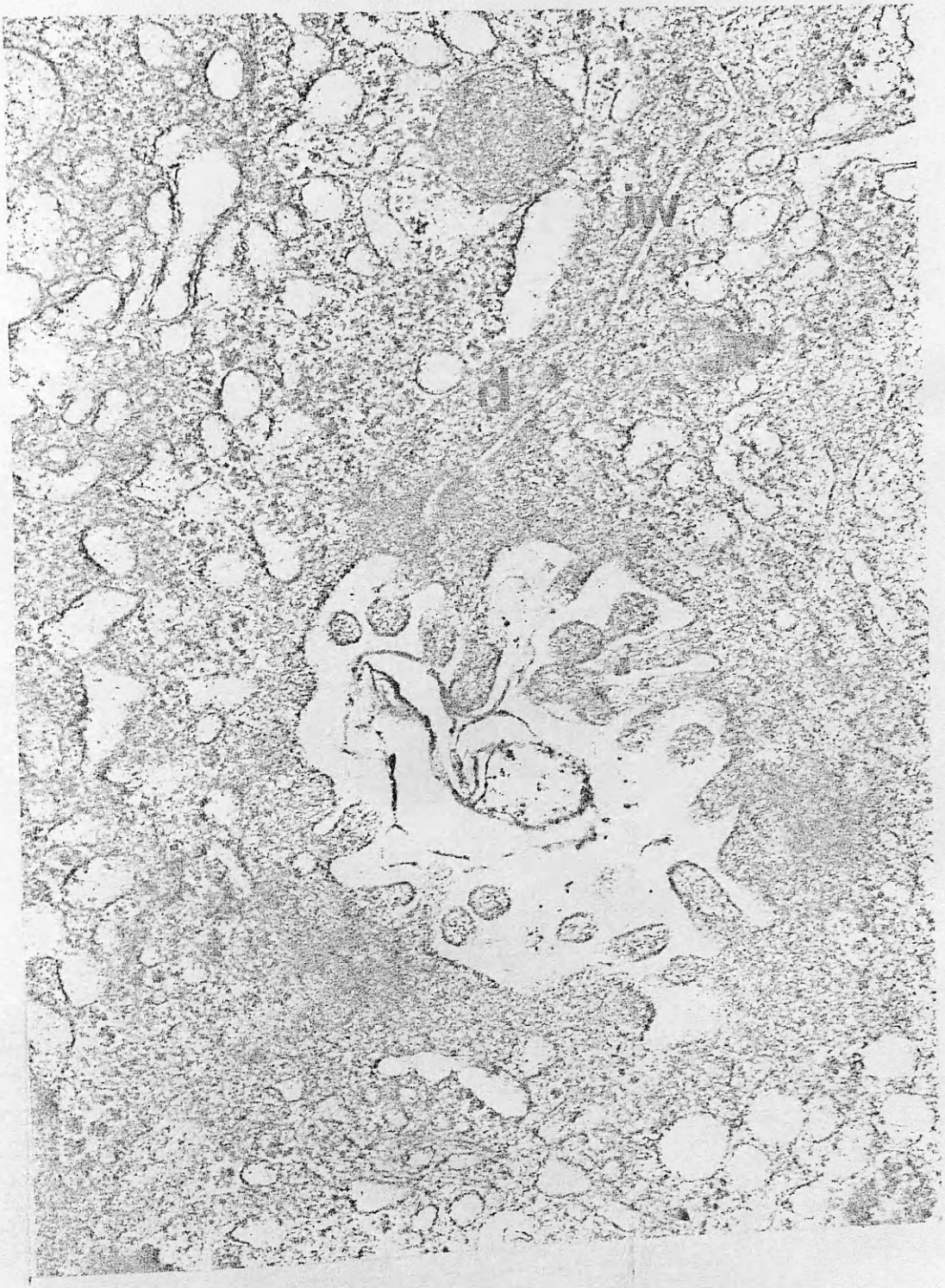

FIGURE 56.1

TEM of pre-cirrhotic PBC. Parts of hepatocytes showing three bile canaliculi (bc) adjacent to each other and appearing to be separated by the junctional complexes only. Note the microvilli filling the lumen, the thickness of the pericanalicular region and the dilated Golgi complex. (X 22050)

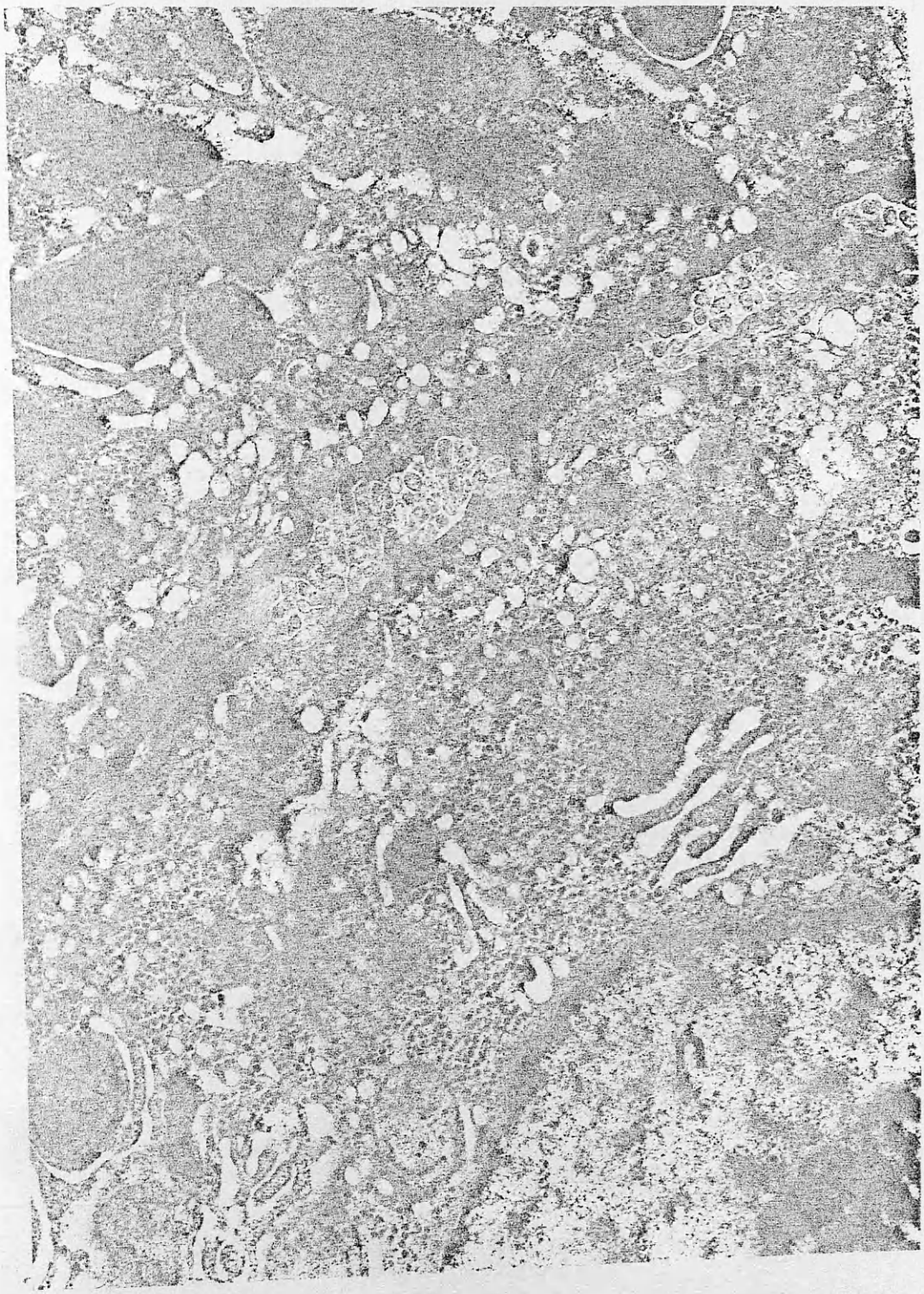

Figure 56.1

FIGURE 56.2

TEM of pre-cirrhotic PBC. Bile canaliculi are shown with marked increase of microfilaments in the pericanalicular ectoplasm. Note the striking dilatation of Golgi complex (gi) and the intercellular space. (tj : tight junction). (X 49500)

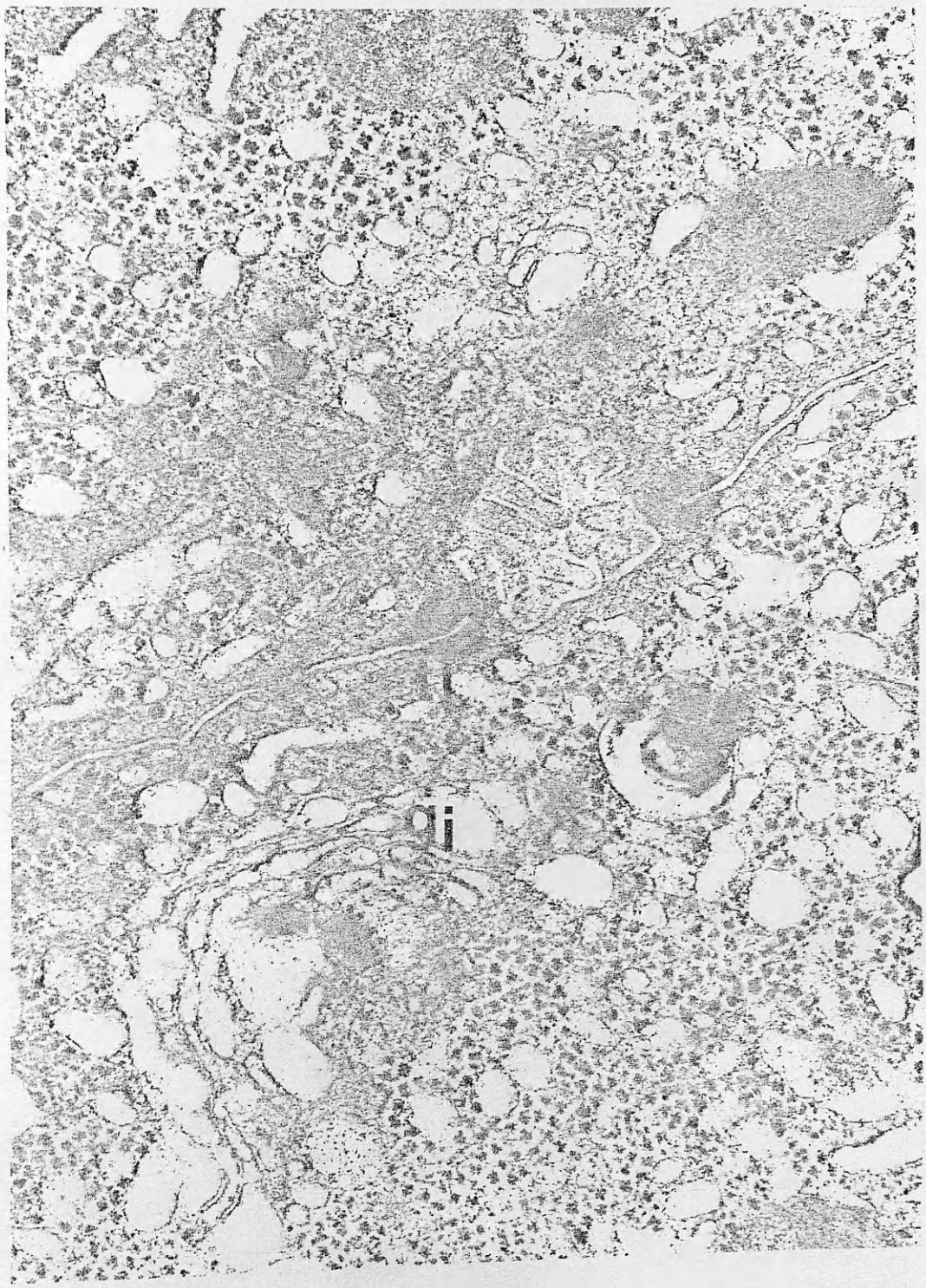

Figure 56.2

FIGURE 57

TEM of pre-cirrhotic PBC. Shows several hepatocytes (h) and sinusoids (s). Within the dilated sinusoid, enlarged Kupffer cells cling to the endothelial lining. Plasma cell (pc) and lymphocyte are present. Note the smaller sinusoids packed with tissue debris, the abundant mitochondria with the paracrystalline inclusions and the bile deposition within the bile canaliculi. (X 4050)

Figure 57

FIGURE 58.1

TEM of pre-cirrhotic PBC. Hepatic sinusoid showing marked swelling of the endothelial cell (ed) which contains numerous electron dense lysosomes adjacent to the enlarged Kupffer cell (k). The space of Disse (ds) appears devoid of microvilli, filled with medium electron dense and finely granular material in which embedded various thickness collagen bundles (co). (X 13275)

Figure 58.1

FIGURE 58.2

TEM of pre-cirrhotic PBC. Hepatic sinusoid with adjacent hepatocytes showing markedly swollen Kupffer cell (k) filling the lumen and contains various sizes bile pigment within the lysosomes. A small lymphocyte (lm) is evident. Ito cell (it) wedged between the endothelial lining and hepatocyte. Slender bundles of collagen fibres are evident in the space of Disse. (X 8100)

Figure 58.2

FIGURE 59.1

TEM of pre-cirrhotic PBC. Hepatic sinusoid with adjacent parts of hepatocytes (h). The sinusoid (s) is packed with tissue debris. Note the Kupffer cell, Ito cell (it) in the space of Disse containing numerous fat droplets which display a dark outer band and light centre. Some of the fat droplets are present in the cytoplasm of the adjacent hepatocytes. (X 6300)

Figure 59.1

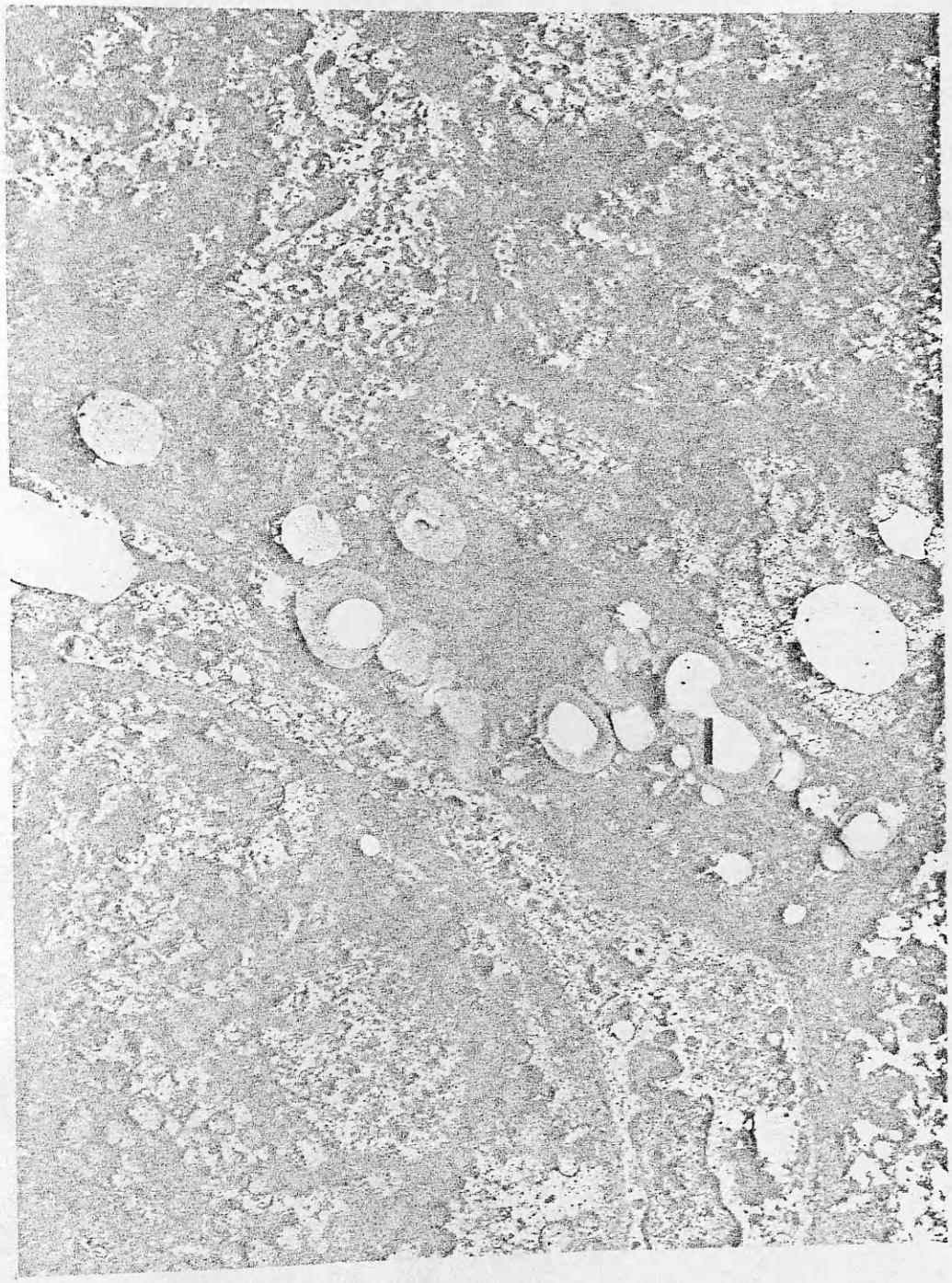

FIGURE 59.2

TEM of pre-cirrhotic PBC. High magnification micrograph of the Ito cell showing details of lipid vacuoles. Note the fine granularity of the medium electron-dense outer band, the many vacuoles in the process of fusion and a band of collagen adjacent to the Ito cell. (X 13275)

Figure 59.2

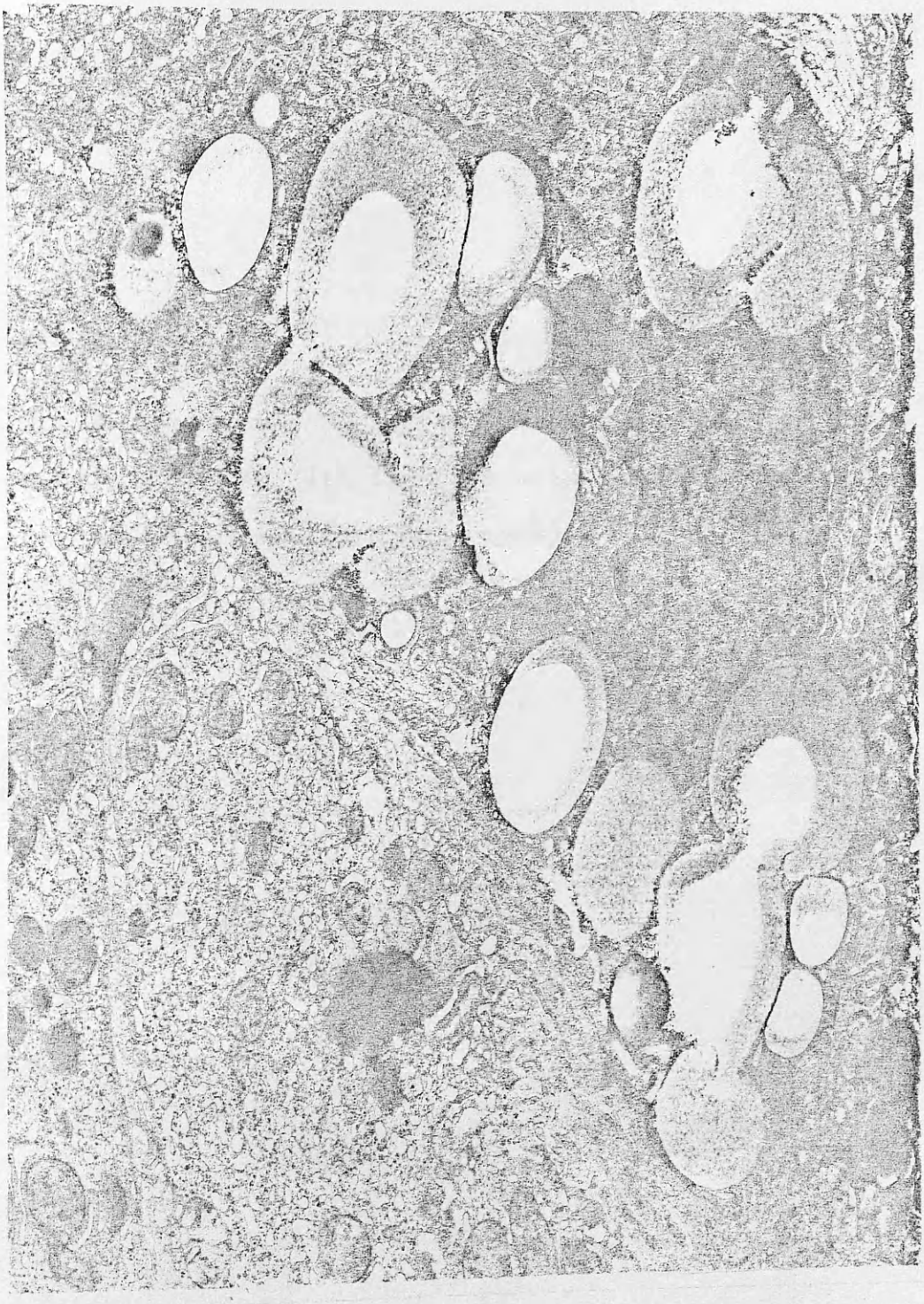

FIGURE 59.3

TEM of pre-cirrhotic PBC. High magnification micrograph showing details of Ito cell (it). Light and medium electron dense lipid droplets are present. (ds : Disse space). (X 22050)

Figure 59.3

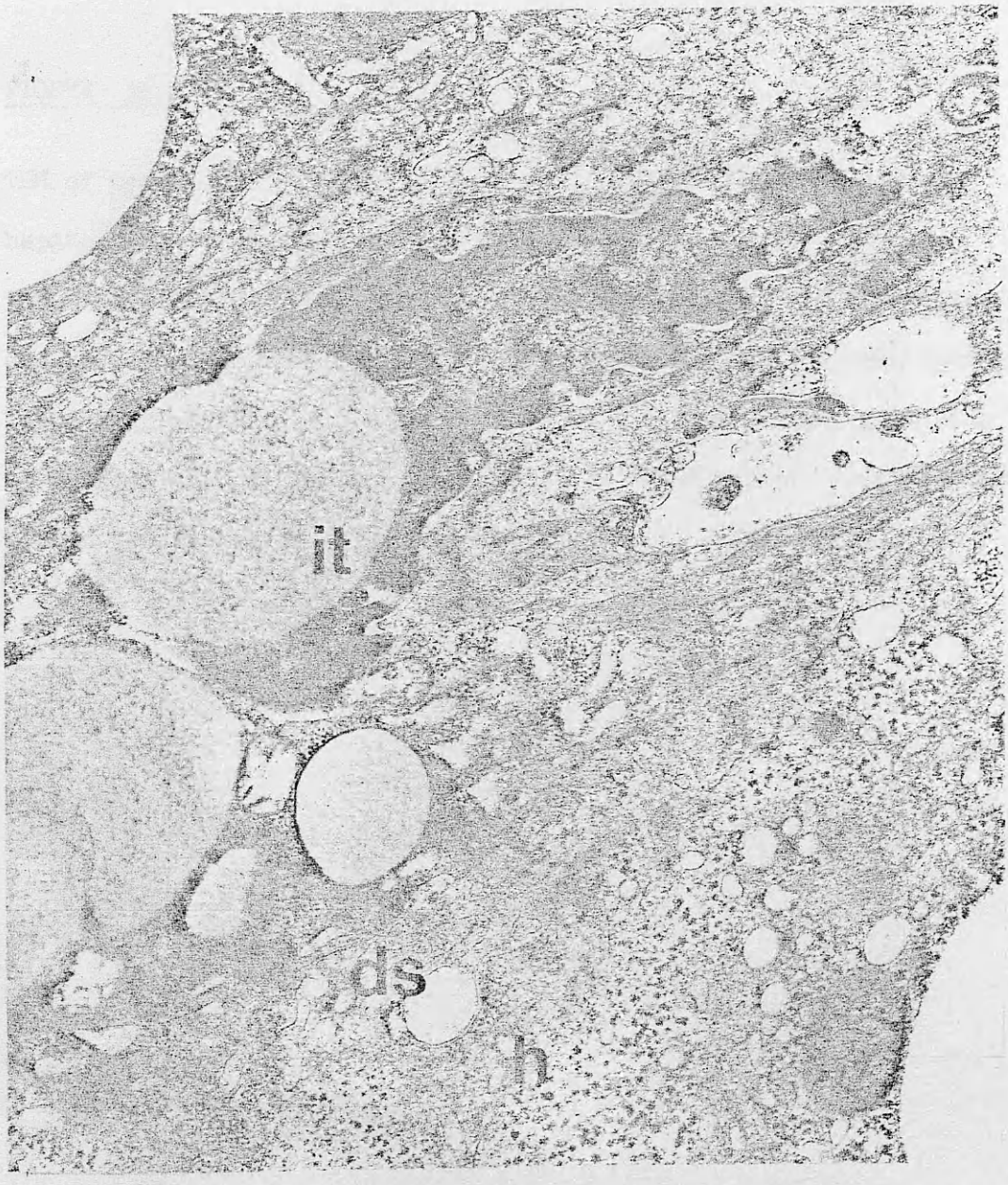

FIGURE 59.4

TEM of pre-cirrhotic PBC. Hepatic sinusoid and adjacent part of hepatocyte are shown. Kupffer cell (k) seems enlarged and fills the sinusoid. The cytoplasm contains abundant amount of lysosomes and one lipid droplet with dark outer band and light centre. Another lipid droplet is present in the space of Disse in close apposition to Kupffer cell while several other seen in process of fusion found within the cytoplasm of the hepatocyte (h). (X 9675)

Figure 59.4

FIGURE 60.1

TEM of pre-cirrhotic PBC. Hepatic sinusoid with adjacent parts of hepatocytes (h) showing lymphocyte (lm) in space of Disse in close contact with the hepatocytic cytoplasm. Note the space of Disse is devoid of microvilli, thickened and contains slender bundle of collagen fibres (co). The sinusoids are packed with tissue debris including membranous structures and bile pigment deposition . (rb : RBC). (X 13275)

Figure 60.1

FIGURE 60.2

TEM of pre-cirrhotic PBC. High magnification micrograph showing lymphocyte (lm) in close apposition to the hepatocytic cytoplasm (h). The lymphocyte is surrounded by double layered membranes (arrows) which appeared to be disrupted in several places and ill-defined in other. (X 22050)

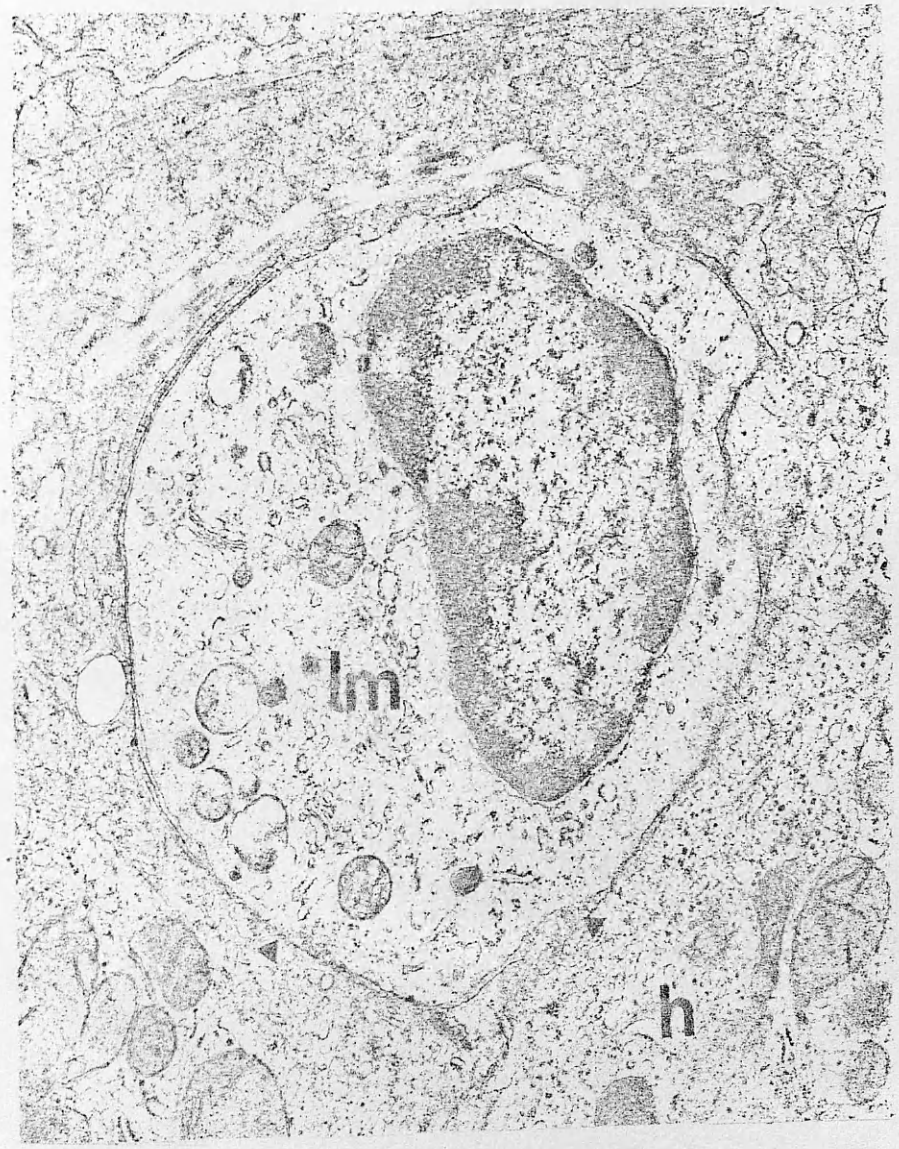

Figure 60.2

FIGURE 60.3

TEM of pre-cirrhotic PBC. Hepatic sinusoids with adjacent parts of hepatocytes. The sinusoids are packed with mononuclear cells, tissue debris and RBCs. A lymphocyte (lm) seen in the space of Disse under the endothelial lining demonstrating a cytoplasmic protrusion in contact with remnants of degenerate cells. Note the few mitochondria, laminated bile deposition and several vacuoles. (X 8100)

Figure 60.3

FIGURE 61.1

TEM of cirrhotic PBC. Apical part of bile ductule showing scanty and short microvilli, some appearing with striking oedematous swellings projecting into the lumen (lu) forming a pseudopodium-like (ps) processes. There is marked increase in the microfilament (mf) which run single and in bundles. (tj: tight junction). (id : interdigitation) (X 22050)

Figure 61.1

FIGURE 61.2

TEM of cirrhotic PBC. Part of the bile ductule showing the thickening and the stratification of the basement membrane (bm) which is disrupted in some places. Note the lumen (lu) is devoid of microvilli; a macrophage (ma) is wedged between the epithelial cells and there is increased amount of microfilament within the epithelial cells. (ly : lysosomes). (X 8100)

FIGURE 61.3

TEM of cirrhotic PBC. High magnification micrograph showing details of the microfilament (mf) which run in long bundles crossing the entire cytoplasm.(lu : lumen). (X 16870)

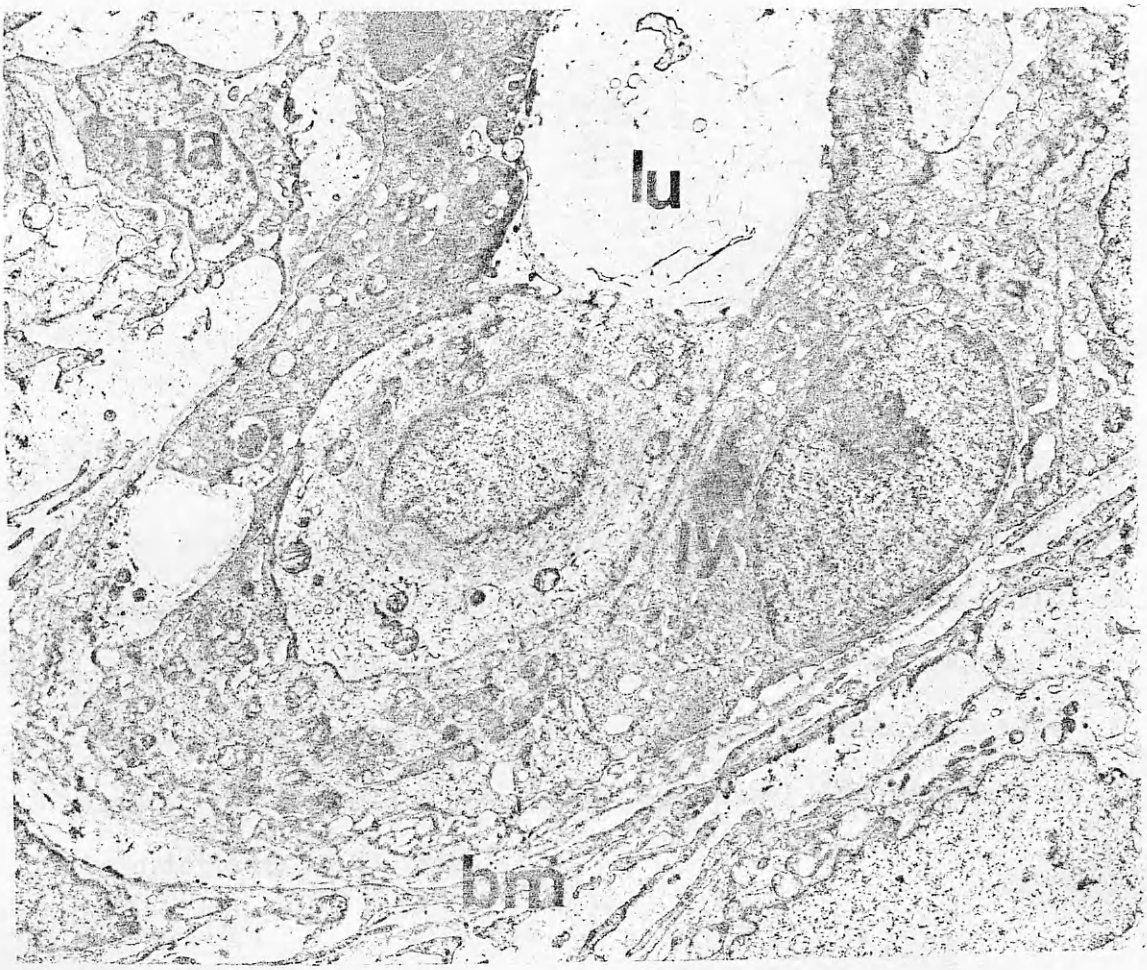

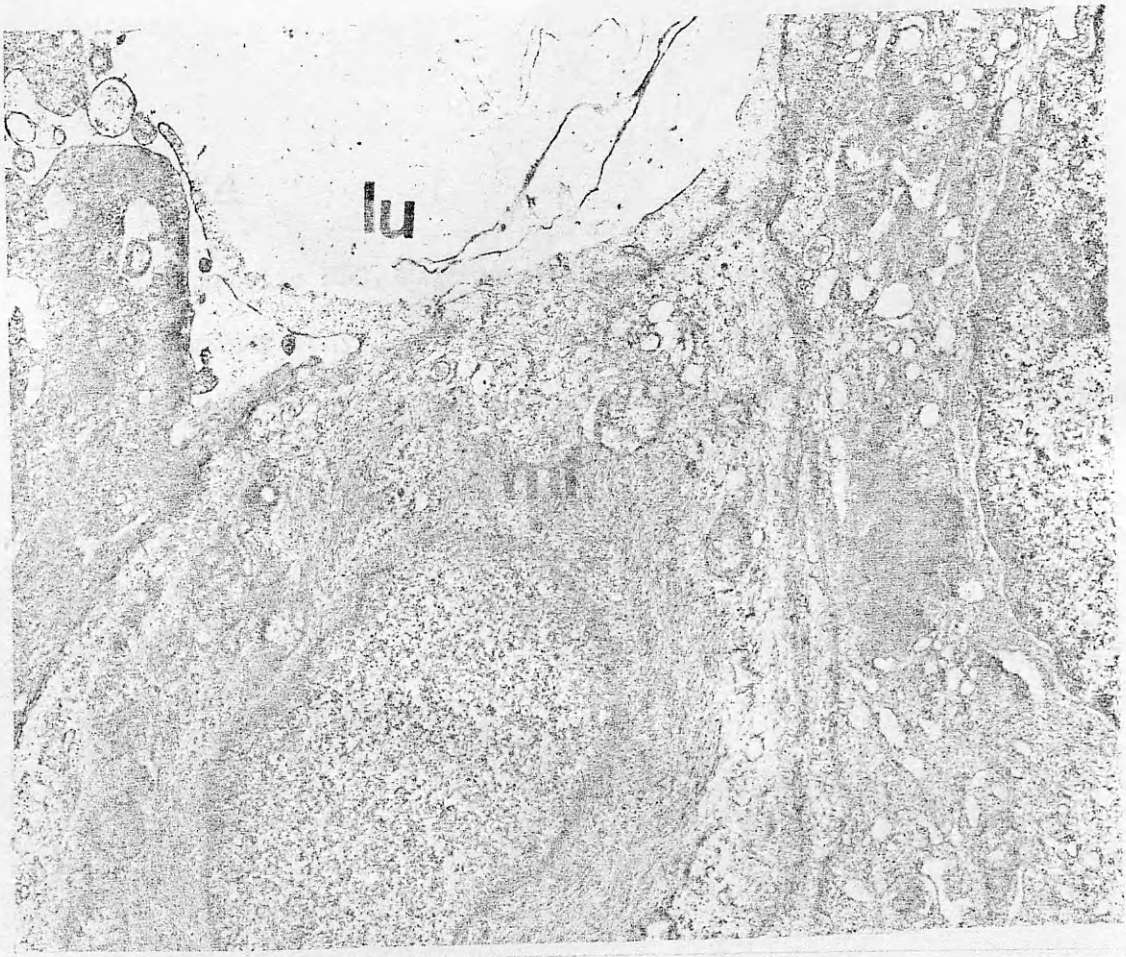

Above : Figure 61.2 Below : Figure 61.3

FIGURE 62.1

TEM of cirrhotic PBC. Part of bile ductule showing profound damage to the epithelial cell. The lumen is narrowed and the microvilli are swollen and contain granular materials. Note the vacuolar transformation of the cytoplasmic organelles with abundant bile pigment (bp) deposition and laminar structures occupying most of the cytoplasm. (X 9675)

FIGURE 62.2

TEM of cirrhotic PBC. High magnification micrograph showing details of the laminar body (lb) which consist of whorls of high electron-dense fibre-like structure between which dense granules are deposited (X 40500)

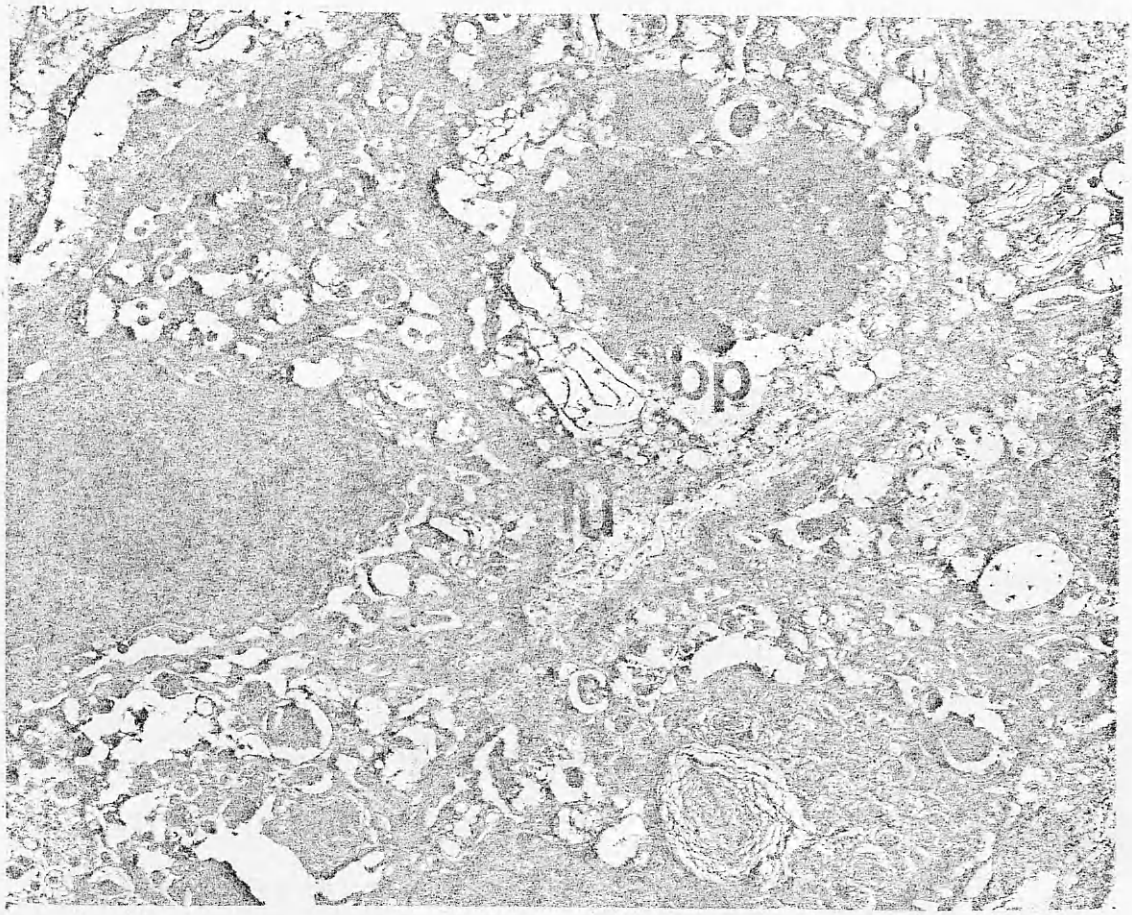

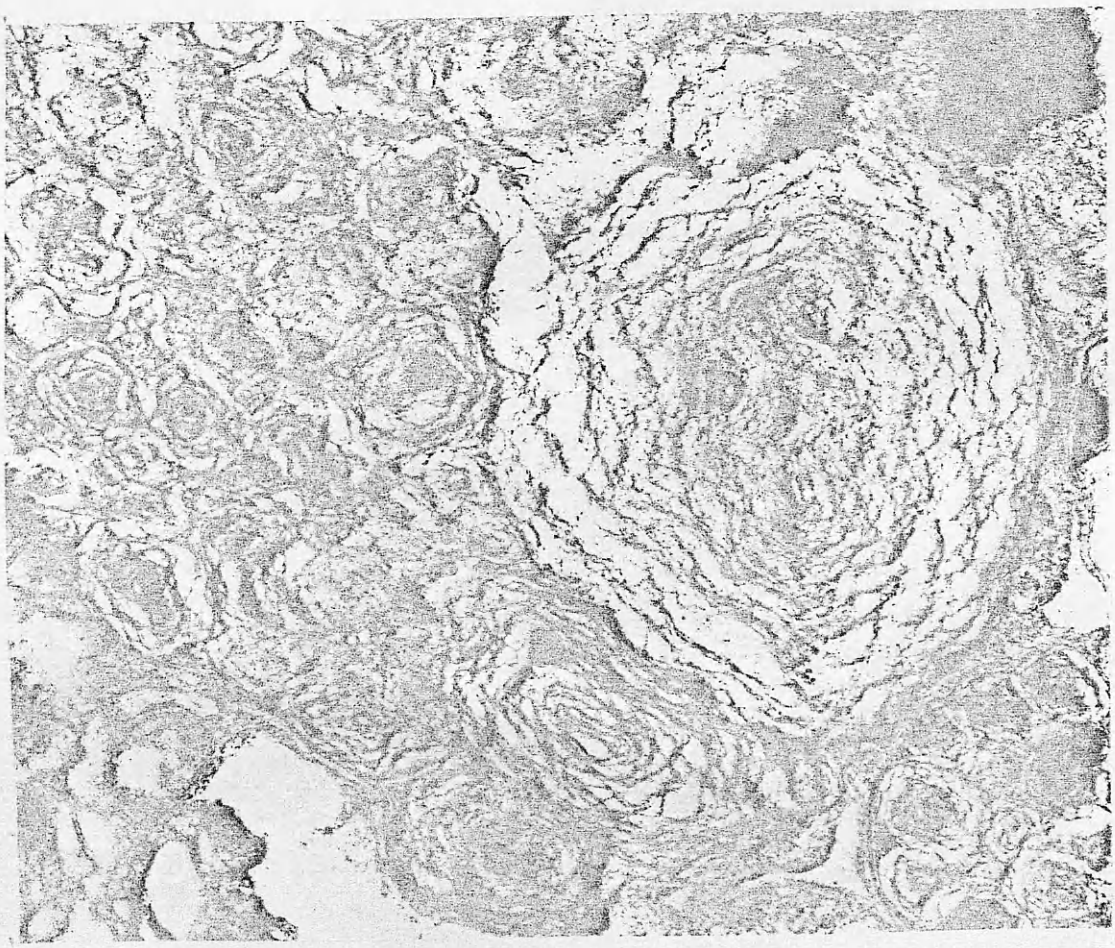

Above : Figure 62.1

Below : Figure 62.2

FIGURE 63

TEM of cirrhotic PBC. Part of hepatocyte showing bizarre-shaped as well as giant mitochondria (gm) with matrical paracrystalline inclusions. The majority of the mitochondria showed increased matrical density. (X 16870)

Figure 63

FIGURE 64.1

TEM of cirrhotic PBC. Part of hepatocyte (h) adjacent to a sinusoid showing Mallory body (mb) occupying great portion of the cytoplasm and appearing as microfilamentous structure. (bc : bile canaliculus). (X 6300)

Figure 64.1

FIGURE 64.2

TEM of cirrhotic PBC. High magnification micrograph of Mallory hyaline showing the tubular structure of some microfilaments among them a small laminated bodies are evident. (X 40500)

Figure 64.2

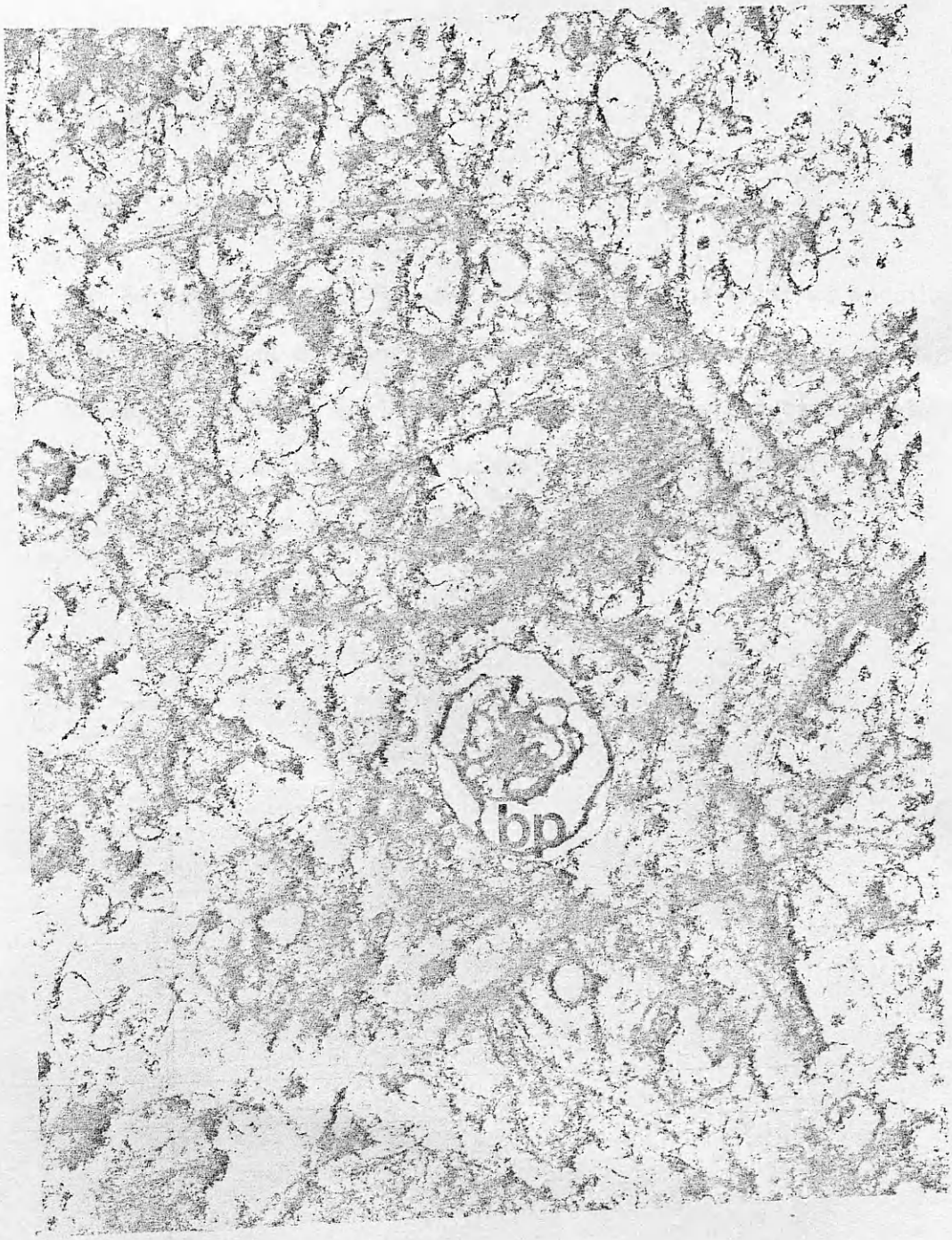

FIGURE 65.1

TEM of cirrhotic PBC. Hepatic sinusoid showing enlarged endothelial cell (ed) which contains numerous dense granules of biliary origin. The space of Disse (ds) is thickened and contained tissue debris, dense granules and a thick bundle of collagen fibres (co).
(h : hepatocyte). (n : nucleus). (X 16870)

Figure 65.1

FIGURE 65.2

TEM of cirrhotic PBC. High magnification micrograph of the space of Disse (ds) showing parallel bundles of collagen fibrils (co). Note the flattened smooth vascular surface of the hepatocyte. (ed : endothelium). (X 49500)

Figure 65.2

FIGURE 66

TEM of cirrhotic PBC. Parts of adjacent hepatocytes (h) showing dilatation of the intercellular space. The lateral surface of the hepatocyte is covered by rich array of microvilli. A thick bundle of collagen fibres (co) lying in the intercellular space is shown (pericellular fibrosis). Note the bile pigment deposition within the lumen of the injured bile canaliculus (bc). (X 13275)

Figure 66

FIGURE 67.1

SEM of PBC. Fractured surface shows numerous various sized spheroidal cells embedded in connective tissue. Note the tissue debris and the several holes and depressions corresponding to the places of the avulsed cells. In the adjacent area, fibrous bundles run parallel in the space of Disse outlining the hepatocytes which have crumbled surfaces. (wb : WBC). (X 450)

Figure 67.1

FIGURE 67.2

SEM of PBC. Fractured surface showing details of the spheroidal cells embedded in tissue stroma. Some possess slightly wrinkled surface, others have short flat blebs or microvilli and a third group left deep depressions in their places. (X 1125)

Figure 67.2

FIGURE 67.3

SEM of PBC. High magnification micrograph of spheroidal cell showing details of the surfaces which are rough irregular with few tiny flat plump microvilli and different size protrusions. Note a thick band crossing over the cell, probably of fibrous origin, adjacent to a depression in the other cell. (X 6750)

Figure 67.3

FIGURE 68.1

SEM of PBC. Fractured surface showing a band of thick twisted fibre encircling part of hepatocyte. The majority of the cells have crumbled surfaces. Others appeared to be arranged in two cells thick plates or in rosette form around a sinusoid (s) which is filled with cells and cellular debris. Note some collagen running along the sinusoid, and some crossing over the broken surface. (h: hepatocyte).(ft : fibrous tissue) (X 2250)

Figure 68.1

FIGURE 68.2

SEM of PBC. Fractured surface showing several hepatocytes arranged around a sinusoid (s). A cell with deeply folded surface appears within the lumen of the sinusoid. Bile canaliculi (bc) running across the surface of the hepatocyte. Thick collagen bundle (cb) crossing the fractured surface. (X 7875)

Figure 68.2

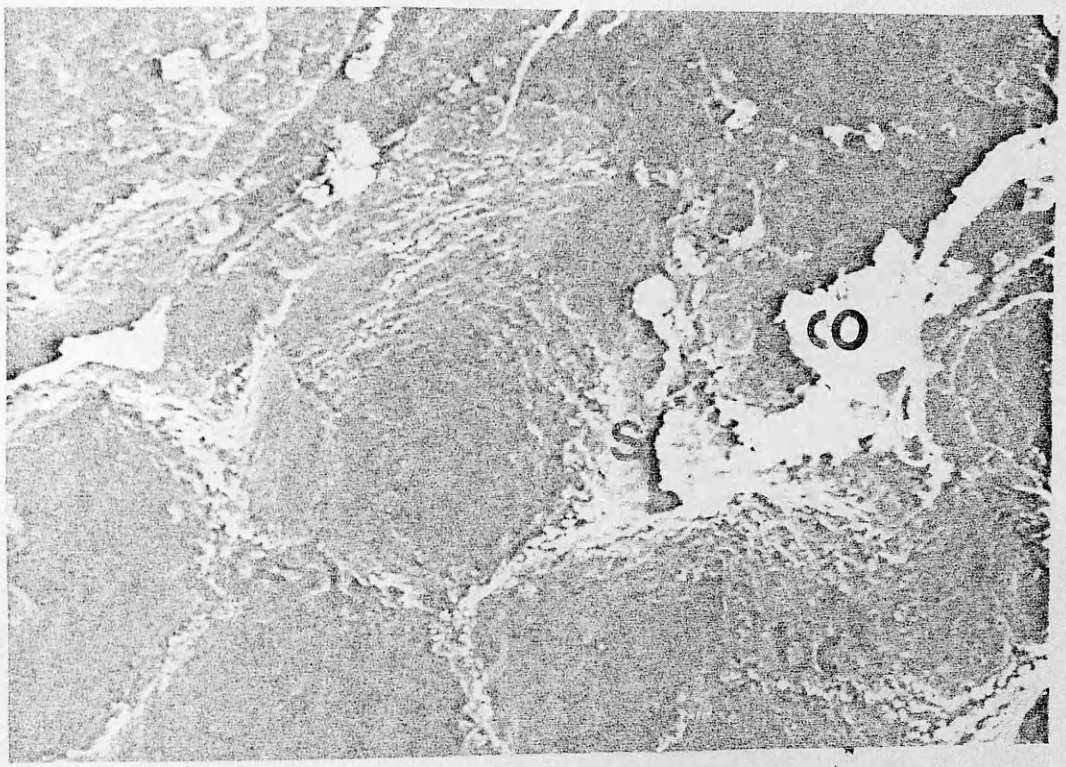

FIGURE 69.1

SEM of PBC. High magnification micrograph showing part of hepatocyte, bile canaliculi crossing the surfaces and joining with other canaliculi, numerous microvilli projecting into the surface and the hepatocytic surface itself appearing slightly wrinkled near the canaliculi, has tiny flat microvilli and small holes corresponding to the intercellular connections. (s : sinusoid). (X 16000)

FIGURE 69.2

SEM of PBC. High magnification micrograph of the hepatic sinusoid showing adjacent hepatocytes, few microvilli on the vascular pole. Within the lumen two cells with deeply folded surfaces are present. (bc : bile canaliculus). (X 20000)

Figure 69.1

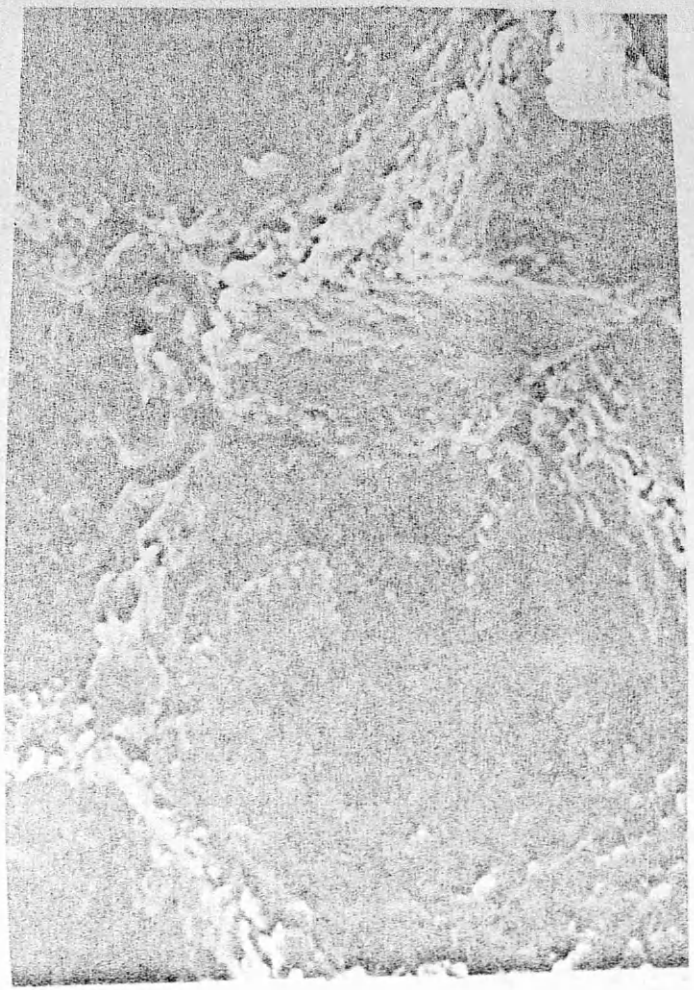

Figure 69.2

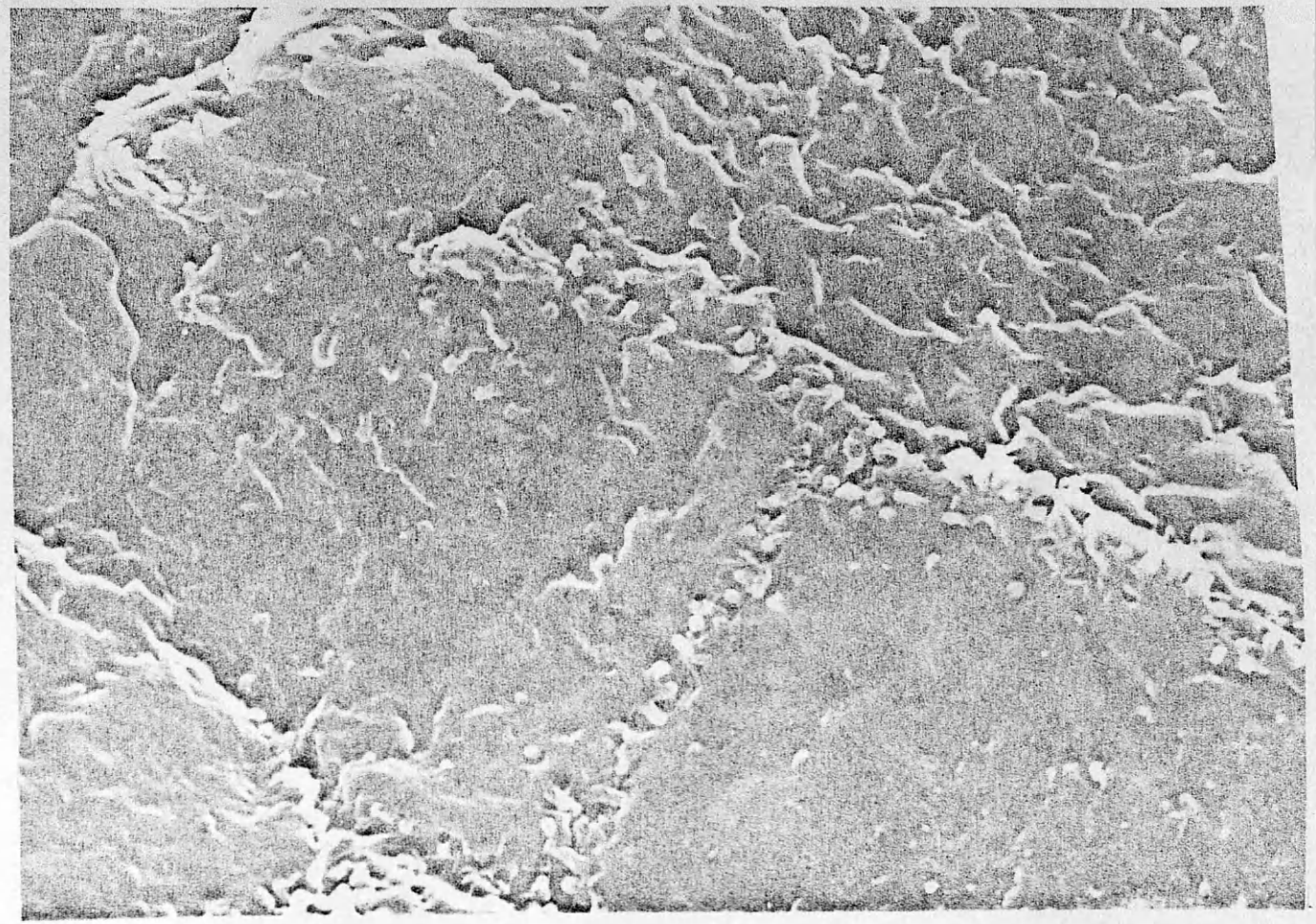

FIGURE 70.1

SEM of PBC. Fractured surface showing several hepatocytes (h) with sinusoid filled with RBCs. The hepatocytes have a smooth clear surface. Bile canaliculi run across the surface. Thick twisted band of collagen (co) crossing the fractured surface is shown. (X 1800)

Figure 70.1

FIGURE 70.2

SEM of PBC. High magnification micrograph showing details of hepatic surface. Bile canaliculi run across the surface and thin bundle of collgen cling to the side of the hepatocyte (h) in the space of Disse where the endothelial lining is ripped away by the fracturing technique. (X 3375)

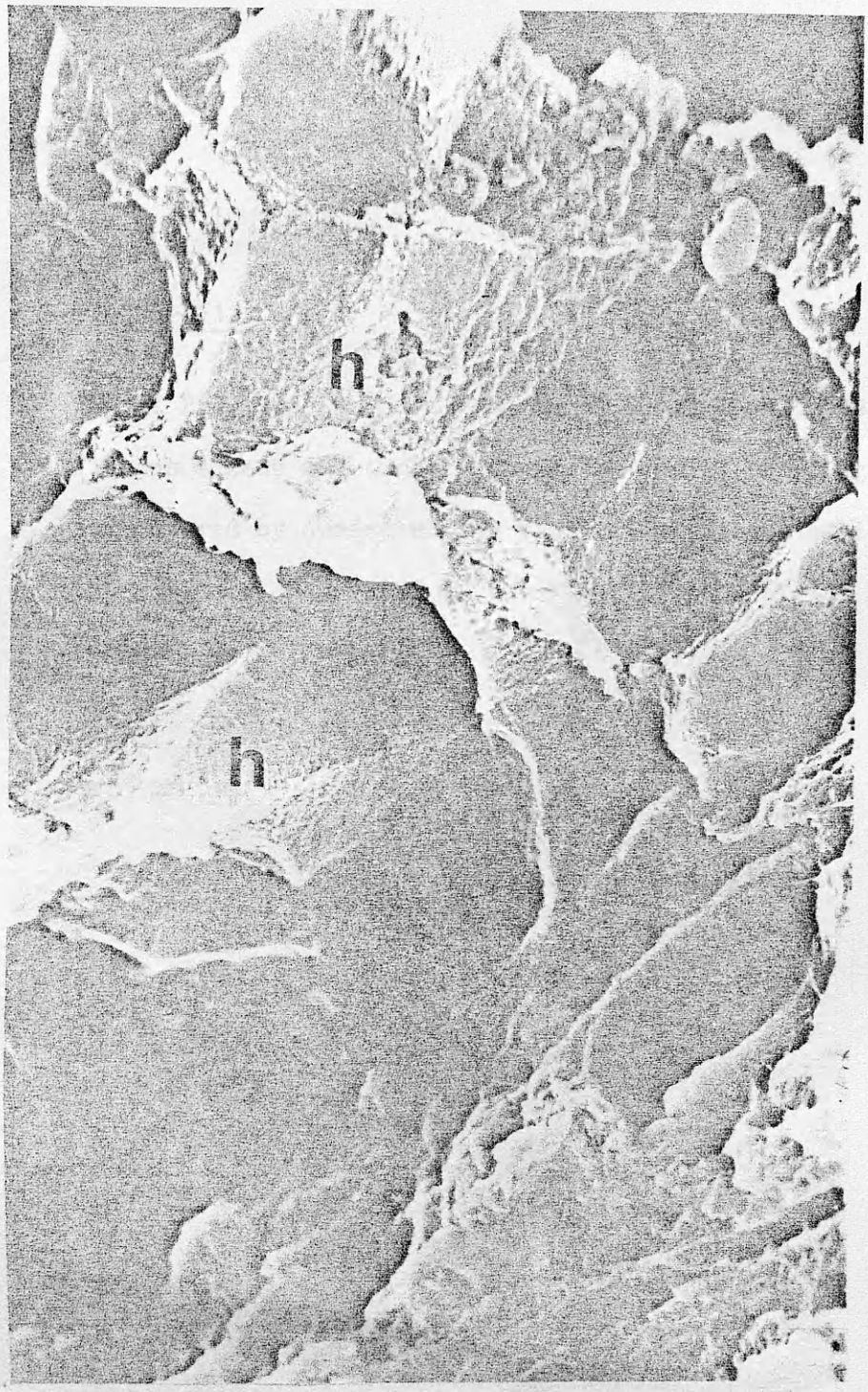

Figure 70.2

FIGURE 71.1

SEM of PBC. Fractured surface showing two hepatocytes (h) among fibrous tissue and tissue debris.The surface is rough, irregular and covered by numerous tiny microvilli. Bile canaliculi run across the surface. Microvilli of the vascular pole of the hepatocyte are evident. (co : collagen) (X 7875)

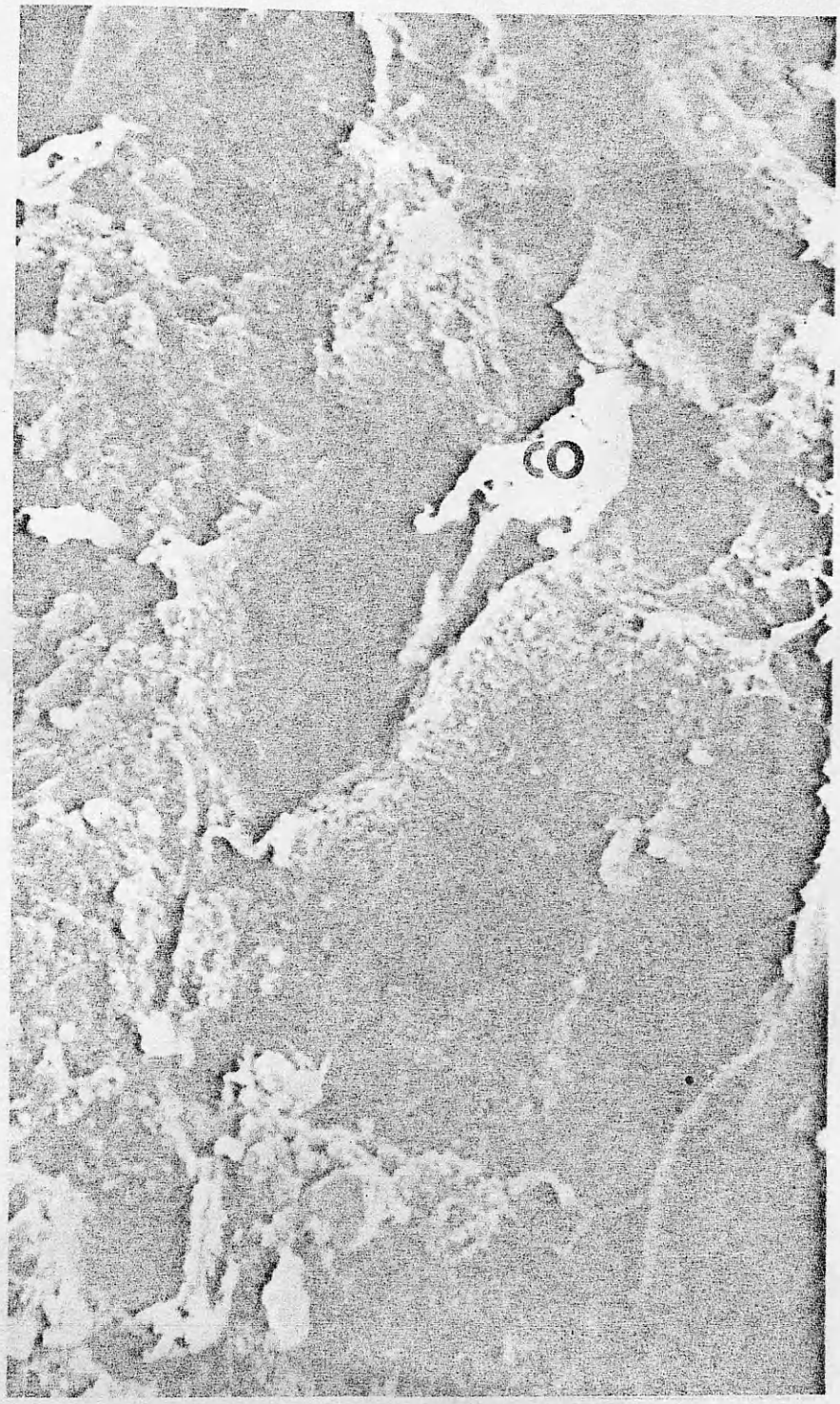

Figure 71.1

FIGURE 71.2

SEM of PBC. Fractured surface showing several hepatocytes (h) and a thick bundle of fibrous tissue connected to the hepatocyte with tiny slender fibrils. Note the surface of the hepatocyte covered by abundant microvilli.(s : sinusoid).(co : collagen). (X 7875)

Figure 71.2